The Role of Mitochondrial Dysfunction in Acute Pancreatitis

Thesis submitted in accordance with the requirements of the University of Liverpool for the degree of Doctor of Philosophy

By:

David Michael Booth

September, 2010

Abstract

Acute pancreatitis is a serious and often lethal inflammatory disease. Its causes are diverse and incompletely understood; however, gallstones and alcohol abuse are the principal triggers. Oxidative stress has been proposed as a determinant of acute pancreatitis (AP) severity, and has been the subject of recent clinical trials. The major AP precipitants, alcohol, alcohol metabolites and bile salts, were investigated for their potential role in the production of reactive oxygen species (ROS), and their effects upon cell fate.

Application of the bile salt taurolithocholic acid sulphate (TLC-S) to isolated human and murine pancreatic acinar cells generated significant Ca^{2+}-dependent mitochondrial ROS which were inhibited with the antioxidant *N*-acetyl-L-cysteine (NAC), and promoted with dimethoxy-2-methylnaphthalene (DMN), an inhibitor of the antioxidant enzyme NAD(P)H quinone oxidoreductase (NQO1). Elevations of ROS mediated by bile salts were crucial in the determination of cell fate, producing apoptosis rather than necrosis.

In contrast, ethanol and its metabolites, both oxidative (acetaldehyde) and non-oxidative (fatty acid ethyl esters: FAEEs), were shown to produce no significant ROS in similar circumstances. Assessment of ethanol and its metabolites revealed that ethanol and acetaldehyde showed little effect on cell fate. Low concentrations of ethanol with fatty acid, however, induced toxic elevations of $[Ca^{2+}]_C$, mitochondrial dysfunction and necrosis when oxidative metabolism was compromised. This effect was reversed by inhibition of FAEE synthase, suggesting important deleterious actions of non-oxidative alcohol metabolism in the pancreas.

Acknowledgements

First and foremost I wish to thank Dr David Criddle and Professor Robert Sutton for their help, support, advice and enthusiasm. Without their excellent supervision, this Ph.D project would not have been possible.

I would like to thank Professor Ole Petersen and Professor Alexei Tepikin for the benefit of their knowledge, astute guidance, wisdom and somewhere to sit.

Further thanks to Svetlana Voronina and Mischa Chvanov for giving me the benefit of their time, practical experience and patience.

Special thanks go to external collaborators Mohammed Jaffar and Bhupendra Kaphalia who have provided vital tools.

Thanks to Mark Houghton for protecting me from a world of admin. You deserved each and every one of the 1,347 cups of tea.

Thanks to all the members of Blue Block, past and present you have made it a special place to be for over 3 years. Gyuri Lur, Wei Huang, Matt Cane, Hayley Dingsdale & Rishi Mukherjee all deserve special thanks, as do members of physiology outside Blue Block: Chris Holmberg, Chris Thorne, Ciara Walsh and Jon Woodsmith for a wide variety of things.

Thanks to Jacqueline Wrench – for being there. Thanks to Rick and Carl, for not.

Finally many thanks to the Medical Research Council for funding this project.

Abbreviations

3MA	3-methyladenine
4MP	4-methylpyrazole
Ac	Acetaldehyde
ACh	Acetyl Choline
ADH	Alcohol dehydrogenase
AO	Acridine Orange
AP	Acute pancreatitis
ARDS	Acute respiratory distress syndrome
ATP	adenosine triphosphate
BAPTA	(1,2-bis(o-aminophenoxy)ethane-N,N,N',N'-tetraacetic acid)
BNPP	Bis-(4-nitrophenol) phosphate
BSA	Bovine serum albumin
cADP	cyclic Adenosine diphosphate
cAMP	cyclic Adenosine 3,5 monophosphate
$[Ca^{2+}]_c$	cytosolic Ca^{2+} concentration
$[Ca^{2+}]_m$	mitochondrial Ca^{2+} concentration
CEL	Carboxyl ester lipase
ChE	Cholesterol esterase
CYP2E1	Cytochrome p450 2E1
CCCP	Carbonyl cyanide m-chlorophenlyhydrazone
CCK	Cholecystokinin
CDE	Choine-defficient, ethionine supplemented
CICR	Ca^{2+}-induced Ca^{2+}-release
DAG	Diacylglycerol
DCFDA	5-(and-6)-chloromethyl-2',7'-dichlorodihydrofluorescein diacetate
DMN	2,4-dimethoxy-2-methylnapthalene
DMSO	Dimethyl sulphoxide
DPI	Diphenylene iodonium
EB	Ethidium bromide
EGTA	Ethylene glycol tetraacetic acid
ER	Endoplasmic reticulum
ERCP	Endoscopic retrograde cholangiopancreatography
ETC	Electron transport chain
EtOH	Ethanol
$FAD(H_2)$	Flavin adenine dinucleotide
FA	Fatty acid
FAEE	Fatty acid ethyl ester
Fluo4	Fluorescein-based Ca^{2+}-indicator
GPBAR1	G-protein coupled bile acid receptor 1
GPx	Glutathione peroxidase
GSH	Glutathione
GSSG	Glutathione disulphide
HEPES	4-(2-hydroxyethyl)-1-piperazineethaqnesulphonic acid

HepG2	human hepatocarcinoma cell line
IP_3	Inositol 1,4,5 trisphosphate
IP_3R	Inositol 1,4,5 trisphosphate receptor
MAOS	Microsomal acetaldehyde oxidising system
MEM	Modified Eagle's medium
MEN	Menadione
MODS	Multiple organ dysfunction syndrome
MnSOD	Manganese superoxide dismutase
NAADP	Nicotinic acid adenine dinucleotide phosphate
NADH	Nicotinamide adenine dinucleotide
NAC	*N*-acetyl-L-cysteine
NADPH	Nicotinamide adenine dinucleotide phosphate
NF- κB	Nuclear factor κ B
NQO1	NAD(P)H quinone oxidoreductase 1
PFA	Paraformaldehyde
PM	Plasma membrane
PI	Propidium iodide
PMCA	Plasma membrane Ca^{2+} ATPase
POA	Palmitoleic acid
POAEE	Palmitoleic acid ethyl ester
RAP	Rapamycin
RNS	Reactive nitrogen species
ROS	Reactive oxygen species
$[ROS]_i$	Intracellular reactive oxygen species
$[ROS]_m$	Mitochondrial reactive oxygen species
RyR	Ryanodine receptor
SERCA	Sarcoplasmic/endoplasmic reticulum Ca^{2+} ATPase
SOCE	Store-operated Ca^{2+}-entry
SOD	Superoxide dismutase
STIM	Stromal interaction molecule
TCA	Tricarboxylic acid
TLC-S	Taurolithocholic acid -3-sulphate
TMRM	Tetramethyl rhodamine methyl ester
VIP	Vasoactive intestinal peptide

Contents

Chapter 1

Introduction

1.1 The Pancreas

The pancreas is a small (<100g) organ located adjacent to the spleen in a retroperitoneal location within the abdomen. The name pancreas derives from the Greek words “pan” and “kreas” meaning “all meat”; a description owing to the fleshy nature of the organ. Anatomically the pancreas is divided into 4 regions termed “head”, “neck”, “body” and “tail”. The head is the largest portion, in closely associated with the duodenum, with the remainder of the organ diminishing in size toward the tail. The pancreas is supplied with blood via the coeliac and superior mesenteric arteries that branch from the aorta. Venous drainage is principally via the hepatic portal vein from the splenic and superior mesenteric veins. The pancreas is innervated by both the sympathetic and parasympathetic branches of the autonomic nervous system, with the parasympathetic pathway being partially responsible for secretory control. Hormonal stimulation of secretion is mediated by cholecystokinin (CCK) (Murphy et al., 2008). The pancreas features an extensive lymphatic drainage system which is relatively inactive under physiological conditions but becomes more active in the diseased pancreas (Bockman et al., 1973). The principal functions of the pancreas are twofold: the production and effective secretion of pancreatic juice containing the digestive enzymes, biocarbonate and fluid by the cells of the exocrine pancreas, and the production of the hormones insulin and glucagon, the hormones responsible for glucose homeostasis, by the endocrine pancreas. This thesis is concerned with the physiology and pathophysiology of the exocrine pancreas.

1.2.1 Structure of the exocrine pancreas

One of the functional units of the exocrine pancreas is the acinus, a latin word meaning “berry” which is in reference to the appearance of the acini and ductal structure. Acini are composed of numerous exocrine pancreatic acinar cells arranged around a common lumen. The ductal structure consists of intralobular and interlobular ducts. The intralobular ducts are situated within lobules and drain pancreatic juice from the lumen of the acini. The interlobular ducts connect the individual lobules connecting eventually to the main pancreatic duct. The intralobular ducts are composed of smooth, flat cuboidal cells termed centroacinar cells which also penetrate into the lumen of the acinar unit (Kern, 1993). The cuboidal epithelium is without features such as microvilli and the clear structural polarity possessed by acinar cells. The function of the epithelial cells is the transport of fluid and ions into the lumen to facilitate transport of the secreted digestive (pro)enzymes (Kern, 1993). The intralobular ducts converge to form larger interlobular ducts which are associated with extensive connective tissue and are lined with pyramidal epithelium (Kern, 1993). These larger ductal structures form organisational foci along which blood vessels and neurons are found (Figure 1.1). The pancreatic duct is the final, largest structure into which the interlobular ducts drain, the secretory products of the interlobular ductal epithelia remain to be fully characterised, but they are known to contain muco-proteins (Kern, 1993). Pancreatic juice is controlled in terms of pH to between 7.6 and 8.2 in order to partially neutralise the acidic chyme received into the small intestine from the stomach (Williams, 1980).

1.2.2 The pancreatic ductal dell

The ductal cell is central to the physiological function of the pancreas. The ductal cells both constitute the intrapancreatic plumbing and are responsible for the secretion of a bicarbonate-rich fuid which has multiple roles. The fluid component effectively transports acinar-derrived enzymes to the duodenum, where the bicarbonate component aids neutralization of the acidic chime (argent, 2006). The secretion of bicarbonate and electrolyte-rich fluid acts as a component in a coordinated system, as demonstrated by the effects of the mutated cystic fibrosis transmembrane conductance regulator protein (CFTR). Loss of CFTR fuction compromises fluid secretion and leads to rapid destruction of the entire organ (Nousia-Arvanitakis, 1999).

1.2.3 Structure of the pancreatic acinar cell

The acinar cell is structurally and functionally polarised (Petersen, 1992, Petersen et al., 1999). The basolateral and perinuclear region of the cell interior is densely packed with membranous rough endoplasmic reticulum (ER) (Petersen et al., 1999). The plasma membrane polarity is defined by the presence of tight junctions. These structures extend from the luminal side of the lateral membrane in three discrete structures; occluding junctions, belt desmosomes and spot desmosomes (Kern, 1993). The apical portion of the cell is packed with mature dense-core vesicles, or zymogen granules. These are sufficiently dense to be clearly visible in both light and electron microscopy. Immediately adjacent to the granules the golgi apparatus is located. This consists of a five-stack structure (Kern, 1993). Surrounding the golgi are numerous coated vesicles approximately 60nm in diameter which

bud from the apical (trans) face of the golgi, in addition to condensing vacuoles which go on to form mature zymogen granules.

The maturation process of condensing vesicles into zymogen granules is characterized by increasing electron density as measured by electron microscopy (Palade, 1975b). Mature zymogen granules forming exocytotic structures with the apical membrane have been captured by electron microscopy (Jamieson and Palade, 1971b, Jamieson and Palade, 1971a). Exocytosis occurs in a compound manner requiring an external signal, intracellular calcium release and a clathrin coated structure (Nemoto et al., 2004).

In addition to the golgi, the zymogen granules are delineated by a “buffer-barrier” of peri-granular mitochondria which serve to polarize and partially contain release of calcium in the apical pole, attenuating it (Tinel et al., 1999). Mitochondria also surround the nucleus and form a belt immediately adjacent to the plasma membrane.

Acinar cells are electrically connected via pore-like structures termed gap junctions. These are composed of connexin proteins (Frossard et al., 2003), which have been shown to form a pore structure complementary to that in a juxtaposed cell, forming an open channel between two cells. The channel formed is approximately 16-20Å, large enough for the passage of ions, metabolites, nucleotides and small peptide such as glutathione but not sufficient in size to allow the passage of macromolecules such as proteins and DNA. Intercellular communication via these channels allows electrical connection, which was demonstrated by the depolarization of one cell

causing an equivalent loss of polarity in neighbouring cells (Petersen, 1975). The extensive nature of interconnected cells (>100) was demonstrated by the free movement of injected non-membrane permeable dyes such as fluorescein, Lucifer Yellow and Procion Yellow (Findlay and Petersen, 1983, Iwatsuki and Petersen, 1979). The role of inter-cell communication may be in part to allow coordination of signalling events by allowing the passage of second messengers such as inositol 1,3,5-trisphosphate (IP_3), Ca^{2+} and cAMP (Saez et al., 1989, Sandberg et al., 1992). This coordination has been observed in diverse cell types such as epithelial (Boitano et al., 1992) and between neurones and astrocytes (Nedergaard, 1994). In the rat pancreatic acinar cell, transmission of calcium waves between cells has been demonstrated and is possibly mediated via intercellular transmission of IP_3, as Ca^{2+} alone was not sufficient to propagate the wave (Yule et al., 1996) Possibly due to the buffering capacity invested in the cytosolic compartment by calcium-binding proteins (Allbritton et al., 1992). The same study (Yule et al., 1996) highlighted the loss of intercellular communication at supramaximal levels of agonist stimulation. Perhaps the most physiologically significant role for intercellular communication is as a possible explanation for the more efficient rate of secretion seen from group, rather than individual cells (Stauffer et al., 1993).

1.2.4 Secretory function

Secretion of enzymes is activated by the gut hormone cholecystokinin (CCK), and the neurotransmitters acetyl choline (ACh) and vasoactive intestinal

polypeptide (VIP). The binding of agonists such as these, occurs at their specific receptors in the basal membrane, stimulating secretion from the apical pole exclusively across the luminal membrane (Palade, 1975a). The interaction of ligands and receptors leads to the mobilization of secondary intracellular messengers such as inositol 1,4,5 trisphosphate (Berridge, 1981). The messenger then initiates a series of reactions culminating in exocytosis and the release of enzymes from the zymogen granules into the lumen. This sequence is termed stimulus-secretion coupling. The ingestion of food triggers the release of the various agonists: ACh from cholinergic nerves, VIP from pancreatic nerves following vagus nerve stimulation, CCK and secretin from the intestinal mucosa. Secretin and VIP are known to stimulate both the cells of the ducts and acinar cells with regard to secretion of the fluid and electrolyte components of the pancreatic juice (Chey et al., 1979). These agonists activate secretion by elevating the intracellular concentration of cyclic adenosine 3,5 monophosphate (cAMP) (Mangos et al., 1973). ACh and CCK are able to activate both enzyme secretion and simultaneous fluid secretion. Fluid secretion in the pancreatic acinar cell is thought to be driven by a rise in $[Ca^{2+}]_c$, which triggers the opening of Ca^{2+}-activated K^+ channels in the basolateral membrane resulting in K^+ efflux (Petersen and Maruyama, 1984). Subsequent influx of + ions back through the membrane via the $Na^+/2Cl^-/K^+$ co-transporter causing uptake of Na^+ and Cl^- ions (Petersen and Maruyama, 1984). In the lumen, the Ca^{2+}-activated Cl^- channels initiate Cl^- efflux into the luminal space. Na^+ ions are pumped out of the cell via the $Na^{+/}K^+$ exchanger and enter the lumen via a para-

cellular route. The overall net secretion of $Na^{+}Cl^{-}$ forces osmotic movement of water in to the lumen (Petersen, 1994).

Secretion of enzymes is achieved by exocytosis and is also an entirely Ca^{2+}-dependent process, whereby stimulation of the cell e.g. with CCK, causes fusion of membrane-bound zymogen granules to the apical membrane. This releases the enzyme contents into the luminal space, which is continuous with the pancreatic duct. Local increases in Ca^{2+} are necessary for this to occur, local increases which also couple stimulus of the cell to metabolism via actions exerted upon the mitochondria (Voronina et al., 2002b).

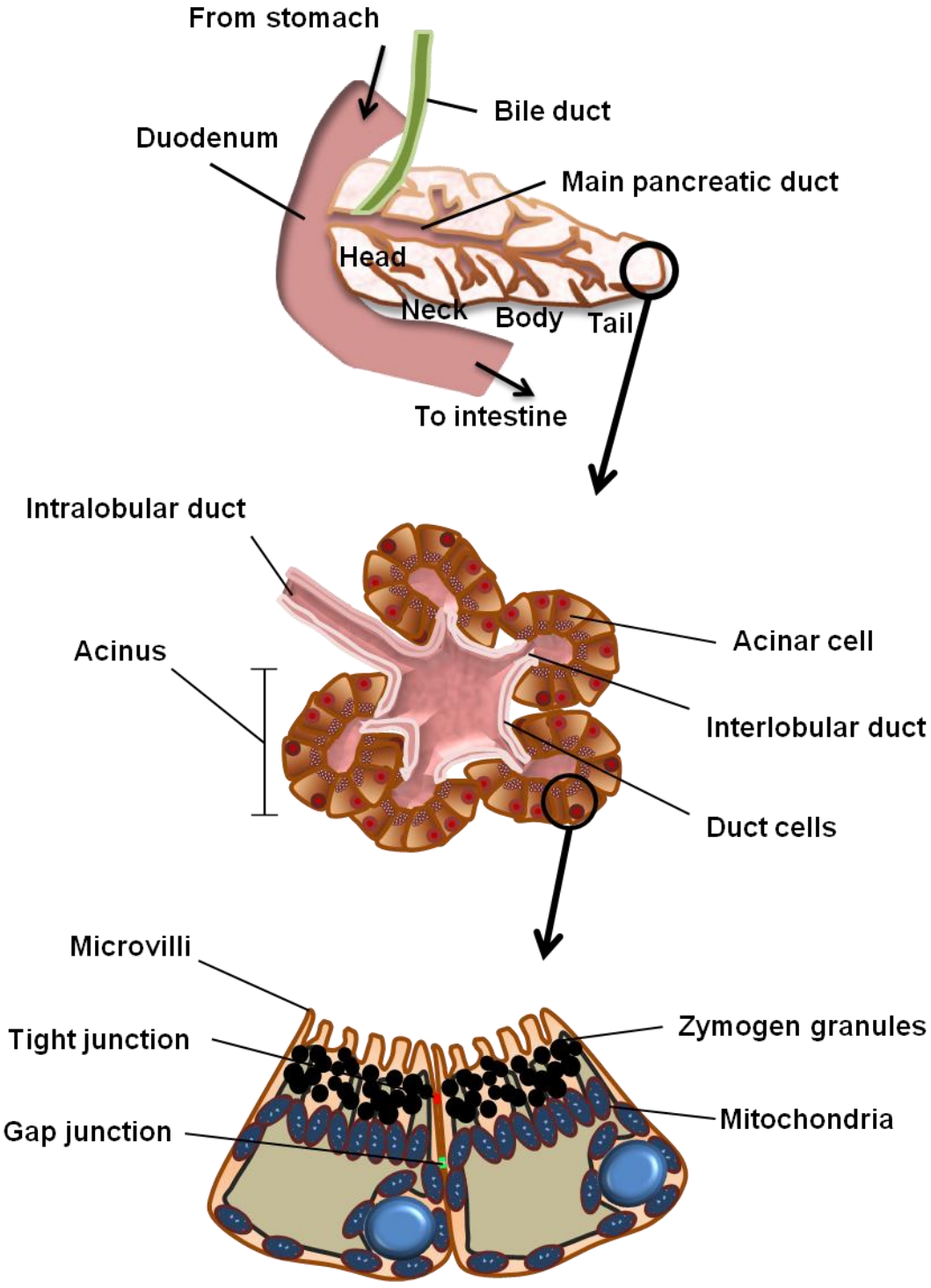

Figure 1.1 Structure of the exocrine pancreas. The pancreas is subdivided into four discrete regions, head, neck,body and tail. All sections produce pancreatic juice, an enzyme-rich fluid which moves through the ductal system into the main pancreatic duct and onward into the duodenum. The exocrine unit is the acini (B) which are composed of cells arranged around the central lumen. The pancreatic acinar cell (C) is defined by its polarity, the zymogen granules are located in the apical pole whereas the ER and nucleus are located in the basolateral region; the mitochondrial belt delineates the two regions.

1.3 Ca^{2+} signalling

The central role of Ca^{2+} in cell biology began as early as 1883, when Sidney Ringer discovered that Ca^{2+} was required for the contractile behaviour of the heart. Since then, Ca^{2+} has been placed at the centre of diverse signalling events. Ca^{2+} is indispensible for cell movement, growth and division (reviewed in (Clapham, 2007)). Ca^{2+} is vital to the control of subcellular processes also; examples include secretion (Petersen, 1992), gene transcription (Berridge et al., 2003) and muscle contraction (Berridge et al., 2003, Clapham, 2007). The role of Ca^{2+} as the master second messenger, owing to its ubiquitous presence in cellular processes, cannot be ignored. The universality of Ca^{2+} as an intracellular messenger leads us to question as to why cells have adapted to use Ca^{2+} over any other water soluble cation? One possibility is the tendency of Ca^{2+} to precipitate phosphate (Clapham, 1995). Cells use phosphate, bound and inorganic, as the currency in their internal energy economy. As such cells are obligated to maintain a sufficiently low concentration of Ca^{2+} in the compartment populated with phosphate; the cytosol. To achieve this, given the high Ca^{2+} external environment, cells have adopted a number of strategies for managing the concentrations of Ca^{2+}. To achieve this cells bind Ca^{2+} to Ca^{2+}-binding proteins and sequester Ca^{2+} into intracellular stores. These actions create Ca^{2+}-gradients, allowing the cell to rapidly change the concentration of Ca^{2+} in the cytosol (Berridge, 2001). The versatility of Ca^{2+} as a signalling molecule evolved as cells themselves evolved new and different ways to interact with and alter the spatio-temporal patterns of Ca^{2+} signalling, and Ca^{2+}interacting molecules.

The life of a Ca^{2+} signal falls broadly into three categories; initiation, propagation and termination. The signalling events, messengers, channels, pumps and organelles pertinent to this work will be discussed in the subsequent sections.

1.3.1 Initiation of the Ca^{2+} signal

Release of Ca^{2+} from one of the many Ca^{2+} stores requires the interaction of a Ca^{2+}-releasing second messenger and a receptor/channel. The second messengers include IP_3 cADP ribose, NAADP and Ca^{2+} itself. IP_3 is formed by the phospholipase C (PLC) cleavage of PI 4,5 P_2, yielding IP_3 and diacylglycerol (DAG). These molecules stimulate divergent signalling pathways. The production of cADP ribose and NAADP are mediated by ADP ribosyl cyclise/CD38, their regulation is still incompletely understood (Cancela et al., 1999) however recent evidence strongly implicates the ecto-enzyme CD38 in pancreatic acinar cells (Cosker et al., 2010).

Each second messenger stimulates its own receptor, of which several isoforms exist and are expressed in the pancreatic acinar cell. The acinar cell expresses IP_3 receptors of type 1,2&3 (Lur et al., 2009, Wojcikiewicz et al., 1999) concentrated in the apical pole (Lur et al., 2009, Ashby and Tepikin, 2002). Importantly, a combination of type 2 and 3 IP_3 receptors (IP_3R) appears to be essential for Ca^{2+} signal generation linked to exocrine secretion in pancreatic acinar cells, since Ca^{2+}-signals and secretory responses to CCK and ACh were absent in double knockout mice, but not in single knockouts for each individual IP_3R subtype (Futatsugi et al., 2005).

The second messenger cADP ribose acts on ryanodine receptors, of which type 2 is expressed in the pancreatic acinar cell (Leite et al., 1999). The actions of NAADP are not well understood in terms of molecular targets (Aarhus et al., 1996) although strong evidence is emerging implicating the recently discovered and characterised two-pore channel (TPC) (Ruas et al., 2010, Tugba Durlu-Kandilci et al., 2010).

Physiological stimulation with acetylcholine (ACh) via muscarinic receptors yields IP_3, CCK stimulation yields cADP ribose and NAADP and the bile acid receptor GPBAR1 may yield cAMP, but certainly releases Ca^{2+} from IP_3 sensitive stores (Perides et al., 2010, Voronina et al., 2002a). IP_3 and Ryanodyne receptors respond to the binding of second messengers by dramatically increasing their open probability, releasing ER Ca^{2+} through the channel. All three second messengers evoke Ca^{2+} release from the apical pole (Thorn et al., 1993, Kasai et al., 1993, Thorn et al., 1994, Cancela et al., 2002, Ashby et al., 2002), as these messengers are freely diffusible from their origin to the apical region of the cell.

1.3.2 Propagation of the Ca^{2+} signal

The propagation of Ca^{2+} signals in the acinar cell is of tremendous physiological significance, and differing concentrations reached during spikes have been demonstrated to elicit discrete actions within the acinar cell (Ito et al., 1997). The principal mechanism of propagation in the acinar cell is Ca^{2+}-induced Ca^{2+}-release (CICR) (Wakui et al., 1990). This requires the coordination of one or more types of Ca^{2+}-release channels (Ashby et al.,

2002), allowing messengers produced in the basal area of the cell to elicit coordinated Ca^{2+} release from receptors in the apical pole of the cell, where all physiological Ca^{2+} signals originate (Thorn et al., 1993).

1.3.4 Termination of the Ca^{2+} signal

The termination of a Ca^{2+} signalling event relies upon two factors: 1: a change in the biophysical properties of Ca^{2+}-release channels, i.e. a significant decrease in their open probability. 2: removal of free Ca^{2+} by active sequestration or extrusion. Ca^{2+} release channels regulate their own open probability by having a bell-shaped Ca^{2+} response curve (Bezprozvanny et al., 1991). Initial stimulation of Ca^{2+} release by Ca^{2+} is replaced by negative-feedback inhibition at higher concentrations.

1.3.5 Ca^{2+} influx

Apart from release of Ca^{2+} from intracellular stores, the main source of Ca^{2+} in the cytosol is Ca^{2+} entry from the exterior of the cell. This is not only important for replenishing intracellular stores but is essential for maintaining sustained Ca^{2+} elevations such as those seen in hyperstimulation events triggered by supramaximal agonist stimulation (Putney, 1976a, Putney, 1976b, Putney, 1977) . Stimulation of Ca2+ entry follows depletion of the intracellular stores. The state of store depletion is sensed by the recently discovered Ca^{2+}-sensing Stromal interacting molecule (STIM) (Roos et al., 2005) and its mammalian homologue STIM1 (Liou et al., 2005). Stim1 is homogenously distributed throughout the ER membrane in resting cells, upon store depletion it rapidly translocates to punctate structures that include the protein Orai1. Orai1 is the functional, pore-forming subunit of store operated Ca^{2+}-entry (SOCE) (Prakriya et al., 2006, Feske et al., 2006), Once STIM1

oligomerises and co-localises with Orai1, its c-terminal domain couples with Orai1 and stimulates channel opening, allowing Ca2+ entry down he large electrochemical gradient (10,000 fold) between the extracellular environment and the cytosol (Putney, 1986, Park et al., 2009).

1.3.6 Ca^{2+} efflux

The plasma membrane of the pancreatic acinar cell is has been demonstrated to contain a Ca^{2+} sensitive Mg^{2+}-dependent ATPase which operates as the principal Ca^{2+}-extrusion mechanism in the pancreatic acinar cell (Tepikin et al., 1992). This pump is termed the plasma membrane Ca^{2+}-ATPase (PMCA) and belongs to the P-type family of ATPases along with the functionally similar sarco-endoplasmic ATPase (SERCA) pump. The two pumps share a similar mechanism of action, (Carafoli and Brini, 2000). Its mechanism is well defined and involves the transfer of a γ-phosphate from ATP to a specific aspartate residue within the pump (Knauf et al., 1974). This is followed by a Mg^{2+}-sensitive conformational change and Ca^{2+}-extrusion (reviewed in (Strehler and Treiman, 2004)). In many cell types, Ca^{2+} extrusion is mediated via Na^{+}/Ca^{2+} exchange pumps, however these appear to be of little functional importance in the pancreatic acinar cell (Muallem et al., 1988) and may even be absent.

1.4 Acute Pancreatitis

The principal disease of the exocrine pancreas is Acute Pancreatitis (AP), a devastating and sometimes fatal disease. It currently affects in excess of 50 per 100,000 people annually, and is predominantly caused by gallstones or alcohol excess. Diverse agents may also induce the disease, including viral infection, hypercalcaemia, hyperlipidaemia, ductal tumour, autoimmunity, and

surgical techniques such as endoscopic retrograde cholangiopancreatography (ERCP) (Pandol et al., 2007, Saluja et al., 2007, Swaroop et al., 2004). Importantly, the incidence of AP is increasing, a phenomenon which is likely to be at least partly due to increased alcohol consumption. Approximately 20% of patients with AP develop a severe form of the disease, characterised by pancreatic necrosis and multiple organ failure, which carries substantial morbidity and mortality. Although overall pancreatitis has a mortality rate of approximately 5% (Banks and Freeman, 2006), the presence of necrosis raises this to 17% (Pandol et al., 2007). Complications such as infected necrosis may further raise the risk of mortality. Despite the considerable social and economic burden associated with the disease, there remains no specific therapy for AP. This highlights the fundamental need for detailed research into the pathogenesis of pancreatitis to identify potential drug targets.

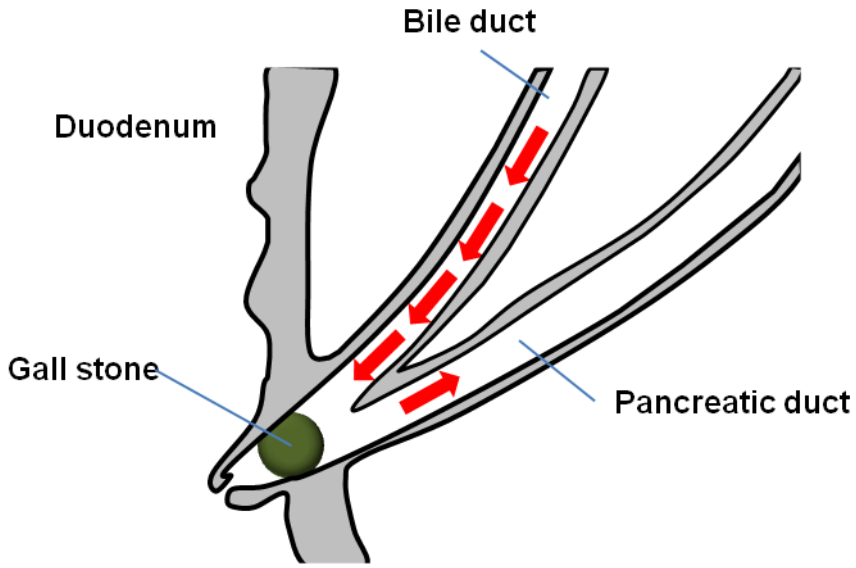

Figure 1.2 The "common duct" theory of gall stone-induced pancreatitis. A schematic representation of a theory proposed by Opie in 1901 to explain the development of acute pancreatitis. The gall stone (*green*) is impacted at the ampulla of Vater blocking the exit of both the pancreatic and bile ducts to the lumen of the duodenum. The bile duct and pancreatic duct are linked allowing reflux of bile (*red*) from the gall bladder into the pancreatic duct.

1.4.1 Bile Acids and Pancreatitis

Bile is produced in the liver and contains numerous excretory products, pigments from the breakdown of haemoglobin and cytochromes, bile acids, cholesterol and bicarbonate. The neutralising and detergent effects of bile are vital to breakdown and absorption of fats and fat soluble vitamins (reviewed in (Strange, 1984)). The concentration of bile acids in mammalian bile varies from 2-45mM with 10mM being an approximate figure for humans. The proximal bile acid; cholic acid is a 24-carbon compound from which all other bile acids are derived. Commonly occurring bile acids differ in the number of free hydroxyl groups: cholate, chenodeoxycholate, and lithocholate having 3, 2 and 1 respectively. The free hydroxyl groups affect the level of solubility in aqueous media, cholate being more soluble than lithocholate. Conjugation of lithocholate to the amino acids glycine or taurine increases the solubility. The pool of bile salts varies enormously between species and individuals, but the most abundant is glycine-conjugated cholate with chenodeoxycholate representing ~40% and ~35% of the pool respectively (Hillman et al., 1986). Bile salts are secreted into the small intestine and eventually 90-99% are reabsorbed, returning to the liver via the portal vein. (Strange, 1984, Johnson, 1994) The systemic circulating concentration of bile acids in the serum is 4.8µM (Lindblad et al., 1977), where they are purported to exert control over systemic metabolic rate (Watanabe et al., 2006).

Bile salts are produced and secreted from hepatocytes into the biliary ductal system which drains to the gall bladder, this drains into the cystic duct,

followed by the common bile duct before entering the duodenum at the ampulla of Vater. The common bile duct and pancreatic may (although not always) join a short distance from the duodenum. The make-up of bile is a critical factor; an imbalance of constituents in favour of cholesterol over bile acids can lead to precipitation. Migration of these precipitates into the common duct may cause obstruction at the ampulla of Vater (see Figure 1.2). This constitutes the “common duct theory” proposed by Eugene Opie in 1901 (Opie, 1901). The theory proposes that an obstruction of the common duct at the ampulla of Vater increases pressure and allows reflux of bile into the pancreas. In support of this theory, studies by Kohut et al. examined the bile from patients with acute pancreatitis throughout the disease course. The density of microcrystalline precipitates was greatest on the first day following disease onset and a progressive decrease in density with time (Kohut et al., 2002). The common duct theory is not without controversy in the field. A recent editorial by Lerch and Aghdassi examined the current theories and evidence supporting them (Lerch and Aghdassi, 2010). Evidence suggests that in many patients the common duct is either insufficient in length or completely absent (Sterling, 1954). In addition experiments in the opossum demonstrated that obstruction of the pancreatic duct alone was sufficient to cause pancreatitis (Lerch et al., 1992). The species differences between human, opossum and mouse are great, and opossum experiments also demonstrated increased severity of pancreatitis from ligation of the bile duct, possibly suggesting a role for increased circulating bile acids (Senninger et al., 1986) which would be free to act via the G-protein coupled bile acid receptor (Perides et al., 2010).

1.4.2 Abnormal Ca^{2+} signalling

Disruption of normal Ca^{2+}-signalling was postulated as a trigger for pancreatitis over a decade ago (Ward et al., 1995). Hyperstimulation of acinar cells with CCK-8 caused large sustained cytosolic Ca^{2+} elevations, premature intracellular digestive enzyme activation and necrosis (Raraty et al., 2000). Subsequently, it transpired that other precipitants of acute pancreatitis, including bile salts (Voronina et al., 2002a, Kim et al., 2002) and non-oxidative metabolites of ethanol (Criddle et al., 2006b, Criddle et al., 2004), also generate toxic elevations of Ca^{2+}.

Ca^{2+} release from internal stores in response to these precipitants was found to be dependent on IP_3R opening (Voronina et al., 2002a, Criddle et al., 2006b, Gerasimenko et al., 2009). However, sustained Ca^{2+} entry triggered by ER store depletion was required to raise cytosolic Ca^{2+} to detrimental levels; abrogation of the cytosolic Ca^{2+} rise with intracellular Ca^{2+} chelators prevented deleterious changes such as trypsinogen activation, vacuolisation and necrosis (Raraty et al., 2000, Kim et al., 2002, Criddle et al., 2006c). In ductal epithelial cells, higher doses of bile acids caused inhibition of the coordinated Ca^{2+}-dependent secretion seen with lower doses (Venglovecz et al., 2008). The inhibition of bicarbonate and therefore fluid secretion could serve to promote pancreatic damage by preventing washout of both inactive and activated enzymes, and crucially shares the feature of mitochondrial inhibition (Maleth et al., 2010). The mechanism of cellular necrosis was investigated in further detail with respect to non-oxidative ethanol metabolites, which produced a Ca^{2+}-dependant inhibition of mitochondrial

function, resulting in loss of membrane potential, NAD(P)H and ATP production (Criddle et al., 2006c). Recent experiments using mitochondria-targeted luciferase in pancreatic acinar cells have demonstrated that bile acids and non-oxidative ethanol metabolites cause profound decreases of mitochondrial ATP levels, in addition to cytosolic reductions (Voronina et al., 2010, Criddle et al., 2006c). The effect of Ca^{2+} overload of the acinar cell would thus appear to be a dramatic cessation of mitochondrial energy production which leads to a change in IP_3R function (Betzenhauser et al., 2008) and inhibition of ATP-requiring Ca^{2+} pumps, namely the PMCA and SERCA, thereby impeding clearance of elevated cytosolic Ca^{2+} from the cell (Petersen et al., 2006). Supply of intracellular ATP via a patch pipette abrogated the development of sustained Ca^{2+} elevations and necrosis in response to non-oxidative ethanol metabolites (Criddle et al., 2006c) highlighting the fundamental importance of the maintenance of mitochondrial function for Ca^{2+} homeostasis and cell integrity under conditions of pancreatic insult (Mukherjee et al., 2008).

1.4.3 Bile acids and Ca^{2+} signalling

Physiological Ca^{2+}-signals are restricted to the apical pole because of a “buffer barrier” composed of peri-granular mitochondria that temporarily take up Ca^{2+} released from the ER, thereby up-regulating ATP production, and preventing global waves from permeating to the basolateral area (Tinel et al., 1999, Voronina et al., 2002b). However, when stimulation reaches sufficient intensity, or when mitochondria are inhibited e.g. by carbonyl cyanide m-chlorophenylhydrazone (CCCP) in the presence of the Ca^{2+}-releasing

messenger IP_3, this barrier may be overcome and local repetitive Ca^{2+} responses in the granular area are transformed into global Ca^{2+}-waves that propagate from the apical to basal pole. Multiple 2^{nd} messengers may combine to generate calcium-induced calcium release (CICR) under physiological conditions, via opening of both IP_3R and ryanodine receptors (RyR), which may enable stimulation of ATP production in mitochondria distant from the apical pole and regulation of multiple signalling cascades (Williams, 2001).

In order that the acinar cell remains viable, it is paramount that homeostatic mechanisms are recruited to prevent sustained global elevations of Ca^{2+} and to preserve mitochondrial function. Thus, Ca^{2+} must be cleared from the cytosol in order to restore the resting state. To this end, Ca^{2+} is returned to the ER stores by the sarco-endoplasmic Ca^{2+} ATPase (SERCA) pump or extruded from the cell by the plasma membrane ATPase (PMCA), both processes consume ATP and are therefore dependant on viable mitochondria. These two pumps also function to clear Ca^{2+} that is continuously leaked from the ER and resting Ca^{2+}-concentration is dictated by a balance between extrusion/reuptake mechanisms and Ca^{2+} entry. Ca^{2+} must periodically be allowed into the cell to refill intracellular stores via store-operated Ca^{2+} entry (SOCE) which has recently been shown to occur by the interaction of the ER sensor protein Stim1 and the plasma membrane channel Orai1 which form a complex at ribosome-free ER PM junctions in acinar cells (Lur et al., 2009). Control of fluid secretion from the pancreas, principally mediated via bicarbonate secretion from the ductal epithelial cells, is also mediated via Ca^{2+}-signalling. Bile acids principally un-conjugated

variants such as chenodeoxycholate trigger bicarbonate and fluid secretion at low doses (Venglovecz et al., 2008). Secretion was abolished by chelation of intracellular Ca^{2+}, demonstrating a coordinated response. However, higher doses of bile acids may reach the ductal system and cause significant dysregulation of acid base balance via inhibition of basolateral Na^+/H^+ and Na^+/HCO_3^- exchangers and luminal Cl^-/HCO_3^- co-transporters which [produces significant falls in ion and consequent fluid secretion. The effects of bile acids on these transported is insensitive to the effects of intracellular Ca^{2+} chelation, perhaps due to the non ATP-dependent nature of these transporters (Venglovecz et al., 2008). Direct damage to the ductal system, and inhibition of its function prevents the ducal tissue acting as an effective barrier against toxic bile acids and enzymes (Maleth et al., 2010).

1.5 Reactive oxygen species

Reactive oxygen species (ROS) are chemically active oxygen containing molecules. They can be organic and inorganic in nature. The term ROS often refers to species generated by the incomplete reduction of molecular oxygen, such as the radicals superoxide ($O_2^{-}\cdot$) and the hydroxyl radical ($OH\cdot$) and the non-radical hydrogen peroxide (H_2O_2), and their downstream products, such as reactive nitrogen species (RNS). ROS are thought to mediate the toxic effects of oxygen because of the more favourable nature of their reaction with susceptible molecules. ROS may also act as signalling molecules, a phenomenon widely documented in the literature, but which still attracts controversy. The controversy may originate from the apparent disparity in specificity between non-covalently bound ligand-receptor macromolecular complexes and the covalent relationship between ROS and

their targets (Nathan, 2003). However, ROS do achieve specificity (reviewed in (D'Autreaux and Toledano, 2007)) and the sequestration, compartmentalization, deactivation and changing rates of production are both analogous to and influenced by Ca^{2+}.

1.5.1 ROS generation

Before discussion of the potential involvement of ROS in cellular toxicity, it is pertinent to highlight where and how ROS occur. ROS are generated under physiological conditions as a necessary part of the ATP-producing machinery of the cell. Growing evidence suggests that the balance between ROS producing and ROS scavenging systems underpins the proper functioning of the cell.

Mitochondria account for 90% of the total oxygen consumption and are the principal source of ROS under physiological conditions (Herst et al., 2004). It has been estimated that approximately 1-2% of all O_2 consumed is linked to production of radicals. In order to generate ATP mitochondria oxidize NADH and $FADH_2$, produced by the TCA cycle or via β-oxidation of fatty acids, in a series of reactions catalysed by enzyme complexes I-IV located on the inner mitochondrial membrane that form the electron transport chain (ETC). These complexes generate ROS as a by-product (Chen et al., 2003, Nicholls and Budd, 2000, Turrens, 2003). It is thought that 10 or more components of mitochondria produce ROS (Adam-Vizi and Chinopoulos, 2006), however, the main sources of superoxide (O_2^{-}•) are complexes I and III (Figure 1.3).

During the course of AP there is significant recruitment of immune cells to the organ. ROS induce both activation and proliferation of immune cells (Sundaresan et al., 1995, Irani et al., 1997, Suh et al., 1999). Moreover, the recruited cells generate copious ROS production via the NOX family of NAD(P)H oxidases (Bedard and Krause, 2007). Upon activation, NAD(P)H oxidase assembles in the plasma membrane and reduces molecular oxygen to superoxide. Phagocytes have been shown to employ NAD(P)H oxidase 2 to destroy pathogens within the phagosomal space (Nauseef, 2007). Within neutrophils, hydrogen peroxide, formed from superoxide, is further converted to hypochlorous acid by myeloperoxidase (Winterbourn et al., 2006), a common marker of pancreatitis severity (Bhatia et al., 2005). The activity of NAD(P)H oxidase and myeloperoxidase is vital for immune cells to mount effective host defence, but should these oxidants be directed against host tissue, inflammatory diseases such as pancreatitis may result (Pullar et al., 2000). ROS production is enhanced in neutrophils obtained from patients with AP (Tsuji et al., 1994) and ROS derived from neutrophil NADPH oxidase may be key to implementing damage in experimental AP (Gukovskaya et al., 2002b). However, it is unlikely that NADPH oxidase is important for ROS production in pancreatic acinar cells since ROS generation induced by menadione was unaffected by the enzyme inhibitor diphenyliodonium chloride (DPI) (Criddle et al., 2006a). Furthermore, its presence could not be confirmed by immunohistochemistry and may even be absent in pancreatic acinar cells (Gukovskaya et al., 2002b).

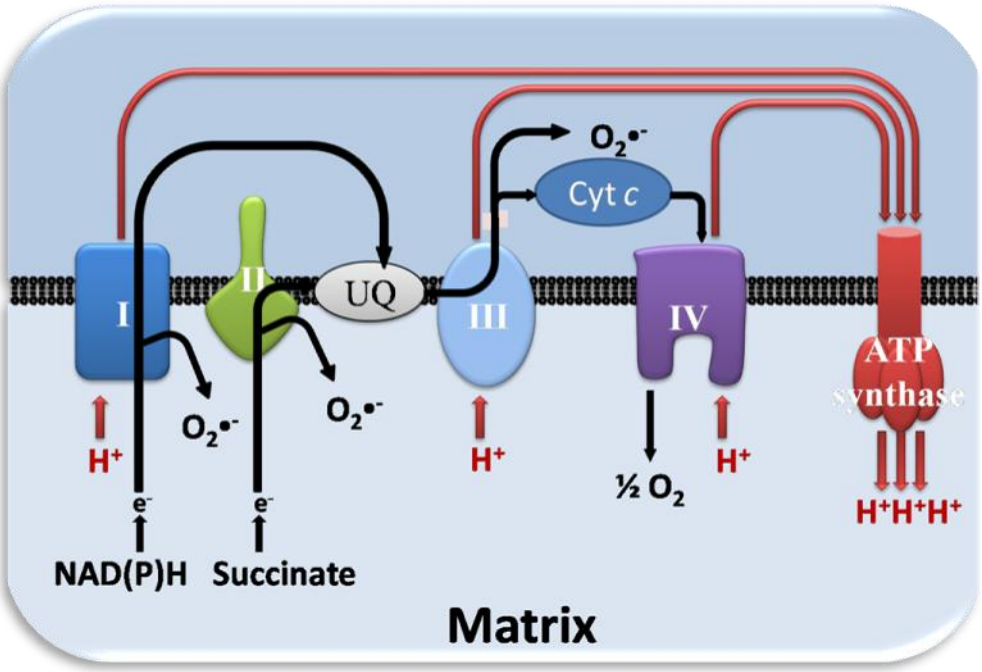

Figure 1.3 The production of reactive oxygen species by mitochondria. A schematic representation of mitochondrial oxidative phosphorylation. Electrons (*black*) donated by NAD(P)H and other substrates such as succinate are used to reduce molecular oxygen at complex IV. The electron flux drives proton transport (*red*) from the matrix (*light blue*) to the intermembrane space (*blue*). Some of the electron flux may become diverted at complexes I,II and III producing superoxide ($O_2^{\bullet -}$). Ejected protons flow back to the matrix driving ATP synthesis via ATP synthase.

1.5.2 ROS defence mechanisms

In order to regulate the concentration and localisation of ROS, numerous antioxidant strategies have been developed by the cell. The principal ROS generated within mitochondria is the superoxide anion ($O_2•^-$), which at neutral pH is a moderately stable radical generally confined within mitochondria, provided the organelle membrane is intact. Toxicity is reliant upon onward generation of further reactive species which may react directly with bio-molecules such as proteins lipids and DNA (Palmieri et al., 2007, Letko et al., 1991, Kadlubar et al., 1998). In general, the deleterious effects of ROS formed within the mitochondria are prevented by numerous antioxidant systems. $O_2•^-$ is converted to H_2O_2 by a family of metaloenzymes; the superoxide dismutases (Fridovich, 1995). While $O_2•^-$ dismutates to H_2O_2 spontaneously, the rate is slow and $O_2•^-$ may either reduce transition metals (particularly Fe^{2+}) which in turn react with H_2O_2 to produce fiercely reactive OH• or peroxynitrite. Therefore it is important that the cell maintains $O_2•^-$ at the lowest concentration possible. The majority of $O_2•^-$ is produced and released into the matrix that contains a specific form of SOD with manganese at its active site (MnSOD) which eliminates $O_2•^-$ formed by the components of the ETC (Fridovich, 1995). Expression of MnSOD can be upregulated by activation of pro-survival NF-kB, thus limiting further ROS production.

The oxidation of GSH to glutathione disulphide (GSSG) is an important step in the control of potentially harmful radicals (Winterbourn, 2008). GSH is synthesised from the precursor N-acetyl-L-cysteine (NAC) and consists of 3 amino-acid residues, glutamate, cysteine and glycine, in which the central thiol group accounts for the reducing activity of the molecule. The pancreas

contains high levels of GSH, approximately 2µmol/g tissue, which represents the fourth highest among the visceral organs (Neuschwander-Tetri et al., 1997, Githens, 1991). Furthermore, the rate of metabolic GSH turnover is high in the pancreas, with only the liver and kidneys possessing higher activities (Githens, 1991), the pancreas therefore appears well adapted to deal with ROS. The actions of glutathione are dependent upon the turnover between reduced (GSH) and oxidised (GSSG) forms; GSSG is created and can be shuttled back to GSH via GSH reductase. Crucially this requires the donation of an electron from NAD(P)H primarily generated within the TCA cycle. However, although glutathione is present in millimolar (mM) concentrations the rate constant for reaction with H_2O_2 is negligible and therefore intracellular diffusion of H_2O_2 *per se* would not be markedly affected by GSH (Winterbourn and Metodiewa, 1999). It is the presence of the selenium-containing enzyme GSH peroxidise (GPx), which catalyses the reduction of peroxides to water (or related alcohols) and the concomitant oxidation of GSH, that makes this a favourable reaction.

There are various enzyme systems that perform important antioxidant defence roles. For example, NAD(P)H quinone oxidoreductase 1 (NQO1/DT diaphorase) is an FAD-containing (flavoprotein) obligate 2-electron reductase that functions as an endogenous cellular detoxifying mechanism (Dinkova-Kostova and Talalay, 2000, Robertson et al., 1992). It is ubiquitously expressed in all tissues and its expression is upregulated in both AP and pancreatic adenocarcinoma (Lind et al., 1990, Lyn-Cook et al., 2006, Hammons et al., 1995). NQO1 also uses NAD(P)H derived from the TCA cycle as a reducing cofactor in multiple reactions such as the production of

relatively stable hydroquinones from endogenously generated quinone species e.g. the tocopherol quinone and coenzyme Q_{10} (Siegel et al., 1997, Beyer et al., 1996). The near universal expression pattern of NQO1 implies a generalized function, including direct scavenging of superoxide (Siegel et al., 2004) and stabilization of p53 (Asher et al., 2002) which controls the transcription of multiple genes involved in oxidative stress. In addition, it may also directly scavenge superoxide (Siegel et al., 2004). Recent work from our lab has highlighted the role of NQO1 in the pancreatic acinar cell as an important detoxifying mechanism. Inhibition of this enzyme with the inhibitor 2,4-dimethoxy-2-methylnaphthalene (DMN) dramatically increased the generation of reactive oxygen species (Criddle et al., 2006a), because 1-electron reduction directly to the relatively stable hydroquinone was prevented, leaving 2-electron reductive pathways to generate unstable semiquinone intermediates within redox cycles (Figure 1.4). The increased levels of NQO1 in pancreatic disease strongly suggest a function to limit oxidative stress under pathophysiological stimulation.

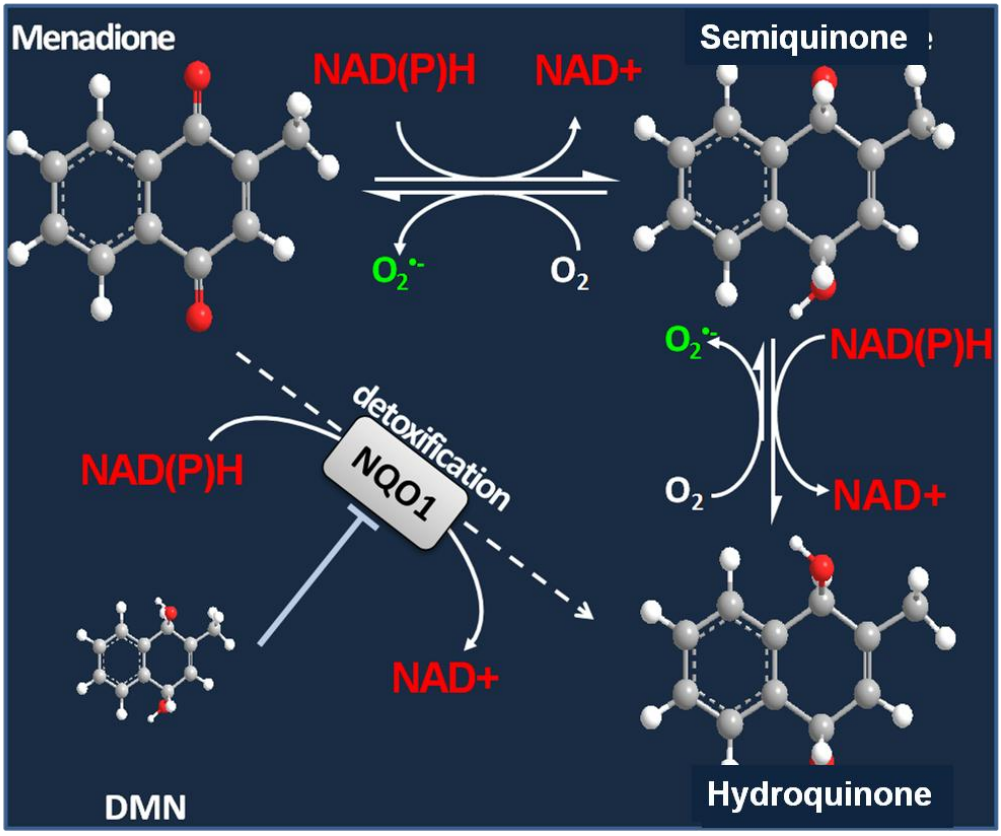

Figure 1.4. **Schematic representation for the proposed mechanism of action of DMN**. One-electron ($1e/H^+$) reduction of menadione generates the unstable semiquinone radical prone to further reduction to the stable hydroquinone. Backoxidation generates ROS ($O_2^{\bullet-}$) when in the presence of molecular oxygen. Menadione may also be metabolized by a one-step two-electron ($2e/2H^+$) reductive process, ***e.g.*** NQO1, directly to the hydroquinone with no ROS production. All reductive processes utilize NAD(P)H as cofactor. Inhibition of NQO1 by DMN blocks two-electron reduction of menadione and promotes one-electron reductive processes leading to enhanced ROS generation.

1.5.3 Influence of ROS on Ca^{2+} signalling

Given the importance of restricting cytosolic Ca^{2+} levels within physiological limits and defined micro domains, the cell must finely coordinate Ca^{2+} entry, release and exit mechanisms to ensure that pathological changes do not ensue. Although thorough research is still lacking in pancreatic acinar cells, studies in diverse cell types suggest that many of these homeostatic processes are sensitive to, and are modulated by, ROS. For example, both IP_3R and RyR contain reactive cysteine residues that may be modified by ROS, changing their activity (Eu et al., 2000, Sun et al., 2001, Meissner, 2002) thereby modulating intracellular Ca^{2+} release events which have already been shown to be responsible for deleterious trypsinogen activation (Husain et al., 2005). Furthermore, thiol oxidation prevents negative regulation of the IP_3R by calmodulin by inhibiting its binding to the receptor (Hamilton and Reid, 2000, Zissimopoulos and Lai, 2006, Foskett et al., 2007). Although not specifically investigated in the acinar cell, the general effect of oxidation of the RyR is to increase channel activity, a process which enhances subunit assembly and inhibits calmodulin binding, a negative regulator of the receptor (Hamilton and Reid, 2000). The situation with respect to the IP_3R is more complex. ROS sensitize the IP_3R to activation by IP_3, but inhibit channel function (Joseph et al., 1995, Joseph et al., 2006). Thiol oxidizing agents may sensitize the channel in a manner sufficient to produce cytosolic oscillations in the absence of stimulation (Missiaen et al., 1991, Bootman et al., 1992) and may preserve the IP_3R-linked Ca^{2+} oscillations necessary for exocrine secretory function (Camello-Almaraz et

al., 2006). In a wider context, exogenously applied ROS enhanced the release of Ca^{2+} in vascular smooth muscle cells. However, when non-hydrolysable analogues of IP_3 were used, no difference was detected, suggesting a role for ROS in the breakdown of IP_3 (Suzuki and Ford, 1992)

Recent progress has been made with respect to elucidation of the vital Ca^{2+} entry mechanism in pancreatic acinar cells, which is now thought to involve formation of a STIM1-Orai complex (Lur et al., 2009). Under conditions of store depletion STIM1 senses Ca^{2+} changes within the ER and translocates to the plasma membrane forming a functional complex with Orai1 (Mercer et al., 2006). Interestingly, the Ca^{2+} release (IP_3R) and Ca^{2+} entry (STIM1-activated channels) mechanisms appear to be spatially distinct in the acinar cell, with ribosome-free portions of ER forming close associations with the plasma membrane (Lur et al., 2009). Recently, differential redox regulation of the Orai channels has been reported in T-cells that may function to tune cellular Ca^{2+} signalling (Bogeski et al., 2010). Whether ROS sensitivity plays a role in Orai-mediated Ca^{2+} entry in acinar cells is likely but as yet undetermined.

Ca^{2+} pumping mechanisms that control cytosolic Ca^{2+} are sensitive to the redox environment. For example, H_2O_2 applied to pancreatic acinar cells altered the normal pattern of CCK or ACh-evoked Ca^{2+} signals, resulting in more global, sustained responses as the concentration of H_2O_2 increased (Bruce and Elliott, 2007). More recently, H_2O_2 induced PMCA inhibition has been demonstrated, thereby decreasing Ca^{2+} clearance from the cytosol through the plasma membrane (Baggaley et al., 2008). The SERCA pumps are also subject to oxidative modification, as they possess redox-sensitive

cysteine residues which exhibit varied effects upon oxidation (Sharov et al., 2006). Current data suggest that mild oxidative conditions oxidize Cys674, up regulating activity (Adachi et al., 2004), whereas prolonged exposure to oxidative stress can cause suphonylation of the same residue and oxidation of other residues, eliciting irreversible SERCA inhibition (Adachi et al., 2004, Grover and Samson, 1988, Suzuki et al., 1992). Such divergent effects highlight the complexity of the partially understood relationships between Ca^{2+}-signalling and ROS, suggesting fine-tuning in the levels of localised, subcellular ROS may affect Ca^{2+} homeostasis positively or negatively.

1.5.4 Ca^{2+}, ROS and cell death

The severity and/or duration of stress applied to pancreatic acinar cells are likely to be crucial in the control of cell death modality (Criddle et al., 2007). Apoptosis and necrosis represent distinct ends of a wide cell death spectrum (Melino et al., 2005). Apoptosis is genetically controlled and occurs via caspase-dependent or caspase-independent mechanisms (Orrenius et al., 2007), whilst necrosis is considered the unregulated default mechanism of cell death, although this view has been questioned (Golstein and Kroemer, 2007). Recently, autophagy has become of interest within pancreatology. Autophagy is classically viewed as an intracellular degradation mechanism for both long-lived proteins and whole organelles. It primarily operates under stress conditions to promote survival under starvation conditions or cell death when apoptosis is inhibited (Yu et al., 2004). The degradation within autolysosomes is catalysed by hydrolases, specifically cathepsins such as L and B

(Bohley and Seglen, 1992), and functions to recycle vital nutrients such as amino acids (Mizushima et al., 2008). Although currently the role and significance of autophagy in disease states is incompletely understood, recent pioneering work has shed light upon this process in pancreatitis (Hashimoto et al., 2008). The study showed that mice deficient in Atg5, a protein central to autophagy, exhibited reduced trypsinogen activation and almost no acute pancreatitis. Subsequent work has reported that impaired autophagic flux mediates vacuolization and trypsinogen activation in rodent models of acute pancreatitis, possibly due to an imbalance between cathepsins L & B (Mareninova et al., 2009).

The principal mechanism of pancreatic acinar cell death is necrosis (Kloppel and Maillet, 1993), which determines the severity and outcome of the disease, characterised by markers such as mitochondrial swelling, vacuolization, loss of plasma membrane integrity and crucially, leakage of the intracellular contents. However, apoptosis, unlike necrosis, involves a regulated cascade of signalling events which result in the “clean” removal of the dead cell from the tissue, as opposed to the “dirty” process of necrosis, which is characterised by loss of membrane integrity and leakage of intracellular components, eliciting inflammation (Melino et al., 2005). The major forms of cell death, apoptosis and necrosis, co-exist to differing extents in established models of pancreatitis induced by caerulein, bile acids (taurolithocholic acid sulphate, TLC-S), choline deficient, ethionine supplemented (CDE) diet and pancreatic ductal obstruction (Esrefoglu et al., 2006, Kaiser et al., 1995, Perides et al., 2010). Studies have indicated that

induction of apoptosis reduces severity of caerulein-induced pancreatitis (Bhatia et al., 1998), while inhibition of caspase activity (and therefore apoptosis) leads to severe necrotising pancreatitis (Mareninova et al., 2006). The control of apoptosis in the pancreatic acinar cell remains to be fully elucidated; however, considerable progress into the subject was made by elucidating the link between intracellular ROS generation and apoptosis (Criddle et al., 2006a). This work demonstrated that redox cycling by the oxidant menadione produced large increase in intracellular ROS, in a manner completely abolished by the antioxidant NAC. ROS was promoted by inhibition of NQO1 by DMN and apoptosis was preferentially increased in cells where ROS generation was highest. This led to proposal that ROS production in the pancreatic acinar cell led to apoptosis and not to necrosis. Thus the balance of cell death between apoptosis and necrosis may be critical for the outcome of the disease, and ROS may be central to the control of this, a hypothesis that requires thorough testing.

1.5.5 Clinical experience with antioxidants and ROS

Antioxidants contribute to the removal of free radicals and are grouped into agents that are either free radical scavenging enzymes (e.g. SOD), enzyme cofactors (e.g. selenium), enzyme substrates (e.g. Vitamins A,C & E) or non-enzymatic antioxidants (e.g. Ebselen, CV-3611). The rationale for the use of such therapy for the treatment of AP is essentially two-fold. Firstly, an increase in oxidative stress is implicated in the pathogenesis of many systemic phenomena such as systemic inflammatory response syndrome (SIRS) and sequelae, such as acute respiratory distress syndrome (ARDS)

and multiple organ dysfunction syndrome (MODS), all of which are major features of AP. Greater oxidative stress has been observed in patients with severe and mild AP compared to healthy volunteers. (Tsai et al., 1998) In remote organ injury, oxidative damage to plasma constituents such as proteins and lipids is a mortality predictor in patients with established ARDS (Quinlan et al., 1996, Quinlan et al., 1994a, Quinlan et al., 1994b, Quinlan et al., 1997). Secondly, a decrease in anti-oxidant levels has been demonstrated in a variety of AP animal models, including those induced by caerulein, CDE diet and Na-taurocholate (Schoenberg et al., 1994, Dabrowski et al., 1988, Nonaka et al., 1989c, Nonaka et al., 1989b)

Unfortunately, the theoretical promise of antioxidant therapy has not been borne out by animal experimental pancreatitis studies and human trials, which have produced conflicting findings. There may be a number of reasons for these different results and indeed the conflicting findings with other anti-oxidants, including differences between combinations of agents, doses or physiological differences between species and types of model. Importantly though, antioxidant treatments have frequently been given simultaneously, or prior to, AP induction in animal models which is incompatible with the human clinical situation. The main focus of animal studies has tended towards proving the involvement of oxidative stress and not the standardised testing of the efficacy of specific antioxidant therapies.

Human trials have generally concentrated on scavenging free radicals via the glutathione pathway, selenium, a non-metal cofactor required for glutathione peroxidase function, and N-acetyl- L-cysteine (NAC), have been used extensively. Other studies have used vitamins A, C (ascorbate) and E, to

augment the antioxidant defence. Unlike animal studies, enzymes have not been directly administered and also studies frequently use combinations of antioxidants, making it difficult to isolate the effects of individual compounds. A combination of antioxidants, featuring NAC and selenium, was assessed using an observational study on patients (Virlos et al., 2003) showing that the antioxidants were safe, with no reported side effects, and restored antioxidant levels towards normal, though only vitamin C and selenium were significantly improved. However, the authors could not demonstrate a significant impact on mortality in severe AP. A further prospective study assessed efficacy of high dose vitamin C treatment in patients with AP (Du et al., 2003). The high dose group demonstrated greater levels of plasma antioxidants, and reduced levels of lipid peroxidation and recovery from clinical symptoms was significantly quicker. This study demonstrated promising results, however, the fate of the patients with severe AP was not documented adequately and this must be a crucial endpoint for any potential treatment. A further major criticism of these trials and others is a lack of randomisation and blinding, impeding accurate conclusions about the potential benefits of anti-oxidant therapy.

A recent single-centre study in the UK addressed the criticism of lack of randomisation in prior investigations, being the first reported randomised controlled trial of anti-oxidant therapy in AP (Siriwardena et al., 2007). This was a relatively small trial (43 patients) which evaluated the effects of administration of a combination of NAC, selenium and vitamin C to AP patients over 3 years. The authors found that relative serum levels of antioxidants rose while markers of oxidative stress fell in the active treatment

group during the course of the trial. However, at 7 days, there was no statistically significant difference in the primary end point, organ dysfunction, between test and control groups (antioxidant vs. placebo: 32% vs. 17%, p = 0.33) or for any secondary end-point of organ dysfunction or patient outcome. Furthermore, this study highlighted a trend towards a more deleterious outcome in patients given antioxidant therapy and the potential to manipulate ROS in the treatment of AP remains far from clear at present.

1.6 Ethanol and pancreatitis

Alcohol abuse is the main cause of pancreatitis (Petersen and Sutton, 2006). Its incidence is directly related to the level of alcohol consumption. However, it is only a small minority of heavy drinkers who suffer from the disease (Apte et al., 2008). With regards to the pancreatic acinar cell, even extremely high concentrations of ethanol (up to 850mM), only produce small changes in cytosolic calcium and have no major effect on oscillations generated by agonists such as acetylcholine (ACh). Cells do not lose the ability to control their calcium homeostasis (Criddle et al., 2004). The findings highlighted that ethanol alone does not consistently cause deleterious effects in the pancreatic acinar cells. Experimentally, ethanol alone is unable to produce pancreatitis (Apte et al., 2006, Petersen and Sutton, 2006), neither high ethanol diets or even continuous intragastric infusion of ethanol is able to induce pancreatitis(Deng et al., 2005). Alcohol is principally linked with the pathology of the liver, where the oxidative metabolite of ethanol, acetaldehyde, is implicated in the development of alcoholic liver disease

(Hoek et al., 2002). When acetaldehyde was applied to pancreatic acinar cells, the effects of calcium homeostasis were minimal (Criddle et al., 2004). The apparent paradox of alcohol and pancreatic pathophysiology, may relate to convincing evidence that the mediators of damage to the pancreas are non-oxidative ethanol metabolites formed from the esterification of ethanol and free fatty acids.

1.6.1 Ethanol metabolism

Ethanol may be absorbed in an unmodified way along the entire length of the alimentary canal. Absorption takes place rapidly from the stomach (20%) and most rapidly from the small intestine (80%). Absorption from the gut into the bloodstream quickly equilibrates ethanol concentrations throughout total body water. Ethanol is subsequently metabolised at a steady rate (reviewed in (Pawan, 1972)). Ethanol metabolism in man and other mammals is principally achieved via the oxidative pathway. Oxidative ethanol metabolism may occur in one of three ways: Alcohol dehydrogenase, Cytochrome P4502E1 (CYP2E1) and catalase, which are apportioned into the cytosol, microsomes and peroxisomes respectively. Alcohol dehydrogenase (ADH) is an intensely studied enzyme and there is considerable literature concerning its structure and function (reviewed in (Hawkins and Kalant, 1972)). The reaction catalysed by ADH can be represented by the following equation:

$$CH_3CH_2OH + NAD^+ \leftrightarrows NADH + H^+ + CH_3CHO$$

Following absorption, it is this reaction which is considered the rate limiting step in the full and complete degradation of ethanol. Human ADH displays

maximum activity at 170mM but is remarkably non-specific and will readily oxidize poisonous methanol and ethylene glycol, to even more deleterious intermediates, and often treated with the ADH inhibitors such as pyrazole derivatives or even ethanol (reviewed in (Hawkins and Kalant, 1972)).

Catalase was one of the first proteins to be crystallized, this was achieved by Sumner and Dounce in 1937, since then structures have been solved representing a variety of states of binding and oxidation.

The action of catalase on ethanol can be represented by the following equation:

$$CH_3CH_2OH + H_2O_2 \rightarrow CH_3CHO + 2H_2O$$

Like ADH, catalase is not specific for ethanol and methanol is also well catalyzed. It is interesting to note that the forward progression of this reaction removes the ROS H_2O_2. The role of catalase in the metabolism of ethanol in vivo may, however, be limited. If catalase activity is significantly inhibited (>90%) with 3-amino-1,2,4-triazole, no effect upon hepatic ethanol oxidation is noted whether in vitro or in vivo (Smith, 1961). This is perhaps because of the limited availability of H_2O_2 to act as a co-factor in the peroxidation of ethanol (Goodman and Tephly, 1968). As such, in physiological conditions, catalase may play only a very small part in ethanol metabolism. However, in pathological conditions there is considerable scope for dramatic increases in H_2O_2 production.

Due consideration should be given to the 3rd component of the oxidative ethanol degradation pathway, that catalyzed in the NADPH-dependent microsomal acetaldehyde-oxidising system (MAOS). The MAOS is an

inducible system. Isolated rat hepatic microsomes display up to 24-fold increase in ethanol oxidising ability following ethanol administration to rats (Kunitoh et al., 1997). While the MAOS contains numerous cytochrome p450, inactivation of CYP2E1 by antibody reduced total activity by 90%.(Kunitoh et al., 1997). Importantly, CYP2E1 is both present and active within the pancreas, and furthermore is induced by chronic administration of ethanol (Norton et al., 1998).

The ability of cells of the pancreas to process ethanol via the oxidative pathway has been assessed by Haber *et al.* (Haber et al., 1998), with direct comparison to cultured hepatocytes. 14C-labelled ethanol was used to evaluate the production of 14C-labelled acetate, a downstream metabolite. The rate of pancreatic oxidative metabolism of ethanol was judged to be comparable to that of the hepatocytes exposed to the same conditions. This work was corroborated in isolated rat acini, where interestingly 4-methylpyrazole, a classical inhibitor of the isoforms ADHI and ADHII, was found to have no effect (Gukovskaya et al., 2002a).

The contribution of the MAOS in pancreas has not been fully explored, although it was initially found not to provide a significant contribution to overall ethanol metabolism (Haber et al., 1998). However, studies detailing the contribution of CYP2E1 following induction of the enzyme are conspicuous by their absence, although it should be noted that in hepatocyte models, over expression of CYP2E1 was not able to rescue cells from ADH-deficiency, suggesting ADH as the dominant factor in ethanol metabolism (Bhopale et al., 2006, Wu et al., 2006).

1.6.2 Non-oxidative ethanol metabolism

The alternative pathway of ethanol metabolism is the non-oxidative pathway. Non-oxidative ethanol metabolism involves the formation of fatty acid ethyl esters (FAEE). FAEE are the products of esterified ethanol and fatty acids (Laposata, 1999) which were observed in vitro (Newsome and Rattray, 1965) and in vivo (Goodman and Deykin, 1963) as early as 1965 and 1963 respectively. However twenty years were needed for the significance of FAEE to become apparent. In 1983, Lange and Sobel observed that although alcohol was known to affect the heart, there was only very low level production of acetaldehyde, a metabolite demonstrated to be involved in pathogenesis of the liver for example. Their work led to the discovery of FAEE in isolated perfused rabbit hearts following administration of physiologically relevant concentrations of fatty acids and ethanol (Lange and Sobel, 1983). The same study subsequently found that FAEE were present at up to 115µM in the hearts of cadavers that had died while acutely intoxicated. Furthermore, the study highlighted the role of mitochondrial dysfunction in alcohol mediated heart damage, and proposed a model whereby FAEE could act to shuttle fatty acids to the mitochondria. Therefore resulting in a build-up of free fatty acids within the mitochondria and uncoupling oxidative phosphorylation (Lange and Sobel, 1983).

A landmark study by Laposata and Lange in 1986 demonstrated that it was the organs most frequently damaged by alcohol, the brain, liver, pancreas and heart, which possessed the highest concentrations of FAEE following alcohol intake that led to the death of the individuals (Laposata and Lange,

1986). Furthermore the study demonstrated that it was these same organs that possessed the greatest ability for *de novo* synthesis of these metabolites. Considerable time passed until the toxicity of FAEE was assessed. Exposure of HepG2 cells to LDL packaged, physiologically relevant concentrations of FAEE showed markers of toxicity, such as decreased proliferation and protein synthesis (Szczepiorkowski et al., 1995). Toxicity was also demonstrated in whole animal in vivo studies (Werner et al., 1997) where pancreatic, injury was specifically highlighted by increases in trypsinogen activation peptide.

The source of FAEE is still unclear, initially at least, it was assumed that FAEE accumulation in the pancreas may occur following production in distant sources and transported (or even synthesised in) the blood itself (Doyle et al., 1994). The liver was a natural candidate for production given its high level of FAEE synthase activity (Werner et al., 2001), however subsequent work demonstrated the presence of FAEE synthase activity in the pancreas (Gukovskaya et al., 2002a, Werner et al., 2001), showing that FAEE accumulation in the pancreas is likely due to synthesis within the gland itself. This is strongly supported by reports of FAEE synthase activity being 3.5-10-fold higher than in similar hepatocyte preparations (Gukovskaya et al., 2002a, Werner et al., 2001).

1.6.3 Oxidative vs. Non-oxidative metabolism

In light of the significant evidence that the pancreatic acinar cell is able to metabolise ethanol via both the oxidative and non-oxidative pathways, it was a natural progression to establish the relative contributions of either pathway to the sum of pancreatic ethanol metabolism. Experiments with radio

labelled ethanol have demonstrated that the oxidative pathway consistently forms a larger part of total metabolism than the non-oxidative pathway (Gukovskaya et al., 2002a). This does not detract from the effect of the non-oxidative metabolites, as levels of synthesis are adequate to produce pancreatic injury (Haber et al., 1993). Crucially the balance between oxidative and non-oxidative ethanol metabolism is linked. Experiments with rat pancreatic homogenates demonstrated that inhibition of oxidative metabolism with the ADH-inhibitor 4-methylpyrazole caused an increase in the generation of non-oxidative metabolites (Werner et al., 2001). This concept was expanded with in vivo work where 4-methylpyrazole was infused with ethanol into rats, leading to an accumulation of pancreatic FAEE (Werner et al., 1997). These data provided a conceptually important link between the two forms of metabolism, whereby non-oxidative metabolism can be greatly increased by inhibition of the oxidative pathways. This leads to the synthesis and accumulation of FAEE, and their subsequent accumulation in mitochondria and inhibition of mitochondrial function (Lange and Sobel, 1983).

1.6.4 Role of non-oxidative metabolites in acinar cell injury

The role of non-oxidative ethanol metabolites in pancreatic injury has become generally accepted in the literature (Pandol et al., 2007). A significant step was experimental data that linked the actions of exogenously applied FAEE to the abnormal Ca^{2+}-activity that is central to acinar cell pathology. Direct application of the FAEE palmitoleic acid ethyl ester (POAEE) to isolated murine pancreatic acinar cells caused large increase in

intracellular calcium ($[Ca^{2+}]_i$) (Criddle et al., 2004). These effects were not limited to POAEE since a variety of other FAEE produced similar results. Crucially the effects were completely dissimilar to the effects of ethanol alone, which was largely without effect (Criddle et al., 2004). Application of palmitoleic acid (POA) non-esterified free fatty acid (FA) was also able to produce concentration-dependent rises in $[Ca^{2+}]_i$ which like the FAEE were acutely dependent upon the presence of extracellular calcium. Further investigation demonstrated that the non-oxidative metabolites were able to cause release of Ca^{2+} from the ER, demonstrated by the absence of further effect by the ER specific SERCA pump inhibitor thapsigargin (Criddle et al., 2006b). The mechanism by which Ca^{2+} release from the ER was shown to be, at least in part ,dependent upon functional IP_3 receptors, as low-level POAEE elicited spiking was inhibited by use of caffeine as an IP_3R antagonist (Criddle et al., 2006b). The effects of POA were completely unaffected by caffeine demonstrating at least two separate mechanisms behind FAEE/FA induced Ca^{2+} elevation. The proposed generation of FA from FAEE involves the cleavage of the ester bond by intracellular esterase activity. Inhibition of this activity with bis-(4-nitrophenyl) phosphate (BNPP) converted POAEE-evoked sustained rises in $[Ca^{2+}]_i$ to short lasting transient events (Criddle et al., 2006b). This clearly highlighted the role of free fatty acid formation in the toxicity of FAEE. The nature of the $[Ca^{2+}]_i$, rise, principally the insensitivity to IP_3R inhibition and slow progressive onset of the sustained $[Ca^{2+}]_i$ increase suggested inhibited Ca^{2+} clearance by the Ca^{2+}-dependent ATPases present on the ER and plasma membrane. Given the ATP-dependent nature of the Ca^{2+}-clearance machinery, depletion of

cellular ATP was a prime candidate for the inhibitory effect on these pumps. Experiments with fluorescent indicators and later genetically encoded mitochondrial luciferase probes demonstrated that inhibition of mitochondrial ATP production was a feature of both POA and POAEE (Criddle et al., 2006b, Voronina et al., 2010). This model was effectively tested by supplementing acinar cells with exogenous ATP introduced into the cell via whole cell patch pipette. In this case POA was completely unable to produce the slow sustained rises in $[Ca^{2+}]_i$ that characterised the response in the absence of ATP (Criddle et al., 2006c). The large sustained $[Ca^{2+}]_i$ rises caused by high levels of POAEE were converted to the transient spikes seen with lower levels in the presence of supplementary ATP. These data give rise to the plausible explanation of a double effect as caused by non-oxidative ethanol metabolites. FAEE are both generated and accumulate in the pancreas, where, within acinar cells they are able to open Ca^{2+} release channels such as the IP_3R. Subsequent hydrolysis yields free fatty acids which induce the mitochondrial dysfunction first postulated by Lange and Sobel (Lange and Sobel, 1983). This induces dysfunction of the mitochondria and renders them unable to produce sufficient ATP (Voronina et al., 2010, Criddle et al., 2006b). Falling intracellular ATP levels do not allow the cell to clear the $[Ca^{2+}]_i$ load induced by IP_3R-mediated Ca^{2+}-release, because the ATPase pumps mounted on the ER and plasma membrane lack sufficient ATP substrate leading to Ca^{2+}-dependent necrosis. Alternative mechanisms for removing Ca^{2+} such as the Na^+/Ca^{2+} antiporter have very little activity in pancreatic acinar cells and may even be absent (Muallem et al., 1988). When ER stores become depleted store operated Ca^{2+}-entry

occurs, further exacerbating the Ca^{2+} overload (Lur et al., 2009). Excessive $[Ca^{2+}]_i$ leads to enzyme activation, and eventually cellular necrosis (Raraty et al., 2000, Criddle et al., 2006b).

The increased understanding of lipids and lipid-derivatives has shed considerable light on the pathogenesis of acute pancreatitis. In common with other protagonists such as caerulein and bile acids, the role of Ca^{2+} is again pivotal. The development of a rational therapy against alcohol induced pancreatitis may prove difficult. Previous work indicates that the Ca^{2+}-handling machinery may be an attractive target. Blockade or partial inhibition of Ca^{2+}-release may prove an option. This is supported by the small but significant protective effect that coffee drinking has on the severity of alcoholic pancreatitis (Morton et al., 2004). Coffee is known to contain many compounds including caffeine, which may be exerting an effect on IP_3R-mediated Ca^{2+}-release. Prevention of initial FAEE-formation is an attractive target as this would prevent abnormal Ca^{2+}-release events and subsequent shuttling of free fatty acids to the mitochondria. To prevent formation of FAEE, the identity of the enzyme forming the molecules is extremely useful information. There are currently several candidates. The association of a gene polymorphism in the locus responsible for carboxyl ester lipase (CEL) with increased risk of alcohol-induced pancreatitis has been demonstrated (Miyasaka et al., 2005). While this is fascinating, there has been no data with regard to the functional significance of the mutation. Perhaps the most interesting is the variously titled FAEE synthase (Cholesterol esterase/triacylglycerol lipase/bile salt activated lipase). This membrane-bound and cytosolic enzyme is released into the circulation of patients with

pancreatitis (Aleryani et al., 1996) and can be found abundantly in mammalian liver and pancreas. The enzyme has been specifically purified from rat pancreata and characterised to be triacylglycerol lipase and Cholesterol esterase (ChE) (Riley et al., 1990, Kaphalia and Ansari, 2003). Crucially the enzyme was found to be structurally and functionally distinct from the enzyme found abundantly in the liver (Kaphalia et al., 1997, Kaphalia and Ansari, 2001). Recent work has highlighted the role of this particular enzyme with studies in rat AR42J cells. Most exciting was the use of 3-benzyl-6-chloro-2-pyrone (3-BCP), a purported FAEE synthase inhibitor. Addition of this compound prevented both FAEE synthesis and caspase-3 dependent apoptosis (Wu et al., 2008). This compound represents an interesting candidate as a possible therapeutic agent. However, as yet it has not been investigated in murine primary pancreatic acinar cells or human acinar cells. Crucially, AR42J cells appear to undergo apoptosis in response to FAEE exposure, as demonstrated by caspase-3 inhibition (Wu et al., 2008), whereas freshly isolated acinar cells tend to undergo necrosis, and different mechanisms of cell death may belie different modes of action.

1.7 Aims and objectives

- To establish the properties of common precipitants of acute pancreatitis as generators of reactive oxygen species
- To explore the mechanism of ROS generation
- Evaluate the effects of ROS generation on the fate of pancreatic acinar cells
- To establish the effects of oxidative and non-oxidative alcohol metabolism on pancreatic acinar cell calcium homeostasis and mitochondrial function

- To assess the effects of alcohol metabolism on pancreatic acinar cell fate.

Chapter 2

Materials and methods

2.1 Pancreatic acinar cell isolation

Male CD-1 or C57B6 mice were stunned and then killed by cervical dislocation, in accordance with the Animal (Scientific Procedures) Act (A(SP)A) 1986. The animal was laid on its right side before a section of the flank was washed in 100% ethanol to wet the fur and prevent contamination. A large incision was made through the skin to reveal the abdominal wall. This was further incised to allow access to the peritoneal cavity. The pancreas is located underneath and delicately attached to the spleen, clearly visible owing to its dark colouration and thin rounded shape. Using dissection scissors and forceps the pancreas was carefully dissociated from the spleen before being removed from the proximity of the duodenum. The excised pancreas was placed in 4-5 ml of NaHEPES buffered salt solution, containing in mM: NaCl 140, KCl 4.7, $MgCl_2$ 1.13, HEPES 10, glucose 10, $CaCl_2$ 1, pH 7.3. This was used to remove any excess blood and other fluids and non-pancreatic cells. The wash is repeated if needed. The pancreas was then transferred, along with minimal excess solution, to a second dish where 1ml of warm collagenase (220 units/ml, Worthington Biochemical Corporation, Lakewood, NJ) solution was injected into the pancreas at multiple points to introduce collagenase solution into the ductal structure. The pancreas was incubated at 36.5 °C for between 13 and 18mins depending upon batch variations in collagenase.

After collagenase incubation the pancreas was placed in a 15 ml polycarbonate tube (Sarstedt, Leicester UK) with 3 ml of NaHEPES solution. The pancreatic tissue was dissociated by triturating with micropipette tips of progressively decreasing diameter. A cloudy supernatant is formed by cells suspending in the solution. The supernatant was removed to an additional identical tube, and replaced with fresh NaHEPES solution. This process was continued until cloudy solution was no longer obtained. The second tube was then centrifuged at 260 G for 1 minute to form a pellet. This pellet was then re-suspended in NaHEPES solution for loading with fluorescent indicators.

2.2 Human pancreatic tissue sample retrieval

During surgery (pancreatic resection), a small piece (~1 cm^3) of pancreas was cut from the transection margin of the remaining pancreas with a new scalpel blade to limit gross macroscopic cell damage. Efforts were made by the surgeon to minimise the time period in which the sample was both ischemic and warm. The sample was immediately washed in cold extracellular solution to remove debris and blood products. The sample was immediately taken to the laboratory in the extracellular solution described above, on ice with care to ensure that the ice was not below 0 °C. The time from sample collection to the start of cell isolation was less than 10 minutes in all cases.

2.3 Human pancreatic acinar cell isolation

Single acinar cells and small acinar cell clusters were isolated by a method adapted and modified from the rodent work outlined above (2.1). Small sections of pancreatic tissue were manually dissected using fine forceps into

sections of approximately 100 mg wet weight. Care was taken to remove all non-acinar tissue, adipose tissue was a common contaminant and if the tissue floated, it was further dissected to remove excess fat. The sample was then injected at several points with collagenase (220 U/ml) (Worthington, Lakewood, NJ). During the injection, fat droplets were often released and became visible on the surface of the collagenase solution; fresh collagenase solution was substituted to prevent onward transfer of fat. Unlike murine pancreas, uniform delivery of collagenase to every portion of the pancreatic sample was impossible, as there usually was no intact pancreatic ductal system following the initial surgical resection of the sample. In an attempt to overcome this, the sample was partially sliced with a fresh surgical blade (size 23) to increase the surface area exposed to the collagenase, repeated washes were performed to remove damaged cellular material. The sample was then incubated in an agitating water bath for 15 – 30 mins at 36ºC. Following digestion, the pancreas was placed into a 15 ml polycarbonate tube (Sarstedt; Leicester UK) containing around 4 – 5 ml standard extracellular solution. Trituration through micropipette tips of progressively diminishing diameter produced the final population of pancreatic acinar cells, which were re-suspended twice in an extracellular solution buffer following a period of 1 minute centrifugation at 260 G in each case. Tubes were exchanged 2-3 times to remove fat adhering to the walls. The final cell pellet was resuspended in 2 ml extracellular solution. All experiments were performed at room temperature and cells used within three hours of isolation, and cells were stored at 4 °C.

2.4 Pancreatic acinar cell culture

Long term (<48 hr) culture of pancreatic acinar cells was achieved by modification of the standard extracellular solution. The standard NaHEPES based extracellular solution was supplemented with MEM amino acids, 292 µg/ml L-glutamine, 100 units/ml penicillin, 100 units/ml streptomycin, (GIBCO/Invitrogen, Paisley, UK), 2 pM cholecystokinin and 1 mg/ml soybean trypsin inhibitor (CCK, Sigma, Gillingham UK). pH was adjusted to either pH7.3 or 7.5 to compensate for acidification when used in 5% CO2 incubator. The solution was sterile filtered (0.2 µm) and stored in sterile conditions. Cells derived from several murine pancreata were dispersed and seeded onto poly-D-lysine coated glass-bottom culture dishes (MatTek; Ashland, MA) and allowed to attach for ~1 hr. Media was changed frequently, ~12 hrs, to prevent build-up of dangerous cell degradation products.

2.5 Confocal microscopy

Confocal imaging was performed on a Zeiss LSM510 confocal microscope (Carl Zeiss; Jena, Germany). Excitation laser lines and emission collection parameters were selected to obtain maximum signal to noise ratio with the indicators used according to the manufacturer's instructions. In all cases cells were visualized with either a C-Apochromat 63X water immersion objective, numerical aperture 1.2, or a Plan-Apochromat 40X oil immersion objective, numerical aperture 0.8. The pinhole was set according to the needs of the experiment; for whole-cell imaging of Fluo4 or DCFDA the maximum light intensity is required. As such, the microscope was set with the pinhole at maximum; 18.21 Airy units representing an optical slice of 141

µM. For imaging of organelles, such as the mitochondria, the pinhole was set at an intermediate level of 2.5 Airy units representing an optical slice of 20 µM. Cells fixed for immunofluorescence were imaged with the pinhole set to 1 Airy unit (8.9 µM) for maximum resolution.

2.6 Use of fluorescent indicators

Cytosolic Ca^{2+} was imaged with the Fluo3-derived calcium indicator Fluo4 (Invitrogen; Paisly, UK). This is loaded in cell permeable aceto-methoxyester (AM) form. This allowed free passage across cell membranes before the AM group is cleaved by non-specific intracellular esterase activity. The affinity of Fluo4 for calcium is 345 nM, which was ideal for the range of Ca^{2+} concentrations encountered in the cytosolic compartment (50 nM-5 µM (Ward et al., 1995)). Fluo4 is prepared by first creating a 20 mM solution in high-grade di-methyl sulphoxide (DMSO; Sigma, Gillingham UK). This is added to the cell preparation by calculating the volume of stock required to create a 3 µM loading concentration. The exact volume is then pipetted into a fresh tube, NaHEPES extracellular solution was then used to dilute this before being added to the cell preparation to reduce osmotic shock associated with DMSO. DMSO concentrations were kept below 0.01% at all times. Fluo4 was loaded in the dark at room temperature (21-23 °C) on a cell shaker at 100 RPM for 30 minutes. Once complete the cells were washed in NaHEPES extracellular solution and re-suspended. Fluo4 was excited with a 488nm laser line and emission collected between 505-530 nm.

Mitochondrial Ca^{2+} was imaged with the calcium-sensitive rhodamine-derived indicator Rhod-2 (Invitrogen; paisley, UK). Like Fluo4, Rhod-2 was loaded in

cell permeable AM form; however intracellular cleavage of the AM group yields a cationic moiety which preferentially partitions to the mitochondrial compartment. Rhod-2 was loaded at 2.5 µM for 30 mins at room temperature in the same manner as Fluo4. Excitation was with a 543 nm laser line and emission collected from 560-650 nm. Rhod-2 exhibited extremely low fluorescence in the resting state, but upon stimulation increases in fluorescence >10 fold, and so care must be taken to avoid saturation of the optical equipment.

Several fluorescent indicators were used throughout this project to measure intracellular reactive oxygen species; $[ROS]_i$, cytosolic calcium; $[Ca^{2+}]_c$, mitochondrial calcium $[Ca^{2+}]_m$, and mitochondrial membrane potential $[\Psi]_m$.

Dynamic changes in $[ROS]_i$ were visualized with the fluorescien-derived 5-(and 6-)carboxy-2',7'-dichlorofluorescein diacetate, CM-DCFDA, this dye becomes fluorescent upon oxidation within the cell interior. This was loaded at 2.5 µM for 30 mins at room temperature in the same manner as Fluo4, with special attention given to prevent unnecessary exposure to light. DCFDA was excited with a 488 nm laser line and emission collected from 505-550 nm. Extreme caution was taken to avoid unnecessary exposure to light throughout the experimental series. Cells were stored at 4 ºC in the dark prior to experiments, in order to slow the normal physiological generation of $[ROS]_i$ and prevent unintentional photo activation of the indicator. Confocal microscopy of DCFDA loaded cells was also adapted to minimise the

exposure of cells to laser light. Detector and amplifier gain were maximized and resolution (x,y and t) and laser intensity minimised.

Mitochondria were specifically stained with tetra methyl rhodamine methyl ester (TMRM). TMRM, at low concentrations, selectively and reversibly accumulates in the mitochondrial matrix acting as a sensor for the changes in the mitochondrial membrane potential ($\Delta\Psi$). TMRM was loaded at 37.5 nM for 30 mins at room temperature before the cells were washed and re-suspended in standard extracellular solution. TMRM was visualised with 543 nm excitation and emission collected at 560-650 nm. If fluorescence at the beginning of the experiment displayed the correct mitochondrial distribution, but insufficient intensity, an additional on-stage loading was performed (50 nM, ~3mins) and their metabolism assessed by NAD(P)H autofluorescence (excitation 363 nm, emission 390-450 nm).

The LSM510 confocal microscope is able to resolve and separate multiple loaded indicators in addition to NAD(P)H autofluorescence. NAD(P)H is a vital intracellular reducing equivalent which displays autofluorescence which was visualized with 351 nm excitation and 390-450 nm emission. As with DCFDA, every caution was exercised to ensure the minimum UV illumination was used to record experimental data.

2.7 Immunofluorescence

Cells were isolated as described above before being seeded onto poly-L-lysine coated cover slips in a 6 well plate and allowed to adhere for 30 mins at room temperature in the dark. Cells were then fixed in either ice-cold 4%

paraformaldehyde or methanol at -20ºC for 15 min. Once fixed cells were washed once in phosphate buffer (PB) and once in phosphate buffered saline (PBS). The washed cells were then permeabilized PBS containing 0.1% Triton X-100 for 5 min. Once permeabilized, non-specific protein-protein interactions were blocked with a PBS solution containing 5% goat serum and 1% acetylated bovine serum albumin (BSA, Ambion; Austin, TX) and non-specific binding blocked with 10% goat serum and 1% bovine serum albumen in phosphate buffered saline for 60 min. The cells were then incubated with blocking solution containing monoclonal primary antibodies against NQO1 (Cell Signalling Technologies, Beverly, MA; 1:100 dilution) and β-actin (Sigma; 1:100). Nuclei were stained with Hoechst 33342 (10 μM) for 20 min. Cells were then washed three times in PBS before incubation in blocking containing the corresponding secondary antibody(s). Alexa 488 (1:1000), 594 (1:500), 647 (1:500) or phalloidin-633 (F-actin), conjugated secondary antibodies (Invitrogen, Paisley, UK) for 20 mins at room temperature. Cells were then washed a further three times in PBS and cover slips were then mounted on slides with ProlongGold (Invitrogen, Paisley, UK) anti-fade medium before being allowed to air-dry overnight at 4 ºC in the dark.

2.8 Determination of cell death in pancreatic acinar cell death

For detection of apoptosis and necrosis two separate methods were used, early apoptosis was detected with a Rhodamine110-linked general caspase substrate (Invitrogen; Paisley, UK) while the nuclear condensation was visualised by the nuclear aggregation of acridine orange (Sigma; Gillingham, UK). In both assays, necrosis was visualised by nuclear staining with

propidium iodide or ethidium bromide respectively (Sigma) and all nuclei visualised with Hoechst 33342 (Invitrogen). For early apoptosis Cells were isolated as described earlier, with the last wash and re-suspension performed with Ca^{2+} omitted from the solution. 500 µl of cell suspension was added to 500 µl pre-prepared blinded solutions containing in: Ca^{2+}-free NaHEPES extracellular solution, EGTA (2 mM), general caspase substrate 20 µM and the test substance/vehicle control. Cells were then incubated for 30 mins in the dark at room temperature (21-23 °C) on a cell shaker at 100RPM for 30 minutes. Once complete the cells were washed in Ca^{2+}-free NaHEPES extracellular solution and re-suspended. Propidium iodide (PI, 1 µM) and the cell permeable nuclear Hoechst 33342 (50 µg/ml) were added and the cells taken immediately to the microscope for assessment. Thirty separate fields of view were recorded for each condition with the lowest (closest to cover slip) feasible field used in every case. A plan-apochromat 40X oil-immersion objective was used to record 512x512 pixel images. Cells were counted off-line at a later time point to save time and prevent operator influence. Hoechst 33342 (excitation 364 nm, emission 405-450 nm) stained the nucleus of all cells. Non membrane permeable Propidium iodide becomes visibly fluorescent (excitation 488 nm, emission 630-693 nm) when bound to DNA, therefore a nucleus stained with both Hoechst 33342 and PI was counted as a necrotic cell. Apoptosis was defined by generalised cytosolic distribution of R110-linked general caspase substrate (excitation 488 nm, emission 505-550) exceeding a pre-selected threshold value. Experiments were repeated, a minimum of three mice per condition were used. Each experiment consisted of a minimum of 15 separate fields per condition. All

visualisation and counting was blinded with the code revealed after data processing was complete.

For determination of late-stage apoptosis an adapted acridine orange ethidium bromide protocol (Galluzzi et al., 2009) was used. Cells were isolated in the manner described above. Following isolation the cells were seeded on poly-L-lysine coated 35 mm glass bottom dishes (MatTek; Ashland, MA) and allowed to attach for 30 mins at room temperature in the dark. The media was exchanged to remove unattached cells and to introduce the long term culture media described previously. Cells were exposed to TLC-S or DMN or NAC or Rapamycin (RAP, to stimulate autophagy (Mareninova et al., 2009)) or 3MA or combinations of these for 3 h before further incubation for 10 h at 35 ºC, in the presence of a humidified 5% CO_2 atmosphere. Cells were then stained with acridine orange (AO, 2 µg/ml; excitation 488 nm, emission 505-530 nm) to detect chromatin condensation and ethidium bromide (EB, 2 µg/ml; excitation 488 nm, emission >650 nm) to detect plasma membrane rupture. Hoechst 33342 (excitation 364 nm, emission 405-450 nm, 5 µg/ml) was used to count total cells. The cells were visualised with a 40x Plan-Apochromat oil-immersion objective, 15 maximal intensity projections from 15 to 20 confocal slices 3 µm thick. Experiments were repeated in triplicate and all visualisation and counting was blinded with the code revealed after data processing was complete.

2.9 Image analysis

Image analysis was carried out using the Zeiss LSM510 image analysis software (Version 4.2), Zen 2009 image analysis software (Carl Zeiss; Jena, Germany), or ImageJ V1.43.

Chapter 3

Results: The role and source of bile salt induced reactive oxygen species in the isolated pancreatic acinar cell

3.1 Calcium-dependent pancreatic acinar cell death induced by bile acids: a protective role for reactive oxygen species

The aim of the work contained within this chapter was to use real-time confocal microscopy of freshly dispersed pancreatic acinar cells to assess the effects of TLC-S on the generation of sustained elevations of cytosolic and mitochondrial Ca^{2+} ($[Ca^{2+}]_C$ and $[Ca^{2+}]_M$ respectively). Furthermore, to assess the level of ROS generation, ($[ROS]_I$ and $[ROS]_M$), generated via prolonged rises in $[Ca^{2+}]_C$ and of the mitochondrial Ca^{2+} concentration ($[Ca^{2+}]_M$). The role of TLC-S and its resultant ROS on the fate of the acinar cell, will also be assessed for potential roles of ROS elevations in the promotion/inhibition of apoptosis or necrosis. The oxidant scavenging enzyme NAD(P)H quinone oxidoreductase (NQO1), has a proven role in the control of both the intracellular redox environment of the acinar cell and the determination of apoptosis and as such its role with respect to TLC-S will be assessed.

3.2 TLC-S induces concentration-dependent elevation of cytosolic calcium

At the lower concentration of 200 μM, TLC-S predominantly induced prolonged, global, oscillatory $[Ca^{2+}]_C$ increases. 80% (n = 16 of 20 cells) showed oscillatory changes of $[Ca^{2+}]_C$, (Figure 1A). In the majority of cases the cytosolic calcium level returned to baseline, consistent with similar observations of the same bile salt (Voronina et al., 2002a). In some cases (31%; 5/16 cells) the oscillatory cells exhibited a sustained component whilst

20 % (4/20) cells exhibited a sustained increase only. No indicated oscillatory component or return to baseline $[Ca^{2+}]_C$ was seen. Furthermore oscillatory rises of $[Ca^{2+}]_C$, induced by 200μM TLC-S produced co-incident, synchronised oscillations in NAD(P)H autofluorescence indicative of stimulus-metabolism coupling previously demonstrated in this cell type (Voronina et al., 2002a, Criddle et al., 2006b) .

In contrast to the predominantly oscillatory responses seen with 200 μM TLC-S, 500 μM TLC-S induced elevations in $[Ca^{2+}]_C$ that were prolonged, global and sustained in all cases (20/20 cells, Figure 1B). In all cases these consisted of a larger initial release component coupled to a sustained elevated plateau of $[Ca^{2+}]_C$ as previously described (Voronina et al., 2002a). NAD(P)H autofluorescence was initially stimulated (Figure 3.1B; 120-200 s) by 500 μM TLC-S but was followed by pronounced, sustained falls of NAD(P)H levels (Figure 1B; 200-800 s).

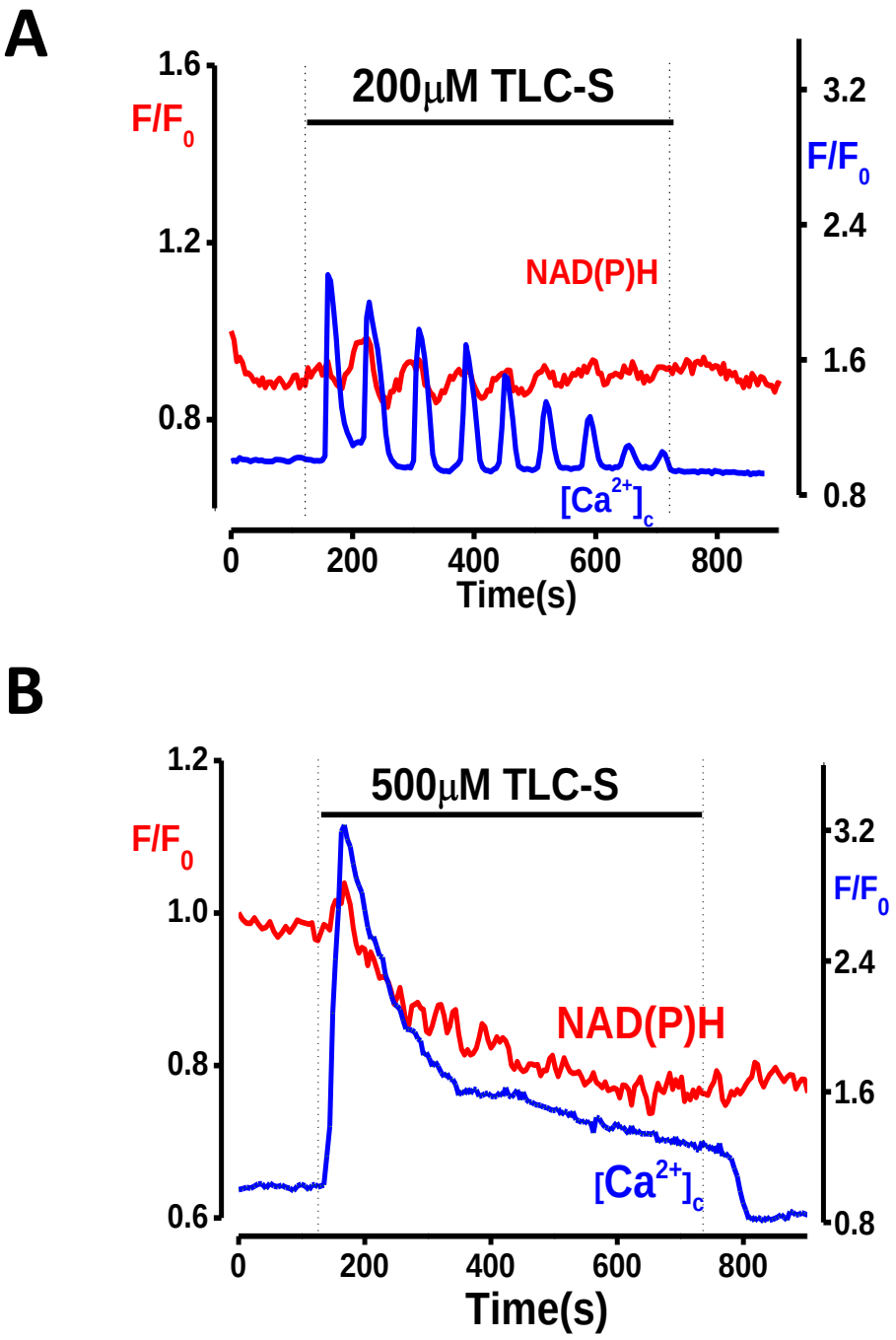

Figure 3.1. TLC-S induced concentration-dependent increases of cytosolic Ca^{2+}. Representative traces showing the different effects of 200 μM and 500 μM taurolithocholic acid sulphate (TLC-S) on cytosolic calcium ($[Ca^{2+}]_C$, *blue*), and NAD(P)H levels (*red*) in pancreatic acinar cells. (A) At the lower concentration of TLC-S, an oscillatory pattern of $[Ca^{2+}]_C$ elevation was seen in a majority of cases (16 of 20 cells). (B) At the higher concentration of TLC-S, sustained, non-oscillatory signals were consistently obtained (20 of 20 cells). Oscillatory increases of NAD(P)H occurred in tandem immediately following rises of $[Ca^{2+}]_C$ induced by 200 μM TLC-S, (A) whereas a small initial rise followed by a sustained fall of NAD(P)H levels occurred as a result of the sustained elevation of $[Ca^{2+}]_C$ induced by 500 μM TLC-S (B). Data are shown as normalized changes from basal (pre-stimulation) fluorescence levels (F/F_0).

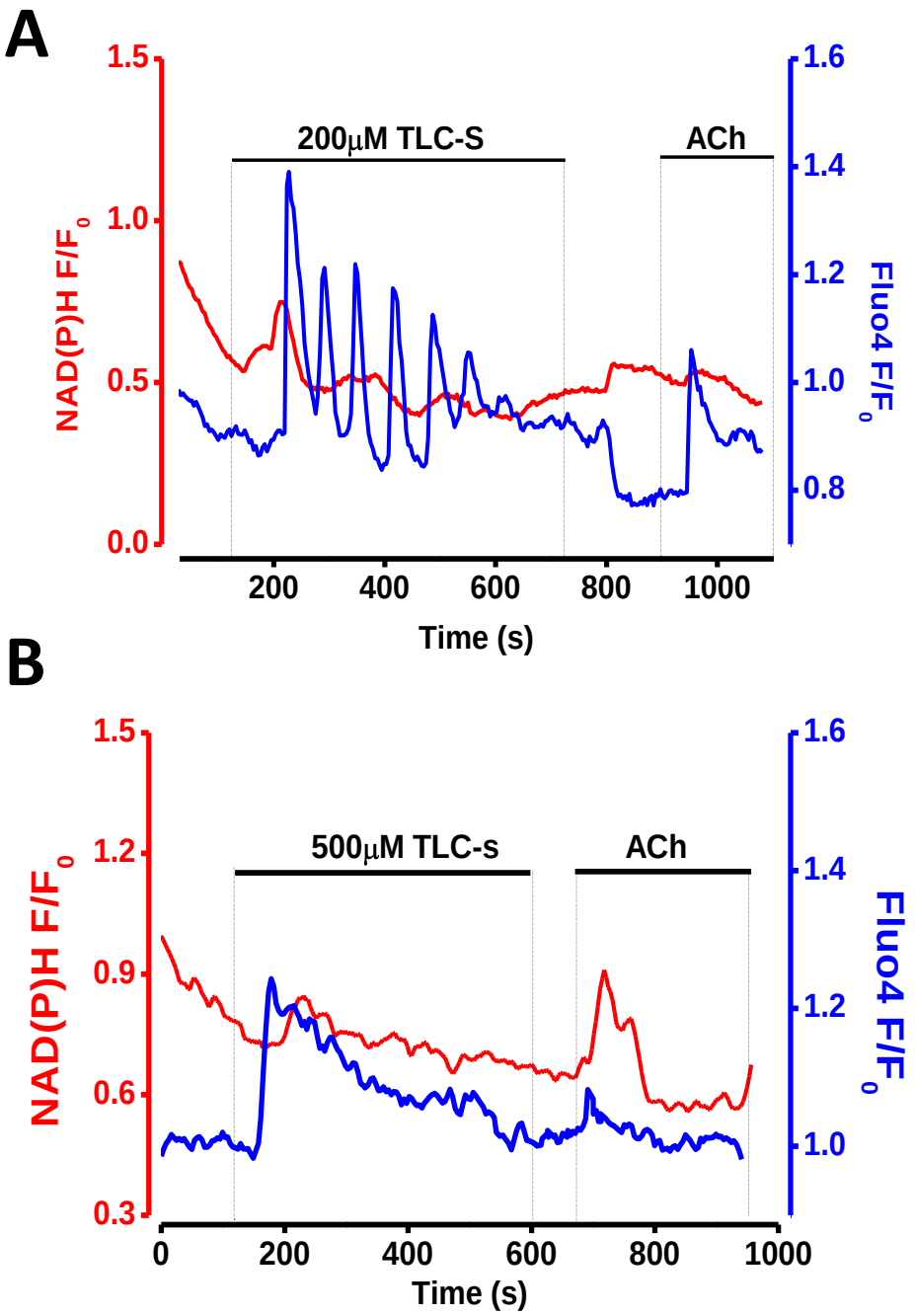

Figure 3.2. TLC-S induced concentration-dependent increases of cytosolic Ca^{2+} in acutely isolated human pancreatic acinar cells. Representative traces showing the different effects of 200 µM and 500 µM taurolithocholic acid sulphate (TLC-S) on cytosolic calcium ($[Ca^{2+}]_C$, *blue*), and NAD(P)H levels (*red*) in isolated human pancreatic acinar cells. (A) At the lower concentration of TLC-S, an oscillatory pattern of $[Ca^{2+}]_C$ elevation was seen in a majority of cases (26 of 26 cells). (B) At the higher concentration of TLC-S, sustained, non-oscillatory signals were consistently obtained (4 of 4 cells). Oscillatory increases of NAD(P)H occurred in tandem immediately following rises of $[Ca^{2+}]_C$ induced by 200 µM TLC-S, (A) whereas a small initial rise followed by a sustained fall of NAD(P)H levels occurred as a result of the sustained elevation of $[Ca^{2+}]_C$ induced by 500 µM TLC-S (B). Data are shown as normalized changes from basal (pre-stimulation) fluorescence levels (F/F_0).

Further to experiments in isolated murine pancreatic cells, samples of normal pancreatic tissue were taken from adult patients undergoing surgery for left-sided or small pancreatic tumours which were not causing duct obstruction, as described (Voronina et al., 2002a, Murphy et al., 2008). Cells were freshly isolated, loaded with cell permeant Fluo4, and imaged in the same manner as murine cells (Figure 3.1 A and B). Representative traces show prolonged, global, predominantly oscillatory rises in $[Ca^{2+}]_C$, (Figure 3.2 A ; 26 of 26 cells) in a manner similar to isolated murine cells (Figure 3.1 A). NAD(P)H autofluorescence also followed an oscillatory pattern in all experiments. Stronger stimulation of isolated human acinar cells with 500μM TLC-S (Figure 3.2 B) produced global sustained rises in $[Ca^{2+}]_C$, initial increases in NAD(P)H autofluorescence (Figure 3.2 B; 200-300 s) followed by a pronounced decrease.

In this group of experiments sufficient data is presented to draw close parallels between the responses of freshly isolated, murine pancreatic acinar cells, and cells isolated from surgical samples of normal human pancreatic tissue. When exposed to a 200μM concentration of the bile salt TLC-S, both murine and human acinar cells respond with large, global but primarily oscillatory rises in $[Ca^{2+}]_C$. NAD(P)H autofluorescence also follows a synchronised oscillatory pattern characteristic of stimulus-metabolism coupling. The greater dose; 500 μM TLC-S produced large sustained increases in $[Ca^{2+}]_C$ and depression of NAD(P)H.

3.3 TLC-S Causes NAC-sensitive elevation of intracellular ROS

In isolated murine pancreatic acinar cells, loaded with the ROS-sensitive indicator DCFDA, loaded in carboxy-methoxyester (CM) form, application of 500 µM TLC-S produced a small but significant, generalised and sustained elevation of $[ROS]_I$ (n = 14), (Figure 3.3 A, B and *inset*). The redox cycling quinone, menadione (30 µM), caused typical pronounced elevation of $[ROS]_I$ identified by a marked rise of DCFDA fluorescence that was generalised throughout the cells, but sparing the granular area (Figures 3A and 3B). In contrast, application of 200 µM TLC-S produced no detectable increase of $[ROS]_I$ (n = 11, see Figure 3.3 B and *inset*) although the cells were still capable of producing a pronounced generalized increase in $[ROS]_I$ in response to menadione, as described previously (Criddle et al., 2006a).

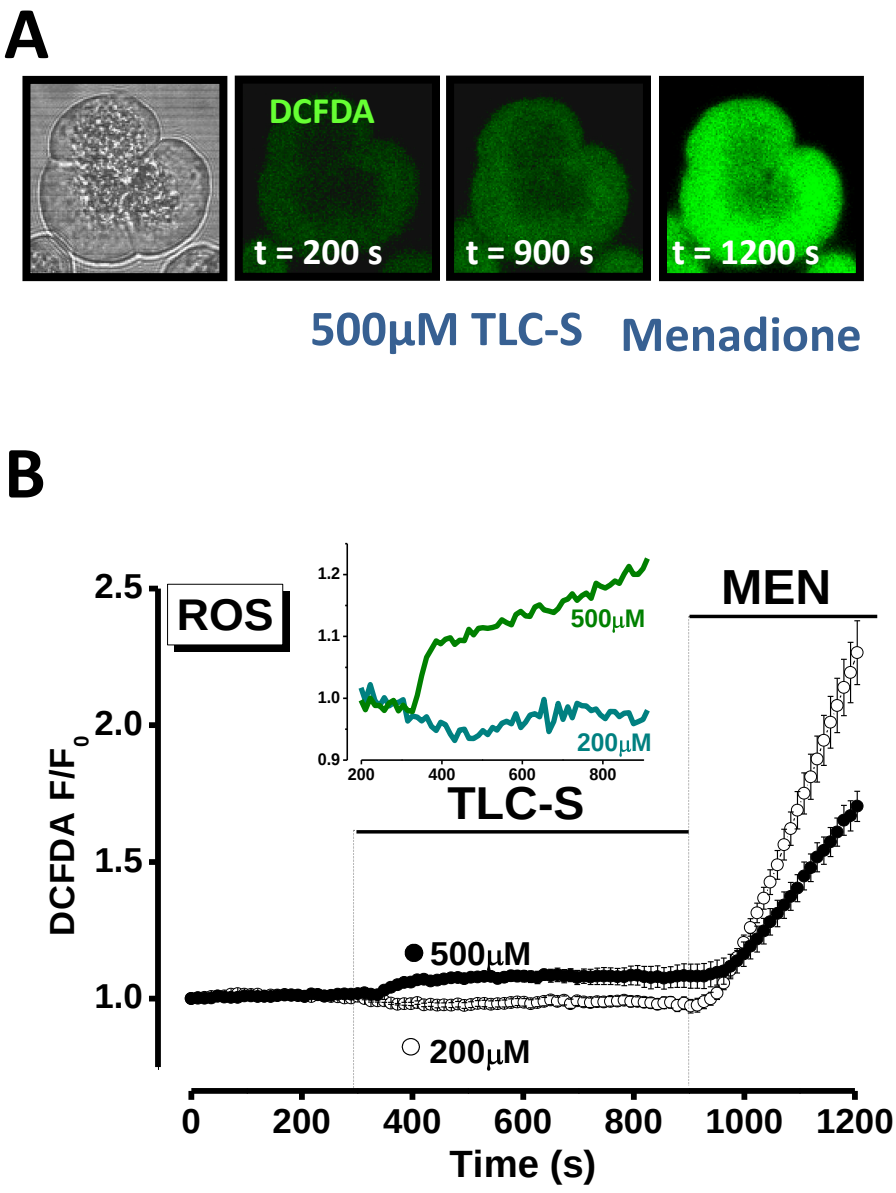

Figure 3.3. Increases in the intracellular concentration of reactive oxygen species ($[ROS]_I$) induced by TLC-S in isolated murine pancreatic acinar cells. (A) Transmitted light and CM-H_2DCFDA fluorescence (*green*) images of a triplet of murine acinar cells showing changes in $[ROS]_I$ induced by 500 µM TLC-S; changes in $[ROS]_I$ induced by menadione (MEN: 30 µM) are shown at the end as a positive control. (B) Mean data from experiments on murine cells demonstrating that $[ROS]_I$ was not increased by 200 µM TLC-S (n = 11), whereas 500 µM TLC-S produced a sustained elevation of $[ROS]_I$ above basal levels (n = 14, see inset for sample trace). Data are shown as normalized changes from basal (pre-stimulation) fluorescence levels (F/F_0).

The application of 200μM TLC-S to isolated human acinar cells produced moderate generalised sustained elevations of $[ROS]_I$, (Figure 3.4 A; 16 of 19 cells). NAD(P)H autofluorescence displayed peak immediately following application of TLC-S (Figure 3.4 A; 120-250 s) followed by a plateau (Figure 3.4 A 250-720 s). Application of 500 μM TLC-S to human cells produced a very large, sustained, generalised increase in $[ROS]_I$ (Figure 3.4 B; 16 of 16 cells). NAD(P)H autofluorescence displayed a profile similar to that previously demonstrated (Figure 3.4 A).

The increase in $[ROS]_I$ generated by 500 μM TLC-S was prevented in all cases when TLC-S application was preceded by application of the antioxidant scavenger *N*-acetyl-L-cysteine (NAC, 10 mM). Murine cells were without overall change in the rate of $[ROS]_I$ generation when NAC and TLC-S were applied (Figure 3.5 A and B, 18 of 18 cells). NAD(P)H autofluorescence remained diminished following TLC-S application. The much larger rise in $[ROS]_I$ generation seen in human cells was also effectively blocked by NAC (Figure 3.6 A and B; 10 of 10 cells).

Following each experiment in this series, the oxidant quinone menadione (30 μM) was used at the end of the experiment to illustrate the capacity of the cells to produce $[ROS]_I$ and confirm the presence of loaded DCFDA. In experiments where NAC was applied, NAC was not included in menadione perfusion solutions as even the pronounced generation of ROS by menadione was effectively scavenged by NAC (Criddle et al., 2006a).

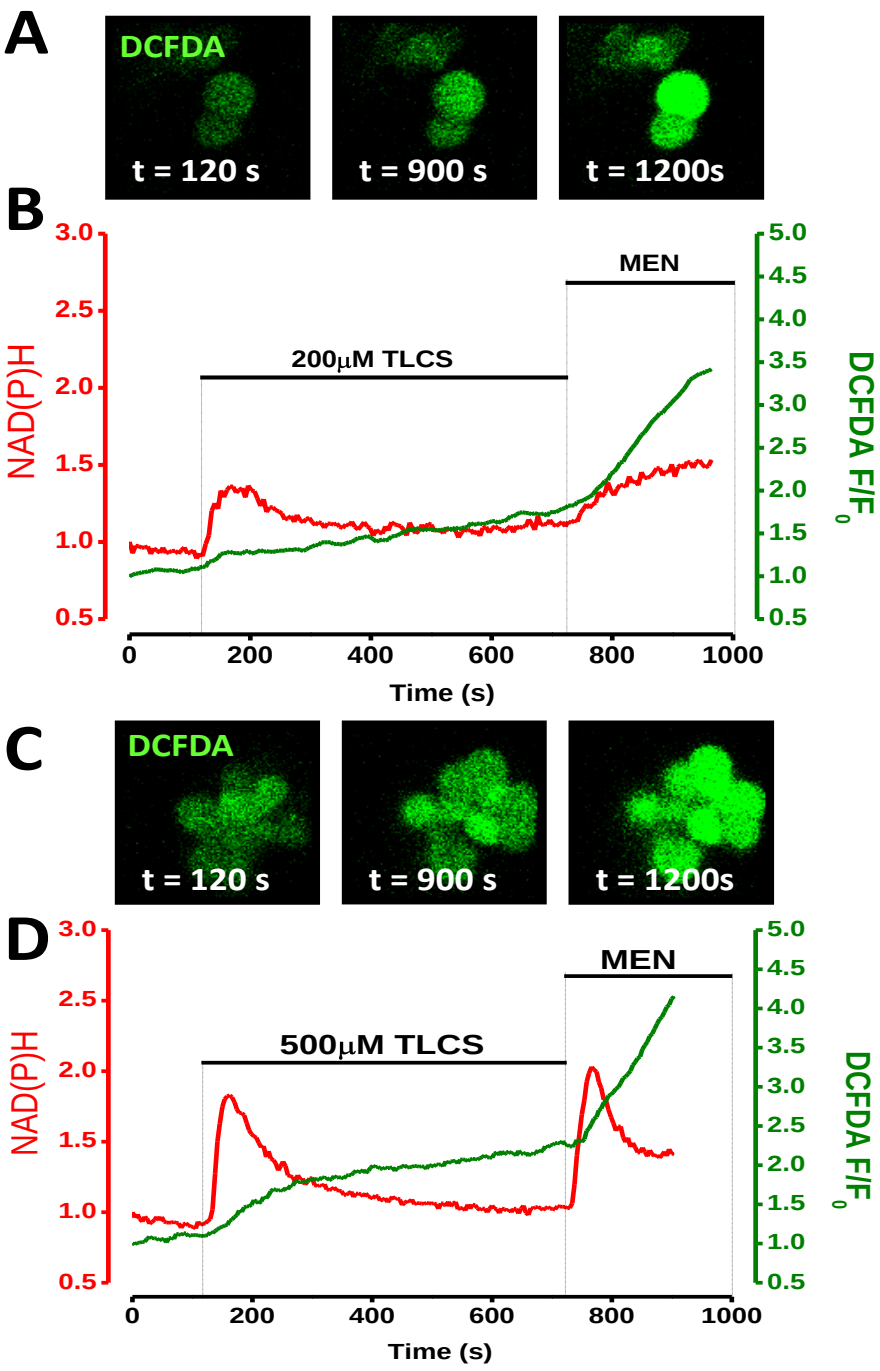

Figure 3.4. Increases in the intracellular concentration of reactive oxygen species ($[ROS]_I$) induced by TLC-S in isolated human pancreatic acinar cells. (A) CM-H_2DCFDA fluorescence (*green*) images of a doublet of human acinar cells showing changes in $[ROS]_I$ induced by 200 μM TLC-S; increases of $[ROS]_I$ induced by menadione (MEN: 30 μM) are shown at the end as a positive control. (B) Representative traces from experiments on isolated human pancreatic acinar cells demonstrating an changes in $[ROS]_I$ in response to 200 μM TLC-S, changes in NAD(P)H (red) occurred in tandem immediately following rises of $[ROS]_I$ induced by 200 μM TLC-S, (n = 16 of 19 cells). (C) CM-H_2DCFDA fluorescence (*green*) images of a group of seven human acinar cells showing increases of $[ROS]_I$ induced by 500 μM TLC-S; increases of $[ROS]_I$ induced by menadione (MEN: 30 μM) are shown at the end as a positive control. (D) Representative traces from experiments on isolated human pancreatic acinar cells demonstrating changes in $[ROS]_I$ in response to 500 μM TLC-S, increases of NAD(P)H (red) occurred in tandem immediately following rises of $[ROS]_I$ induced by 500 μM TLC-S, (n = 16 of 16 cells). Data are shown as normalized changes from basal (pre-stimulation) fluorescence levels (F/F_0).

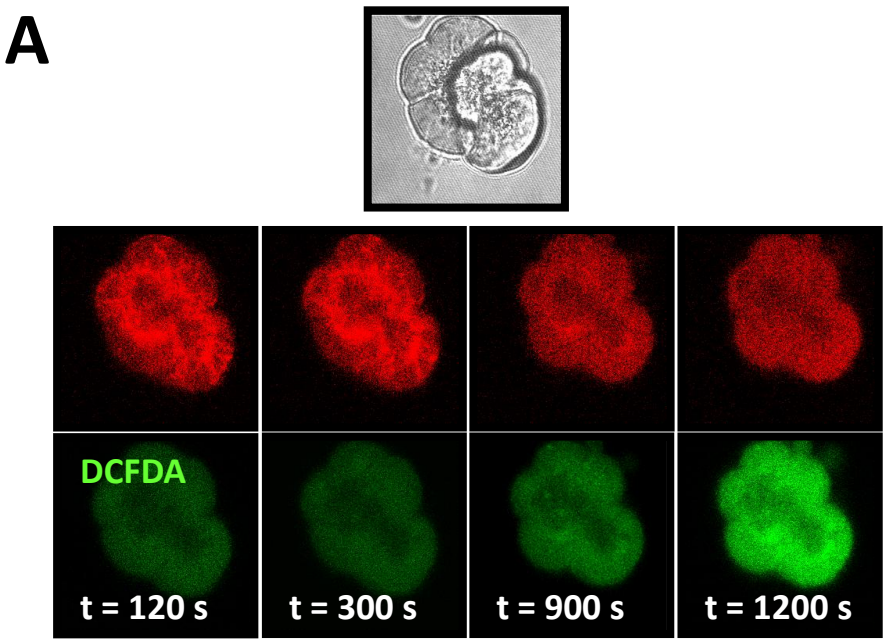

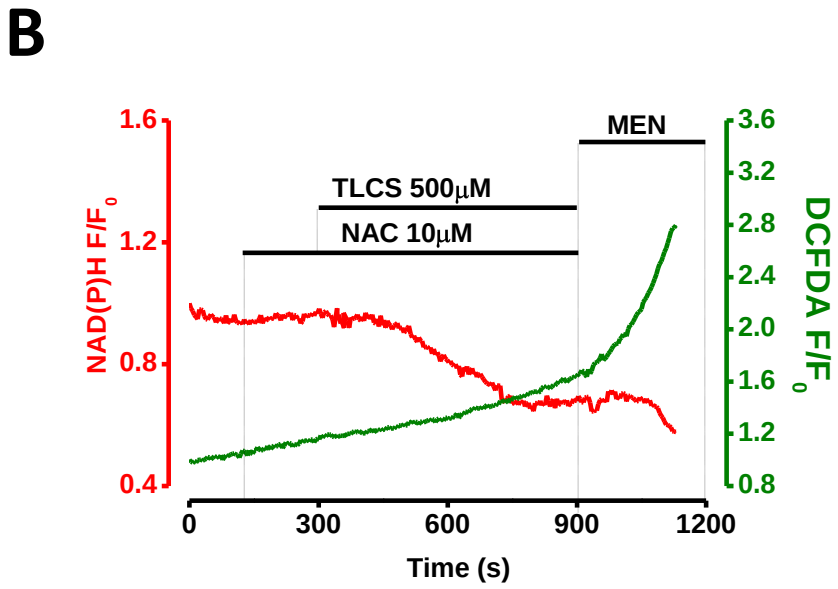

Figure 3.5. Antioxidant scavenging of the intracellular reactive oxygen species ($[ROS]_I$) induced by TLC-S in isolated murine pancreatic acinar cells. (A) Transmitted light and CM-H_2DCFDA fluorescence (*green*) images of a group of murine acinar cells show the changes in $[ROS]_I$ induced by 500 μM TLC-S; increases of $[ROS]_I$ induced by menadione (MEN: 30 μM) are shown as a positive control. (B) Representative traces from experiments on isolated murine pancreatic acinar cells demonstrating $[ROS]_I$ response to 500 μM TLC-S as abolished by 10mM *n*-acetyl-L-cysteine. Changes in NAD(P)H (red) occurred in tandem immediately following perfusion with 500 μM TLC-S, (n = 18 of 18 cells). Data are shown as normalized changes from basal (pre-stimulation) fluorescence levels (F/F_0).

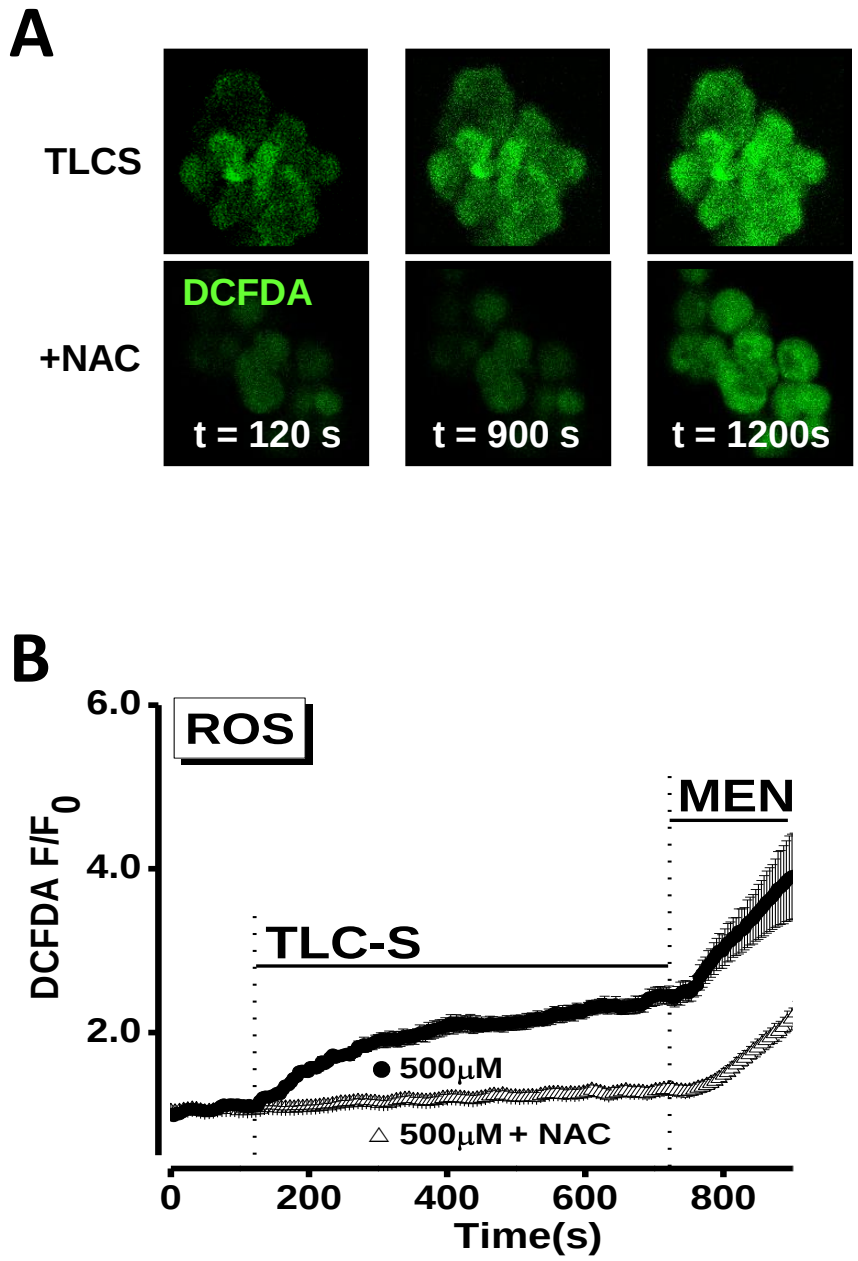

Figure 3.6. Increases in the intracellular concentration of reactive oxygen species ($[ROS]_i$) induced by TLC-S in isolated human pancreatic acinar cells. (A) Transmitted light and CM-H_2DCFDA fluorescence (*green*) images of isolated human acinar cells showing changes in $[ROS]_i$ induced by 500 μM TLC-S and *N*-acetyl-L-cysteine (NAC, 10 mM, n = 10; no further NAC applied during menadione application to check human cells capable of ROS generation); increases of $[ROS]_i$ induced by menadione (MEN: 30 μM) are shown as a positive control. (B) Mean data from experiments on isolated human pancreatic acinar cells demonstrating changes in $[ROS]_i$ in response to 500 μM TLC-S (n = 12), abolished by simultaneous incubation with *N*-acetyl-L-cysteine (NAC, 10 mM, n = 10; no further NAC applied during menadione application to check human cells capable of ROS generation).

3.4 Distribution of the oxidant scavenging enzyme NAD(P)H quinone oxidoreductase (NQO1) and effects of NQO1 inhibition on the elevation of $[ROS]_i$ induced by TLC-S in pancreatic acinar cells

Murine pancreatic acinar cells display a uniform intracellular distribution of NQO1 (*green*) (Figure 7) with noticeably lower levels of fluorescence seen in areas labelled with the nuclear stain Hoechst 33342 (*blue*). Fluorescence levels in cells incubated in the absence of the anti-NQO1 primary antibody were significantly lower and consistent with autofluorescence in unstained PFA-fixed pancreatic acinar cells (data not shown). Additional staining of F-actin (AlexaFluor633 Phalloidin; Invitrogen, Paisley, UK) was used to demonstrate maintained cell polarity and orientation. F-actin has been previously shown to be located at the apical pole and periphery of the pancreatic acinar cell (Singh et al., 2001) number of cells visualised in all cases was >20.

Human cells stained in the same way also exhibited a cytosolic distribution of NQO1. Figure 8 shows a maximal intensity projection of a group of freshly isolated human acinar cells stained in the same manner as the murine cells (Figure 7). The distribution of F-actin (*red*), NQO1 (*green*) and Hoechst 33342 (*blue*) is essentially the same as seen with murine experiments. In a single confocal slice (Figure 3.9 A; 5 µM), images of the same cluster show that nuclear exclusion of NQO1 appears common to both human and murine acinar cells (Figure 3.8 and 3.9 A). Figure 3.9 B displays graphically the relative intensity of NQO1 immunofluorescence (*green*) and Hoechst33342 fluorescence (*blue*) in the area depicted by the arrow (Figure 3.9 A; *white*). Where nuclear staining is strong NQO1 staining is relatively weak.

Perfusion of murine pancreatic acinar cells with 200 µM TLC-S yielded no significant increase in $[ROS]_I$, compared to pre-stimulation baseline (Figure 3). Inhibition of NQO1 with 1,4-dimethoxy-2-methylnaphthalene (DMN; 30 µM) unmasked the generation of intracellular ROS by 200 µM TLC-S and potentiated the $[ROS]_I$, increases seen with 500 µM TLC-S (Figure 3.10 A and B). Mean data from these experiments (Figure 10A) show that ROS production induced by both 200 µM (n = 11) and 500 µM (n = 12) TLC-S was greater in the presence of DMN. Real-time dynamic increases of $[ROS]_I$, were observed in the presence of NQO1 inhibition with DMN for both murine (Figure 3.11 A and B n = 12 of 12 cells) and human acinar cells (Figure 3.12 A and B n = 12 of 12 cells) Data are displayed as normalized changes from basal (pre-stimulation) fluorescence levels (F/F_0).

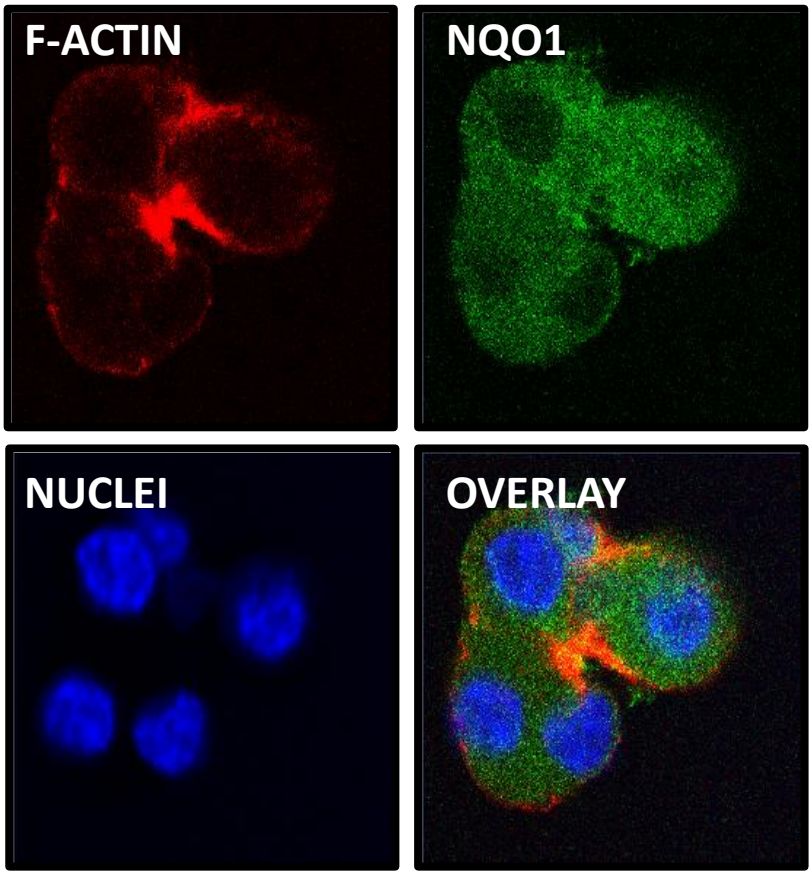

Figure 3.7. Distribution of the oxidant scavenging enzyme NAD(P)H quinone oxidoreductase (NQO1) in isolated murine pancreatic acinar cells. Confocal image (5μM) of PFA fixed cells. Cytosolic distribution of NQO1 *(green)* as shown by immunofluorescence (F-actin *(red)* and Hoescht 33342 *(blue)* counter-stains).

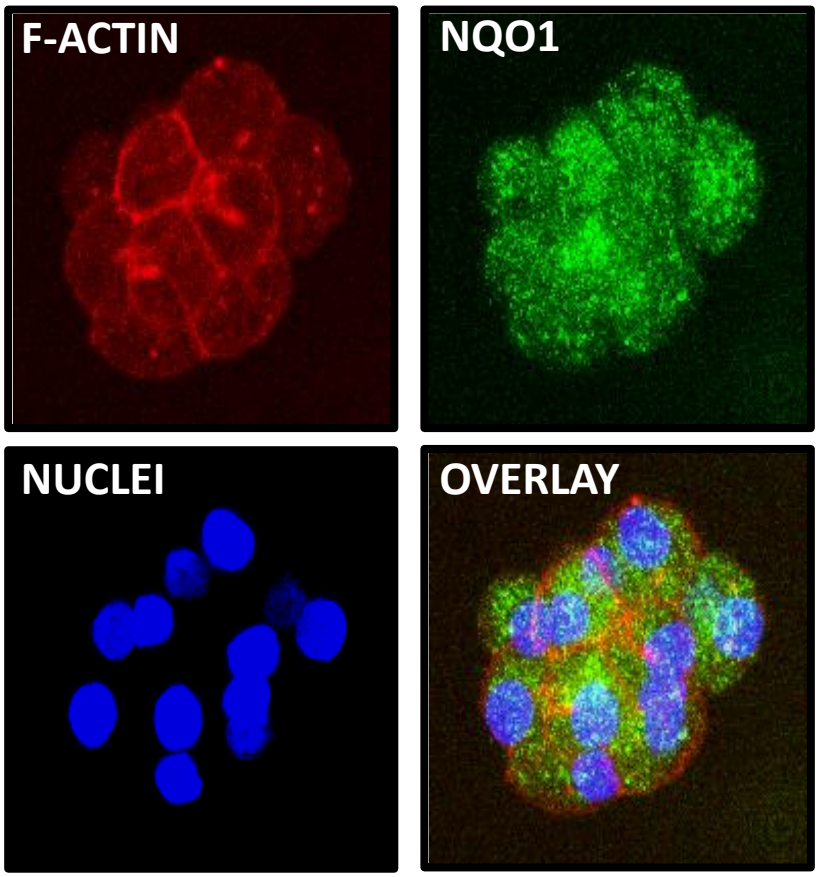

Figure 3.8. Distribution of the oxidant scavenging enzyme NAD(P)H quinone oxidoreductase (NQO1) in isolated human pancreatic acinar cells. Maximal intensity projection of PFA fixed cells. Cytosolic distribution of NQO1 *(green)* as shown by immunofluorescence is seen to be similar in human and murine pancreatic acinar cells (F-actin *(red)* and Hoechst 33342 *(blue)* counter-stains

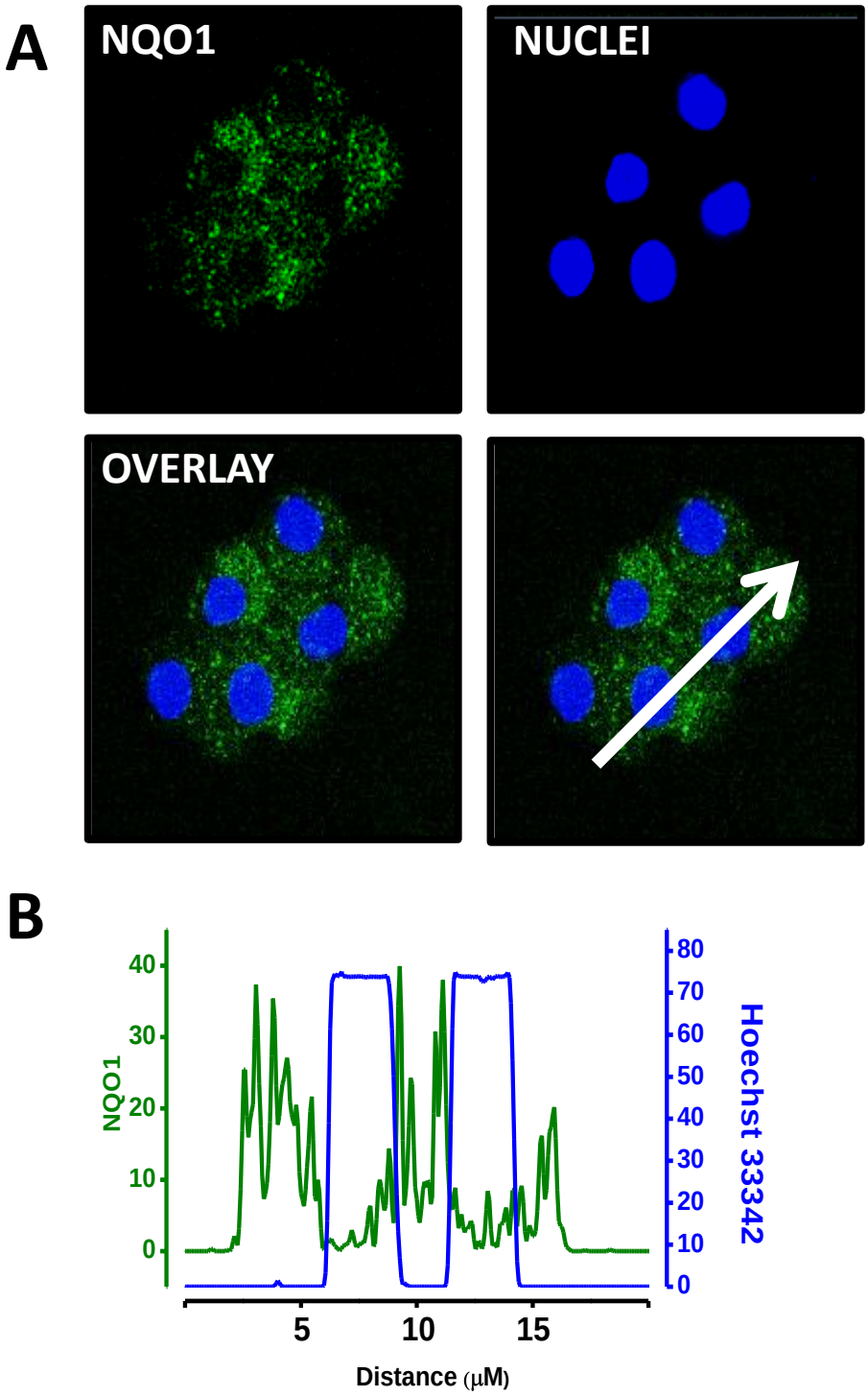

Figure 3.9. Distribution of the oxidant scavenging enzyme NAD(P)H quinone oxidoreductase (NQO1) in isolated human pancreatic acinar cells. (A) Confocal image (5 μM) of PFA fixed cells. Cytosolic distribution of NQO1 *(green)* is seen to be excluded from the nucleus *(blue)* as shown by immunofluorescence. (B) Line graph depicting relative fluorescence along white arrow. NQO1 immunofluorescence is inversely correlated with nuclear (Hoechst 33342) fluorescence.

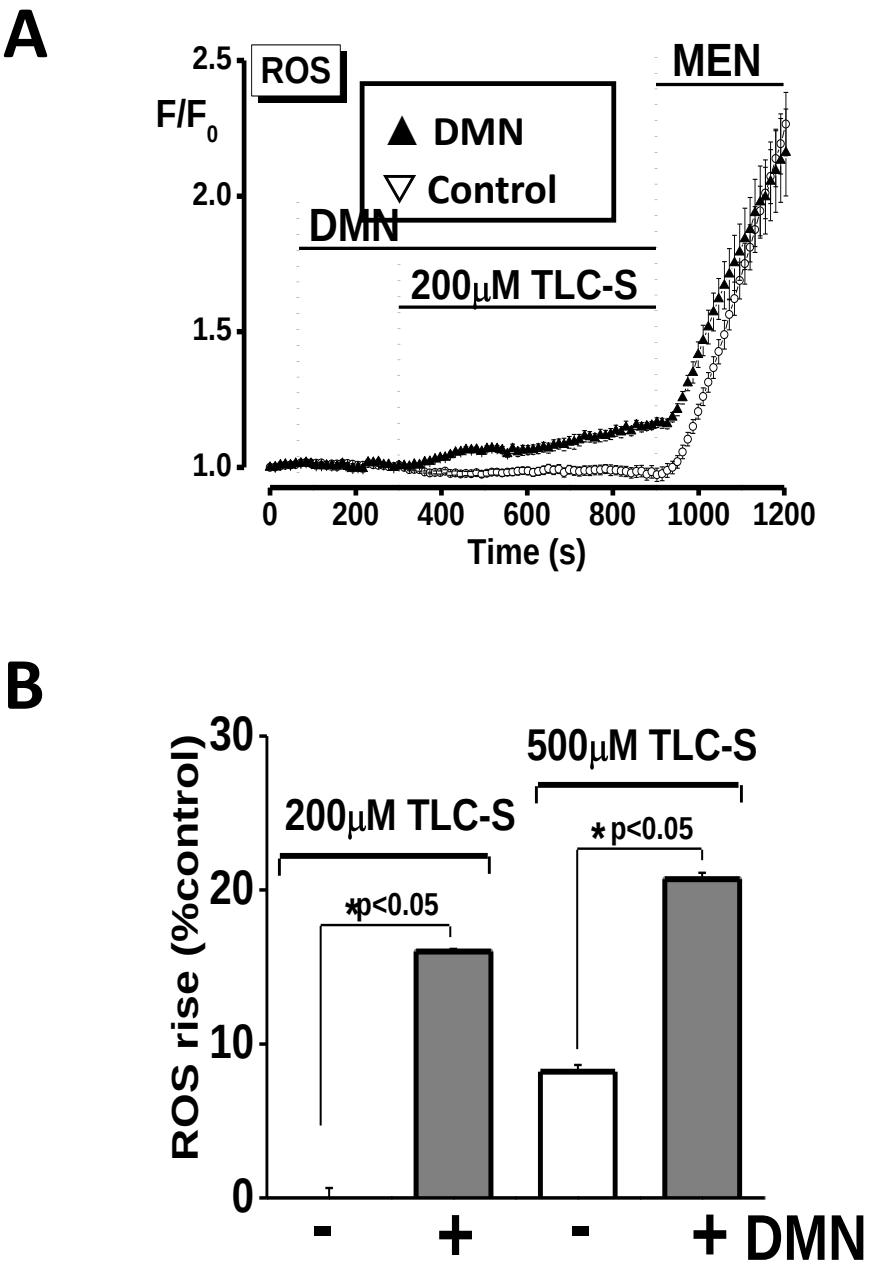

Figure 3.10. Effects of NQO1 inhibition on the elevation of $[ROS]_I$ induced by TLC-S in pancreatic acinar cells (A) Inhibition of NQO1 with DMN (1,4-dimethoxy-2-methylnaphthalene; 30 μM) unmasked the generation of ROS induced by 200 μM TLC-S, as measured by CM-H_2DCFDA fluorescence (*green*) (n = 11). (B) Mean data from these experiments show that ROS production induced by both 200 μM (n = 11) and 500 μM (n = 12) TLC-S was greater in the presence of DMN (30 μM). Data are displayed as normalized changes from basal (pre-stimulation) fluorescence levels (F/F_0).

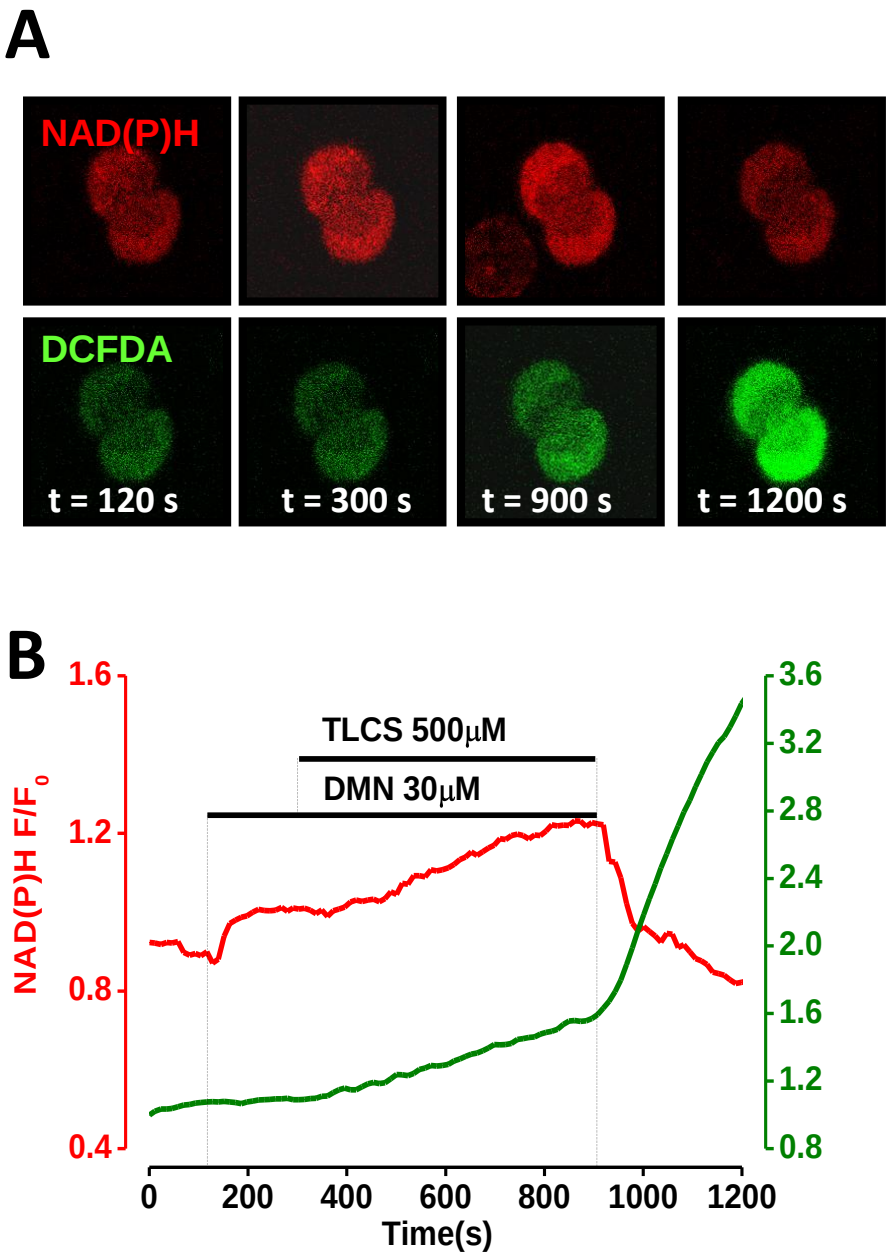

Figure 3.11. Increases in the intracellular concentration of reactive oxygen species ($[ROS]_I$) induced by TLC-S in isolated murine pancreatic acinar cells in the presence of DMN. (A) CM-H_2DCFDA fluorescence (*green*) images of a group of murine acinar cells showing increases of $[ROS]_I$ induced by 500 μM TLC-S in the presence of NQO1 inhibition DMN (30 μM); increases of $[ROS]_I$ induced by menadione (MEN: 30 μM) are shown at the end as a positive control. (B) Representative traces from experiments on isolated murine pancreatic acinar cells demonstrating an increase of $[ROS]_I$ in response to 500 μM TLC-S, increases of NAD(P)H (red) occurred in tandem immediately following rises of $[ROS]_I$ induced by 500 μM TLC-S, (n = 12 of 12 cells). Data are shown as normalized changes from basal (pre-stimulation) fluorescence levels (F/F_0).

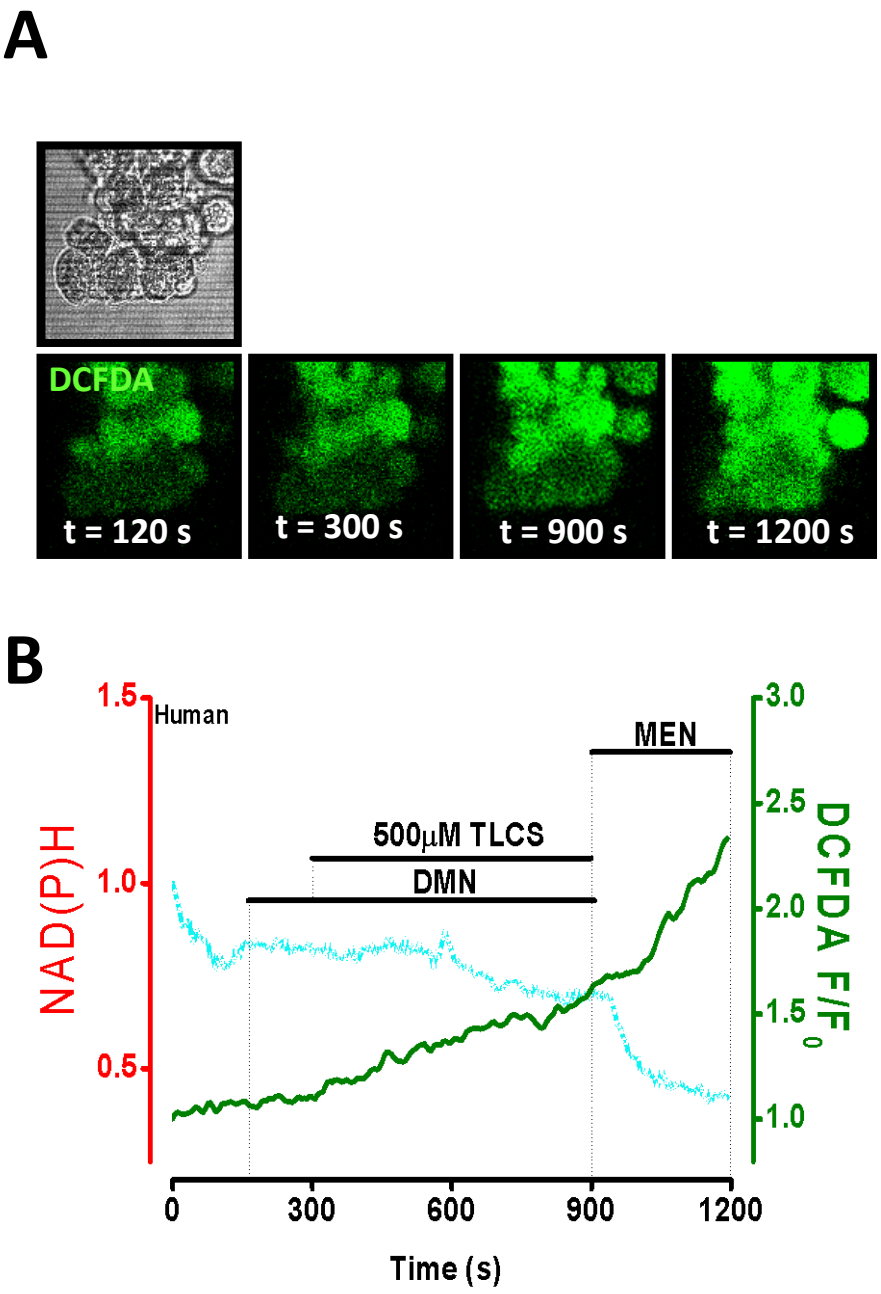

Figure 3.12. Increases in the intracellular concentration of reactive oxygen species ($[ROS]_I$) induced by TLC-S in isolated human pancreatic acinar cells in the presence of DMN. (A) CM-H_2DCFDA fluorescence (*green*) images of a group of human acinar cells showing increases of $[ROS]_I$ induced by 500 μM TLC-S in the presence of NQO1 inhibition DMN (30μM); increases of $[ROS]_I$ induced by menadione (MEN: 30 μM) are shown at the end as a positive control. (B) Representative traces from experiments on isolated human pancreatic acinar cells demonstrating an increase of $[ROS]_I$ in response to 500 μM TLC-S, increases of NAD(P)H (red) occurred in tandem immediately following rises of $[ROS]_I$ induced by 500 μM TLC-S, (n = 12 of 12 cells). Data are shown as normalized changes from basal (pre-stimulation) fluorescence levels (F/F_0).

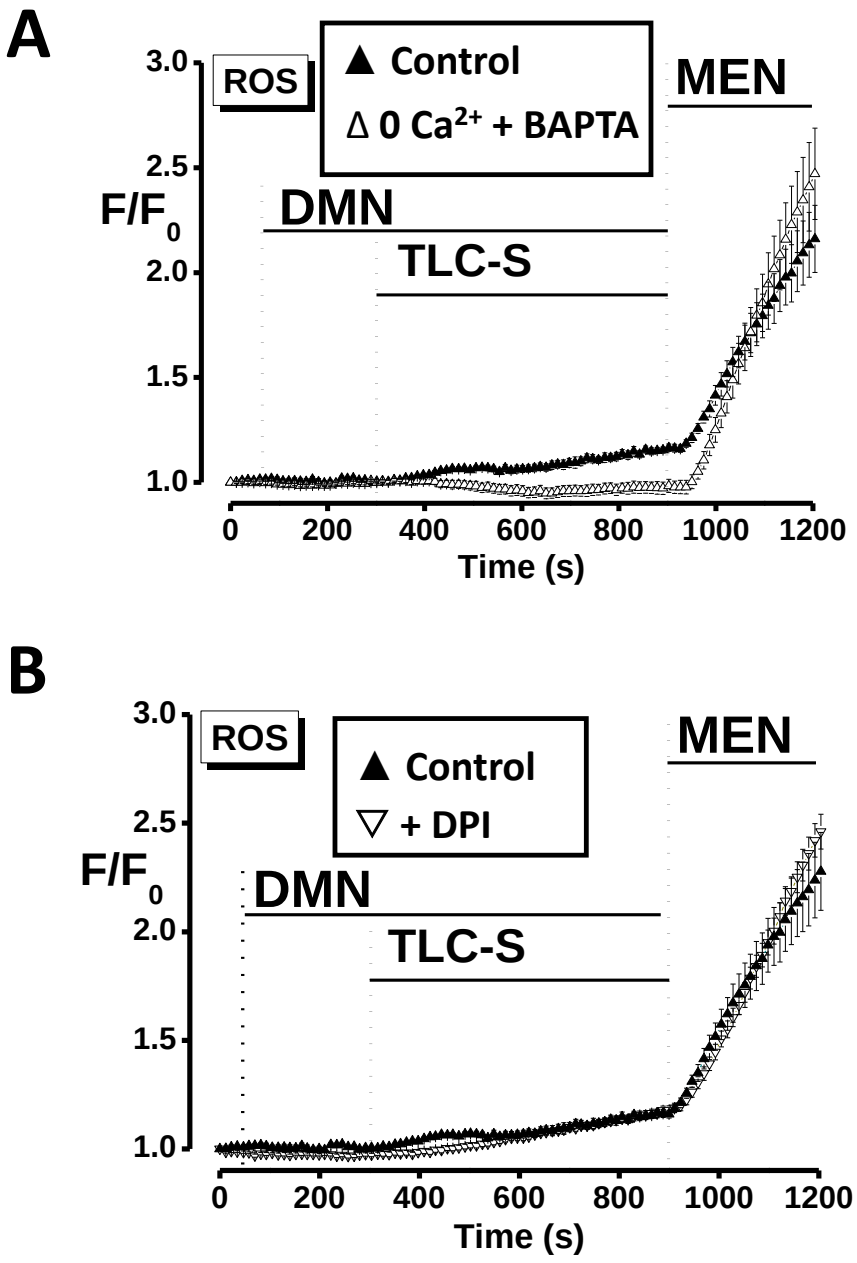

Figure 3.13. Effects of Ca^{2+} chelation or NADPH oxidase inhibition on TLC-S-mediated elevation of $[ROS]_I$ in pancreatic acinar cells. (A) The generation of ROS induced by 200 µM TLC-S in the presence of DMN (30 µM) and absence of external Ca^{2+} was completely blocked by 30 min pre-treatment with the Ca^{2+} chelator BAPTA-AM, whereas that induced by MEN (30 µM) was unaffected (control, n = 11; BAPTA, n = 14). (B) Increases in $[ROS]_I$ elicited by either TLC-S or MEN were not inhibited by the NADPH oxidase inhibitor diphenyleneiodonium (DPI, 10 µM; control n = 15; DPI, n = 12). Mean data are shown as normalized changes from basal (pre-stimulation) fluorescence levels (F/F_0) +/- SEM.

3.5 - Effects of Ca^{2+} chelation or NADPH oxidase inhibition on TLC-S-mediated elevation of $[ROS]_I$ in pancreatic acinar cells

The generation of ROS induced by 200 µM TLC-S in the presence of NQO1 inhibition (DMN; 30 µM) (Figure 3.13 A; *black triangles*) was completely blocked by 30 min pre-treatment with the intracellular Ca^{2+} chelator 1,2-bis(*O*-aminophenoxy)ethane-N,N,N',N'-tetraacetic acid (BAPTA; 25 µM), loaded in AM form (Figure 3.13 A; *white triangles*). The characteristic increase in ROS induced by MEN (30 µM) was unaffected by intracellular calcium chelation and occurred in a similar manner in both experimental groups (control, n = 11; BAPTA, n = 14).

The role of NAD(P)H oxidase is vital to immune function and as a prodigious source of superoxide, the proximal ROS. As such it cannot be discounted despite little evidence for its presence in primary pancreatic acinar cells (Gukovskaya et al., 2002b). However, in rat acinar cell derived AR42J cells, NADPH oxidase has been identified as a source of ROS in response to hyperstimulation with cholecystokinin (CCK) (Yu et al., 2005) and its inhibition with diphenyleneiodonium (DPI) linked to suppression of apoptosis (Yu et al., 2007). Increases in $[ROS]_I$ elicited by either TLC-S or MEN were not inhibited by the NADPH oxidase inhibitor diphenyleneiodonium (Figure 3.13 B DPI, 10 µM; control n = 15; DPI, n = 12). Mean data are shown as normalized changes from basal (pre-stimulation) fluorescence levels (F/F_0) +/- SEM.

Limited data obtained with freshly isolated human acinar cells, while not extensive, shows that calcium chelation (BAPTA; 25 µM), loaded in AM form prevents even the much larger rises in $[ROS]_I$ as detected by DCFDA

fluorescence (Figure 3.14 A; *green*). The lack of response (Figure 3.14 B) is in stark contrast to the large, generalized rises seen with human acinar cells and 500 µM TLC-S (Figure 3.4 B).

3.6 TLC-S elevates $[Ca^{2+}]_M$ and inhibits mitochondrial function

Events triggering release of calcium into the cytosol enable calcium to move down an electro chemical gradient into the mitochondrial matrix via multiple channels (reviewed in (Szabadkai and Duchen, 2008)). As shown (Figure 1 A and B), both 200 µM and 500 µM TLC-S cause substantial increases in the $[Ca^{2+}]_C$.

In cells loaded with the mitochondrial calcium indicator ($[Ca^{2+}]_M$) Rhod-2, 200 µM TLC-S induced small, localised elevations of fluorescence in the typical peri-granular mitochondrial region (Petersen and Tepikin, 2008) in the majority of cells (Figure 3.15 A;10/15 cells), indicative of rises of $[Ca^{2+}]_M$. Simultaneous measurement of NAD(P)H

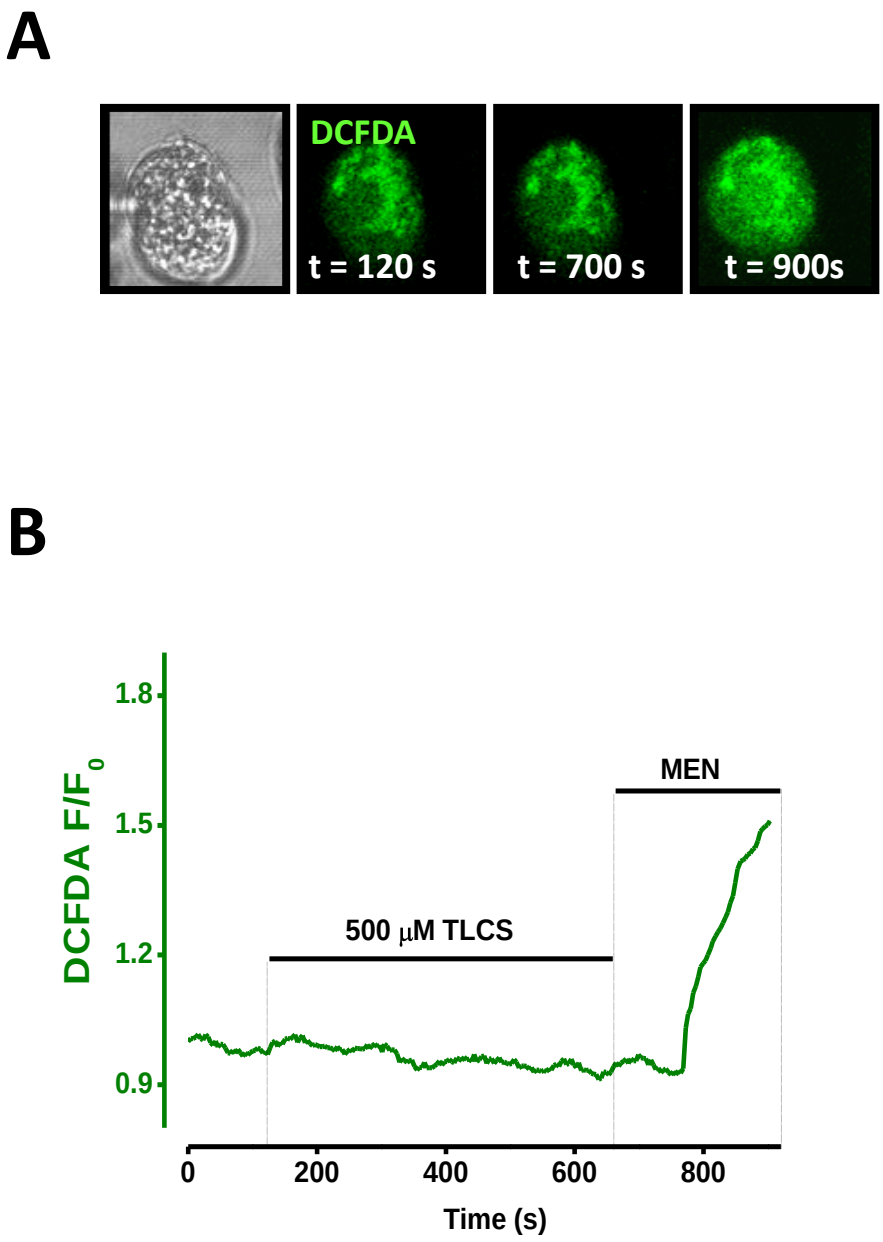

Figure 3.14. Effects of Ca^{2+} chelation on TLC-S-mediated elevation of $[ROS]_I$ in pancreatic acinar cells. (A) Transmitted light and CM-H_2DCFDA fluorescence (*green*) images of isolated human acinar cells show no increase of $[ROS]_I$ induced by 500 μM TLC-S. (B) The generation of ROS induced by 500 μM TLC-S was completely blocked by 30 min pre-treatment with the Ca^{2+} chelator BAPTA-AM (25 μM), whereas that induced by MEN (30 μM) was unaffected (n = 4).

Mean data are shown as normalized changes from basal (pre-stimulation) fluorescence levels (F/F_0).

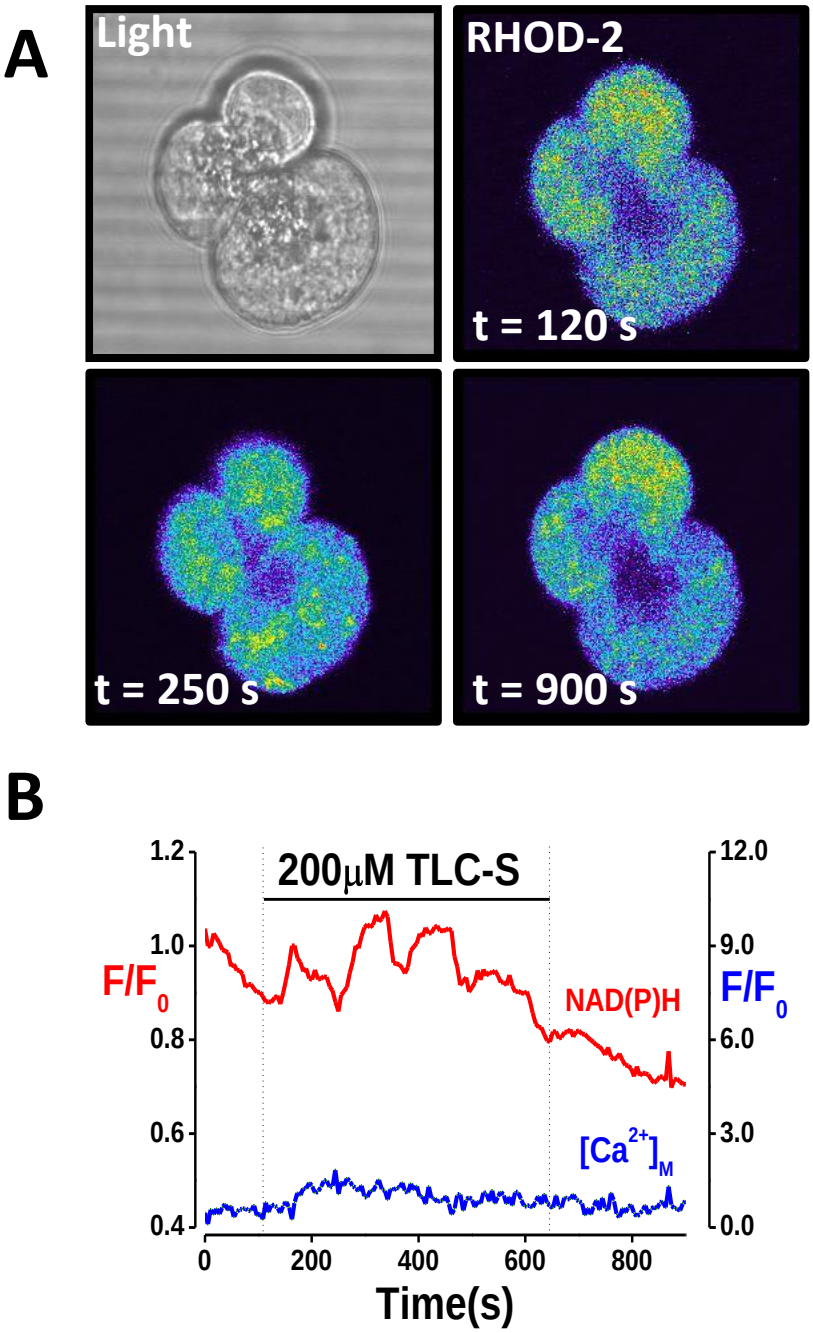

Figure 3.15. 200 μM TLC-S induced modest changes in mitochondrial calcium. Representative traces showing the effect of 200 μM taurolithocholic acid sulphate (TLC-S) on mitochondrial calcium ($[Ca^{2+}]_M$, *blue*) and NAD(P)H levels (*red*) in pancreatic acinar cells. (A) Light-transmitted, and Rhod-2 *(rainbow)* fluorescence images of a triplet of acinar cells showing small changes in $[Ca^{2+}]_M$ *(blue)* induced by 10 min application of 200 μM TLC-S. (B) Changes of $[Ca^{2+}]_M$ (*blue*) were predominantly small and not sustained and changes of NAD(P)H (*red*) elicited by 200 μM TLC-S were predominantly oscillatory in nature (10 of 15 cells,), although some sustained $[Ca^{2+}]_M$ increases were obtained (5 of 15 cells).

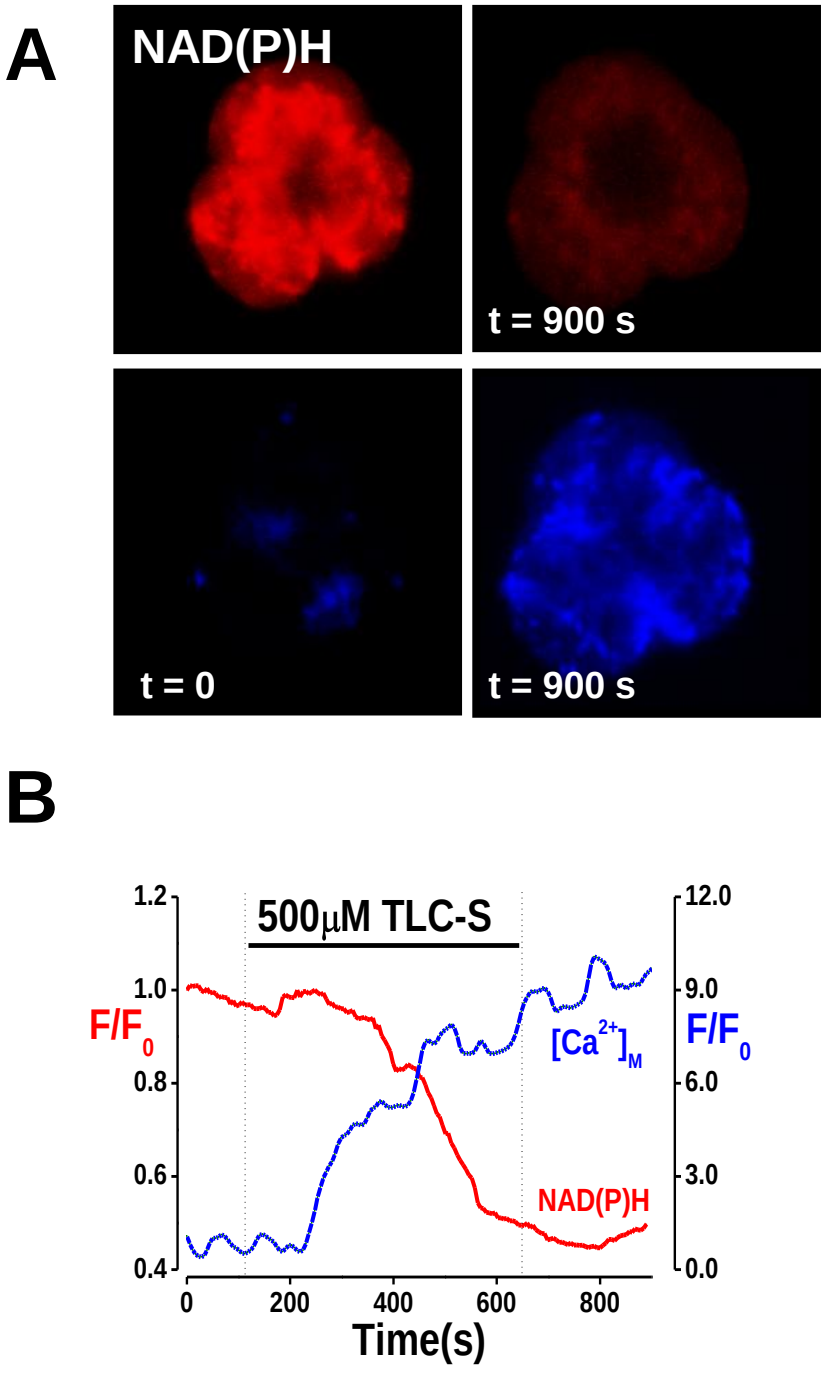

Figure 3.16. 500 μM TLCS induced large sustained changes in mitochondrial calcium. Representative traces showing the different effects of 500 μM taurolithocholic acid sulphate (TLC-S) on mitochondrial calcium ($[Ca^{2+}]_M$, *blue*) and NAD(P)H levels (*red*) in murine pancreatic acinar cells. (A) Light-transmitted, NAD(P)H (*red*) and Rhod-2 *(blue)* fluorescence images of a triplet of acinar cells showing concomitant elevations of $[Ca^{2+}]_M$ *(blue)* and decreases of NAD(P)H *(red)* induced by 10 min application of 500 μM TLC-S. Sustained elevations of $[Ca^{2+}]_M$ and concomitant decreases of NAD(P)H were consistently induced by 500 μM TLC-S (20 of 20 cells, example shown in right hand graph), indicative of mitochondrial Ca^{2+} overload

autofluorescence showed an oscillatory pattern typical of the stimulus-metabolism coupling effects of transient $[Ca^{2+}]_C$. increases. In contrast, 500 µM TLC-S induced sustained elevations of $[Ca^{2+}]_M$ and typical marked falls of NAD(P)H (Voronina et al., 2004) in all cells examined (20/20 cells, Figure 16 A and B), with 50% (10/20 cells) also showing some superimposed quasi-oscillatory increases of $[Ca^{2+}]_M$, that were not reversible on washout of the bile acid (Figure 3.16 B)**.**

The changes in acinar cell function caused by the high, 500 µM, level of TLC-S include rises in $[Ca^{2+}]_C$ (Figure 1B) and $[Ca^{2+}]_M$ (Figure 3.16) were accompanied by a fall in the autofluorescence of NAD(P)H in the mitochondrial regions. This is illustrated when TLCS-S is applied and cells subject to thin-section high quality confocal imaging. Application of 500µM TLCS caused a complete loss of the mitochondrial distribution of NAD(P)H (Figure 3.17 (*Red*)). Concomitant with this was a rise in DCFDA fluorescence (*green*). In these experiments, high quality thin-section images, revealed the increasing DCFDA fluorescence to correlate with decreasing NAD(P)H autofluorescence in characteristic mitochondrial regions such as the peri-granular, peri-nuclear and subplasmalemmal locations. The fall in NAD(P)H and rise in DCFDA fluorescence in these regions is indicative of inhibition of mitochondrial function.

Murine pancreatic acinar cells incubated with the mitochondrial dye tetra methyl rhodamine methyl ester (TMRM, 50 nM) display a typical mitochondrial distribution as demonstrated previously (Tinel et al., 1999, Voronina et al., 2004). Upon stimulation with TLC-S (500 µM 10 mins), cells co-loaded with TMRM (*red*) and DCFDA (*green*) display co localization (3.19;

overlay: orange). A mitochondrial distribution of DCFDA was not seen in cells perfused without TLC-S (Figure 19; left image set).

Application of 500 µM TLC-S to murine and human acinar cells was accompanied by an increase in $[Ca^{2+}]_C$; (Figure 1B) and a dramatic increase in $[Ca^{2+}]_M$;(Figure 3.16). Within seconds NAD(P)H autofluorescence temporarily increases before becoming progressively diminished (Figure 3.1 B, 3.2 B, 3.16 B and 3.20 B). These phenomena are accompanied by increased production of $[ROS]_I$ (Figure 3.3, 3.4 and 3.20), which displays a mitochondrial distribution in fluorescently labelled cells (Figure 17 and 18). Effective blockade of the electron transport chain can be achieved at two separate points; complex 1 and complex 3 (Rotenone; 5 µM and Antimycin A 10 µM respectively). Application of rotenone and antimycin A was able to completely block the effects of TLC-S on ROS but caused a marked increase in NAD(P)H autofluorescence *per se* (Figure 3.20 A and B, n = 21 of 21 cells). Application of

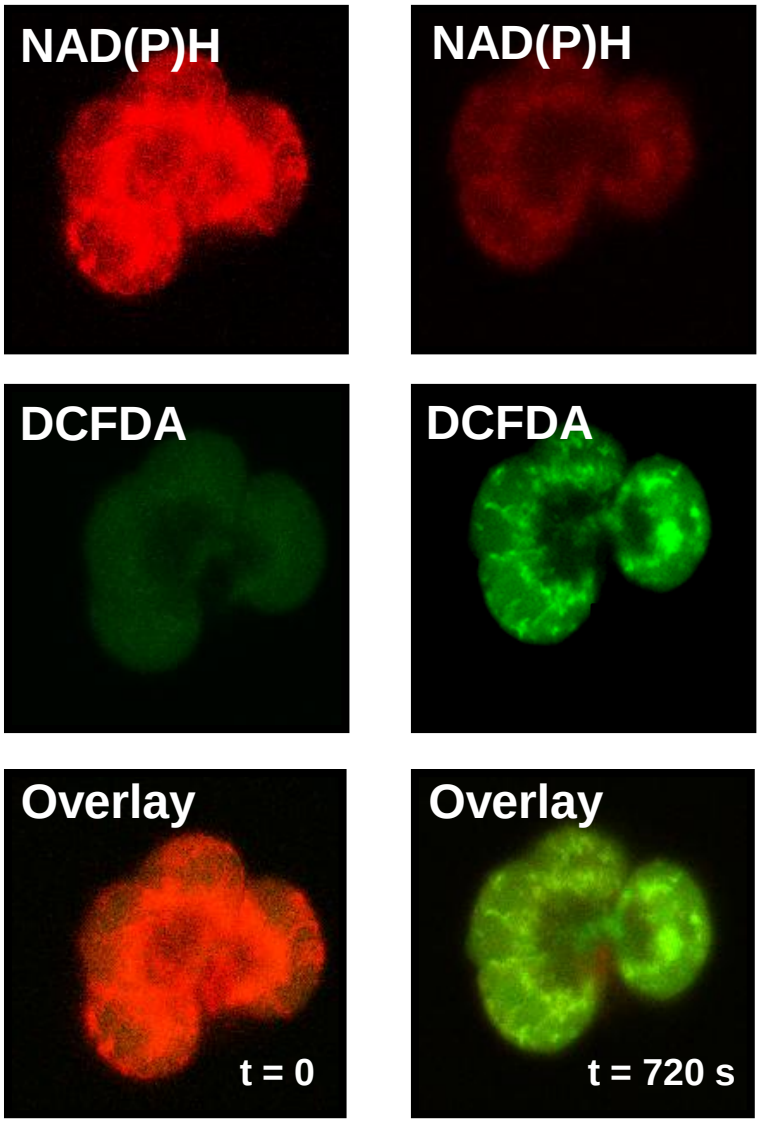

Figure 3.17 500 µM TLCS induced mitochondrial ROS. Typical thin slice (<2 µm) confocal fluorescent images of changes in $[ROS]_I$ and NAD(P)H induced by 500 µM TLC-S. Increases of ROS are seen within mitochondria ($[ROS]_M$) (*green*), co-localised with decreasing NAD(P)H (*red*) autofluorescence indicative of impaired mitochondrial metabolism, in characteristic peri-granular, peri-nuclear and sub-plasmalemmal locations.

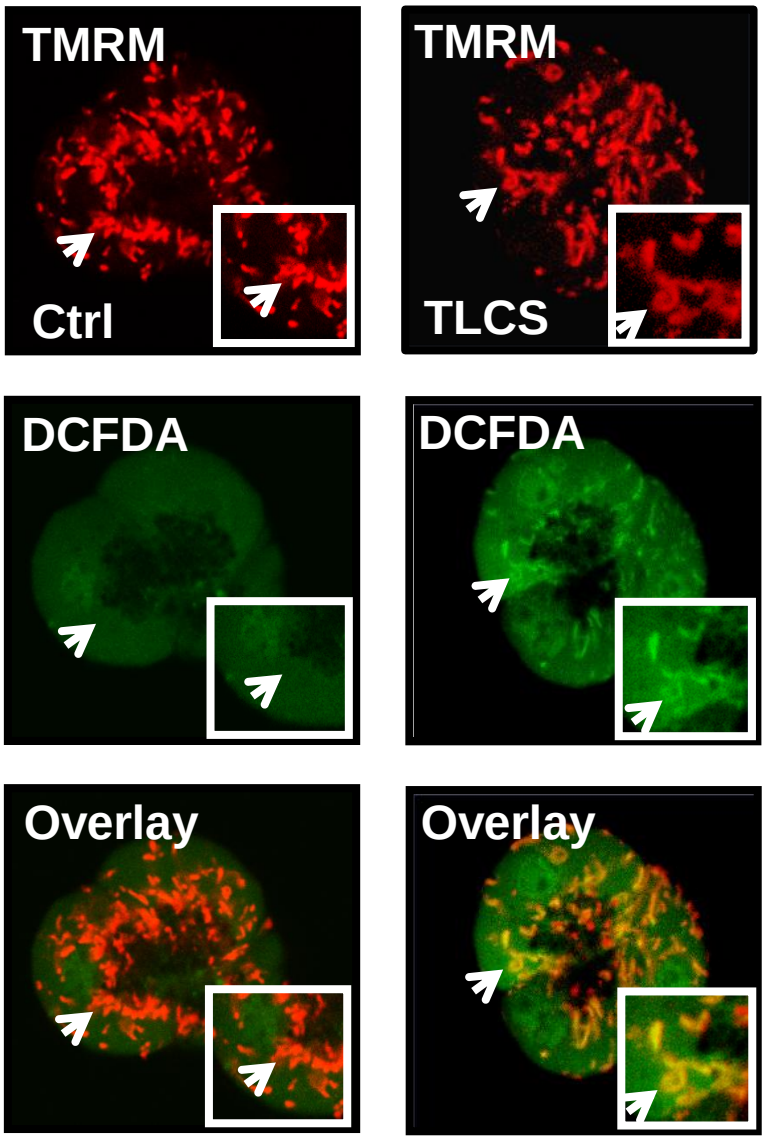

Figure 3.18 Mitochondrial ROS co-localised with mitochondria. Typical thin slice (<2 µm) confocal fluorescent images of changes in $[ROS]_I$ and NAD(P)H induced by 500 µM TLC-S. Increases of ROS are seen within mitochondria ($[ROS]_M$) (*green*), co-localised with the mitochondria specific dye TMRM (*red*) forming a yellow structures in characteristic peri-granular, peri-nuclear and sub-plasmalemmal locations

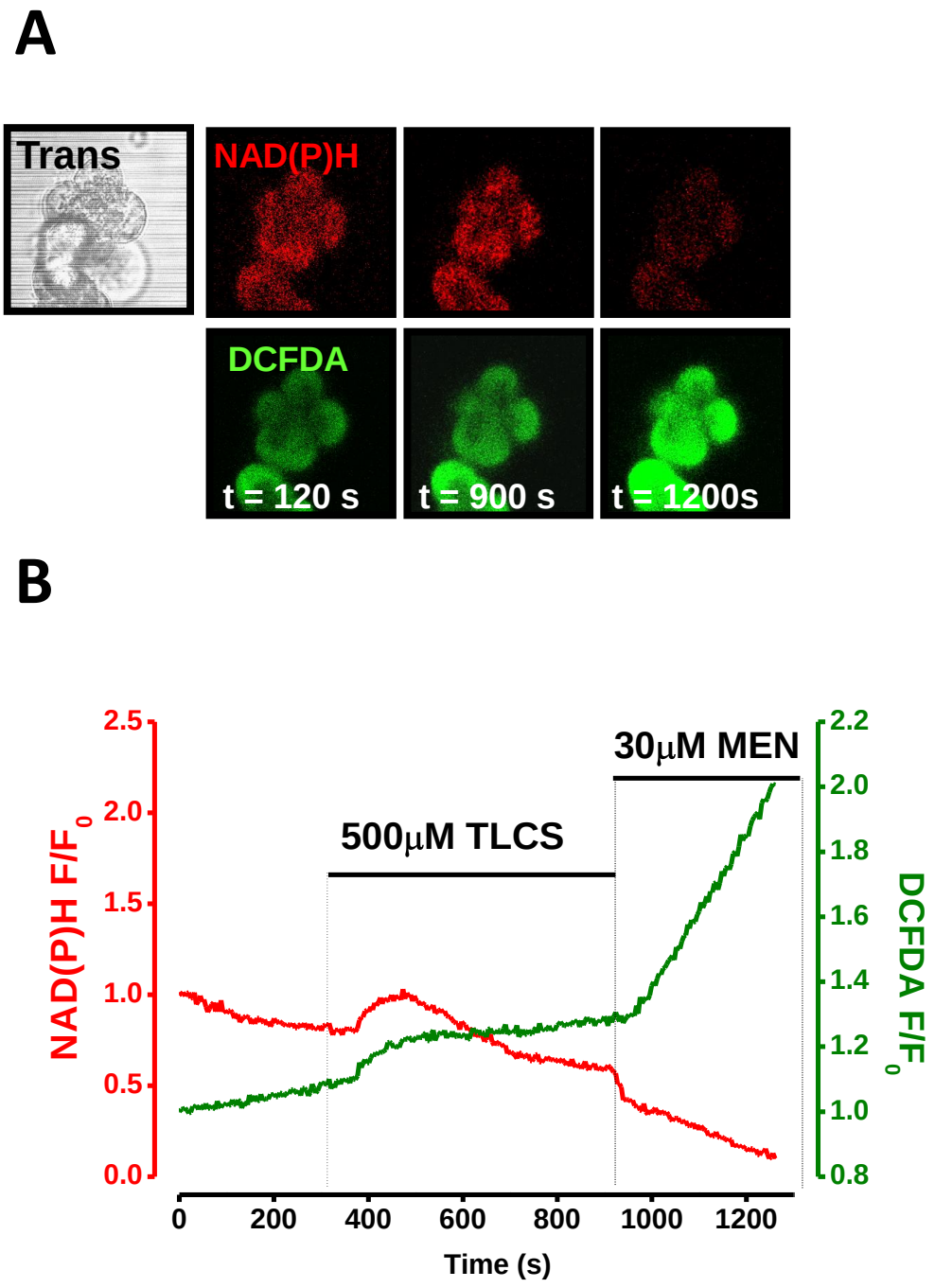

Figure 3.19 Increases in the intracellular concentration of reactive oxygen species ($[ROS]_I$) induced by TLC-S in isolated murine pancreatic acinar cells. (A) Transmitted, CM-H_2DCFDA fluorescence (*green*) and NAD(P)H autofluorescence images of a group of murine acinar cells showing changes in NAD(P)H and increases of $[ROS]_I$ induced by 500 μM TLC-S; increases of $[ROS]_I$ induced by menadione (MEN: 30 μM) are shown at the end as a positive control. (B) Representative traces from experiments on isolated murine pancreatic acinar cells demonstrating an increase of $[ROS]_I$ in response to 500 μM TLC-S, changes of NAD(P)H (red) occurred in tandem immediately following rises of $[ROS]_I$ induced by 500 μM TLC-S, (n = 21 of 21 cells). Data are shown as normalized changes from basal (pre-stimulation) fluorescence levels (F/F_0).

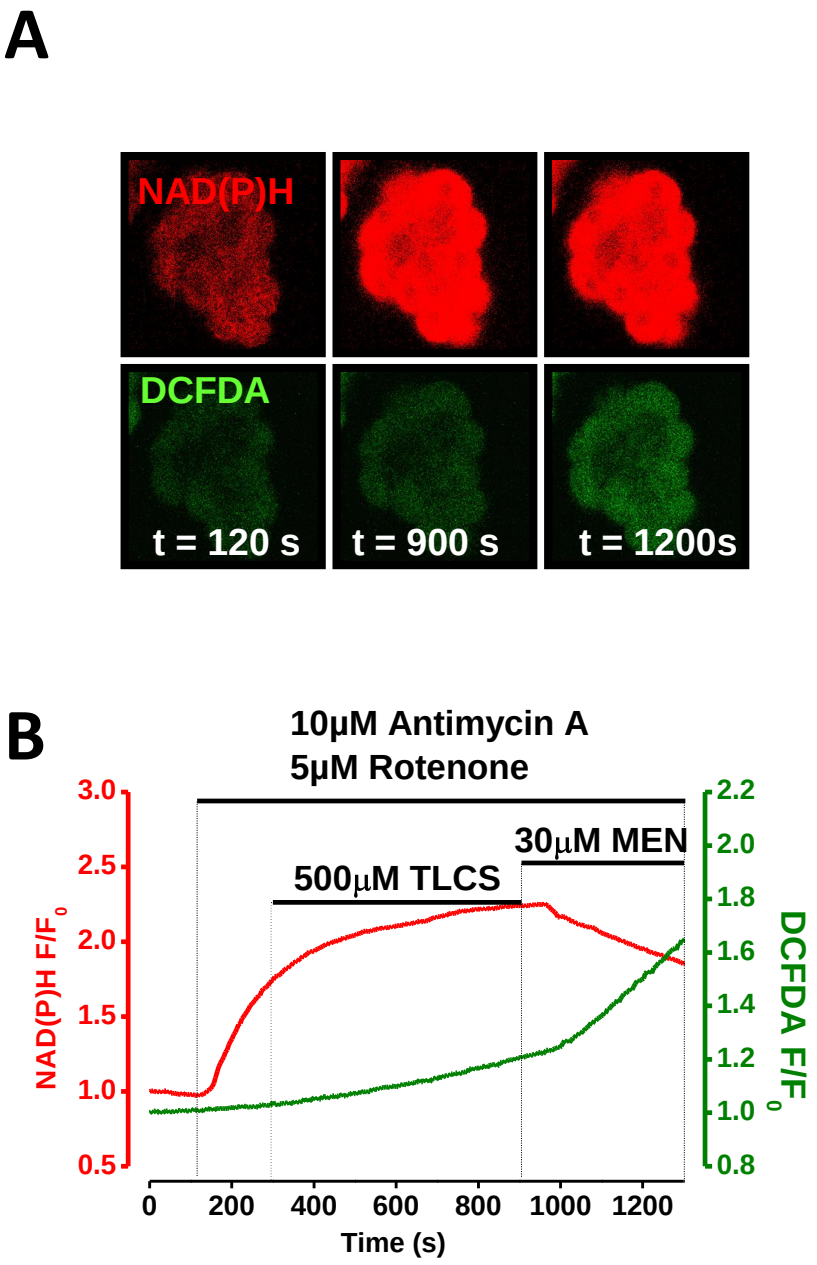

Figure 3.20 Effects of mitochondrial electron transport on the intracellular concentration of reactive oxygen species ($[ROS]_I$) induced by TLC-S in isolated murine pancreatic acinar cells. (A) Transmitted, CM-H_2DCFDA fluorescence (*green*) and NAD(P)H autofluorescence images of a group of murine acinar cells showing changes in NAD(P)H and $[ROS]_I$ induced by 500 μM TLC-S; increases of $[ROS]_I$ induced by menadione (MEN: 30 μM) are shown at the end as a positive control. (B) Representative traces from experiments on isolated murine pancreatic acinar cells demonstrating an no increase of $[ROS]_I$ in response to 500 μM TLC-S in the presence of Antimycin A and Rotenone, changes of NAD(P)H (red) occurred in tandem immediately following application of Antimycin A and Rotenone, (n = 34 of 34 cells). Data are shown as normalized changes from basal (pre-stimulation) fluorescence levels (F/F_0).

rotenone and antimycin A alone had no effect on the rate of $[ROS]_I$ production compared to control but always produced a large increase of NAD(P)H autofluorescence (18 of 18 cells data not shown).

3.7 Relative importance of $[Ca^{2+}]_C$, $[Ca^{2+}]_M$ and $[ROS]_I$ in pancreatic acinar cell fate

Incubation of isolated murine acinar cells in the presence of the oxidant menadione (MEN; 30 µM) the antioxidant *N*-acetyl-L-cysteine (NAC; 10 mM) or a combination of both produced differential effects on overall cell death. Antioxidant treatment alone had no significant effect on apoptosis (Figure 21B; *white*) or necrosis (Figure 21B; *grey*). Application of the oxidant menadione (MEN; 30 µM) produced significant increase in the number of cells exhibiting bright fluorescence of the fluorescent-indicator linked general caspase substrate (Figure 21A; *green,* Figure 21B; *white*). The changes in caspase activation as measured by the fluorescent general caspase substrate were completely abolished by simultaneous incubation with antioxidant (MEN; 10 mM, Figure 21A and B). Data are presented as mean ± s.e. mean, (number of cells in parenthesis).

Simultaneous detection of apoptosis and necrosis was applied to the agonist TLC-S. Unlike the oxidant menadione (Figure 21), TLC-S induced significant necrosis as visualized by propidium iodide fluorescence (Figure 22; *red*). Application of TLC-S at 200 µM and 500 µM evoked a concentration-dependent rise in both necrosis (Figure 23A; *grey*) and apoptosis (*white*). After 30 min application of 200 µM and 500 µM TLC-S respectively, 13.3% (n = 96 of 724) and 15.3% (n = 221 of 1446) were apoptotic; 24.7% (n = 179 of

724) and 48.6% (n = 703 of 1446) were necrotic (Figure 3.23 A). In contrast 10min pre-incubation with BAPTA, loaded in AM form, produced a marked decrease in visible necrotic cells (Figure 22A; *red*). Overall a reduction of necrosis was observed, decreasing by 63.4% at 200 µM and 65.7% at 500 µM TLC-S respectively, (Figure 3.22 B *grey*).

Experiments were undertaken to alter $[ROS]_I$ production and/or clearance to assess directly the role of $[ROS]_I$ on apoptosis and necrosis induced by TLC-S. NAC (10 mM) pre-treatment diminished TLC-S-induced apoptosis by 81.7% with 200 µM TLC-S and by 64.9% with 500 µM TLC-S (Figure 3.23 B; *white*). At 500 µM TLC-S, NAC significantly increased necrosis by 34.8%, although no difference was detected at

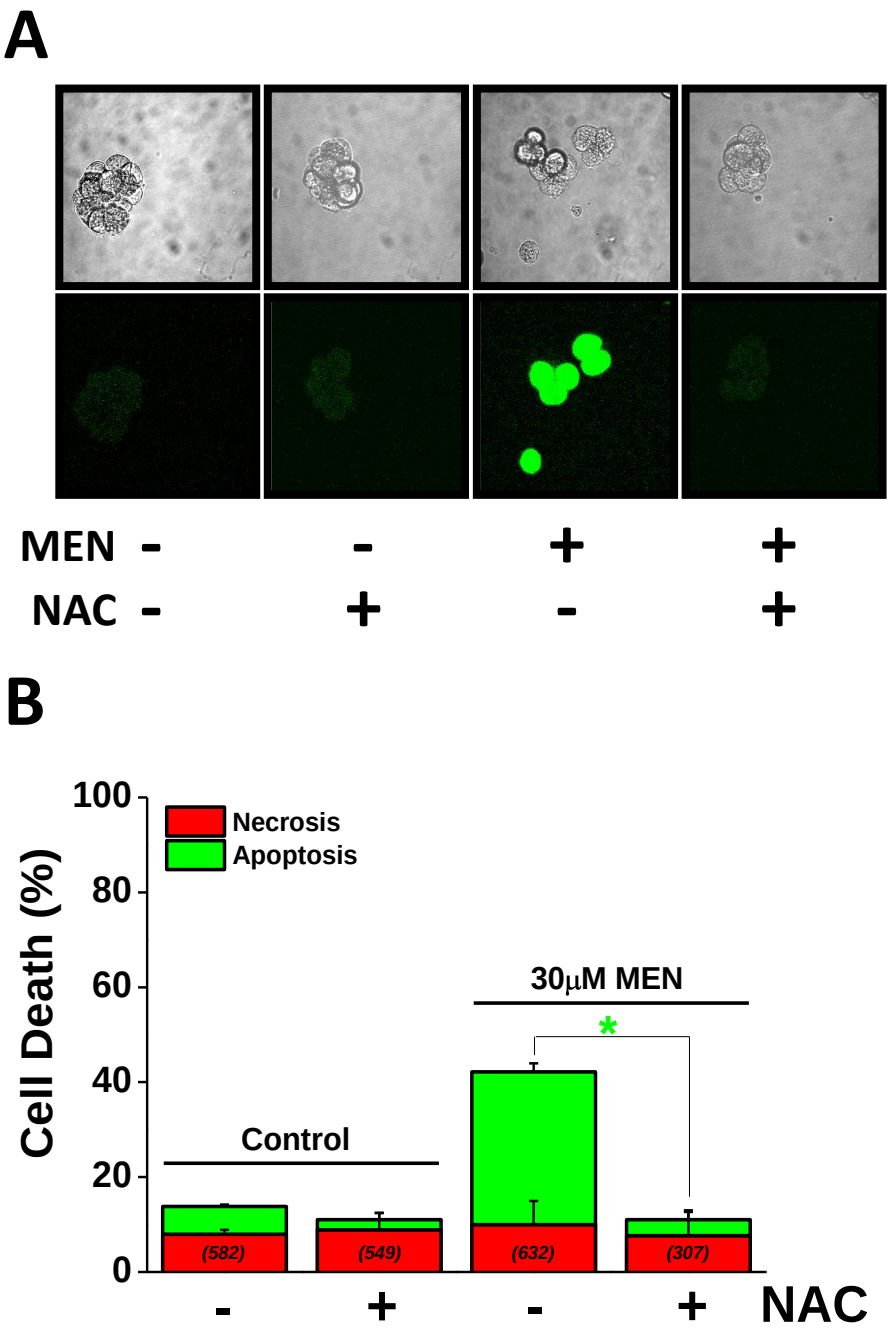

Figure 3.21 Menadione-induced reactive oxygen species cause antioxidant-sensitive apoptosis. Effects of NAC (10 mM) on 30 μM MEN-induced pancreatic acinar cell death. (A) Transmitted and fluorescent general caspase substrate (*green*) images of murine pancreatic acinar cells showing that apoptosis induced by MEN was completely prevented by the antioxidant NAC. (B) Chart depicting the increase in caspase activation by MEN as completely abolished by NAC (* = P = < 0.05). All data are presented as mean ± s.e. mean (number of cells shown in parentheses).

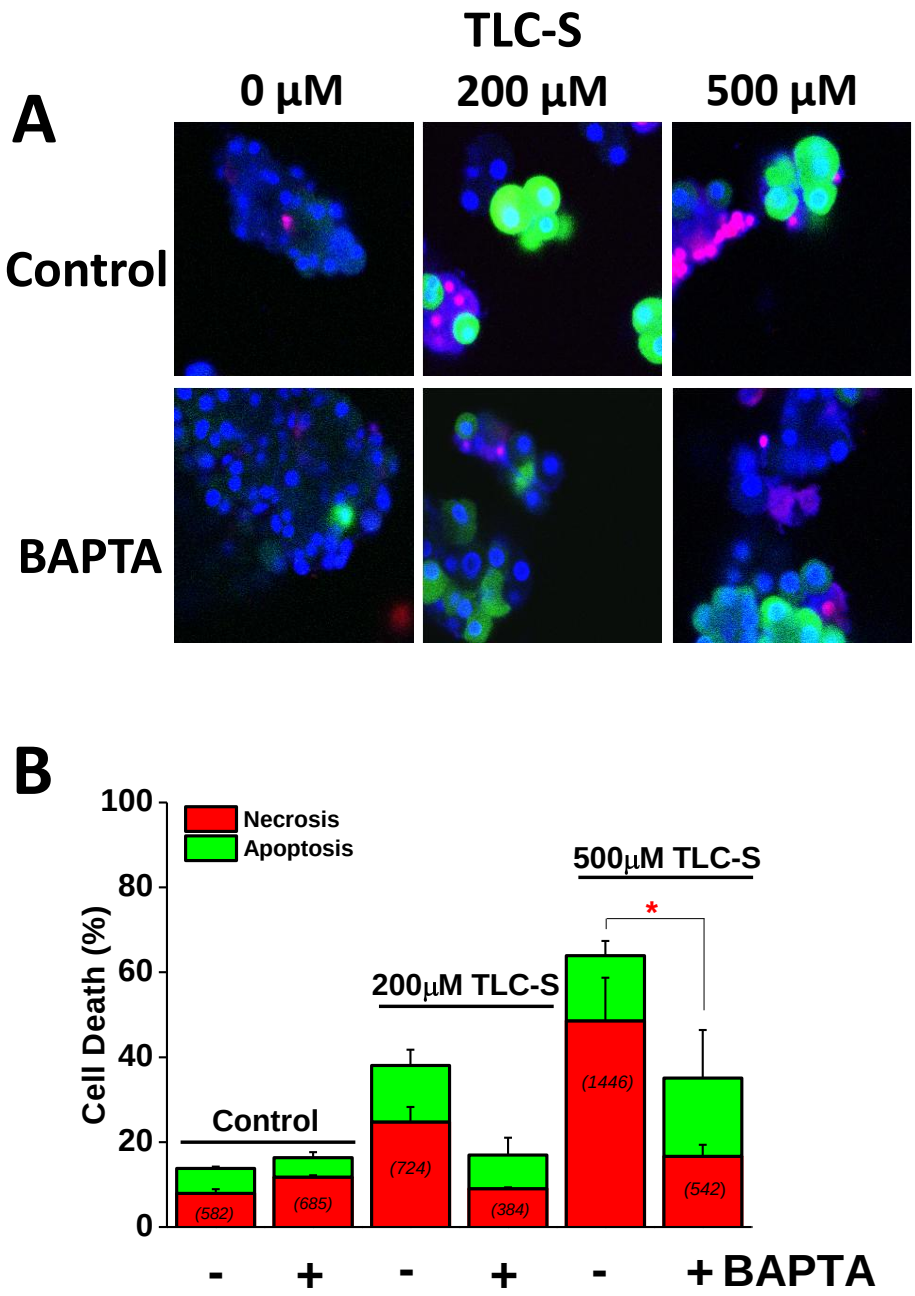

Figure 3.22 Chelation of intracellular calcium reduces pancreatic acinar cell necrosis. Effects of changes made in $[Ca^{2+}]_C$ and $[Ca^{2+}]_M$ using the intracellular Ca^{2+} chelator BAPTA-AM (10 min pre-treatment with Ca^{2+} in external medium) on pancreatic acinar cell death pathways induced by TLC-S. A) Representative images of apoptosis, detected with a fluorescent general caspase substrate *(green)*, necrosis, detected with propidium iodide *(red)*, and all cells, stained with the nuclear stain Hoechst 33342 *(blue)*. With 30 min exposure to increasing concentrations of TLC-S, a progressive increase in both apoptosis and necrosis is seen, while BAPTA-AM has reduced the relative number of necrotic cells. B) Total percentages (mean $\pm$ s.e. mean) of apoptotic and necrotic cells following 30 min exposure to increasing concentrations of TLC-S, showing chelation of intracellular Ca^{2+} with BAPTA-AM significantly (* = P = < 0.05) reduced necrotic and total cell death induced by the bile acid. The BAPTA-AM protocol also resulted in a relative increase in apoptosis induced by the bile acid, most evident at 500 µM TLC-S.

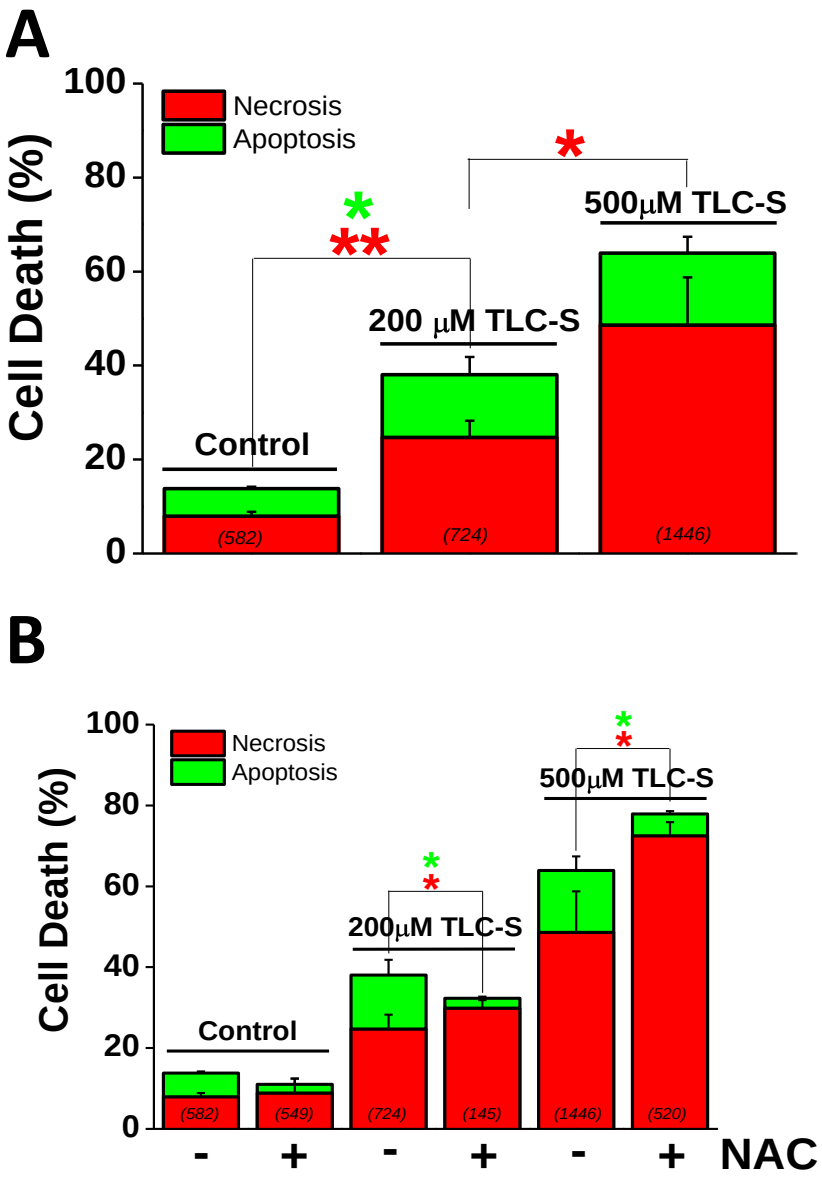

Figure 3.23 Antioxidant treatment abolishes acinar cell apoptosis. Effects of Increasing concentrations of TLCS and Antioxidant treatment on cell fate in murine pancreatic acinar cells. (A) Cells exhibited a concentration-dependent increase in overall cell death, (also seen in B) both apoptosis and necrosis, when exposed to increasing concentrations of TLCS. (B) The antioxidant NAC had no significant effects alone, but abolished the apoptosis stimulated by TLCS. At the higher concentration of TLCS, NAC markedly increased necrosis. TLC-S induced a concentration-dependent increase in both apoptosis and necrosis. The antioxidant NAC (10 mM) markedly reduced apoptosis at both concentrations of TLC-S, while necrosis and total cell death induced by 500 μM TLC-S were increased. All data are presented as mean ± s.e. mean (number of cells shown in parentheses) (* = P = < 0.05).

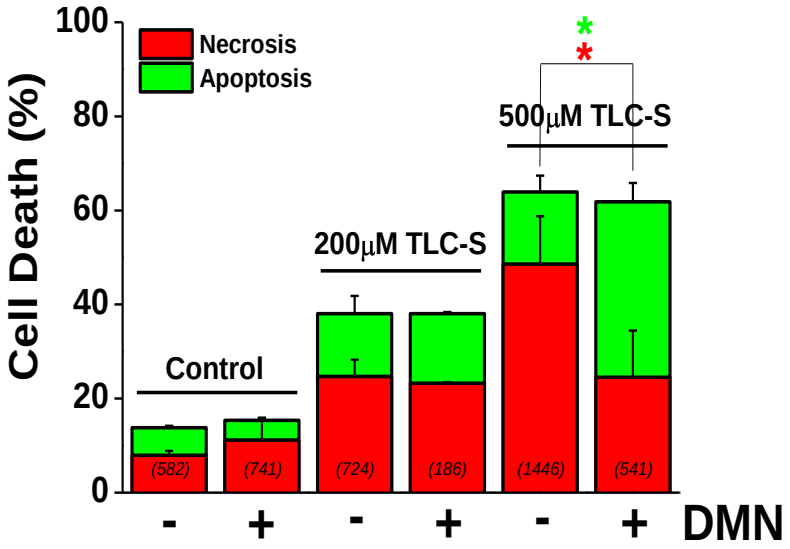

Figure 3.24 Inhibition of NQO1 promotes apoptosis and reduces necrosis in pancreatic acinar cells. Effects of agents changing $[ROS]_I$ on pancreatic acinar cell death pathways induced by TLC-S DMN (30 μM), an inhibitor of the cytosolic antioxidant NQO1, increased the proportion of apoptotic cells induced by 200 μM and 500 μM TLC-S, whilst concomitantly reducing necrosis.

All data are presented as mean ± s.e. mean (number of cells shown in parentheses) (* = P = < 0.05).

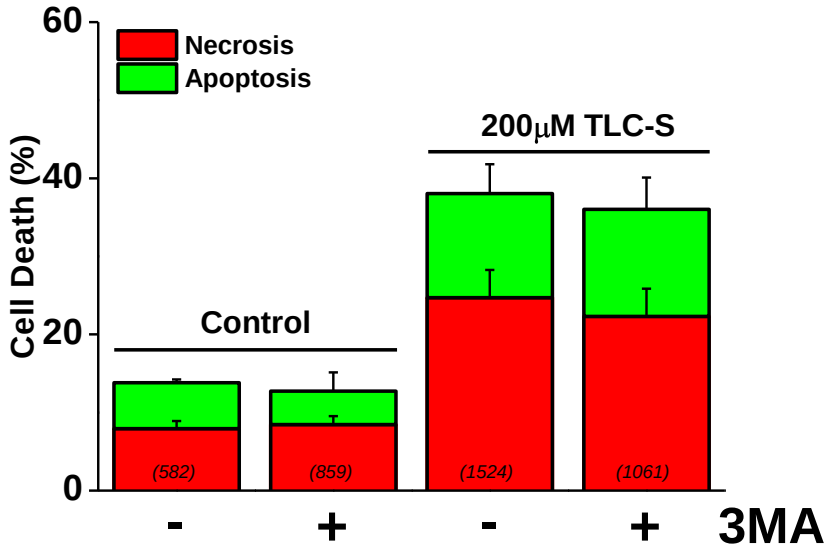

Figure 3.25 Inhibition of autophagy does not change cell fate in pancreatic acinar cells. Effect of the inhibition of autophagy on cell death induced by TLC-S in isolated murine pancreatic acinar cells. Specific inhibition of autophagy with 3-methyladenine (3-MA 5 mM) had no effect on caspase activation or necrosis *per se*. In the presence of 200 μM TLC-S necrosis (*grey*) and caspase activation (*white*) displayed no significant difference. All data are presented as mean ± s.e. mean (number of cells shown in parentheses).

200 µM TLC-S (Figure 23B; *grey*). NAC did not, however, affect $[Ca^{2+}]_C$ elevations nor NAD(P)H depletion induced by 500 µM TLC-S (n = 10 of 10; data not shown). NQO1 inhibition with DMN (30 µM) caused no significant reduction of total cell death *per se*, however it increased TLC-S-induced apoptosis by 37.5% at 200 µM TLC-S and by 44.3% at 500 µM TLC-S, simultaneously reducing necrosis by 24.3% and 36.2% respectively (Figure 3.24).

Autophagy has been demonstrated to have a significant role in the pathogenesis of acute experimental pancreatitis (Hashimoto et al., 2008). To establish the role of autophagy on pancreatic acinar cell fate, autophagy was prevented with the specific inhibitor 3-methyladenine (3MA; 5 mM). Inhibition of autophagy had no significant effect on acinar cell fate *per se*, In the presence of 200 µM TLC-S no significant effect was seen on necrosis or apoptosis (Figure 3.25; *grey* and *white* respectively).

Long term culture of murine pancreatic acinar cells (> 16 hrs) was used to establish apoptosis and necrosis by alternative means. Late stage apoptosis is characterised by chromatin condensation visualised by acridine orange aggregation (Figure 3.26 A; acridine orange; *green*) co localising with the nucleus (Figure 3.26 A; Hoechst 33342; *blue*), while necrosis is visualised by the presence of ethidium bromide fluorescence (Fig 3.26 A; *red*) in the nucleus. The method showed that promotion of $[ROS]_I$ by inhibition of NQO1 (DMN; 30 µM) reduced necrosis (Figure 3.26 B; *white;* 2.5% of total cell death) and increased apoptosis (Figure 3.26 B; *green;* 7.29% of total cell

death) compared to 200 µM TLC-S alone. Antioxidant treatment (NAC; 10mM) significantly reduced apoptosis (3.25 B; *green; 7.74%* of total cell death) and increased necrosis (Figure 3.25 B; *red;* 20.47%of total cell death).

The same method was used to evaluate the role of autophagy. Autophagy was promoted with rapamycin (Rap; 100 nM) or inhibited with 3-methyladenine (3MA; 5 mM). Neither inhibition nor promotion of autophagy significantly abrogated overall cell death (Figure 3.27).

The increase in apoptosis was completely reversed by NAC, confirming the dependence of MEN-induced apoptosis on ROS production. Taken together the data indicate that $[ROS]_I$ and $[ROS]_M$ elevations induce death of acinar cells predominantly by apoptosis, whereas sustained $[Ca^{2+}]_C$ and $[Ca^{2+}]_M$ elevations are major triggers of necrosis.

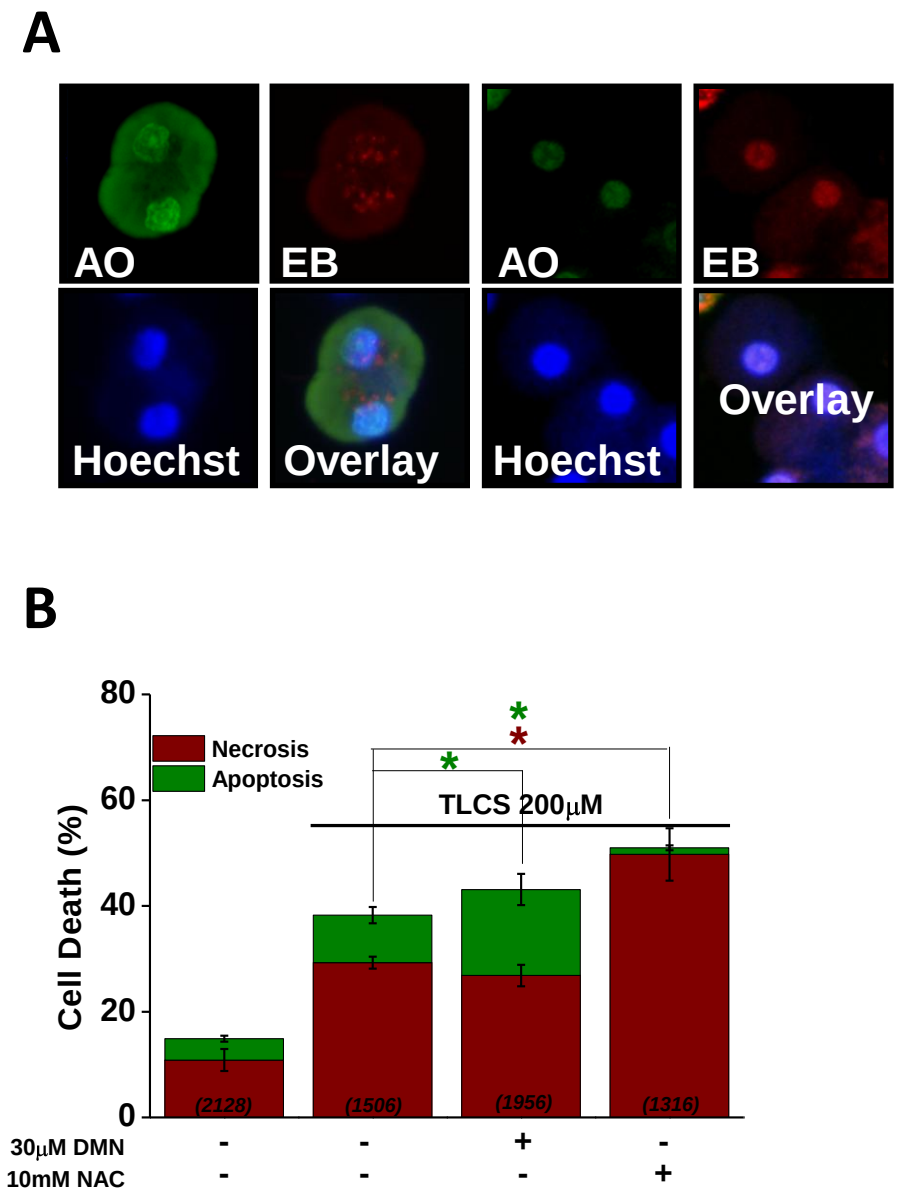

Figure 3.26 Promotion and inhibition of ROS change cell fate. Effect of agents changing $[ROS]_l$ on pancreatic acinar cell death pathways induced by TLC-S (A) Representative images of apoptosis: acridine orange, (AO) staining throughout the cytoplasm with brightly stained nuclei *(green)* and necrosis: loss of cytoplasmic AO staining and ethidium bromide within the nucleus *(red)*. All nuclei were stained with Hoechst 33342 *(blue)*. (B) With 3 h stimulation with TLC-S and 11 h incubation with pro/anti oxidants, increases in both apoptosis and necrosis are seen. NAC (10 mM) markedly reduces apoptosis as measured by chromatin condensation, while necrosis and total cell death are increased. DMN (30 μM) increased apoptosis and reduced necrosis as seen in (Fig. 5 B). All data are presented as mean ± s.e. mean (number of cells shown in parentheses) (* = P = < 0.05).

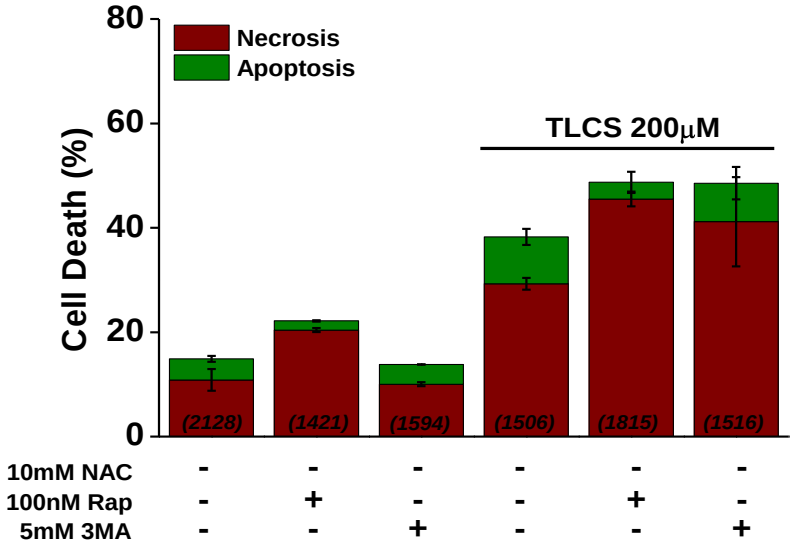

Figure 3.27 Promotion and inhibition of autophagy do not reduce cell fate. Effect of agents promoting, or inhibiting autophagy on pancreatic acinar cell death pathways induced by TLC-S. Both promotion (Rapamycin 100 nM) and inhibition (3-methyladenine 5 mM) of autophagy did not significantly reduce overall cell death. All data are presented as mean ± s.e. mean (number of cells shown in parentheses).

In conclusion, the data indicate that TLC-S promotes large increases in both $[Ca^{2+}]_C$ and $[Ca^{2+}]_M$. Without these increases the pancreatic acinar cell does not generate significant $[ROS]_I$ and $[ROS]_M$. This is shown by the lack of $[ROS]_I$ and $[ROS]_M$ response when intracellular calcium is chelated with BAPTA. However, when $[ROS]_I$ is effectively scavenged with NAC, the apoptotic response to TLC-S is lost. Necrosis is unaffected by NAC and is only significantly abrogated by BAPTA. These data suggest that $[ROS]_I$ and $[ROS]_M$ elevations induce cell death in acinar cells predominantly by apoptosis, whereas large, sustained $[Ca^{2+}]_C$ and $[Ca^{2+}]_M$ elevations are major triggers of necrosis.

The alternative combination of AO and EB (Figure 3.26 and 3.27) confirmed the patterns of cell death identified by rhodamine 110-aspartic acid amide and PI, since DMN with TLC-S induced an increase in chromatin condensation without plasma membrane rupture compared to TLC-S alone, while NAC with TLC-S induced the reverse (Figure 3.5 C). Neither stimulation (RAP) nor inhibition (3MA) of autophagy significantly altered and did not lessen total cell death pathway activation obtained with TLC-S compared to TLC-S alone (Figure 3.5 C), although there was a tendency towards more plasma membrane rupture with both, significant in the case RAP (as with RAP alone in control cells), presumed due to non-specific effects.

Chapter 4

Results: Effects of ethanol and its metabolites on reactive oxygen species production in the pancreatic acinar cell

4.1 Introduction

Strong evidence suggests that radical species may be produced as a by-product of the oxidative metabolism of ethanol to substances such as acetaldehyde and acetate via cytochrome P450 2 E1 (CYP2E1) (Cederbaum, 2003) or from the electron transport chain within the mitochondria (Lumeng and Crabb, 2000). As such, the aim of the experiments within this chapter was to determine the effect of ethanol and its metabolites, both oxidative and non-oxidative, on the generation of ROS in the freshly isolated murine pancreatic acinar cell.

4.2 Ethanol and acetaldehyde cause varied effects on $[ROS]_I$ and NAD(P)H autofluorescence

Freshly isolated murine pancreatic acinar cells were loaded with the ROS-sensitive indicator DCFDA loaded in carboxy-methylester (CM) form. Perfusion of increasing concentrations of ethanol (EtOH; 10-850 mM) produced varied results. In all cases 10-100mM EtOH was unable to increase the basal rate of $[ROS]_I$ production as demonstrated by the increase in fluorescence (Figure 4.1 A; *green*) and representative trace (Figure 4.1 B 24 of 24 cells). Perfusion of 850mM produced a sharp increase in the level of DCFDA fluorescence in some cells (17 of 24 cells) along with the appearance of bleb structures (12 of 24 cells). At the end of the experiment the oxidant menadione was added as a positive control (Figure 3.1 A and B showing increased $[ROS]_I$). The change in $[ROS]_I$ was accompanied by a fall in the level of intracellular NAD(P)H (Figure 3.1 A and B; *red*), this was

pronounced upon perfusion with 850 mM. Data are displayed as normalized changes from basal (pre-stimulation) fluorescence levels (F/F_0).

As previously demonstrated with TLC-S, inhibition of the cytosolic antioxidant enzyme NQO1 with 1,4-dimethoxy-2-methylnaphthalene (DMN; 30 µM) was able to unmask $[ROS]_I$ generation following exposure to 200µM TLCS in the acinar cell. DMN produced no ROS alone compared to the pre-stimulated baseline (Figure 3.2A and B; *green* 16 of 16 cells), but was able to evoke a characteristic rise in NAD(P)H autofluorescence primarily in the peri-granular mitochondrial belt region (Figure 2A *red*). 100mM EtOH prevented further rise in NAD(P)H autofluorescence whereas 850 mM showed a marked depression (Figure 3.2 B *red*). Perfusion with either 100 mM or 850 mM EtOH in addition to DMN produced no increase in the level of $[ROS]_I$ production.

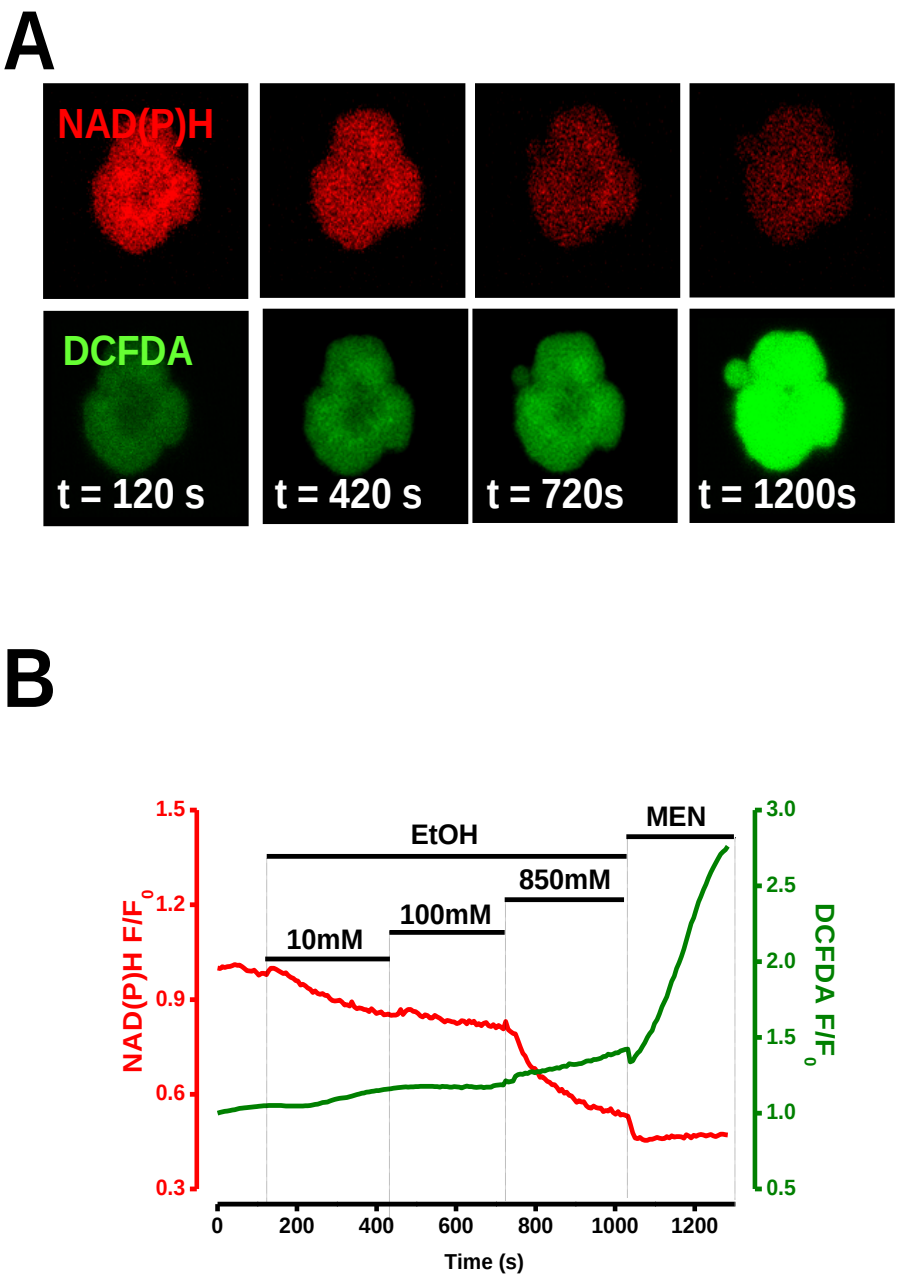

Figure 4.1 Ethanol causes minimal elevation of intracellular reactive oxygen species. Effect of ethanol (EtOH) on the generation of intracellular reactive oxygen species ($[ROS]_I$) in isolated murine pancreatic acinar cells. (A) Transmitted light, CM-H_2DCFDA fluorescence (*green*) and NAD(P)H autofluorescence (*red*) images of a triplet of murine acinar cells show the changes of $[ROS]_I$ induced by increasing concentrations of ethanol; increases of $[ROS]_I$ induced by menadione (MEN: 30 µM) are shown as a positive control. (B) Representative traces from experiments on isolated murine pancreatic acinar cells demonstrating $[ROS]_I$ response to 10,100 and 850 mM EtOH. Changes in NAD(P)H (red) occurred in tandem immediately following perfusion with Ethanol, (n = 24 cells). Data are shown as normalized changes from basal (pre-stimulation) fluorescence levels (F/F_0).

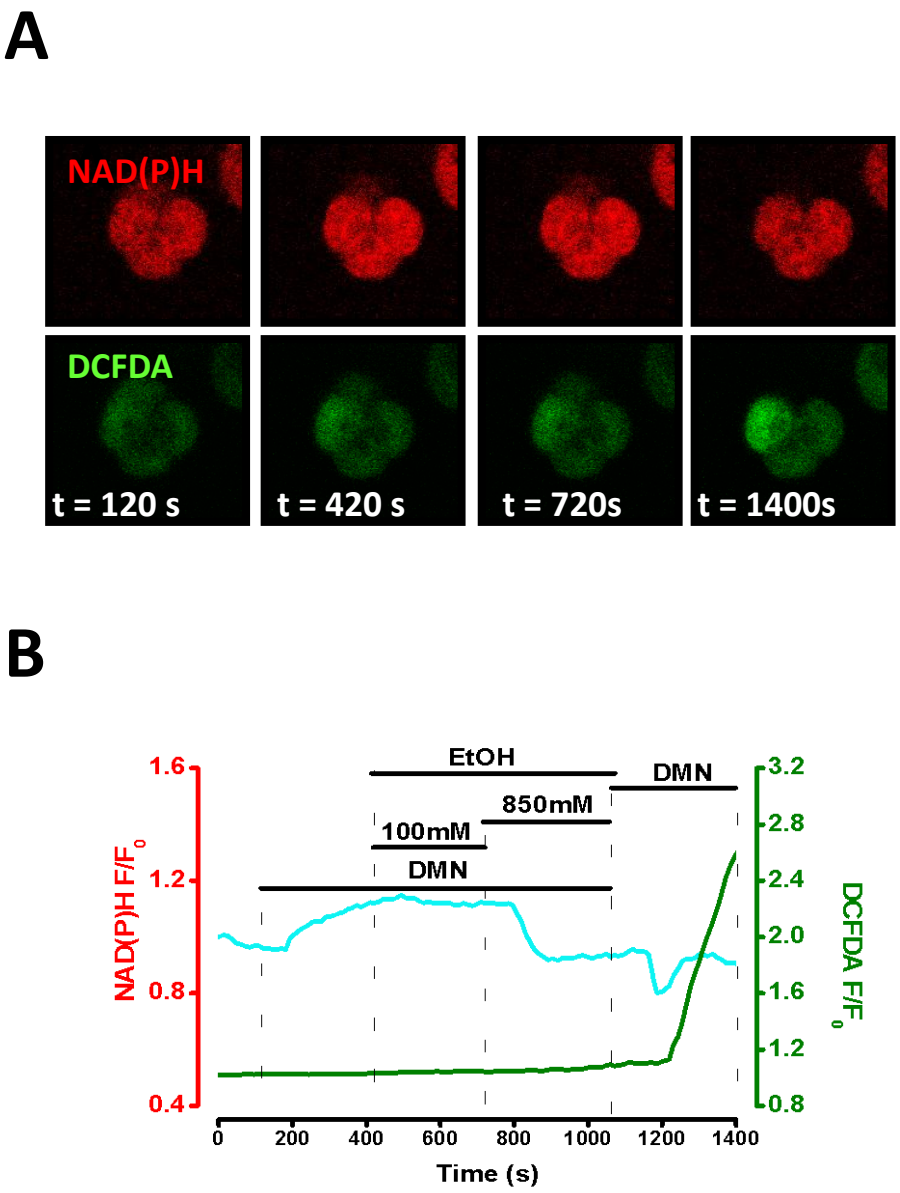

Figure 4.2 Ethanol causes minimal elevation of intracellular reactive oxygen species in the presence of NQO1 inhibition. Effect of NQO1 inhibition on the generation of intracellular reactive oxygen species ($[ROS]_I$) in response to ethanol in isolated murine pancreatic acinar cells. (A) CM-H_2DCFDA fluorescence (*green*) and NAD(P)H (*red*) autofluorescence images of a triplet of murine acinar cells show the changes of $[ROS]_I$ induced by increasing concentrations of ethanol (EtOH) during inhibition of NQO1 with DMN (1,4-dimethoxy-2-methylnaphthalene; 30 µM) increases of $[ROS]_I$ induced by menadione (MEN: 30 µM) are shown as a positive control. (B) Representative traces from experiments on isolated murine pancreatic acinar cells demonstrating $[ROS]_I$ response to 10,100 and 850mM EtOH. Changes in NAD(P)H (red) occurred in tandem immediately following perfusion with Ethanol, (n = 16 cells). Data are shown as normalized changes from basal (pre-stimulation) fluorescence levels (F/F_0).

The principal oxidative metabolite of ethanol in mammals is acetaldehyde. Ethanol is readily metabolised to acetaldehyde by alcohol dehydrogenase (ADH) and other enzymatic systems such as Cytochrome P2 E1 (CYP2E1) and peroxisomal catalase. As such, it is available in relatively high concentrations shortly after the administration of ethanol. In acinar cells loaded with DCFDA, perfusion of acetaldehyde in increasing concentrations (10-200 µM) produced no detectible increase in $[ROS]_{I.}$ As measured by DCFDA fluorescence (Figure 3.3A and B; *green*). Contemporaneous measurements of NAD(P)H autofluorescence show a stepwise, concentration-dependent increase (Figure 3B; *red*) in a punctuate distribution associated with mitochondria in the acinar cell (Figure 3.3A; *red* 18 of 18 cells). At the end of the experiment the oxidant menadione (MEN; 30 µM) was applied to produce a maximal effect.

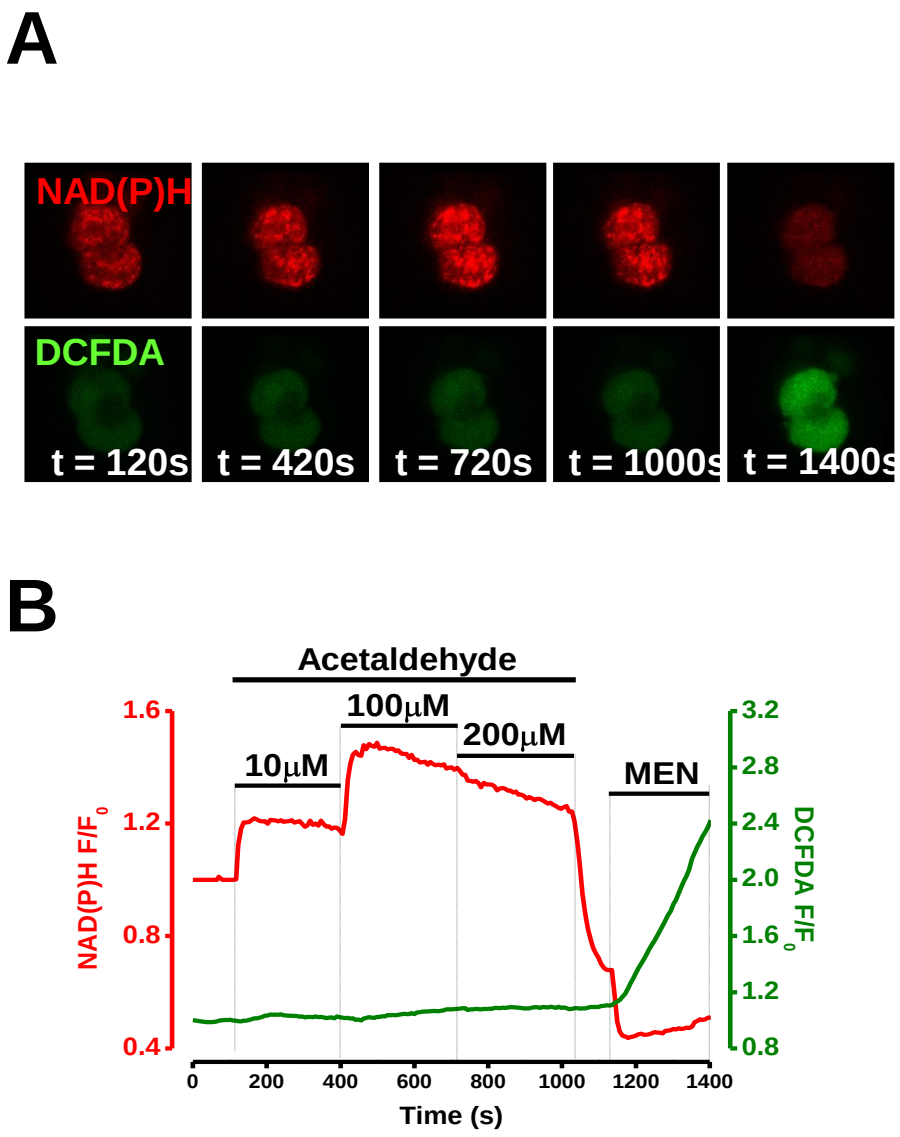

Figure 4.3 Acetaldehyde causes minimal elevation of intracellular reactive oxygen species. Effect of acetaldehyde on the generation of intracellular reactive oxygen species ($[ROS]_I$) in isolated murine pancreatic acinar cells. (A) CM-H_2DCFDA fluorescence (*green*) and NAD(P)H autofluorescence (*red*) images of a doublet of murine acinar cells show the changes of $[ROS]_I$ induced by increasing concentrations of acetaldehyde; increases of $[ROS]_I$ induced by menadione (MEN: 30 μM) are shown as a positive control. (B) Representative traces from experiments on isolated murine pancreatic acinar cells demonstrating $[ROS]_I$ response to 10,100 and 200 μM EtOH. Changes in NAD(P)H (red) occurred in tandem immediately following perfusion with acetaldehyde, (n = 18 cells). Data are shown as normalized changes from basal (pre-stimulation) fluorescence levels (F/F_0).

4.3 Fatty acids and fatty acid ethyl esters produce no change in intracellular ROS but deplete NAD(P)H

Application of non-oxidative ethanol metabolites to pancreatic acinar cells loaded with the $[ROS]_{I}$-sensitive indicator DCFDA revealed no overall increase in $[ROS]_{I.}$ production. The free fatty acid, palmitoleic acid (POA) and its ethyl ester, palmitoleic acid ethyl ester (POAEE) were without effect (POA; Figure 3.4 A and B *green* 21 of 21 cells. POAEE Figure 4.5A and B *green* 19 of 19 cells). The oxidant menadione (MEN; 30 µM) was applied at the end of the experiment in all case to ensure the cells were capable of a response. The response of NAD(P)H autofluorescence was similar in the case of both non-oxidative metabolites. Upon application there was a small increase followed immediately by a prolonged downward trend which did not recover or deplete further upon application of menadione (POA; Figure 4.4A and B *red* 21 of 21 cells. POAEE Figure 4.5 A and B *red* 19 of 19 cells).

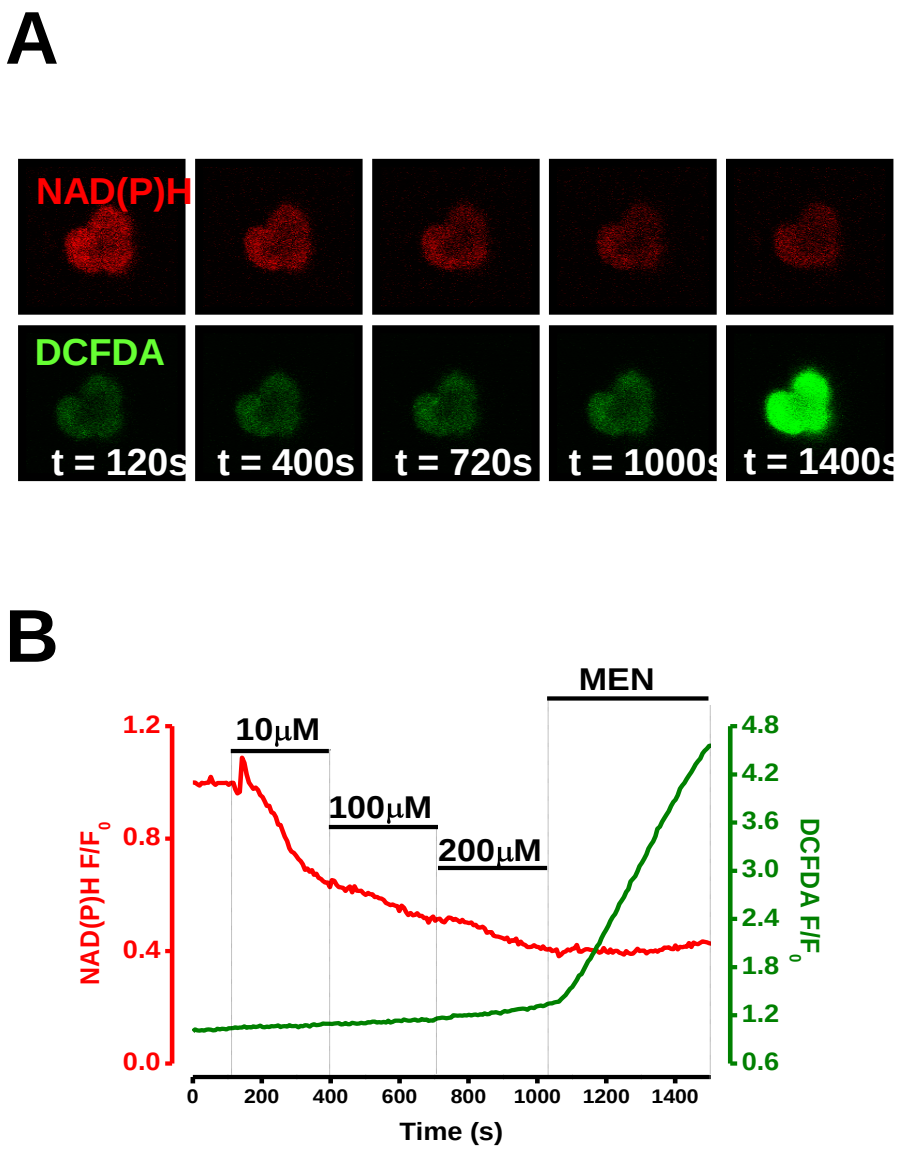

Figure 4.4 Palmitoleic acid causes minimal elevation of intracellular reactive oxygen species. Effect of palmitoleic acid on the generation of intracellular reactive oxygen species ($[ROS]_I$) in isolated murine pancreatic acinar cells. (A) CM-H_2DCFDA fluorescence (*green*) and NAD(P)H autofluorescence (*red*) images of a triplet of murine acinar cells show the changes of $[ROS]_I$ induced by increasing concentrations of palmitoleic acid (POA); increases of $[ROS]_I$ induced by menadione (MEN: 30 μM) are shown as a positive control. (B) Representative traces from experiments on isolated murine pancreatic acinar cells demonstrating $[ROS]_I$ response to 10,100 and 200 μM POA. Changes in NAD(P)H (red) occurred in tandem immediately following perfusion with acetaldehyde, (n = 21 cells). Data are shown as normalized changes from basal (pre-stimulation) fluorescence levels (F/F_0).

A

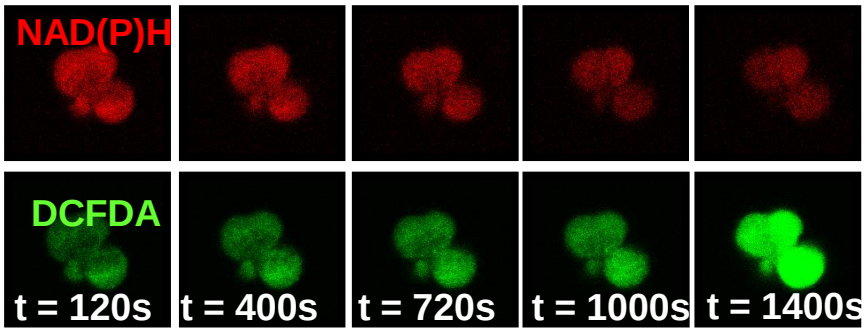

B

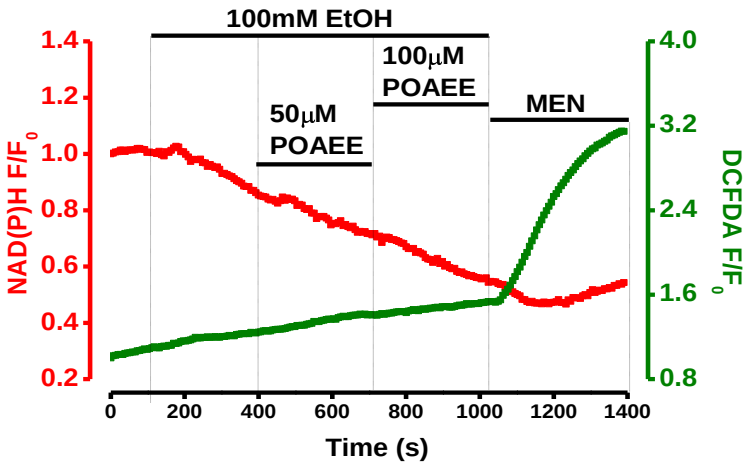

Figure 4.5 Palmitoleic acid ethyl ester causes minimal elevation of intracellular reactive oxygen species. Effect of palmitoleic acid ethyl ester on the generation of intracellular reactive oxygen species ($[ROS]_I$) in isolated murine pancreatic acinar cells. (A) CM-H_2DCFDA fluorescence (*green*) and NAD(P)H autofluorescence (*red*) images of a triplet of murine acinar cells show the changes of $[ROS]_I$ induced by increasing concentrations of palmitoleic acid ethyl ester (POAEE); increases of $[ROS]_I$ induced by menadione (MEN: 30 μM) are shown as a positive control. (B) Representative traces from experiments on isolated murine pancreatic acinar cells demonstrating $[ROS]_I$ response to 10,100 and 200 μM POAEE. Changes in NAD(P)H (red) occurred in tandem immediately following perfusion with acetaldehyde, (n = 19 cells). Data are shown as normalized changes from basal (pre-stimulation) fluorescence levels (F/F_0).

Chapter 5

Results: effects of ethanol metabolism on pancreatic acinar cell fate

5.1 Introduction

Excessive ethanol consumption is the principal cause of pancreatitis, however the realitively mild effects of ethanol on critical pathological indicators such as $[Ca^{2+}]c$ suggest that non oxidative metabolites, FAEEs may have a central role (Criddle et al., 2004). FAEEs and FA's exogenously applied may mediate necrosis in isolated acinar cells, however the relative contributions of apoptosis and necrosis have not been previously assessed. Furthermore, measurement of cell death in the presence of agents manipulating ethanol metabolism may provide insights into the mechanism of both non-oxidative metabolite generation and the subsequent effects of those metabolites.

5.2 Ethanol and acetaldehyde produce opposing effects upon pancreatic acinar cell fate.

Acutely isolated murine pancreatic acinar cells were loaded with a fluorescent general caspase substrate (Rhodamine-110 bis-(L-aspartic acid amide); 20 µM; Molecular Probes) for the detection of intracellular caspase activation in response to a selection of agents. Detection of necrosis is achieved by the addition of propidium iodide (1µM; Sigma, Gillingham). Incubation of isolated murine acinar cells in the presence of ethanol (EtOH) showed an increase in necrosis associated with increasing concentrations of ethanol (Figure 5.1 A; *grey*). Although concentrations of ethanol used were high (100-850 mM) the increase in necrotic cell death was relatively modest; 850 mM induced a 3.4 fold increase compared to control (10.9 Vs. 37.3%). Apoptosis, as measured by caspase activation, was not significantly affected at any concentration with the exception of 850mM where a 2.3 fold inhibition

was produced (11.17 Vs. 4.8%). Application of the non-oxidative ethanol metabolite acetaldehyde (Ac; 100-200 µM) was without any significant effects on cell death compared to control, both necrosis (Figure 5.1 B; *grey*) and apoptosis (Figure 5.1 B; *white*) were without effect.

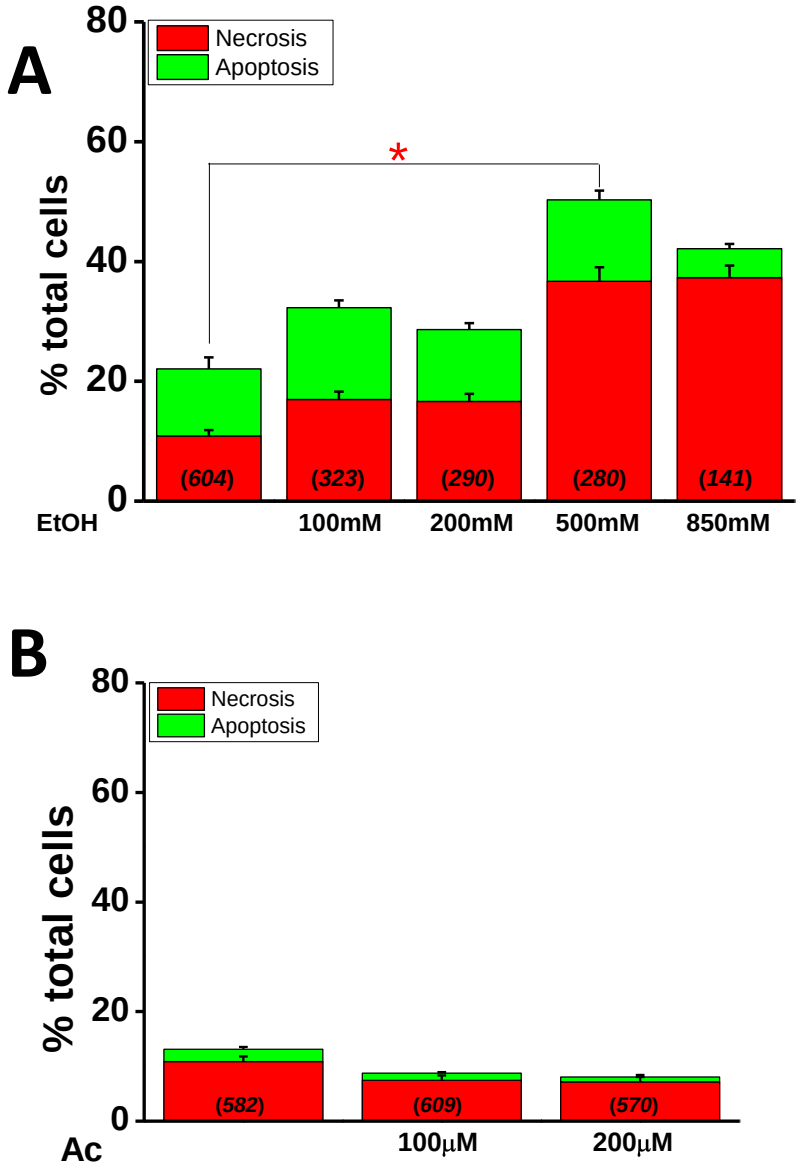

Figure 5.1. Effects of ethanol and the principal oxidative metabolite, acetaldehyde, on pancreatic acinar cell fate (A) Effects of ethanol (EtOH) 100-850 mM on necrosis (*grey*), and apoptosis (*white*). (B) Acetaldehyde (Ac) at increasing concentrations (100-200 μM) showed no overall effect on either necrosis (*grey*) or apoptosis (*white*). All data are presented as mean ± s.e. mean (number of cells shown in parentheses) (* = P = < 0.05).

5.3 Non-oxidative ethanol metabolites induce pancreatic acinar cell death

Non-oxidative ethanol metabolites such as fatty acid ethyl esters and subsequently liberated fatty acids, have previously been shown to be present in human and rodent pancreas following ethanol intake (Laposata and Lange, 1986, Werner et al., 1997) and to cause pathological changes in both in vitro and in vivo models (Criddle et al., 2004, Werner et al., 1997). The effects on the balance of overall cell death remained to be elucidated however. When applied to isolated pancreatic acinar cells, and both necrosis and apoptosis was measured the free-fatty acid palmitoleic acid (POA) produced an overall concentration-dependent increase in necrosis (Figure 5.2 A; *grey*). Apoptosis was also increase by POA: 100 and 200 µM POA produced a 3.3 and 2.5 fold increase in the levels of apoptosis compared to control respectively (Figure 5.2 A; *white*).

Application of the fatty acid ethyl ester; palmitoleic acid ethyl ester (POAEE) increased both necrosis and apoptosis compared to control (Figure 5.2 B; *grey* and *white*). However when the concentration was increased from 50 µM to 100 µM to 200 µM no significant further increase in apoptosis or necrosis was seen. This implies that at the concentrations tested no concentration-dependent effect was observed.

To establish the role of intracellular generation of non-oxidative ethanol metabolites, the oxidative pathway may be inhibited. Blockade of the oxidative metabolism is possible by inhibition of alcohol dehydrogenase (ADH) with 4-methylpyrazole (4MP) (Makar and Tephly, 1975). Cells

exposed to 4MP alone displayed no significant change in necrosis compared to control (Figure 3A; *grey*). Addition of increasing concentrations of ethanol (100-500 mM) caused a concentration-dependent increase in necrosis (Figure 5.3 A; *grey*, 2.0 and 3.6 fold respectively) and apoptosis (Figure 5.3 A *white,* 2.6 and 2.0fold respectively) compared to 4MP alone.

Addition of increasing concentrations of ethanol (50-200 mM) to cells exposed to POAEE (50 µM). In a manner similar to application of POAEE alone (Figure 5.2 B) the POAEE and ethanol combination produced a significant rise in necrosis (Figure 5.3 B; *grey*) in all cases.

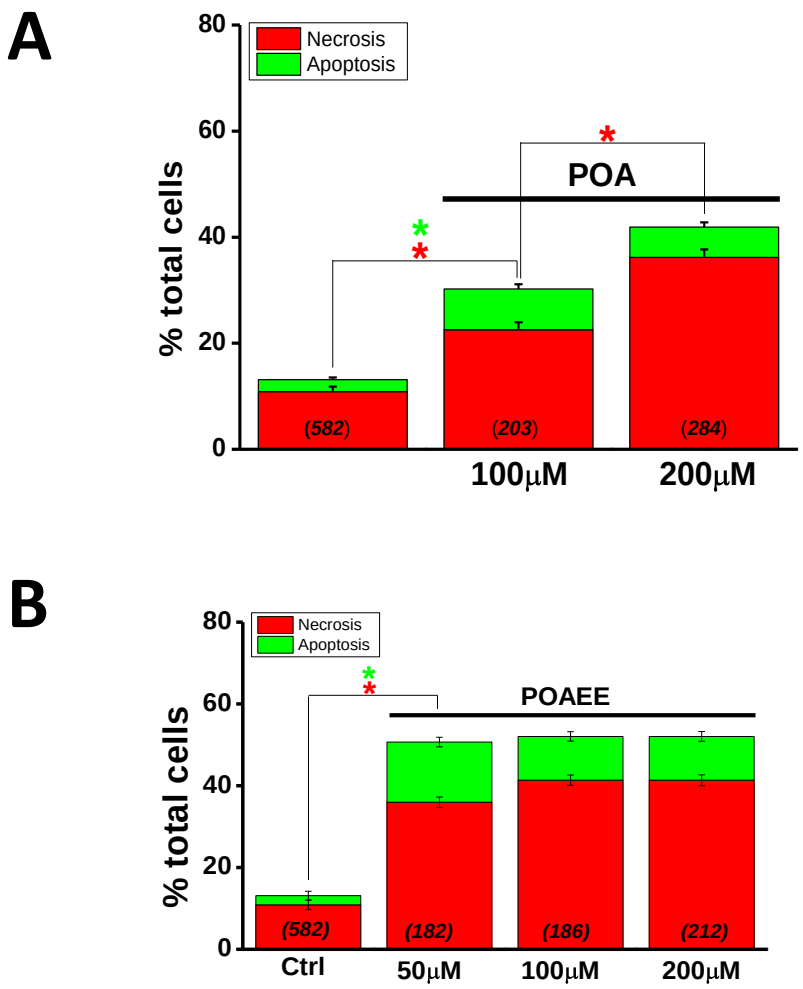

Figure 5.2 Non-oxidative ethanol metabolites cause necrosis. Effects of non-oxidative ethanol metabolites on pancreatic acinar cell fate (A) Palmitoleic acid (POA) 100-200 μM induced a concentration-dependent increase in necrosis (*grey*), varied effects on caspase activation (*white*). (B) Palmitoleic acid ethyl ester (POAEE) at increasing concentrations (50-200 μM) increases in necrosis (*grey*) and apoptosis (*white*) compared to control. All data are presented as mean ± s.e. mean (number of cells shown in parentheses) (* = P = < 0.05).

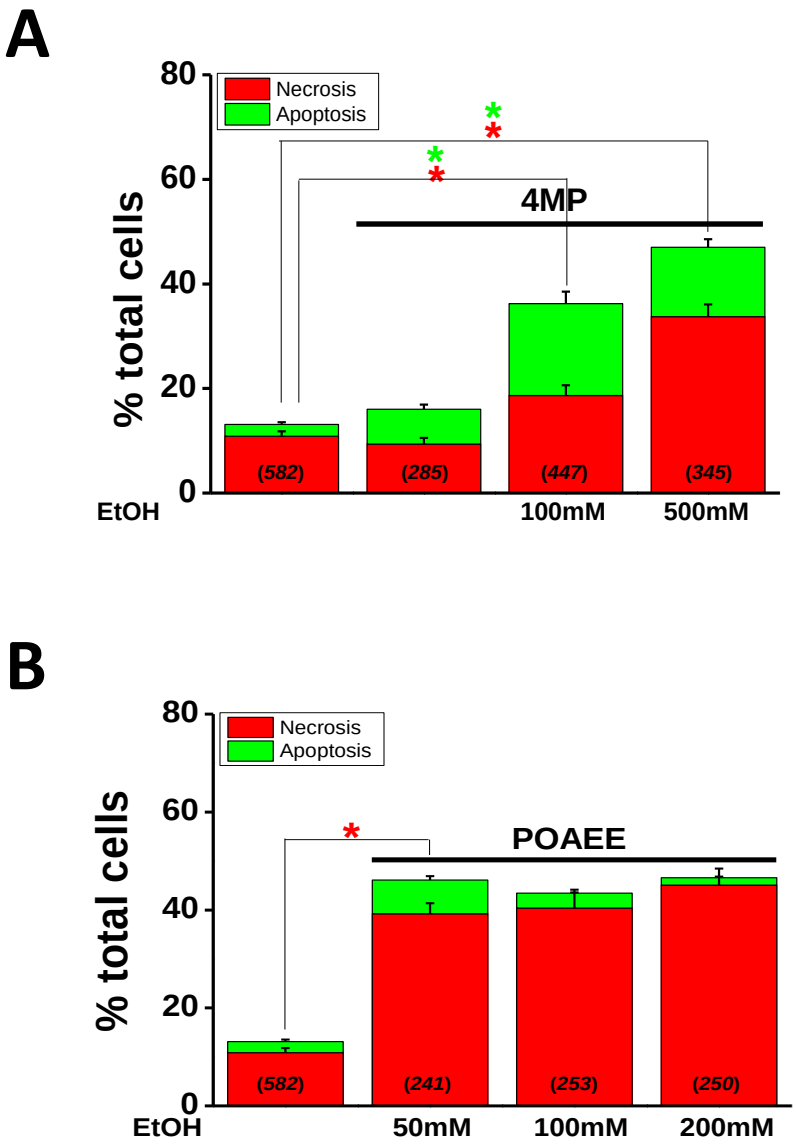

Figure 5.3 Ethanol causes cell death in the presence of oxidative metabolism, palmitoleic acid ethyl ester causes cell death in the presence of ethanol. Effects of the ethanol (EtOH) on pancreatic acinar cell fate in the presence of oxidative ethanol metabolism inhibition: 4-methylpyrazole (4MP) and non oxidative ethanol metabolite: palmitoleic acid ethyl ester (POAEE) (A) Ethanol (EtOH) 100,500mM induced a concentration-dependent increase in necrosis (*grey*) or apoptosis (*white*) in the presence of 4MP, 4MP alone was without effect. (B) Palmitoleic acid ethyl ester (POAEE: 50 µM) in the presence of increasing concentrations of ethanol. Increases in necrosis (*grey*) and varied changes in apoptosis (*white*) compared to control. All data are presented as mean ± s.e. mean (number of cells shown in parentheses) (* = P = < 0.05).

5.4 Modulation of ethanol metabolism mediates varied effects upon cell fate

Application of low concentrations of ethanol (EtOH; 10 mM), palmitoleic acid (POA; 20 µM) or 4-methylpyrazole (4MP; 100 µM) alone produced no significant increase in necrosis or apoptosis (Figure 5.4; *grey* and *white*). However, application of both EtOH and POA while oxidative metabolism was inhibited with 4MP produced a marked increase in both necrosis and apoptosis (Figure 4A; *grey* 8.5 fold, *white* 8.1 fold respectively).

Inhibition of hydrolase activity with bis-(4-nitrophenyl) (BNPP; 200µM) phosphate induced only low level necrosis and apoptosis (Figure 5.4 B; *grey* and *white*) similar to that seen in control conditions (Figure 5.4 A). Application of the combination of the combination of POA and EtOH produced a significant rise in necrosis (Figure 5.4 B; *grey*) compared to control conditions or either EtOH or POA alone (Figure4A; *grey*). Inhibition of oxidative ethanol metabolism in the same conditions produced a further increase in necrosis (Figure 5.4; *grey*) and a significant increase in apoptosis (Figure 5.4 B; *white*) as seen in (Figure 5.4 A). Necrosis was significantly abrogated by addition of the hydrolase inhibitor BNPP (Figure 5.4 B; *grey*), however BNPP was without effect on apoptosis (Figure 5.4 B; *white*).

Generation of FAEEs such as POAEE has been purported to be catalysed by FAEE synthase, which may be inhibited by 3-Benzyl-6-chloro-2-pyrone (3-BCP; 10 µM). Applied to isolated pancreatic acinar cells, 3-BCP was without effect on necrosis (Figure 5.5; *grey*) or apoptosis (Figure 5.5; *white*), compared to control conditions (Figure 5.4 A). When 3-BCP was included

with EtOH, POA and 4MP, 3-BCP induced a significant reduction in both necrosis (Figure 5; g*rey*) and apoptosis (Figure 5; *white*).

The oxidant menadione (MEN; 30 µM) the antioxidant *N*-acetyl-L-cysteine (NAC; 10 mM) or a combination of both produced differential effects on overall cell death. Antioxidant treatment alone had no significant effect on apoptosis (Figure 5.21 B; *white*) or necrosis (Figure 5.21 B; *grey*). Application of the oxidant menadione (MEN; 30 µM) produced significant increase in the number of cells exhibiting bright fluorescence of the fluorescent-indicator linked general caspase substrate (Figure 5.21 A; *green,* Figure 5.21 B; *white*). The changes in caspase activation as measured by the fluorescent general caspase substrate were completely abolished by

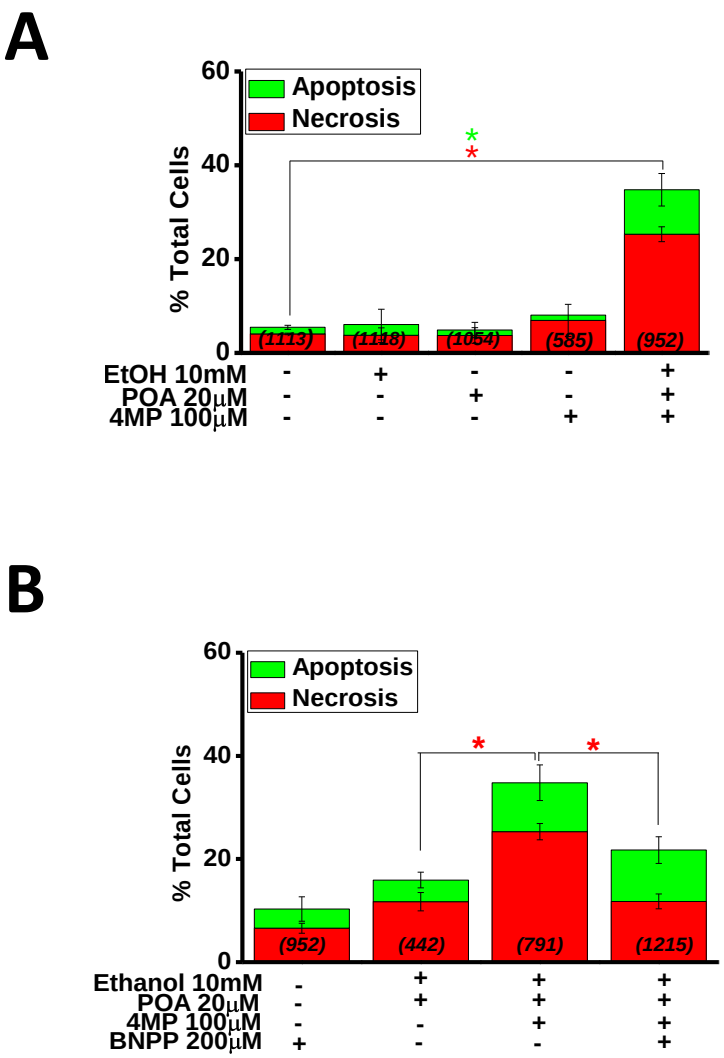

Figure 5.4 Inhibition of oxidative metabolism increases cell death partially abrogated by hydrolase inhibition. Effects of ethanol (EtOH; 10 mM), palmitoleic acid (POA; 20 µM), oxidative ethanol metabolism inhibition: 4-methylpyrazole (4MP) and hydrolase inhibition bis-(4-nitrophenyl) phosphate (BNPP; 200 µM) on pancreatic acinar cell fate. (A) EtOH (10 mM), POA (20 µM) and 4MP (100 µM) induced changes in necrosis (*grey*) or apoptosis (*white*). (B) Changes in necrosis (*grey*) or apoptosis (*white*) compared to control (displayed in (A)) induced by BNPP, EtOH, POA and 4MP compared to control (displayed in (A)). All data are presented as mean ± s.e. mean (number of cells shown in parentheses) (* = P = < 0.05).

A

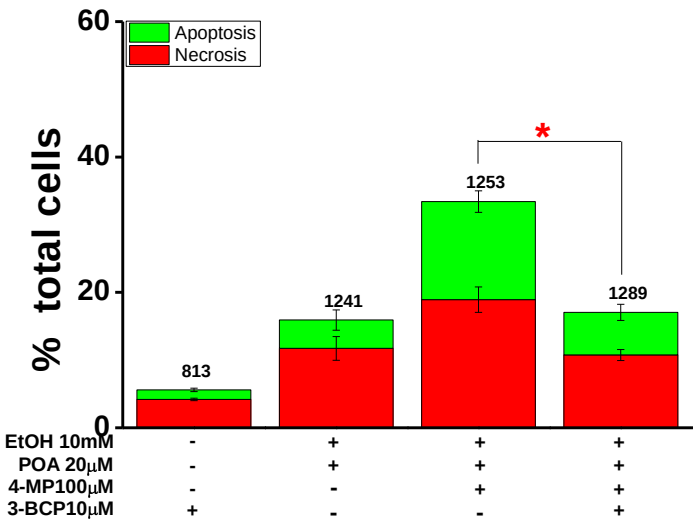

Figure 5.5 Inhibition of FAEE synthase activity reduces cell death. Effects of ethanol (EtOH; 10 mM), palmitoleic acid (POA; 20 µM), inhibition of oxidative ethanol metabolism 4-methylpyrazole (4MP; 100 µM) and FAEE synthase inhibition: 3-benzyl-6-chloro-2-pyrone (3-BCP; 10 µM) on pancreatic acinar cell fate. (A) Changes in necrosis (*grey*) or apoptosis (*white*) induced by combinations of 3-BCP, EtOH and POA produced increases in both necrosis and apoptosis which were markedly potentiated by addition of 4MP as displayed in Fig. 4. Addition of 3-BCP to the combination significantly reduced both necrosis and apoptosis (* = P = < 0.05).

simultaneous incubation with antioxidant (NAC; 10mM, Figure 5.21 A and B). Data are presented as mean ± s.e. mean, (number of cells in parenthesis).

Simultaneous detection of apoptosis and necrosis was applied to the agonist TLC-S. Unlike the oxidant menadione (Figure 5.21), TLC-S induced significant necrosis as visualized by propidium iodide fluorescence (Figure 22; *red*). Application of TLC-S at 200 µM and 500 µM evoked a concentration-dependent rise in both necrosis (Figure 5.23 A; *grey*) and apoptosis (*white*). After 30 min application of 200 µM and 500 µM TLC-S respectively, 13.3% (n = 96 of 724) and 15.3% (n = 221 of 1446) were apoptotic; 24.7% (n = 179 of 724) and 48.6% (n = 703 of 1446) were necrotic (Figure 5.23A). In contrast 10min pre-incubation with BAPTA, loaded in AM form, produced a marked decrease in visible necrotic cells as marked by propidium iodide fluorescence (Figure 5.22 A; *red*). Overall a reduction of necrosis was observed; decreasing by 63.4% at 200 µM and 65.7% at 500 µM TLC-S, (Figure 5.22 B *grey*).

Experiments were undertaken to alter $[ROS]_I$ production and/or clearance to assess directly the role of $[ROS]_I$ on apoptosis and necrosis induced by TLC-S. NAC (10 mM) pre-treatment diminished TLC-S-induced apoptosis by 81.7% with 200 µM TLC-S and by 64.9% with 500 µM TLC-S (Figure 23B; *white*). At 500 µM TLC-S, NAC significantly increased necrosis by 34.8%, although no difference was detected at 200 µM TLC-S (Figure 23B; *grey*). NAC did not, however, affect $[Ca^{2+}]_C$ elevations nor NAD(P)H depletion induced by 500 µM TLC-S (n = 10 of 10; data not shown). NQO1 inhibition

with DMN (30 µM) caused no significant reduction of total cell death *per se*, however it increased TLC-S-induced apoptosis by 37.5% at 200 µM TLC-S and by 44.3% at 500 µM TLC-S, simultaneously reducing necrosis by 24.3% and 36.2% respectively (Figure 5.24).

Autophagy has been demonstrated to have a significant role in the pathogenesis of acute experimental pancreatitis (Hashimoto et al., 2008). To establish the role of autophagy on pancreatic acinar cell fate, autophagy was prevented with the specific inhibitor 3-methyladenine (3MA; 5 mM). Inhibition of autophagy had no significant effect on acinar cell fate *per se*, In the presence of 200 µM TLC-S no significant effect was seen on necrosis or apoptosis (Figure 5.25; *grey* and *white* respectively).

Chapter 6

Results: Effects of ethanol metabolism on Ca^{2+} homeostasis and mitochondrial function

6.1 Introduction

The effects of non-oxidative ethanol metabolites on Ca^{2+} homeostasis and mitochondrial function have been previously investigated, and in line with the prevailing hypothesis that abnormal Ca^{2+} signals are crucial for the initiation of acute pancreatitis (Ward et al., 1995), the deleterious consequences of ethanol metabolism manipulation should be accompanied by Ca^{2+} signals and evidence of mitochondrial dysfunction.

6.1 Promotion of non-oxidative metabolism induced cytosolic Ca^{2+} rises

The aim of this series of experiments was to elucidate the effects of both ethanol and fatty acids in the presence of agents used to modify ethanol metabolism. Freshly isolated pancreatic acinar cells were loaded with Fluo4 in order to monitor changes in cytosolic calcium ($\Delta [Ca^{2+}]_c$). Application of the alcohol dehydrogenase (ADH) inhibitor 4-methylpyrazole (4MP; 100 µM) was without effect (Figure 6.1 A and B) in the majority of cases causing a $\Delta[Ca^{2+}]_c$ in only 7% of cells (Figure 6.4; *white*). In the case of cells exhibiting no $\Delta[Ca^{2+}]_c$, an application of acetylcholine (ACh; 100 nM) was used at the end of the experiment, to confirm the cells were loaded with Fluo4 and that they were viable, and able to exhibit a normal response to classical agonists (Figure 6.1; A and B). Application of the combination of ethanol (EtOH; 10 mM) and palmitoleic acid (POA; 20 µM) produced data less easily interpreted. In the majority of cases, pancreatic acinar cells responded with a

series of large, global and cytosolic $[Ca^{2+}]_c$ spikes which recovered to the baseline (Figure 6.2; A and B). The spiking activity accounted for 61% of all cells, however sustained toxic $\Delta[Ca^{2+}]_c$ were also observed in 23% of cases (Figure 6.4; *light grey*). When oxidative ethanol metabolism was inhibited, via blockade of ADH, the same mix of EtOH and POA produced a more pathophysiological pattern of responses among the cells tested. Overall, 66% of cells exhibited toxic $\Delta[Ca^{2+}]_c$ (Figure 6.4; *dark grey*) typified by an initial global spike which failed to fully recover, and was followed by a progressive rise in $[Ca^{2+}]_c$ to a maximal level (Figure 3 A and B).

Taken together, these data suggest that the inhibition of ADH with 4MP is largely without effect on $[Ca^{2+}]_C$ in the absence of EtOH and POA. When EtOH and POA are applied in isolation, their effect is relatively mild, although there is a significant increase in both global transient and sustained increases in $[Ca^{2+}]_c$.

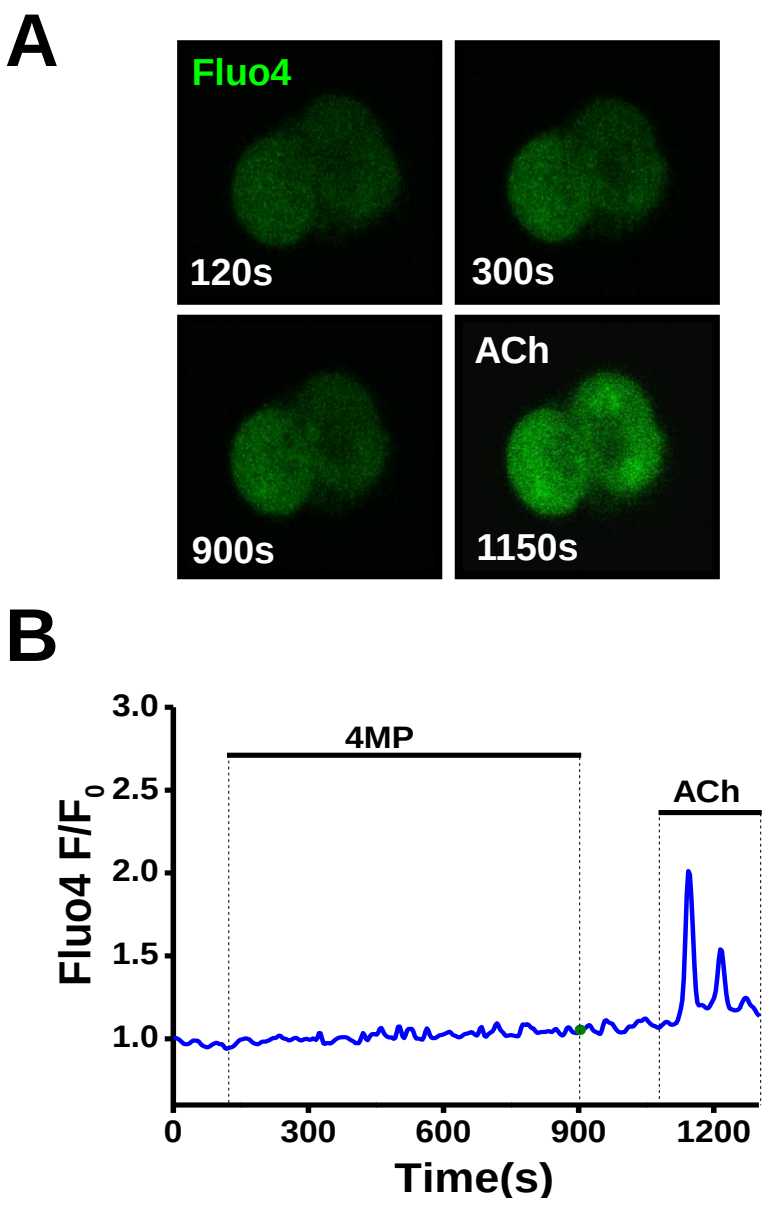

Figure 6.1 4-methylpyrazole is without effect on cytosolic Ca^{2+}. Effect of 4-methylpyrazole (4MP) on cytosolic calcium ($[Ca^{2+}]_C$). (A) Fluo4 fluorescence (*green*) images of a group of murine acinar cells showing no change in $[Ca^{2+}]_C$ induced by 100 µM 4MP. (B) representative trace showing the effect of 4MP on $[Ca^{2+}]_C$. Increases of $[Ca^{2+}]_C$ induced by Acetyl Choline (ACh: 100 nM) are shown at the end as a positive control n = 31 of 42. Data are shown as normalized changes from basal (pre-stimulation) fluorescence levels (F/F_0).

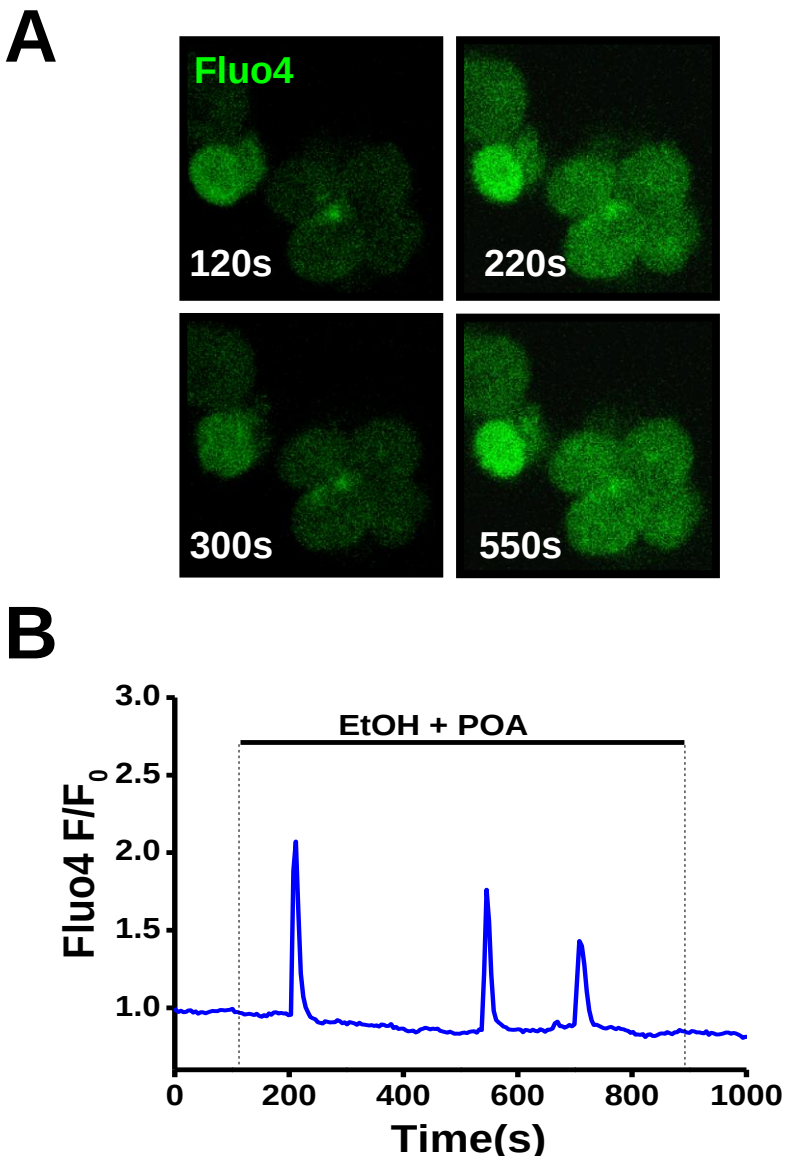

Figure 6.2 Ethanol and fatty acid induce transient Ca^{2+} rises. Effect of Ethanol (EtOH) and palmitoleic acid (POA) on cytosolic calcium ($[Ca^{2+}]_C$). (A) Fluo4 fluorescence (*green*) images of a group of murine acinar cells showing oscillatory changes in $[Ca^{2+}]_C$ induced by 100 µM 4MP. (B) Representative trace showing the effect of EtOH and POA on $[Ca^{2+}]_C$ n = 12 of 26. Data are shown as normalized changes from basal (pre-stimulation) fluorescence levels (F/F_0).

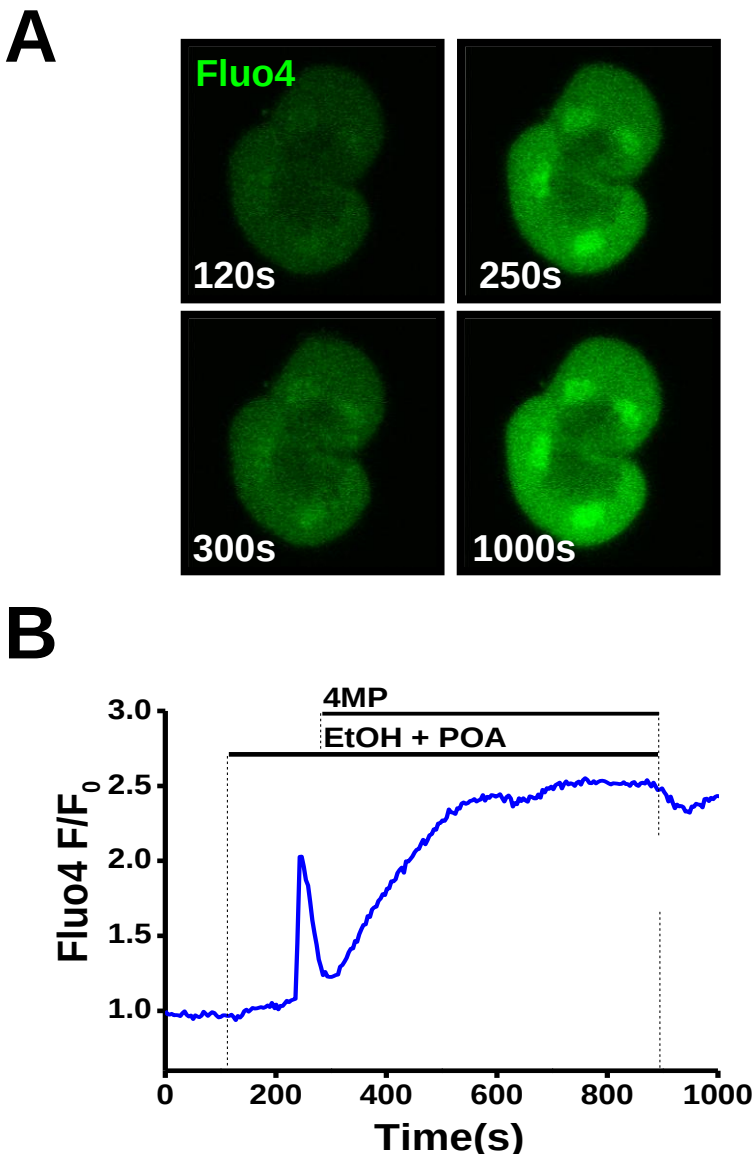

Figure 6.3 Non-oxidative ethanol metabolism promotes sustained Ca^{2+} rises. Effect of oxidative ethanol metabolism inhibition in the presence of Ethanol (EtOH) and palmitoleic acid (POA) on cytosolic calcium ($[Ca^{2+}]_C$). (A) Fluo4 fluorescence (*green*) images of a group of murine acinar cells showing sustained increases in $[Ca^{2+}]_C$ induced by 100 µM 4MP, 10mM EtOH and 20 µM POA. (B) Representative trace showing the effect of EtOH, POA and 4MP on $[Ca^{2+}]_C$ n = 34 of 52. Data are shown as normalized changes from basal (pre-stimulation) fluorescence levels (F/F_0).

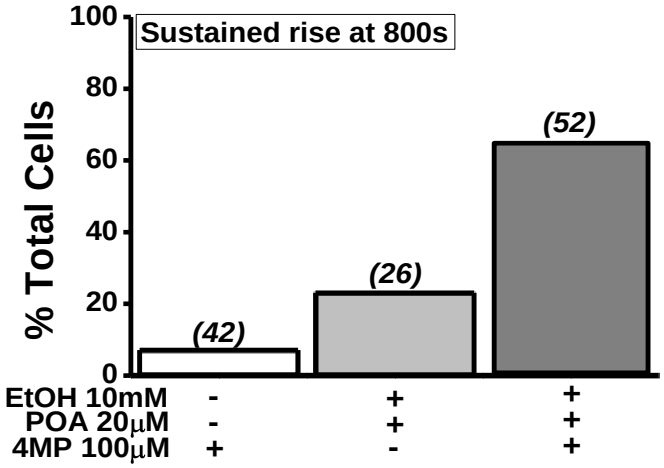

Figure 6.4 Inhibition of oxidative metabolism promotes sustained cytosolic calcium increase. Sustained increases in cytosolic calcium ($[Ca^{2+}]_C$)in response to ethanol (EtOH), palmitoleic acid and 4-methylpyrazole (4MP). Percentage of cells exhibiting sustained rises (F/F^0 = >1.5) at 800 s.

6.2 Promotion of non-oxidative ethanol metabolism negatively affects the mitochondrial membrane potential

The effect of non-oxidative ethanol metabolites such as POA and POAEE on mitochondrial membrane potential ($\Delta\psi_m$) has been previously explored (Criddle et al., 2004). Applications of relatively high concentrations of POA and POAEE were shown to completely depolarize the mitochondria of freshly isolated pancreatic acinar cells. Non-oxidative metabolites also provoked sustained $[Ca^{2+}]_c$ increases. To investigate the possibility that there was a common mechanism connecting these data with the data describe above, assessments of mitochondrial membrane potential were made in isolated pancreatic acinar cells.

Assessment of $\Delta\psi_m$ was made by loading freshly isolated acinar cells with tetra methyl rhodamine methyl ester (TMRM; 37.5 nM), producing a pattern of fluorescence characteristic of the mitochondrial distribution in pancreatic acinar cells (Figure 6.5, 6.6, 6.7 & 6.8 A). Perfusion of 4MP alone was without significant effect; cells displayed a small, linear decrease in TMRM fluorescence (Figure 6.5 B). Application of EtOH and POA combined produced a moderate decrease in mitochondrial TMRM fluorescence (Figure 6.6 A and B). The application of EtOH and POA in the presence of ADH inhibition with 4MP produced a much more pronounced $\Delta\psi_m$ (Figure 6.7 A and B). An effect completely abrogated by concomitant perfusion with the FAEE synthase inhibitor 3-benzyl-6-chloro-2-pyrone (3-BCP; 10 μM) (Figure 6.8; A and B).

6.3 Inhibition of FAEE synthase prevents Ca^{2+} rises and mitochondrial dysfunction

The $[Ca^{2+}]_c$ increases mediated by EtOH, POA and 4MP were completely reversed from the pre-stimulation level in the presence of 3-BCP (Figure 6.9 B). The effect of 3-BCP on $\Delta\psi_m$ was marked, to assess the effect of 3-BCP more fully other intracellular parameters were measured. 3-BCP maintained and even increased mitochondrial function as measured by NAD(P)H autofluorescence (Figure 6.9 A).

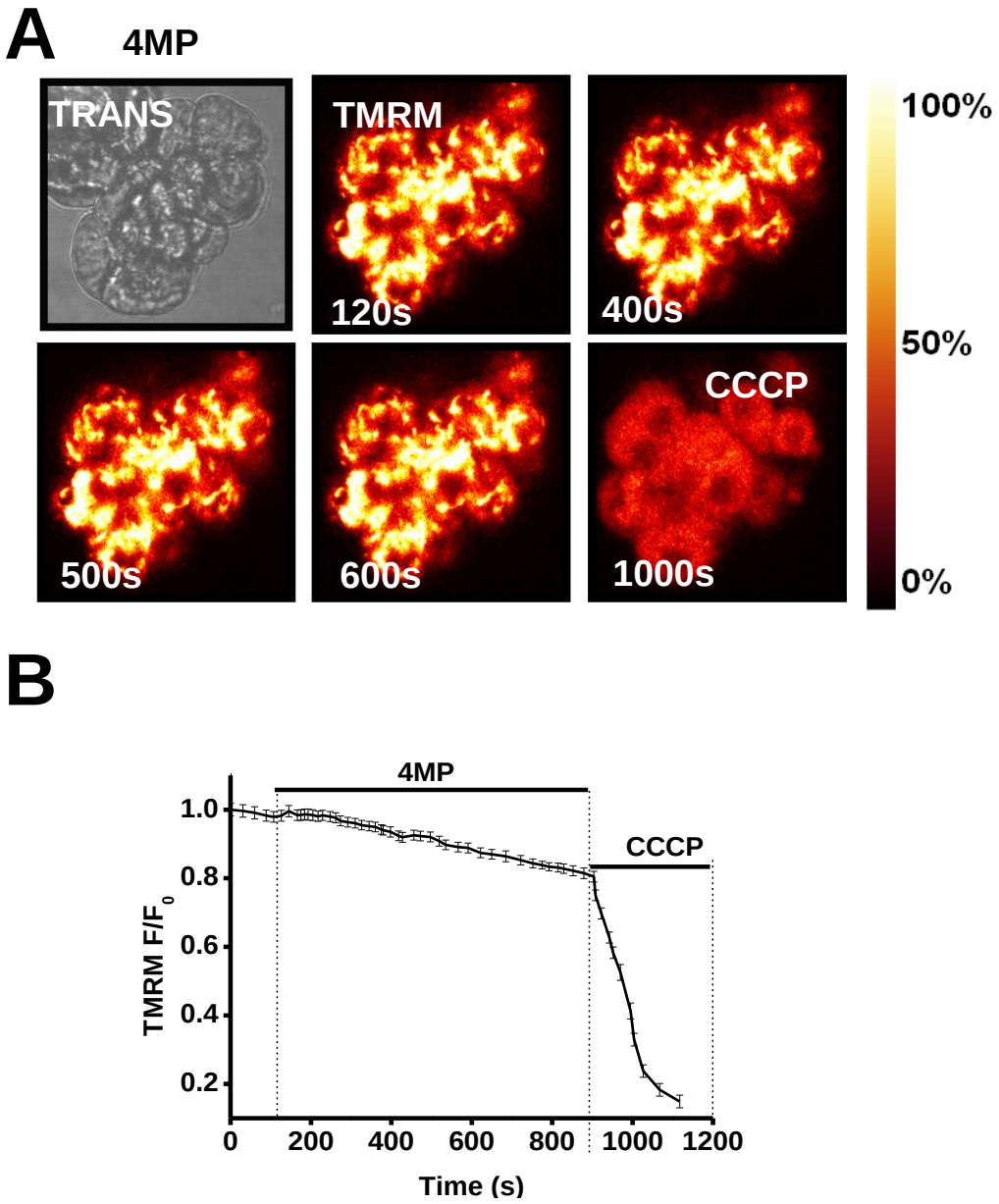

Figure 6.5 4-methylpyrazole causes minimal depolarization of the mitochondrial membrane. Effect of oxidative ethanol metabolism inhibition on mitochondrial membrane potential: ($\Delta\psi_m$). (A) Time course fluorescence images of a group of pancreatic acinar cells loaded with TMRM. The images display no decrease in induced by 4MP. (B) Mean trace (+/- SEM) of the effects of 4MP. At the end of the experiment carbonyl cyanide 3-chlorophenylhydrazone (CCCP 10 µM) was applied to display maximum depolarization. Data are shown as normalized changes from basal (pre-stimulation) fluorescence levels (F/F_0).

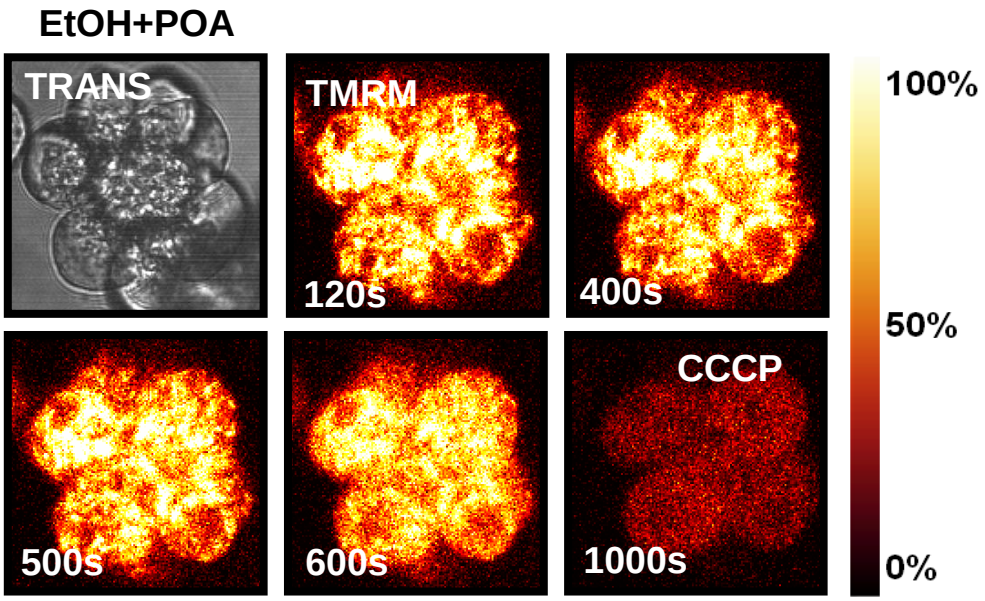

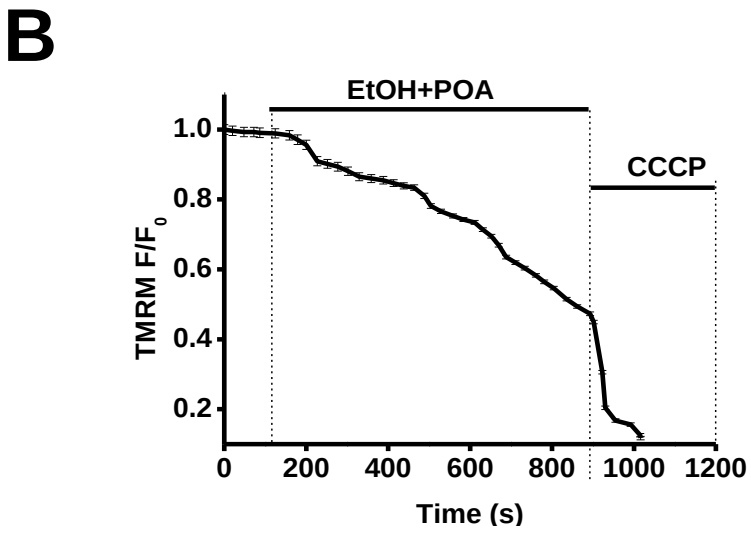

Figure 6.6 Effect of ethanol (EtOH) and palmitoleic acid (POA) on mitochondrial membrane potential: ($\Delta\psi_m$). (A) Time course fluorescence images of a group of pancreatic acinar cells loaded with TMRM. The images display changes in mitochondrial membrane potential induced by EtOH (10mM) and POA (20 µM). (B) Mean trace (+/- SEM) of the effects of EtOH and POA. At the end of the experiment carbonyl cyanide 3-chlorophenylhydrazone (CCCP 10 µM) was applied to display maximum depolarization. Data are shown as normalized changes from basal (pre-stimulation) fluorescence levels (F/F_0).

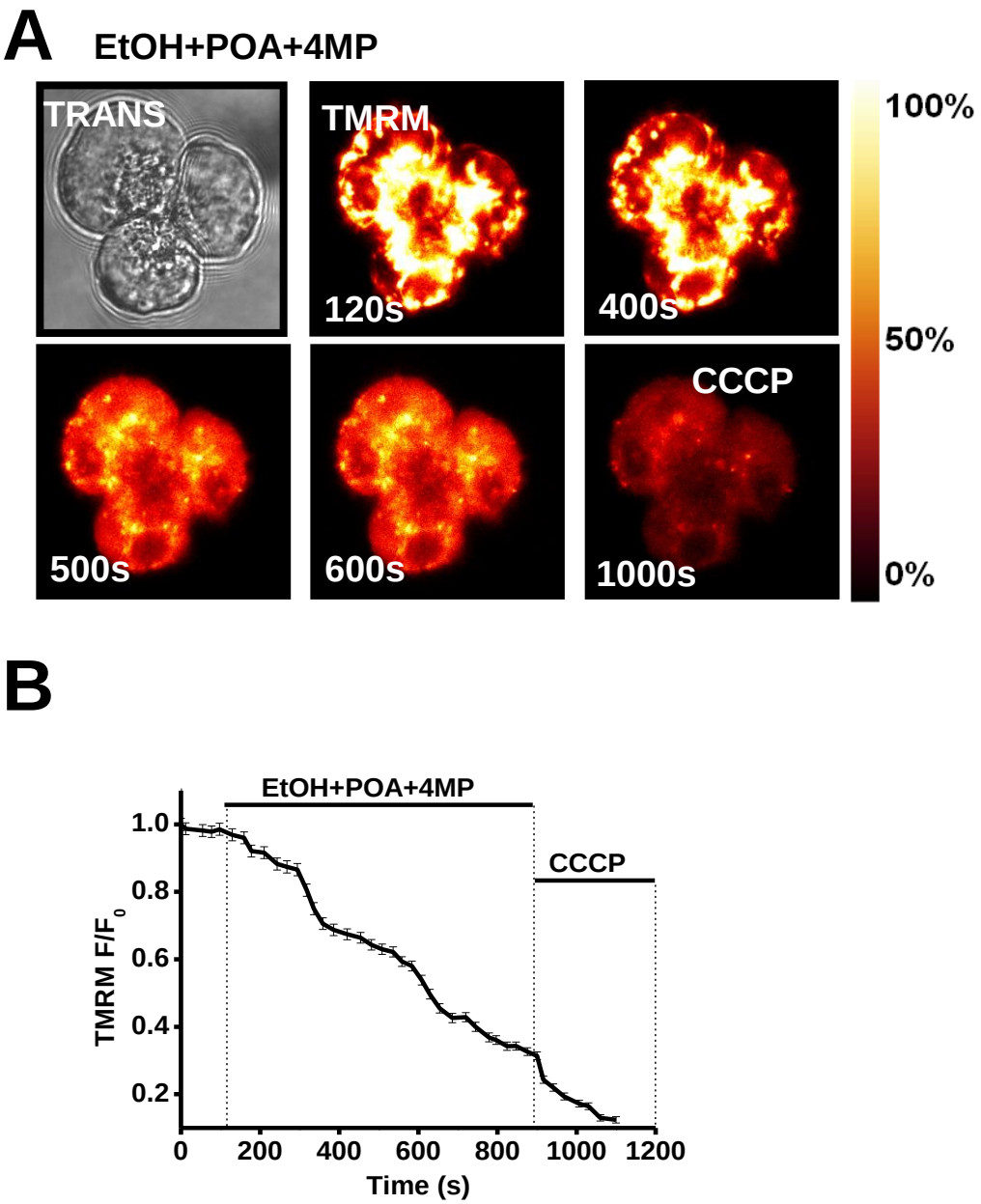

Figure 6.7 Effect of ethanol (EtOH) and palmitoleic acid (POA) and 4-methylpyrazole on mitochondrial membrane potential: ($\Delta\psi_m$). (A) Time course fluorescence images of a group of pancreatic acinar cells loaded with TMRM. The images display marked depolarization in membrane potential induced by EtOH (10 mM), POA (20 µM) and 4MP (100 µM). (B) Mean trace (+/- SEM) of the depolarizing effects of EtOH, POA and 4MP. At the end of the experiment carbonyl cyanide 3-chlorophenylhydrazone (CCCP 10 µM) was applied to display maximum depolarization. Data are shown as normalized changes from basal (pre-stimulation) fluorescence levels (F/F_0).

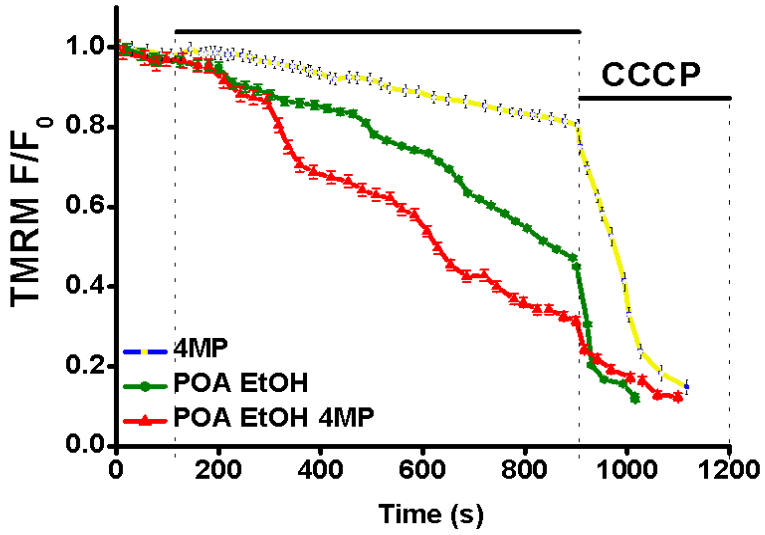

Figure 6.8 Effect of ethanol (EtOH; 10mM), palmitoleic acid (POA; 20 µM), 4-methylpyrazole (4MP; 100 µM) on mitochondrial membrane potential: ($\Delta\psi_m$) – composite figure. Mean (+/- SEM) traces of $\Delta\psi_m$ upon exposure to 4MP (*Blue*) EtOH and POA (*Green*) and EtOH, POA and 4MP (*Red*) Data are shown as normalized changes from basal (pre-stimulation) fluorescence levels (F/F_0).

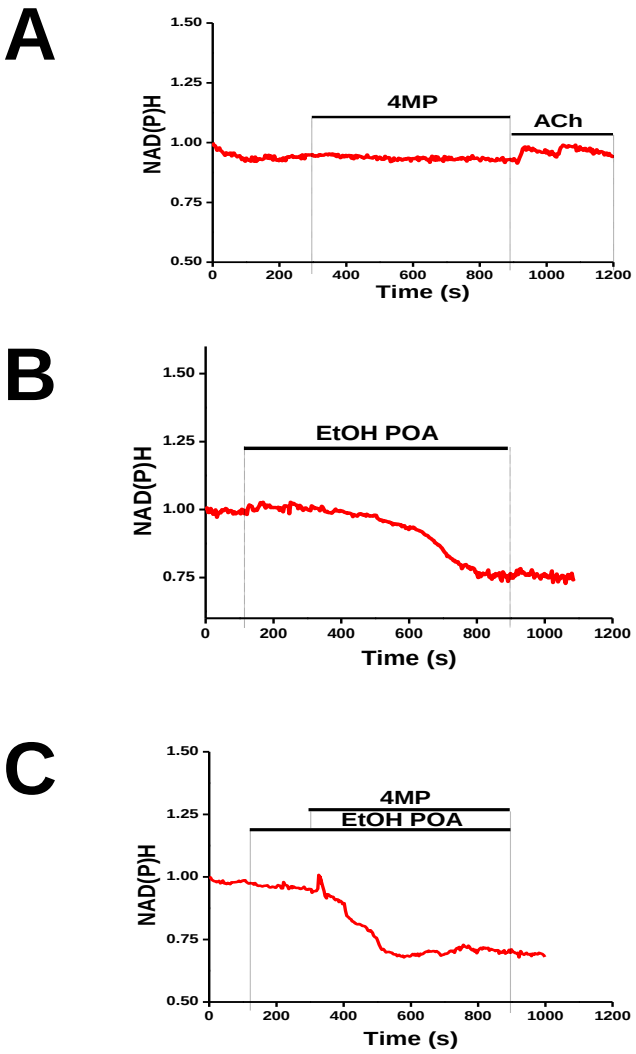

Figure 6.9 Effect of ethanol (EtOH; 10 mM), palmitoleic acid (POA 20 µM) and 4-methylpyrazole (4MP; 100 µM) on NAD(P)H levels. Representative traces showing the effects of (A) 4MP (B) EtOH + POA and (C) EtOH, POA and 4MP Data are shown as normalized changes from basal (pre-stimulation) fluorescence levels (F/F_0).

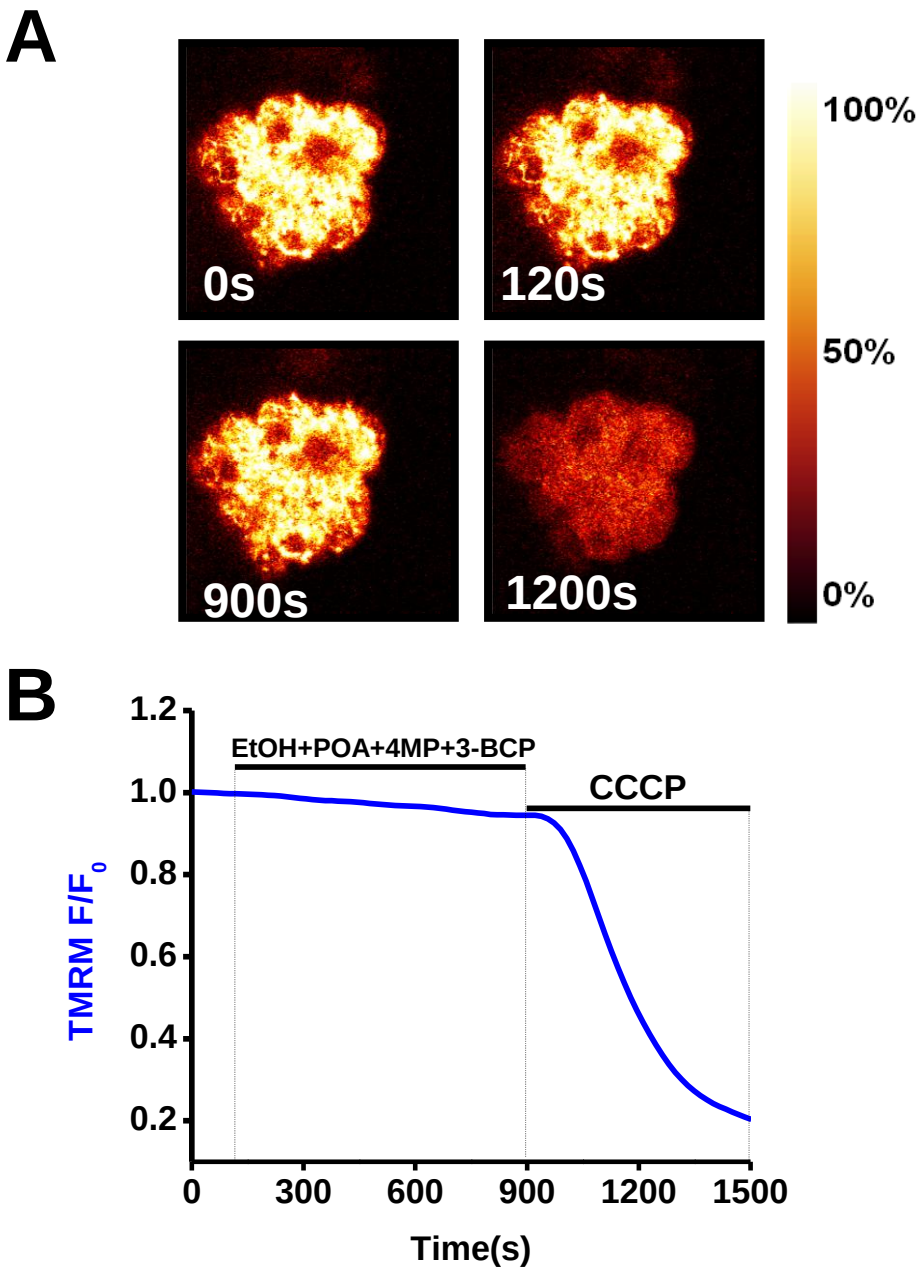

Figure 6.10 Effect of ethanol (EtOH; 10mM), palmitoleic acid (POA; 20 µM), 4-methylpyrazole (4MP; 100 µM) on mitochondrial membrane potential: ($\Delta\psi_m$) – composite figure. (A) Time course fluorescence images of a group of pancreatic acinar cells loaded with TMRM. The images display preserved mitochondrial membrane potential during perfusion with EtOH (10 mM), POA (20 µM), 4MP (100 µM) and 3-BCP (10 µM). (B) representative trace displaying preserved $\Delta\psi_m$ depolarizing effects of EtOH, POA and 4MP with contemporaneous perfusion with 3-BCP. At the end of the experiment carbonyl cyanide 3-chlorophenylhydrazone (CCCP 10 µM) was applied to display maximum depolarization. Data are shown as normalized changes from basal (pre-stimulation) fluorescence levels (F/F_0).

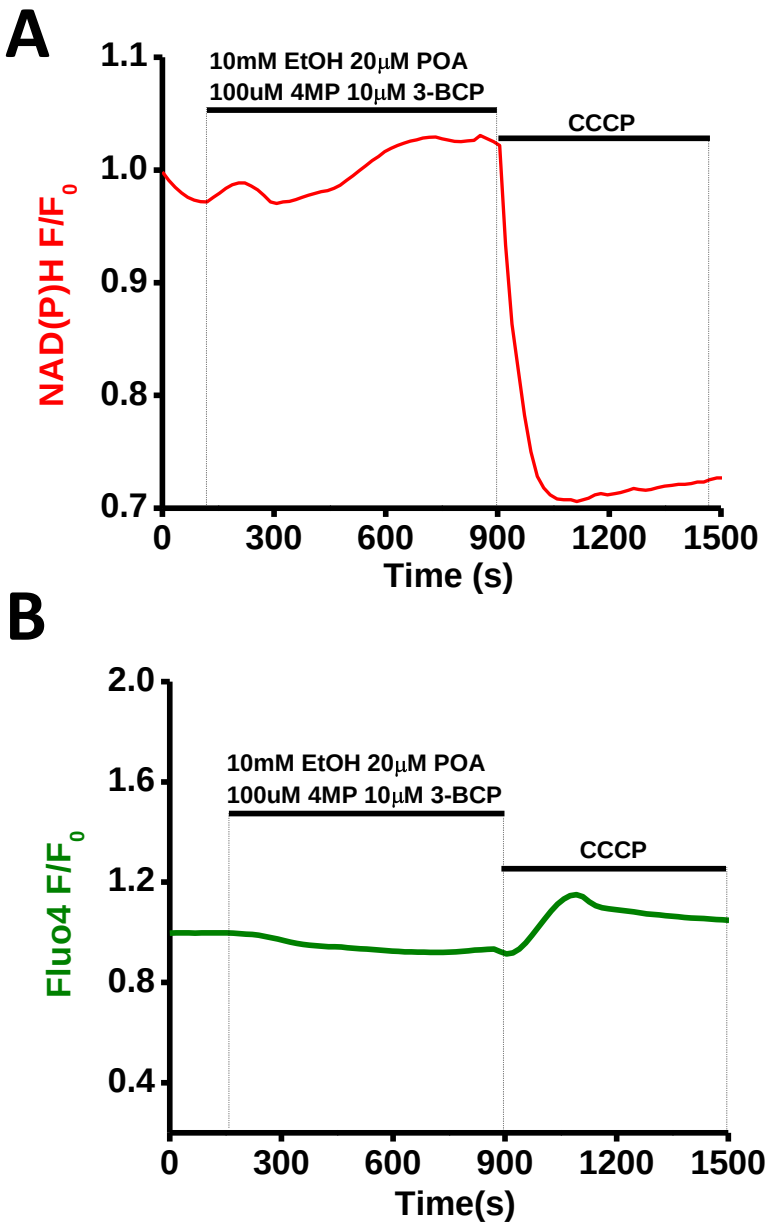

Figure 6.11 Effect of 3-benzyl-6-chloro-2-pyrone in the presence of Ethanol (EtOH) and palmitoleic acid (POA) on NAD(P)H autofluorescence and cytosolic calcium ($[Ca^{2+}]_C$). (A) Representative trace showing the effects of 3-BCP on NAD(P)H autofluorescence when perfused with EtOH, POA and 4MP. NAD(P)H levels are maintained (B) representative traces showing the effects of 3-BCP on $[Ca^{2+}]_C$ when perfused with EtOH, POA and 4MP. No increase in $[Ca^{2+}]_C$ is observed. Carbonyl cyanide 3-chlorophenylhydrazone (CCCP 10μM) was applied at the end of both (A) and (B) CCCP n = 19 of 19. Data are shown as normalized changes from basal (pre-stimulation) fluorescence levels (F/F_0).

Chapter 7

Discussion

7.1 The role and source of bile salt induced reactive oxygen species in pancreatic acinar cells

7.1.1 TLC-S-induced Ca^{2+} elevations

The experiments contained within Chapter 3 clearly demonstrated that application of the bile salt TLCS caused elevations of $[Ca^{2+}]_C$ and changes in NAD(P)H autofluorescence in both freshly isolated human, and murine, pancreatic acinar cells (Figure 3.1 and 3.2). For the first time, these human cells were shown to generate profound $[Ca^{2+}]_C$ elevations in response to a bile salt, in this case TLC-S. The responses underlined the relevance of bile salts in human pancreatitis. This strongly supports the role of Ca^{2+}, particularly Ca^{2+}-overload as the trigger for acute pancreatitis, a theory which although 15 years old, still requires validation (Ward et al., 1995). The patterns of Ca^{2+}-response obtained in isolated human cells were broadly divided into two groups dependent upon the level of stimulation; 200 (Figure 3.2 A) and 500 µM TLC-S (Figure 3.2 B) exhibited distinct patterns. The lower level of stimulation elicited global, transient Ca^{2+}-spikes whereas the higher level of stimulation was always characterised by a large sustained increase in $[Ca^{2+}]_C$ which was characteristic of Ca^{2+}-overload. Experiments with murine cells displayed exactly the same profile as those in human (Figure 3.1) and both were entirely consistent with the responses demonstrated previously (Voronina et al., 2004). The response of NAD(P)H autofluorescence to TLC-S was different according to the level of stimulation. At the lower level of stimulation, (200 µM TLC-S), oscillations in NAD(P)H

autofluorescence were seen in both human and murine cells, (Figure 3.1 A and 3.2 A). This demonstrates that in both human and murine cells the effects of moderate Ca^{2+} release are stimulation of the mitochondrial production of NAD(P)H. This is currently hypothesised to occur via an increase in the rate of three Ca^{2+}-sensitive dehydrogenases which increase the activity of the TCA cycle, these data are in firm agreement with the concept of stimulus-metabolism coupling (Voronina et al., 2002b). At the higher level of stimulation, where $[Ca^{2+}]_C$ was elevated in a sustained fashion, NAD(P)H was steadily depleted, indicating that the mitochondria were inhibited from returning NAD(P)H to a resting level as demonstrated with the lower level of stimulation (Figure 3.1 A). Overall, these data demonstrate the remarkable similarity between the responses of human and murine cells and confirms the common mechanisms at work in both human and mouse that have already been demonstrated with CCK (Murphy et al., 2008). The response of the human cells to TLC-S may suggest that the bile receptor, GPBAR1, is very likely both expressed and functional in human cells. Recent work by Peredes and colleagues (Perides et al., 2010) showed that the bile receptor GPBAR1 was likely responsible for the much of the organ injury in TLC-S-induced experimental pancreatitis. The work presented in this thesis showed that the mechanisms responsible for TLC-S-induced pancreatitis in mice also appear to operate in freshly isolated human tissue.

.

7.1.2 TLC-S induced ROS elevations

Application of TLC-S to cells loaded with ROS-sensitive indicator showed significantly elevated concentrations of $[ROS]_i$ (Figure 3.3), but only at the higher concentration of TLC-S. It is also interesting to note that the elevation of $[ROS]_i$ was relatively modest compared to that seen upon application of menadione at the end of each experiment. The actions of menadione in pancreatic acinar cells have been previously described (Criddle et al., 2006a), and the redox cycling of menadione is demonstrably different in both rate of production, and ultimate level attained. The generation of ROS in freshly isolated human cells was also demonstrated (Figure 3.4). The level of ROS generation in human cells was considerably greater than that seen in murine isolates; in addition, ROS generation was seen in response to application of the lower, (200 µM) concentration of TLC-S. This demonstrated that while human and murine cells both exhibited similar Ca^{2+} and NAD(P)H responses, and that both shared the generation of ROS in response to TLC-S, the level of ROS generated by human cells was much greater than that in murine cells. Due to the difficulty with obtaining surgical samples of human tissue, further analytical experiments could not be undertaken within the time frame of this thesis, and as such exploration into the mechanisms behind the difference in ROS generation awaits completion. One possible explanation is that the mice routinely used in isolated cell experiments are young adult mice, whereas the human patients are frequently older, both numerically and in relation to average lifespan. All human samples in this study were obtained from patients older than 60 years. As such, the antioxidant potential of the young mice may have been greater than the older human cells. In the mouse at least, older animals lose

the ability to maintain proteins in a non-oxidised state, a feature not shared by younger mice (Carney et al., 1991).

Both murine and human cells shared the NAC-sensitive nature of TLC-S-induced ROS generation. As expected application of NAC was sufficient to completely abrogate any indicated elevation in $[ROS]_i$ (Figure 3.5 and 3.6) confirming that it was indeed ROS that was being measured by the indicator.

Previous work has elegantly demonstrated that pancreatic acinar cells use NAD(P)H quinone oxidoreductase 1 (NQO1) as a major part of their antioxidant defence system (Criddle et al., 2006a). This study showed that 2,4-dimethoxy-2-methylnaphthalene (DMN), a novel inhibitor of NQO1, was able to potentiate the ROS generation in response to menadione, without being a ROS producer itself. NQO1 is widely assumed to be of cytosolic localisation within the cell (Jaiswal et al., 1988). To establish if this was the case in the acinar cell, the presence and location of the enzyme was tested in both human and murine acinar cells. Immunofluorescence was used to stain the endogenous enzyme in PFA-fixed cells. The enzyme was located uniformly throughout the cytosol and excluded from the nucleus (Figures 3.7, 3.8 and 3.9). When NQO1 was inhibited with DMN, and the cells subsequently exposed to TLC-S, ROS generation was potentiated (Figure 3.10). This is entirely consistent with the previous study in which menadione-induced ROS is increased by NQO1 inhibition (Criddle et al., 2006a). Crucially, however, the ROS generation induced by 200 µM TLC-S in the presence of DMN was not detectible without NQO1 inhibition in murine acinar

cells (Figure 3.10). This may represent a level of ROS generation induced by this stimulus lay normally within the capacity of the cell's antioxidant defence mechanisms.

With experimental evidence suggesting that TLC-S generated significant ROS when applied to pancreatic acinar cells, further experiments were devised to establish the mechanism of the ROS generation.

Confirmation of the essential role of Ca^{2+} to ROS generation was obtained by experiments designed to prevent the elevation of $[Ca^{2+}]_C$ by pre-incubation with the loadable intracellular Ca^{2+}-chelator BAPTA (in AM form). Rises in $[ROS]_I$ induced by the bile salt TLC-S were significantly inhibited, indicating that the sustained rises in $[Ca^{2+}]_C$ induced by TLC-S were necessary for ROS generation (Figure 3.13 A and 3.14). In many cell types, such as neutrophils, NADPH oxidase is an inducible enzyme capable of producing prodigious amounts of superoxide as part of the "respiratory burst" (Vignais, 2002). To investigate the potential role of this enzyme within the ROS generation observed in pancreatic acinar cells the specific inhibitor DPI was used; no effect upon TLC-S induced ROS generation was observed (Figure 3.13) suggesting that in the pancreatic acinar cell NADPH oxidase provided no detectible contribution to the total generation of ROS. This was consistent with published data indicating that NADPH oxidase is not present in primary pancreatic acinar cells (Gukovskaya et al., 2002b).

Prolonged, global rises in $[Ca^{2+}]_C$ bathe mitochondria in a high Ca^{2+} environment allowing mitochondria to take up Ca^{2+}. This process occurs down a steep electrochemical gradient, principally via the uniporter; a high-

capacity Ca^{2+} channel which has evaded full characterization (Reviewed in (Szabadkai and Duchen, 2008)) however, early recent work may finally be able to shed some light on its regulation (Collins and Meyer, 2010, Perocchi et al., 2010). If the extra mitochondrial Ca^{2+} concentration remains elevated for a significant period of time mitochondrial Ca^{2+} overload may result. This was assessed in the current study and it was found that the greater concentration of TLC-S induced a significant irreversible increase in $[Ca^{2+}]_m$ (Figure 3.16), which was accompanied by the same loss in NAD(P)H autofluorescence seen in earlier experiments (Figure 3.1 B) and reported in the literature (Criddle et al., 2006a, Criddle et al., 2006b). Importantly, the lower concentration of 200 µM TLC-S, which produced only transient increases of $[Ca^{2+}]_{C,}$ was almost without effect upon the uptake of Ca^{2+} into the mitochondria as measured by Rhod-2 (Figure 3.15). This indicated that the sustained global increase in $[Ca^{2+}]_C$ was necessary to cause $[Ca^{2+}]_m$ overload and that both the $[Ca^{2+}]_C$ and $[Ca^{2+}]_m$ elevations were associated with the generation of ROS.

To investigate where in the cell ROS generation occurred, thin-section confocal microscopy was used to isolate thin optical sections <2 µm in the Z-axis. Stimulation with 500 µM TLC-S induced a significant generation of ROS which displayed a distribution characteristic of the mitochondria within the acinar cell (Figure 3.17). This was subsequently confirmed by co-localization with the mitochondria-specific dye TMRM (Figure 3.18). Overall, the data suggest that the sustained $[Ca^{2+}]_m$ and NAD(P)H decreases were

indicative of mitochondrial dysfunction, due at least in part to Ca^{2+} influx in to the mitochondrial matrix causing depolarization of the mitochondria.

Mitochondrial compromise was a principal feature of injury induced by high concentrations of the bile acid TLC-S, characterised by sustained increases in $[Ca^{2+}]_M$ and loss of NAD(P)H concentrations. In normal cells mitochondria are the main source of intracellular ROS, produced by the electron transport chain driving ATP production (Droge, 2002). In addition to ROS production, mitochondria have endogenous capacity to contain and inactivate ROS, including from surrounding subcellular regions (Balaban et al., 2005). From evidence presented within this thesis, it appears that much of the increase in $[ROS]_I$ occurred within mitochondria. This was also demonstrated by the absence of ROS production when the electron transport chain was inhibited in two places, complex I and III, with antimycin A and rotenone (Figure 3.20). Particularly interesting was the significant rise in NAD(P)H observed upon such blockade of electron transport (Figure 3.20), by preventing the transfer of protons from NAD(P)H to complex I (Figure1.3).

The important link between ROS and apoptotic cell death previously proposed (Criddle et al., 2006a) was further investigated with respect to the bile salt TLC-S. The experimental data within this thesis clearly demonstrates that TLC-S generated ROS, and that this ROS promoted apoptosis rather than necrotic acinar cell death. There were however, notable differences between the actions of menadione and TLCS. Menadione is a redox-cycling quinone which was demonstrated to generate ROS in a Ca^{2+}-independent manner (Criddle et al., 2006a). As previously discussed, TLC-S evokes profound Ca^{2+} signals which are dependent upon

the level of stimulation applied. Application of high concentrations of TLC-S induced a moderate but significant increase in ROS generation within the human acinar cell. Real-time, online recordings of ROS within human pancreatic acinar cells, is completely novel. These data demonstrated, for the first time, the propensity for human cells to generate prodigious ROS in response to stimuli such as TLC-S and menadione. Unlike menadione, ROS generated in response to TLC-S application, was always accompanied by Ca^{2+} elevations. However, irrespective of the mechanism of ROS generation, the consequence on cell fate was the same. When ROS is promoted or inactivated, apoptosis is increased or abolished respectively. The effect of bile salts such as TLC-S, on both ROS and cell fate, appear dependent upon $[Ca^{2+}]_c$ although they are possibly not entirely limited in this regard. The results of luciferase ATP measurements upon acinar cells exposed to bile salts, offer a tantalising insight into the actions of ATP. Bile salts interact with GPBAR1 and mediate Ca^{2+} release in a manner which bears a striking resemblance to supramaximal application of secretagogues such as ACh and CCK, however, the effects of CCK and ACh on mitochondrial ATP synthesis were opposite to those of TLC-S (Voronina et al., 2010). Mitochondrial ATP synthesis is partially inhibited by TLC-S in the pancreatic acinar cell. Some evidence has shown that realistic concentrations of bile derivatives, in this case the cholate anion, can inhibit cytochrome c oxidase, the terminal molecule in the electron transport chain (Van Buuren and Van Gelder, 1974). Other inhibitors of cytochrome c oxidase activity, such as carbon monoxide and azide, also cause ROS generation (Chen et al., 2003, Zuckerbraun et al.,

2007) possibly at complex I following blockade of electron transport, a mechanism which may be shared by TLC-S.

When ROS production was inhibited, a profound inhibition of apoptosis was demonstrated. When cells were pre-loaded with BAPTA to prevent significant $[Ca^{2+}]_c$ overload, therefore preventing $[Ca^{2+}]_m$ overload, significantly lower cell death was seen (Figure 3.22). However, when ROS was either specifically generated or inactivated, the situation was simplified greatly. When menadione is applied to acinar cells the effects upon Ca^{2+}-signals are minor (Criddle et al., 2006a). However the ROS generated induced significant apoptosis (Figure 3.21). When cleared with NAC, menadione-induced ROS had no effect upon cell fate (Figure 3.21). Similar effects of NAC were observed upon TLC-S-induced apoptosis (Figure 3.23 B). Without ROS generation, specifically from the mitochondrial electron transport chain, the ability of TLC-S to stimulate apoptosis was lost. The loss of ROS as apoptotic stimuli leaves Ca^{2+} as the main determinant of cell death, which allows for ATP depletion, intracellular trypsinogen activation and cellular necrosis (Criddle et al., 2006c).

ROS-induced cytochrome c release, leading to ATP-dependent caspase activation and apoptosis, occurs in many cell types including acinar cells (Orrenius et al., 2007, Yerushalmi et al., 2001); without ATP, a switch to necrosis is likely (Nicotera et al., 1998, Mukherjee et al., 2008, Criddle et al., 2006b, Orrenius et al., 2007, Yerushalmi et al., 2001). ROS, specifically mitochondrial ROS, may facilitate the detachment of cytochrome *c* from cardiolipin, a molecule specific to the inner membrane of the mitochondria, before release of cytochrome *c* into the cytoplasm via opening of the

mitochondrial permeability transition pore or mitochondrial outer membrane permeabilization. As cytochrome *c* release is a crucial intermediate step in the intrinsic apoptosis pathway (Liu et al., 1996), the earlier it occurs, the sooner apoptosis is correctly initiated.

While prolonged, global rises of $[Ca^{2+}]_C$ induced by bile salts were seen to cause pancreatic acinar cell necrosis by inhibition of mitochondrial function, in this work it was found that bile salt-induced elevations of $[ROS]_I$ initiated apoptosis. Predominant current expectations would imply that antioxidant treatment limit Ca^{2+}-overload by preventing modification of Ca^{2+}-handling machinery. ROS-mediated modifications of the PMCA (Baggaley et al., 2008, Leung and Chan, 2009) SERCA, (Sharov et al., 2006) RyR (Hamilton and Reid, 2000) and IP_3R (Joseph et al., 2006) generally function to increase $[Ca^{2+}]_C$ by inhibiting clearance and increasing release respectively. Specific antioxidant treatment did not affect elevations of $[Ca^{2+}]_C$ but was found to reduce $[ROS]_I$ and thereby change the mechanisms of cell death, increasing the proportion of cells undergoing necrosis.

The role of $[ROS]_I$ in the determination of apoptosis was clearly demonstrated by the action of the oxidant menadione, which generates marked elevations in pancreatic acinar cell $[ROS]_I$ (Criddle et al., 2006a, Galluzzi et al., 2009) whereas stimulation or inhibition of autophagy, also recently implicated in the pathogenesis of acute pancreatitis (Mareninova et al., 2009), were not found to have any significant effect (Figure 3.25 and 3.27). This was perhaps surprising given the astonishing effects reported in mice lacking the ATG5 protein (Hashimoto et al., 2008). The field of research related to autophagy is however, relatively new and its precise

involvement in the pathogenesis of acute pancreatitis is yet to be fully elucidated.

Due to the constraints of obtaining viable samples of human pancreas from surgery, not every experiment conducted on murine cells could be undertaken with human cells. However, I believe that in this thesis, sufficient data were obtained to indicate broad similarity in their behaviour, underlining the relevance of murine data to human pathobiology (Murphy et al., 2008). ROS are frequently alluded to as negative, indiscriminate, chemically reactive molecules that mediate damage to organelles and bio-molecules, and they have been implicated in the pathogenesis of pancreatitis and many other diseases (Sanfey et al., 1984, Sanfey et al., 1985, Rutledge et al., 1987, Leung and Chan, 2009, Park et al., 2003, Bai et al., 2008, Bhardwaj et al., 2009, Gerasimenko et al., 2006). However, the presented data suggest that pancreatic acinar cells harness increases in $[ROS]_I$ to initiate apoptosis during toxic damage, affording a measure of protection, primarily by avoiding necrosis. Thus a certain degree of stress may be resisted by mitochondria until sufficient ROS are generated to turn on controlled apoptotic cell death thus preventing such cells from triggering the inflammatory response associated with necrosis.

As apoptosis is an ATP-dependent process, some preservation of mitochondrial function is required for apoptosis to occur. While increases in $[Ca^{2+}]_C$ and $[Ca^{2+}]_M$ accelerate operation of the electron transport chain (Petersen and Tepikin, 2008, Odinokova et al., 2009), excessive, prolonged elevations in $[Ca^{2+}]_C$ and $[Ca^{2+}]_M$ lead to a collapse of mitochondrial function as measured by the mitochondrial membrane potential and NAD(P)H autofluorescence (Criddle et al., 2006b), followed by

diminished ROS production from the inactivated electron transport chain (Yerushalmi et al., 2001) and impaired ROS clearance (Orrenius et al., 2007, Odinokova et al., 2009). Nevertheless in cells exposed to 200 μM TLC-S increases in NAD(P)H production were seen in response to large oscillations in $[Ca^{2+}]_C$, indicative of increased mitochondrial metabolism, via stimulus-metabolism coupling. In cells exposed to 500 μM TLC-S an early increase in NAD(P)H production was also seen, although in all cases this was followed by a marked depression in NAD(P)H. The data suggest, therefore, that the relative increases of $[Ca^{2+}]_M$ and $[ROS]_M$ play a major role in the relative induction of pancreatic acinar cell necrosis versus apoptosis respectively. Once mitochondria become sufficiently overloaded with Ca^{2+} and Ψ_m collapses, ATP levels fall, apoptosis is inhibited and necrosis ensues.

The experiments within this thesis may also demonstrate a cytosolic contribution to apoptosis-inducing elevations of [ROS]. Application of high concentrations of TLC-S led to a Ca^{2+}-dependent decrease in the concentration of NAD(P)H. NAD(P)H acts as an intracellular supply of reducing equivalents, upon which the enzymatic antioxidant machinery relies. Cytosolic glutathione peroxidase, thioredoxin and peroxiredoxin systems all depend upon available NAD(P)H to specifically deactivate various ROS by facilitating their interaction with small molecule antioxidants such as glutathione (reviewed in (Winterbourn, 2008)). Unlike the prodigious, sharp increase in $[ROS]_I$ induced by menadione, much of which originates from redox cycling via reductive enzymes such as the mitochondrial NADH-ubiquinone oxidoreductase (complex I) (Criddle et al., 2006a), the bile salt induced more modest rises in $[ROS]_I$. In fact inhibition of the cytosolic antioxidant enzyme NQO1 with DMN was required to show increased ROS production in cells exposed to 200 μM TLC-S.

The data presented in this thesis present something of a paradox with regard to the studies of experimental pancreatitis, where antioxidant strategies have been shown to be protective (Sanfey et al., 1984, Leung and Chan, 2009, Bhardwaj et al., 2009). The experimental and clinical studies are not able to isolate the effects of ROS production in the cells of interest, for example; effects of antioxidant strategies on the neutrophil, a major contributor of ROS, as well as inflammatory damage in acute pancreatitis (Pandol et al., 2007, Leung and Chan, 2009, Balaban et al., 2005, Guice et al., 1989, Tsuji et al., 1994, Gukovskaya et al., 2002b), may well account for some of the apparent conflict. Perhaps the best evidence to date is that of the first case controlled, double blind randomised clinical trial conducted by Siriwardena and colleagues (Siriwardena et al., 2007). In this study, administration of multiple antioxidants raised the level of circulating antioxidants to normal but failed to significantly ameliorate the disease state. In fact, in some cases antioxidant treatment was ceased because of increased organ damage. The work outlined within this thesis may provide a mechanistic explanation for these phenomena. Antioxidant treatment may have inhibited apoptosis, leading to $[Ca^{2+}]_C$ overload, mitochondrial injury and necrotic cell death.

The role of ROS as an apoptotic signal within the acinar cell may only be a small part of the total, production of ROS from such cells as recruited neutrophils is considerable. NADPH oxidase, a membrane component of neutrophil granules and secretory vesicles, transports electrons from NAD(P)H in the cytosol across their membranes, reducing molecular O_2 to form superoxide (O_2^-) (Reeves et al., 2002). ROS create charges across granular membranes that must be compensated by cation entry (DeCoursey et al., 2003), without which the charge difference created would inhibit further activity of NADPH oxidase. Although the contribution of NADPH oxidase-derived ROS is unclear, the ion shifts allow solubilisation and activation of

cationic serine proteases, which contribute to innate immunity, break down damaged tissue, and fine tune surrounding immune responses (Reeves et al., 2002). Following injury to the pancreas during acute inflammation, large amounts of trypsinogen are present within the interstitium of the organ (Hartwig et al., 1999), released proteases from recruited neutrophils bear the ability to activate this trypsinogen propagating the damage (Pham, 2006).

7.2 Ethanol, ethanol metabolites and ROS

The role of ethanol in the pathogenesis of acute pancreatitis is still somewhat enigmatic. Initially considered a chronic disease, there is now increased evidence that that pancreatic injury occurs from successive cycles of necrosis and fibrosis. As a precipitant of the disease alcohol abuse is quickly becoming the principal cause (Pandol et al., 2007). However, the mechanism of pathogenesis is still far from complete. Reactive oxygen species have been implicated in the pathogenesis of pancreatitis in both clinical and experimental studies (Sanfey et al., 1984, Schoenberg et al., 1990, Neuschwander-Tetri et al., 1992, Braganza et al., 1993). ROS have the capacity to damage lipid membranes, DNA and proteins, and elevated levels of these products have been found in the pancreatic juice in examples of both acute and chronic pancreatitis (Guyan et al., 1990). Additionally, levels of ROS are elevated in pancreatic tissue where experimental pancreatitis is induced (Nonaka et al., 1989a, Gough et al., 1990).

The source of ROS within the pancreas could conceivably be cells of the pancreas, extra pancreatic inflammatory cells of immune origin, or a combination. In the liver, an organ frequently associate with alcohol pathology, heavy alcohol intake induces hepatic cytochrome P4502E1 which is responsible for generation of hydroxyl radicals and H_2O_2 during the oxidation of ethanol to acetaldehyde (Cederbaum et al., 2001). Recent evidence has suggested that cytochrome P450 2E1 is present, active and inducible in the pancreatic acinar cell (Apte et al., 2005), providing interesting parallels between the organs. In the series of experiments presented in this thesis, the pancreatic acinar cell, the most numerous cell of the pancreas was assessed for generation of $[ROS]_i$ in real time. The data obtained strongly argued against the generation of significant $[ROS]_i$ by the acinar cell in response to ethanol and its immediate oxidative metabolite acetaldehyde.

The lack of acutely generated ROS in response to ethanol and acetaldehyde is an important finding although it could be considered surprising. There is significant evidence to suggest that acute ethanol administration leads to oxidative changes in experiments with rats, indicated by changes in the levels of pancreatic malonaldehyde (a lipid peroxidation product) and a decreased ratio of the reduced: oxidized glutathione (GSH:GSSG) (Altomare et al., 1996). This presents a conflict between data obtained in vivo and in vitro. However, this data is consistent with the literature, previous studies have demonstrated that ethanol and acetaldehyde have little or no effect upon $[Ca^{2+}]_c$, implicating non-oxidative effects instead (Criddle et al., 2004). In the absence of a large, sustained elevation of $[Ca^{2+}]_c$ the $[Ca^{2+}]_m$ would

not be significantly elevated and mitochondrial Ca^{2+} overload would be impossible. In this scenario, the mechanism proposed for bile acid mediated ROS generation is unlikely as a potential mechanism for ethanol and its metabolites. It is therefore, difficult to infer a mechanism common to both TLC-S and ethanol. Application of the extremely high (850mM) concentration of ethanol was carried out on an entirely analytical basis, as this concentration is far in excess of that achieved in the clinic. Even this level of ethanol proved without consistent effects on ROS generation within the pancreatic acinar cell (Figure 4.1). This high concentration was technically troublesome with regard to high-quality recordings of $[ROS]_{i,}$ as the cells frequently lose membrane integrity (Figure 4.1 A). Additionally, as DCFDA is an integrative, non-ratiometric indicator, a change in cell volume or leakage may result in recordings that are difficult to interpret.

Reports in the literature, using similar cells with the same indicator, suggest that ROS production from ethanol was attainable over a similar time period to that demonstrated here (Gonzalez et al., 2006). Experiments with TLC-S have shown that inhibition of NQO1 with DMN is able to reveal $[ROS]_i$ generation, however even with application of DMN ethanol-induced ROS production remained elusive (Figure 4.2). Application of ethanol, particularly high concentrations, was able to negatively affect the NAD(P)H concentration within cells as visualised by NAD(P)H autofluorescence (Figure 4.1 and 4.2), which may suggest a paradox, as oxidative ethanol metabolism by ADH actively produces NADH (Pushpakiran et al., 2004). Clearly further investigation is required with regard to the nature of ethanol metabolism in

the pancreatic acinar cell although these data provide strong evidence that ethanol does not mediate ROS production on a short timescale.

The role of acetaldehyde in the pathogenesis of alcohol mediated liver damage has been established for some time (Lumeng and Crabb, 2000), and cells of the liver are able to produce significant ROS when exposed to acetaldehyde (Novitskiy et al., 2006). In the data presented in this thesis, however, acetaldehyde was without effect on the production of ROS in the pancreatic acinar cell (Figure 4.3). Careful future work needs to be carried out in this area as ROS-mediated effects are present, and acetaldehyde is produced by ethanol oxidation, although the mechanism is not clear. Candidates for ethanol induced pancreatic ROS production may well lie outside the acinar cell, hepatocellular proteins have been shown to become modified following exposure to acetaldehyde, in a process that is not specific to the liver, interestingly these adduct-laden proteins elicit an immune response (Lieber, 1992). This suggests a scenario whereby ethanol consumption and subsequent acetaldehyde production, lead to the formation of acetaldehyde protein adducts (APA), which have been recorded in the pancreas (Iimuro et al., 1996), and other organs (reviewed in (Niemela, 2001)). Subsequent recruitment of inflammatory cells to the pancreas could follow in a similar manner to that demonstrated in the liver (Tuma and Klassen, 1992). Leading to the production of prodigious and deleterious ROS via the NAD(P)H oxidase and myeloperoxidase systems which are abundant in immune cells such as neutrophils.

Further clues from studies in the liver implicate the hepatic stellate cell in the production of ROS mediated by acetaldehyde in the liver (Novitskiy et al., 2006). The hepatic stellate cell is very similar in origin, phenotype and function to the pancreatic stellate cell (Friedman, 2008). Indeed, both cells express NADPH oxidase, and represent a viable mechanism for the generation of ethanol induced ROS in the pancreas (Friedman, 2008, Masamune et al., 2008). Furthermore, it is their activation by ROS (Masamune et al., 2008) and subsequent production of further ROS, which likely constitutes a feed-forward cycle.

The role of non-oxidative ethanol metabolites in the pathogenesis of acute pancreatitis is perhaps a crucial development in understanding of the disease. Unlike ethanol, and the oxidative metabolite acetaldehyde, non-oxidative metabolites have the ability to cause significant elevations of $[Ca^{2+}]_c$ and loss of mitochondrial NAD(P)H (Criddle et al., 2006b, Criddle et al., 2004). Mitochondrial inhibition is a major feature of these molecules, leading to a distinct loss of mitochondrial function and ultimately necrosis (Criddle et al., 2006b, Criddle et al., 2004). The elevation of $[Ca^{2+}]_c$ is pronounced and sustained, therefore the mitochondria are exposed to high concentrations of Ca^{2+} for significant periods of time. However, application of POA and POAEE in the presence of ethanol, were without effect on $[ROS]_i$ generation (Figure 4.4 and 4.5). The absence of effect of non-oxidative metabolites of ethanol is perhaps surprising, given the strong effect upon mitochondrial function as measured by NAD(P)H autofluorescence (Figure 4.4 and 4.5). However, explanation may lie in the initial characterisation of FAEEs in the heart. Lange and Sobel observed direct actions of FAEEs on the

mitochondria of perfused rabbit hearts (Lange and Sobel, 1983). Mitochondrial dysfunction was confirmed in pancreatic acinar cells much more recently (Criddle et al., 2006b, Criddle et al., 2004), and within this the explanation may lie. If FAEEs and subsequently hydrolysed FA disrupt the integrity of the inner mitochondrial membrane, then ROS derived from the normal operation of the electron transport chain would cease; uncoupling of oxidative phosphorylation classically reduces mitochondrial ROS production. However, the depletion of NAD(P)H as a reducing equivalent may render many of the enzymatic ROS defence mechanisms incapable, and the cell extremely vulnerable to exogenously generated ROS. This may impart a partial explanation for the apparent discrepancy with the work of Gonzalez *et al.* where DCFDA-loaded cells were assessed in a cuvette, and showed small elevations of ROS. However, his method does not exclude contamination with non-acinar cells, such as pancreatic stellate cells or neutrophils, which may possess NAD(P)H oxidase and significantly contribute to the total ROS production..

7.3 Ethanol metabolism and cell fate

The pancreas is a major target of ethanol toxicity as mediated via its high rate of FAEE synthase activity and FAEE production during alcohol exposure (Laposata and Lange, 1986, Kaphalia and Ansari, 2001). Non-oxidative metabolites such as ethyl palmitate, cause acinar cell injury as measured by trypsin activation peptide (TAP) and vacuolization (Werner et al., 1997). The fate of cells exposed to ethanol and its metabolites was investigated in this series of experiments (Chapter 5). The relative balance between apoptosis and necrosis is of critical importance to the pathogenesis of acute

pancreatitis, with greater necrosis correlating with a poor prognosis (Pandol et al., 2007). Ethanol alone, at a variety of concentrations, produced an increase in cell death, with higher concentrations producing more cell death (Figure 5.1). The concentrations attainable in the clinic however, (1-100mM) were without significant effect, and although higher concentrations did produce measureable cell injury, this again underlined the remarkable lack of effect of ethanol on the isolated acinar cell. These effects upon cell fate support the literature (Criddle et al., 2004) with regard to the absence of large elevations of $[Ca^{2+}]_c$; a crucial stage in pancreatic acinar cell fate. The assumption that ethanol toxicity is not mediated directly via ethanol or acetaldehyde strongly implicates the non-oxidative pathway. In the absence of exogenously applied free fatty acid, ethanol is less able to form FAEE by esterification.

Further evidence against the involvement of oxidative metabolism was provided in Figure 5.1B. Application of acetaldehyde was without effect on acinar cell fate. This is perhaps surprising, however, acetaldehyde was previously demonstrated to be without effect on $[ROS]_{i,}$ and the results are consistent with the literature where acetaldehyde was without effect on $[Ca^{2+}]_c$ (Criddle et al., 2004). Within this thesis, data in the form of cell fate assays provided convincing evidence against a central role of acetaldehyde in the production of ROS and determination of cell fate. Rapid onset cell injury and necrosis was completely absent from cells treated with acetaldehyde, and prevalent with cells treated with non-oxidative metabolites.

Application of the non-oxidative metabolites of ethanol, FAEE and FA were in marked contrast to both ethanol and acetaldehyde (Figure 5.2). Both FAEE

and FA were capable of inducing significant cell death, primarily necrosis at the same concentrations shown to induce $[Ca^{2+}]_c$ elevations and mitochondrial dysfunction. Interestingly, the FA POA displayed a concentration dependent increase in cellular necrosis, which was entirely consistent with the effects observed on $[Ca^{2+}]_c$ (Criddle et al., 2004). This was in contrast to POAEE, which showed little change between the minimal and maximal concentrations used (Figure 5.2 B). Potentially, POAEE is at a maximal effect, which is supported by the absence of ethanol potentiating further cell death (Figure 5.3 B). This is entirely consistent with the hypothesis that the toxic effects of FAEE are mediated by hydrolysis to FFA. When hydrolase activity was inhibited FAEE ceased to display such marked mitochondrial inhibition (Criddle et al., 2006b).

The disparity between the great amount of people with a very large alcohol intake, and the relatively small number of those suffering from alcohol-induced pancreatitis, is something of a puzzle, and has highlighted the possibility of individual variations in ethanol metabolism as a mechanism for pancreatic injury (Haber et al., 1995). Werner and colleagues initially manipulated ethanol metabolism in experimental studies on rats. They found that the inhibition of ADH with 4-methylpyrazole increased both the generation of FAEE and measured parameters of cellular injury (Werner et al., 2001). General inhibition in a whole animal does not necessarily implicate changed intra-pancreatic alcohol metabolism, especially in the light of the supposedly 4-MP-insensitive ADH isoforms detected by Haber and colleagues (Haber et al., 1998). Data presented here show that 4MP alone was without effect on overall cell fate, (Figure 5.4 A). In the same fashion,

low concentrations of the individual compounds ethanol, POA and the BNPP (a general hydrolase inhibitor) were unable to increase either necrosis or apoptosis (Figure 5.4). Ultimately, the combination of ethanol and POA produced a minor increase in necrosis compared to either substance alone, suggesting a synergistic effect of both compounds presumably via formation of FAEEs (Figure 5.4, B). Previous work has demonstrated that 4-MP did not increase overall cell death compared to ethanol alone (Figure 5.3 A and 5.1 A). However, when much lower concentrations of ethanol, POA and the same concentration of 4MP were used, a significant increase in overall cell death was seen (Figure 5.4). This was a fascinating finding, as cell death could only be demonstrated when the substrates for FAEE synthesis were available and oxidative ethanol metabolism was concurrently inhibited. This strongly suggested that FAEE synthesis occurred within the freshly isolated acinar cell. Given strong evidence suggesting that FAEE toxicity is mediated via re-hydrolysis, yielding free fatty acids (Lange and Sobel, 1983), addition of BNPP would be expected to decrease the toxicity of the POA, ethanol 4-MP mixture. This was observed (Figure 5.4 B), providing evidence for a model whereby FAEE synthesis and re-hydrolysis back to FA may mediate cell damage within the timescale of these experiments, a timescale which may be consistent with an the rapid onset of pancreatic injury which contrasts with the progressive damage seen in the liver.

Recent work in the AR42J cell-line has demonstrated the presence of the 66 kDa. protein FAEE synthase and also demonstrated the efficacy of the FAEE synthase inhibitor 3-benzyl-6-chloro-2-pyrone (3-BCP) (Wu et al., 2008) to prevent formation of FAEEs. Applied to acinar cells, 3-BCP was clearly

effective in reducing both apoptosis and necrosis to the same levels as those seen without 4-methylpyrazole (Figure 5.5). This effect is remarkable, because although FAEE synthase activity has been inhibited in hepatocyte-derived cell lines, with tri-*o*-tolyl phosphate (Kaphalia et al., 1999), and pancreatic-derived cell lines (Wu et al., 2008) with 3-BCP, inhibition and the subsequent effects on cell fate have not been demonstrated upon primary isolated pancreatic acinar cells. Taken together the evidence is compelling, cell fate is not affected by each component in isolation, however when the components of FAEEs are available and oxidative metabolism is inhibited a significant increase in cell death is seen. This increase is largely rescued by inhibition of FAEE synthase with 3-BCP, strongly implicating the influence of FAEE synthase and the subsequent generation of FAEEs.

7.4 Ethanol metabolism, Ca^{2+}-homeostasis and mitochondrial function

Application of low concentrations of ethanol and POA in the presence of 4-MP resulted in greatly increased cell death compared to each compound in isolation and other combinations. Assuming the intracellular generation of FAEEs, it is logical to conclude that 3-BCP and BNPP prevented the formation and re-hydrolysis of FAEE respectively. Experiments designed to establish the role of these compounds and combinations of compounds upon the Ca^{2+}-homeostasis and mitochondrial function were devised. 4-MP was predominantly without effect upon either $[Ca^{2+}]_c$ or $\Delta\psi_m$ (Figure 6.1 and 6.5) suggesting that inhibition of ADH alone is not sufficient, in the absence of

other stimulation, to cause any perturbation of the Ca^{2+}-homeostasis or mitochondrial function. Perfusion of ethanol and POA produced predominantly transient global spiking events, (Figure 6.2) although in some cases sustained Ca^{2+} elevations were seen. This is consistent with the cell death data whereby conditions causing cell death were similar to those causing extreme elevations of $[Ca^{2+}]_c$ and mitochondrial inhibition. Furthermore the combination had a moderate depolarizing effect on the $\Delta\psi_m$, (Figure 6.6). The combination of ethanol, POA and 4-MP produced the most cell death, the same combination demonstrated a strong downward $\Delta\psi_m$, causing rapid depolarization and pronounced dysregulation of $[Ca^{2+}]_c$ (Figure 6.5 and 6.3). Application of free fatty acids, specifically POA, did not cause sharp Ca^{2+} "spikes" (Criddle et al., 2004). Sharp "spikes" were demonstrated to be POAEE-mediated Ca^{2+} events that were acutely sensitive to the classical IP_3R inhibitor caffeine (Criddle et al., 2006b). The sharp Ca^{2+} spikes seen in response to ethanol and POA and the initial component shown in response to ethanol, POA and 4-MP combination are likely to be due to the generation of POAEE from the exogenously applied ethanol and POA. Particularly interesting was the extremely rapid onset of spiking, and subsequent global sustained rises, underlining the rapid rate of intracellular generation of FAEEs and subsequent hydrolysis. However, this is yet to be confirmed by direct biochemical analysis.

Perhaps the most interesting evidence was supplied by experiments performed with the FAEE synthase inhibitor addition of 3-BCP to the combination of ethanol, POA and 4-MP. When 3-BCP was present, $\Delta\psi_m$ was

preserved (Figure 6.8), NAD(P)H was maintained (Figure 6.9 A) and $[Ca^{2+}]_c$ was unaffected in all cases tested (Figure 6.9 B). These data strongly implicate the FAEE-synthase mediated synthesis of FAEE from exogenously applied substrates in pancreatic acinar cells when oxidative metabolism is compromised. Unlike experiments in AR42J cells, which are neoplastic in origin, these data provide the first evidence that FAEEs are synthesised within pancreatic acinar cells and exert deleterious effects consistent with in vitro, in vivo and human studies. The inhibition of FAEE synthase with 3-BCP provides a fascinating opportunity; the compound is tolerated in a wide variety of animal models (Deck et al., 1999, Heidrich et al., 2004), and may to inhibit FAEE synthesis and its downstream effects in human cells.

Chapter 8

Concluding remarks

8.1 Summary

In this present study we have investigated the effects of two of the major precipitants of acute pancreatitis, alcohol and bile salts in pancreatic acinar cells (Pandol et al., 2007). Briefly, we found that bile salt-mediated Ca^{2+} led to an overload of mitochondrial Ca^{2+}, during these events, modest generation of ROS was observed and experimentally confirmed to be Ca^{2+}-dependent ROS which was reliant upon the functional electron transport chain. This ROS generation was crucial to the development of caspase activation and full apoptosis. Within the wider context of pancreatitis, this ROS generation may provide a vital signal in the determination of acinar cell death, stimulating apoptosis rather than necrosis. These data shed light on recent clinical trial upon the wider role of ROS in cell signalling.

Against current expectations, ROS generation was not apparent in acinar cells exposed to ethanol, acetaldehyde or examples of non-oxidative ethanol metabolites. In spite of significant evidence that ROS levels are elevated in alcohol-induced pancreatitis, no evidence was found to implicate ethanol, acetaldehyde or FAEEs in the generation of ROS within the acinar cell. This implicates non-acinar cells as the primary sources of ROS within the pancreas and subsequent injury associated with those species.

We also demonstrated that alcohol is able to produce cellular injury via the intracellular generation of non-oxidative ethanol metabolites: fatty acid ethyl esters. These data demonstrate that the isolated, primary pancreatic acinar cell is capable of synthesising FAEEs, and that those FAEEs mediate Ca^{2+} dysregulation, mitochondrial injury and cellular necrosis. Crucially, the

generation of these toxic intermediates was inhibited by 3-BCP, which represents a clear strategy for amelioration of pancreatitis in experimental studies and beyond.

8.2 Calcium-dependent pancreatic acinar cell death induced by bile salts

The role of ROS in pancreatitis is a subject of much history and debate, and questions still remain as to the wider implications of altering local or systemic ROS levels as treatment for pancreatitis. Substantial evidence supports the notion that oxidants, free radicals and downstream products such as reactive nitrogen species, (RNS) can cause severe deleterious effects when present in excess (Leung and Chan, 2009, Droge, 2002, Orrenius et al., 2007). In spite of this, the generation of free radicals is a feature of all viable cells and highly conserved mechanisms regulate their production, use and control (Droge, 2002, Orrenius et al., 2007, Balaban et al., 2005). ROS and RNS are integral parts of or exert effects on, a range of signalling cascades in both animals and plants (e.g. control of cell growth and differentiation, glucose utilisation, erythropoietin production, vascular tone, ventilation, immune responses) (Droge, 2002). Since ROS production is increased in disease (Orrenius et al., 2007), it might be expected that high levels of $[ROS]_i$ would initiate protective response mechanisms. The balance of protective versus deleterious effects of ROS is complex and subject to dysregulation. A recent meta-analysis of randomized clinical trials has suggested antioxidant supplements may increase mortality in several diseases (Bjelakovic et al., 2007) which would suggest that a generalized ROS removal is a naive strategy. Although there may yet prove to be a role for antioxidants in the

pain management of chronic pancreatitis (Bhardwaj et al., 2009), our data suggest an explanation for the lack of effect of antioxidant therapy in randomized clinical trials for acute pancreatitis (Siriwardena et al., 2007). More coherent strategies may focus on the central problem of pancreatitis, Ca^{2+} overload. Preventing or attenuating Ca^{2+} or entry, may help reduce the Ca^{2+} load, alternatively protection of the mitochondria would prevent ATP depletion, allowing Ca^{2+} clearance or apoptosis.

8.3 Alcohol and alcohol metabolites: ROS generation

ROS generation mediated by alcohol, its oxidative metabolism and its oxidative metabolites, are implicated in the development of alcoholic liver disease and may certainly play a role in the slow progressive component of chromic pancreatitis. However, within the limitations of the experiments presented here, no significant ROS generation was demonstrated in response to any of the precipitants used.

Application of ethanol was perhaps most likely to generate ROS as metabolism via CYP2E1 has been demonstrated to do so (Cederbaum et al., 2001) and is present in the pancreas (Norton et al., 1998). Perhaps longer term experiments would expose the inducible nature of CYP42E1 and subsequent ROS generation (Norton et al., 1998). This poses technical challenges with regard to the integrative nature of indicators designed to measure ROS directly, and indirect methodology such as measurement of peroxidated lipids, does not yield the spatiotemporal resolution afforded by direct measurement.

Non-oxidative metabolites of ethanol have been demonstrated to cause mitochondrial dysfunction in the pancreatic acinar cell (Criddle et al., 2006c,

Voronina et al., 2010). Dysfunctional mitochondria have been associated with ROS production in a number of disease states (Kakkar and Singh, 2007), particularly with regard to Ca^{2+} overload (Brookes et al., 2004). The absence of ROS generation following application of non-oxidative metabolites may be explained by the rapid depolarisation of the mitochondrial membrane potential, inhibiting mitochondrial ROS production.

The data presented within this thesis establish that ROS are likely generated outside of the pancreatic acinar cell, by numerous candidates equipped to do so. However this does not completely remove the possibility, if ROS are generated within the acinar cell the timescale is much different than that of ROS generated in response to bile salts. The implications for the alcoholic pancreatitis are that ROS generation mediated by bile salts and alcohol may be fundamentally different in their generation and effect.

8.4 Alcohol and alcohol metabolites: Cell fate, Ca^{2+} signalling and membrane potential

Non-oxidative metabolites of ethanol have been implicated in the pathogenesis of pancreatitis for some time (Laposata and Lange, 1986). The study suggests multiple sites of generation, however generation within the pancreas itself may be crucial, as FAEEs are rapidly hydrolysed in transit (Saghir et al., 1997). The results presented in this thesis demonstrate for the first time that FAEEs are most likely generated within the acinar cells of the pancreas and promote deleterious changes in Ca^{2+} homeostasis and

mitochondrial function. These effects were blocked by inhibition of pancreatic FAEE synthase, which represents a logical strategy for preventing acinar cell necrosis and wider injury common to alcohol-induced pancreatitis. The implications for the disease focus on the changes elicited by the inhibition of oxidative metabolism, which was able to promote the toxic effects of non-oxidative ethanol metabolites. In a poorly understood disease state, these data may shed some light upon factors contributing to the pathogenesis of acute pancreatitis. However, more investigation is necessary to establish the role of both free fatty acids and FAEE in the pathogenesis of AP, particularly with regard to that caused by alcohol as opposed to other precipitants.

Chapter 9

Bibliography

AARHUS, R., DICKEY, D. M., GRAEFF, R. M., GEE, K. R., WALSETH, T. F. & LEE, H. C. 1996. Activation and inactivation of Ca2+ release by NAADP+. *J Biol Chem,* 271**,** 8513-6.

ADACHI, T., WEISBROD, R. M., PIMENTEL, D. R., YING, J., SHAROV, V. S., SCHONEICH, C. & COHEN, R. A. 2004. S-Glutathiolation by peroxynitrite activates SERCA during arterial relaxation by nitric oxide. *Nat Med,* 10**,** 1200-7.

ADAM-VIZI, V. & CHINOPOULOS, C. 2006. Bioenergetics and the formation of mitochondrial reactive oxygen species. *Trends Pharmacol Sci,* 27**,** 639-45.

ALERYANI, S., KABAKIBI, A., CLUETTE-BROWN, J. & LAPOSATA, M. 1996. Fatty acid ethyl ester synthase, an enzyme for nonoxidative ethanol metabolism, is present in serum after liver and pancreatic injury. *Clin Chem,* 42**,** 24-7.

ALLBRITTON, N. L., MEYER, T. & STRYER, L. 1992. Range of messenger action of calcium ion and inositol 1,4,5-trisphosphate. *Science,* 258**,** 1812-5.

ALTOMARE, E., GRATTAGLIANO, I., VENDEMIALE, G., PALMIERI, V. & PALASCIANO, G. 1996. Acute ethanol administration induces oxidative changes in rat pancreatic tissue. *Gut,* 38**,** 742-6.

APTE, M. V., PIROLA, R. C. & WILSON, J. S. 2005. Molecular mechanisms of alcoholic pancreatitis. *Dig Dis,* 23**,** 232-40.

APTE, M. V., PIROLA, R. C. & WILSON, J. S. 2006. Fatty acid ethyl esters--alcohol's henchmen in the pancreas? *Gastroenterology,* 130**,** 992-5.

APTE, M. V., PIROLA, R. C. & WILSON, J. S. 2008. Individual susceptibility to alcoholic pancreatitis. *J Gastroenterol Hepatol,* 23 Suppl 1**,** S63-8.

ARGENT, B. E. 2006. Cell physiology of the pancreatic ducts. *In:* JOHNSON, L. R. (ed.) *Physiology of the gastrointestinal tract.* 4th ed. San Diego: Elsevier.

ASHBY, M. C., CRASKE, M., PARK, M. K., GERASIMENKO, O. V., BURGOYNE, R. D., PETERSEN, O. H. & TEPIKIN, A. V. 2002. Localized Ca2+ uncaging reveals polarized distribution of Ca2+-sensitive Ca2+ release sites: mechanism of unidirectional Ca2+ waves. *J Cell Biol,* 158**,** 283-92.

ASHBY, M. C. & TEPIKIN, A. V. 2002. Polarized calcium and calmodulin signaling in secretory epithelia. *Physiol Rev,* 82**,** 701-34.

ASHER, G., LOTEM, J., KAMA, R., SACHS, L. & SHAUL, Y. 2002. NQO1 stabilizes p53 through a distinct pathway. *Proc Natl Acad Sci U S A,* 99**,** 3099-104.

BAGGALEY, E. M., ELLIOTT, A. C. & BRUCE, J. I. 2008. Oxidant-induced inhibition of the plasma membrane Ca2+-ATPase in pancreatic acinar cells: role of the mitochondria. *Am J Physiol Cell Physiol,* 295**,** C1247-60.

BAI, Y., GAO, J., ZHANG, W., ZOU, D. & LI, Z. 2008. Meta-analysis: allopurinol in the prevention of postendoscopic retrograde cholangiopancreatography pancreatitis. *Aliment Pharmacol Ther,* 28**,** 557-64.

BALABAN, R. S., NEMOTO, S. & FINKEL, T. 2005. Mitochondria, oxidants, and aging. *Cell,* 120**,** 483-95.

BANKS, P. A. & FREEMAN, M. L. 2006. Practice guidelines in acute pancreatitis. *Am J Gastroenterol,* 101**,** 2379-400.

BEDARD, K. & KRAUSE, K. H. 2007. The NOX family of ROS-generating NADPH oxidases: physiology and pathophysiology. *Physiol Rev,* 87**,** 245-313.

BERRIDGE, M. J. 1981. Phosphatidylinositol hydrolysis and calcium signaling. *Adv Cyclic Nucleotide Res,* 14**,** 289-99.

BERRIDGE, M. J. 2001. The versatility and complexity of calcium signalling. *Novartis Found Symp,* 239**,** 52-64; discussion 64-7, 150-9.

BERRIDGE, M. J., BOOTMAN, M. D. & RODERICK, H. L. 2003. Calcium signalling: dynamics, homeostasis and remodelling. *Nat Rev Mol Cell Biol,* 4**,** 517-29.

BETZENHAUSER, M. J., WAGNER, L. E., 2ND, IWAI, M., MICHIKAWA, T., MIKOSHIBA, K. & YULE, D. I. 2008. ATP modulation of Ca2+ release by type-2 and type-3 inositol (1, 4, 5)-triphosphate receptors. Differing ATP sensitivities and molecular determinants of action. *J Biol Chem,* 283**,** 21579-87.

BEYER, R. E., SEGURA-AGUILAR, J., DI BERNARDO, S., CAVAZZONI, M., FATO, R., FIORENTINI, D., GALLI, M. C., SETTI, M., LANDI, L. & LENAZ, G. 1996. The role of DT-diaphorase in the maintenance of the reduced antioxidant form of coenzyme Q in membrane systems. *Proc Natl Acad Sci U S A,* 93**,** 2528-32.

BEZPROZVANNY, I., WATRAS, J. & EHRLICH, B. E. 1991. Bell-shaped calcium-response curves of Ins(1,4,5)P3- and calcium-gated channels from endoplasmic reticulum of cerebellum. *Nature,* 351**,** 751-4.

BHARDWAJ, P., GARG, P. K., MAULIK, S. K., SARAYA, A., TANDON, R. K. & ACHARYA, S. K. 2009. A randomized controlled trial of antioxidant supplementation for pain relief in patients with chronic pancreatitis. *Gastroenterology,* 136**,** 149-159 e2.

BHATIA, M., WALLIG, M. A., HOFBAUER, B., LEE, H. S., FROSSARD, J. L., STEER, M. L. & SALUJA, A. K. 1998. Induction of apoptosis in pancreatic acinar cells reduces the severity of acute pancreatitis. *Biochem Biophys Res Commun,* 246**,** 476-83.

BHATIA, M., WONG, F. L., CAO, Y., LAU, H. Y., HUANG, J., PUNEET, P. & CHEVALI, L. 2005. Pathophysiology of acute pancreatitis. *Pancreatology,* 5**,** 132-44.

BHOPALE, K. K., WU, H., BOOR, P. J., POPOV, V. L., ANSARI, G. A. & KAPHALIA, B. S. 2006. Metabolic basis of ethanol-induced hepatic and pancreatic injury in hepatic alcohol dehydrogenase deficient deer mice. *Alcohol,* 39**,** 179-88.

BJELAKOVIC, G., NIKOLOVA, D., GLUUD, L. L., SIMONETTI, R. G. & GLUUD, C. 2007. Mortality in randomized trials of antioxidant supplements for primary and secondary prevention: systematic review and meta-analysis. *JAMA,* 297**,** 842-57.

BOCKMAN, D. E., SCHILLER, W. R., SURIYAPA, C., MUTCHLER, J. H. & ANDERSON, M. C. 1973. Fine structure of early experimental acute pancreatitis in dogs. *Lab Invest,* 28**,** 584-92.

BOGESKI, I., KUMMEROW, C., AL-ANSARY, D., SCHWARZ, E. C., KOEHLER, R., KOZAI, D., TAKAHASHI, N., PEINELT, C., GRIESEMER, D., BOZEM, M., MORI, Y., HOTH, M. & NIEMEYER, B. A. 2010. Differential redox regulation of ORAI ion channels: a mechanism to tune cellular calcium signaling. *Sci Signal,* 3**,** ra24.

BOHLEY, P. & SEGLEN, P. O. 1992. Proteases and proteolysis in the lysosome. *Experientia,* 48**,** 151-7.

BOITANO, S., DIRKSEN, E. R. & SANDERSON, M. J. 1992. Intercellular propagation of calcium waves mediated by inositol trisphosphate. *Science,* 258**,** 292-5.

BOOTMAN, M. D., TAYLOR, C. W. & BERRIDGE, M. J. 1992. The thiol reagent, thimerosal, evokes Ca2+ spikes in HeLa cells by sensitizing the inositol 1,4,5-trisphosphate receptor. *J Biol Chem,* 267**,** 25113-9.

BRAGANZA, J. M., SCHOFIELD, D., SNEHALATHA, C. & MOHAN, V. 1993. Micronutrient antioxidant status in tropical compared with temperate-zone chronic pancreatitis. *Scand J Gastroenterol,* 28**,** 1098-104.

BROOKES, P. S., YOON, Y., ROBOTHAM, J. L., ANDERS, M. W. & SHEU, S. S. 2004. Calcium, ATP, and ROS: a mitochondrial love-hate triangle. *Am J Physiol Cell Physiol,* 287**,** C817-33.

BRUCE, J. I. & ELLIOTT, A. C. 2007. Oxidant-impaired intracellular Ca2+ signaling in pancreatic acinar cells: role of the plasma membrane Ca2+-ATPase. *Am J Physiol Cell Physiol,* 293**,** C938-50.

CAMELLO-ALMARAZ, M. C., POZO, M. J., MURPHY, M. P. & CAMELLO, P. J. 2006. Mitochondrial production of oxidants is necessary for physiological calcium oscillations. *J Cell Physiol,* 206**,** 487-94.

CANCELA, J. M., CHURCHILL, G. C. & GALIONE, A. 1999. Coordination of agonist-induced Ca2+-signalling patterns by NAADP in pancreatic acinar cells. *Nature,* 398**,** 74-6.

CANCELA, J. M., VAN COPPENOLLE, F., GALIONE, A., TEPIKIN, A. V. & PETERSEN, O. H. 2002. Transformation of local Ca2+ spikes to global Ca2+ transients: the combinatorial roles of multiple Ca2+ releasing messengers. *Embo J,* 21**,** 909-19.

CARAFOLI, E. & BRINI, M. 2000. Calcium pumps: structural basis for and mechanism of calcium transmembrane transport. *Curr Opin Chem Biol,* 4**,** 152-61.

CARNEY, J. M., STARKE-REED, P. E., OLIVER, C. N., LANDUM, R. W., CHENG, M. S., WU, J. F. & FLOYD, R. A. 1991. Reversal of age-related increase in brain protein oxidation, decrease in enzyme activity, and loss in temporal and spatial memory by chronic administration of the spin-trapping compound N-tert-butyl-alpha-phenylnitrone. *Proc Natl Acad Sci U S A,* 88**,** 3633-6.

CEDERBAUM, A. I. 2003. Iron and CYP2E1-dependent oxidative stress and toxicity. *Alcohol,* 30**,** 115-20.

CEDERBAUM, A. I., WU, D., MARI, M. & BAI, J. 2001. CYP2E1-dependent toxicity and oxidative stress in HepG2 cells. *Free Radic Biol Med,* 31**,** 1539-43.

CHEN, Q., VAZQUEZ, E. J., MOGHADDAS, S., HOPPEL, C. L. & LESNEFSKY, E. J. 2003. Production of reactive oxygen species by mitochondria: central role of complex III. *J Biol Chem,* 278**,** 36027-31.

CHEY, W. Y., KIM, M. S., LEE, K. Y. & CHANG, T. M. 1979. Effect of rabbit antisecretin serum on postprandial pancreatic secretion in dogs. *Gastroenterology,* 77**,** 1268-75.

CLAPHAM, D. E. 1995. Calcium signaling. *Cell,* 80**,** 259-68.

CLAPHAM, D. E. 2007. Calcium signaling. *Cell,* 131**,** 1047-58.

COLLINS, S. & MEYER, T. 2010. Cell biology: A sensor for calcium uptake. *Nature,* 467**,** 283.

COSKER, F., CHEVIRON, N., YAMASAKI, M., MENTEYNE, A., LUND, F. E., MOUTIN, M. J., GALIONE, A. & CANCELA, J. M. 2010. The ecto-enzyme CD38 is a NAADP synthase which couples receptor activation to Ca2+ mobilization from lysosomes in pancreatic acinar cells. *J Biol Chem*.

CRIDDLE, D. N., GERASIMENKO, J. V., BAUMGARTNER, H. K., JAFFAR, M., VORONINA, S., SUTTON, R., PETERSEN, O. H. & GERASIMENKO, O. V. 2007. Calcium signalling and pancreatic cell death: apoptosis or necrosis? *Cell Death Differ,* 14**,** 1285-94.

CRIDDLE, D. N., GILLIES, S., BAUMGARTNER-WILSON, H. K., JAFFAR, M., CHINJE, E. C., PASSMORE, S., CHVANOV, M., BARROW, S., GERASIMENKO, O. V., TEPIKIN, A. V., SUTTON, R. & PETERSEN, O. H. 2006a. Menadione-induced reactive oxygen species generation via redox cycling promotes apoptosis of murine pancreatic acinar cells. *J Biol Chem,* 281**,** 40485-92.

CRIDDLE, D. N., MURPHY, J., FISTETTO, G., BARROW, S., TEPIKIN, A. V., NEOPTOLEMOS, J. P., SUTTON, R. & PETERSEN, O. H. 2006b. Fatty acid ethyl esters cause pancreatic calcium toxicity via inositol trisphosphate receptors and loss of ATP synthesis. *Gastroenterology,* 130**,** 781-93.

CRIDDLE, D. N., RARATY, M. G., NEOPTOLEMOS, J. P., TEPIKIN, A. V., PETERSEN, O. H. & SUTTON, R. 2004. Ethanol toxicity in pancreatic acinar cells: mediation by nonoxidative fatty acid metabolites. *Proc Natl Acad Sci U S A,* 101**,** 10738-43.

CRIDDLE, D. N., SUTTON, R. & PETERSEN, O. H. 2006c. Role of Ca2+ in pancreatic cell death induced by alcohol metabolites. *J Gastroenterol Hepatol,* 21 Suppl 3**,** S14-7.

D'AUTREAUX, B. & TOLEDANO, M. B. 2007. ROS as signalling molecules: mechanisms that generate specificity in ROS homeostasis. *Nat Rev Mol Cell Biol,* 8**,** 813-24.

DABROWSKI, A., GABRYELEWICZ, A., WERESZCZYNSKA-SIEMIATKOWSKA, U. & CHYCZEWSKI, L. 1988. Oxygen-derived free radicals in cerulein-induced acute pancreatitis. *Scand J Gastroenterol,* 23**,** 1245-9.

DECK, L. M., BACA, M. L., SALAS, S. L., HUNSAKER, L. A. & VANDER JAGT, D. L. 1999. 3-Alkyl-6-chloro-2-pyrones: selective inhibitors of pancreatic cholesterol esterase. *J Med Chem,* 42**,** 4250-6.

DECOURSEY, T. E., MORGAN, D. & CHERNY, V. V. 2003. The voltage dependence of NADPH oxidase reveals why phagocytes need proton channels. *Nature,* 422**,** 531-4.

DENG, X., WANG, L., ELM, M. S., GABAZADEH, D., DIORIO, G. J., EAGON, P. K. & WHITCOMB, D. C. 2005. Chronic alcohol consumption accelerates fibrosis in response to cerulein-induced pancreatitis in rats. *Am J Pathol,* 166**,** 93-106.

DINKOVA-KOSTOVA, A. T. & TALALAY, P. 2000. Persuasive evidence that quinone reductase type 1 (DT diaphorase) protects cells against the toxicity of electrophiles and reactive forms of oxygen. *Free Radic Biol Med,* 29**,** 231-40.

DOYLE, K. M., BIRD, D. A., AL-SALIHI, S., HALLAQ, Y., CLUETTE-BROWN, J. E., GOSS, K. A. & LAPOSATA, M. 1994. Fatty acid ethyl esters are present in human serum after ethanol ingestion. *J Lipid Res,* 35**,** 428-37.

DROGE, W. 2002. Free radicals in the physiological control of cell function. *Physiol Rev,* 82**,** 47-95.

DU, W. D., YUAN, Z. R., SUN, J., TANG, J. X., CHENG, A. Q., SHEN, D. M., HUANG, C. J., SONG, X. H., YU, X. F. & ZHENG, S. B. 2003. Therapeutic efficacy of high-dose vitamin C on acute pancreatitis and its potential mechanisms. *World J Gastroenterol,* 9**,** 2565-9.

ESREFOGLU, M., GUL, M., ATES, B. & SELIMOGLU, M. A. 2006. Ultrastructural clues for the protective effect of melatonin against oxidative damage in cerulein-induced pancreatitis. *J Pineal Res,* 40**,** 92-7.

EU, J. P., SUN, J., XU, L., STAMLER, J. S. & MEISSNER, G. 2000. The skeletal muscle calcium release channel: coupled O2 sensor and NO signaling functions. *Cell,* 102**,** 499-509.

FESKE, S., GWACK, Y., PRAKRIYA, M., SRIKANTH, S., PUPPEL, S. H., TANASA, B., HOGAN, P. G., LEWIS, R. S., DALY, M. & RAO, A. 2006. A mutation in Orai1 causes immune deficiency by abrogating CRAC channel function. *Nature,* 441**,** 179-85.

FINDLAY, I. & PETERSEN, O. H. 1983. The extent of dye-coupling between exocrine acinar cells of the mouse pancreas. The dye-coupled acinar unit. *Cell Tissue Res,* 232**,** 121-7.

FOSKETT, J. K., WHITE, C., CHEUNG, K. H. & MAK, D. O. 2007. Inositol trisphosphate receptor Ca2+ release channels. *Physiol Rev,* 87**,** 593-658.

FRIDOVICH, I. 1995. Superoxide radical and superoxide dismutases. *Annu Rev Biochem,* 64**,** 97-112.

FRIEDMAN, S. L. 2008. Hepatic stellate cells: protean, multifunctional, and enigmatic cells of the liver. *Physiol Rev,* 88**,** 125-72.

FROSSARD, J. L., RUBBIA-BRANDT, L., WALLIG, M. A., BENATHAN, M., OTT, T., MOREL, P., HADENGUE, A., SUTER, S., WILLECKE, K. & CHANSON, M. 2003. Severe acute pancreatitis and reduced acinar cell apoptosis in the exocrine pancreas of mice deficient for the Cx32 gene. *Gastroenterology,* 124**,** 481-93.

FUTATSUGI, A., NAKAMURA, T., YAMADA, M. K., EBISUI, E., NAKAMURA, K., UCHIDA, K., KITAGUCHI, T., TAKAHASHI-IWANAGA, H., NODA, T., ARUGA, J. & MIKOSHIBA, K. 2005. IP3 receptor types 2 and 3 mediate exocrine secretion underlying energy metabolism. *Science,* 309**,** 2232-4.

GALLUZZI, L., AARONSON, S. A., ABRAMS, J., ALNEMRI, E. S., ANDREWS, D. W., BAEHRECKE, E. H., BAZAN, N. G., BLAGOSKLONNY, M. V., BLOMGREN, K., BORNER, C., BREDESEN, D. E., BRENNER, C., CASTEDO, M., CIDLOWSKI, J. A., CIECHANOVER, A., COHEN, G. M., DE LAURENZI, V., DE MARIA, R., DESHMUKH, M., DYNLACHT, B. D., EL-DEIRY, W. S., FLAVELL, R. A., FULDA, S., GARRIDO, C., GOLSTEIN, P., GOUGEON, M. L., GREEN, D. R., GRONEMEYER, H., HAJNOCZKY, G., HARDWICK, J. M., HENGARTNER, M. O., ICHIJO, H., JAATTELA, M., KEPP, O., KIMCHI, A., KLIONSKY, D. J., KNIGHT, R. A., KORNBLUTH, S., KUMAR, S., LEVINE, B., LIPTON, S. A., LUGLI, E., MADEO, F.,

MALOMI, W., MARINE, J. C., MARTIN, S. J., MEDEMA, J. P., MEHLEN, P., MELINO, G., MOLL, U. M., MORSELLI, E., NAGATA, S., NICHOLSON, D. W., NICOTERA, P., NUNEZ, G., OREN, M., PENNINGER, J., PERVAIZ, S., PETER, M. E., PIACENTINI, M., PREHN, J. H., PUTHALAKATH, H., RABINOVICH, G. A., RIZZUTO, R., RODRIGUES, C. M., RUBINSZTEIN, D. C., RUDEL, T., SCORRANO, L., SIMON, H. U., STELLER, H., TSCHOPP, J., TSUJIMOTO, Y., VANDENABEELE, P., VITALE, I., VOUSDEN, K. H., YOULE, R. J., YUAN, J., ZHIVOTOVSKY, B. & KROEMER, G. 2009. Guidelines for the use and interpretation of assays for monitoring cell death in higher eukaryotes. *Cell Death Differ,* 16**,** 1093-107.

GERASIMENKO, J. V., FLOWERDEW, S. E., VORONINA, S. G., SUKHOMLIN, T. K., TEPIKIN, A. V., PETERSEN, O. H. & GERASIMENKO, O. V. 2006. Bile acids induce Ca2+ release from both the endoplasmic reticulum and acidic intracellular calcium stores through activation of inositol trisphosphate receptors and ryanodine receptors. *J Biol Chem,* 281**,** 40154-63.

GERASIMENKO, J. V., LUR, G., SHERWOOD, M. W., EBISUI, E., TEPIKIN, A. V., MIKOSHIBA, K., GERASIMENKO, O. V. & PETERSEN, O. H. 2009. Pancreatic protease activation by alcohol metabolite depends on Ca2+ release via acid store IP3 receptors. *Proc Natl Acad Sci U S A,* 106**,** 10758-63.

GITHENS, S. 1991. Glutathione metabolism in the pancreas compared with that in the liver, kidney, and small intestine. *Int J Pancreatol,* 8**,** 97-109.

GOLSTEIN, P. & KROEMER, G. 2007. Cell death by necrosis: towards a molecular definition. *Trends Biochem Sci,* 32**,** 37-43.

GONZALEZ, A., NUNEZ, A. M., GRANADOS, M. P., PARIENTE, J. A. & SALIDO, G. M. 2006. Ethanol impairs CCK-8-evoked amylase secretion through Ca2+-mediated ROS generation in mouse pancreatic acinar cells. *Alcohol,* 38**,** 51-7.

GOODMAN, D. S. & DEYKIN, D. 1963. Fatty acid ethyl ester formation during ethanol metabolism in vivo. *Proc Soc Exp Biol Med,* 113**,** 65-7.

GOODMAN, J. I. & TEPHLY, T. R. 1968. The role of hepatic microbody and soluble oxidases in the peroxidation of methanol in the rat and monkey. *Mol Pharmacol,* 4**,** 492-501.

GOUGH, D. B., BOYLE, B., JOYCE, W. P., DELANEY, C. P., MCGEENEY, K. F., GOREY, T. F. & FITZPATRICK, J. M. 1990. Free radical inhibition and serial chemiluminescence in evolving experimental pancreatitis. *Br J Surg,* 77**,** 1256-9.

GROVER, A. K. & SAMSON, S. E. 1988. Effect of superoxide radical on Ca2+ pumps of coronary artery. *Am J Physiol,* 255**,** C297-303.

GUICE, K. S., OLDHAM, K. T., CATY, M. G., JOHNSON, K. J. & WARD, P. A. 1989. Neutrophil-dependent, oxygen-radical mediated lung injury associated with acute pancreatitis. *Ann Surg,* 210**,** 740-7.

GUKOVSKAYA, A. S., MOURIA, M., GUKOVSKY, I., REYES, C. N., KASHO, V. N., FALLER, L. D. & PANDOL, S. J. 2002a. Ethanol metabolism and transcription factor activation in pancreatic acinar cells in rats. *Gastroenterology,* 122**,** 106-18.

GUKOVSKAYA, A. S., VAQUERO, E., ZANINOVIC, V., GORELICK, F. S., LUSIS, A. J., BRENNAN, M. L., HOLLAND, S. & PANDOL, S. J. 2002b. Neutrophils and NADPH oxidase mediate intrapancreatic trypsin activation in murine experimental acute pancreatitis. *Gastroenterology,* 122**,** 974-84.

GUYAN, P. M., UDEN, S. & BRAGANZA, J. M. 1990. Heightened free radical activity in pancreatitis. *Free Radic Biol Med,* 8**,** 347-54.

HABER, P., WILSON, J., APTE, M., KORSTEN, M. & PIROLA, R. 1995. Individual susceptibility to alcoholic pancreatitis: still an enigma. *J Lab Clin Med,* 125**,** 305-12.

HABER, P. S., APTE, M. V., APPLEGATE, T. L., NORTON, I. D., KORSTEN, M. A., PIROLA, R. C. & WILSON, J. S. 1998. Metabolism of ethanol by rat pancreatic acinar cells. *J Lab Clin Med,* 132**,** 294-302.

HABER, P. S., WILSON, J. S., APTE, M. V. & PIROLA, R. C. 1993. Fatty acid ethyl esters increase rat pancreatic lysosomal fragility. *J Lab Clin Med,* 121**,** 759-64.

HAMILTON, S. L. & REID, M. B. 2000. RyR1 modulation by oxidation and calmodulin. *Antioxid Redox Signal,* 2**,** 41-5.

HAMMONS, G. J., WARREN, G. J., BLANN, E., NICHOLS, J. & LYN-COOK, B. D. 1995. Increased DT-diaphorase activity in transformed and tumorigenic pancreatic acinar cells. *Cancer Lett,* 96**,** 9-14.

HARTWIG, W., JIMENEZ, R. E., WERNER, J., LEWANDROWSKI, K. B., WARSHAW, A. L. & FERNANDEZ-DEL CASTILLO, C. 1999. Interstitial trypsinogen release and its relevance to the transformation of mild into necrotizing pancreatitis in rats. *Gastroenterology,* 117**,** 717-25.

HASHIMOTO, D., OHMURAYA, M., HIROTA, M., YAMAMOTO, A., SUYAMA, K., IDA, S., OKUMURA, Y., TAKAHASHI, E., KIDO, H., ARAKI, K., BABA, H., MIZUSHIMA, N. & YAMAMURA, K. 2008. Involvement of autophagy in trypsinogen activation within the pancreatic acinar cells. *J Cell Biol,* 181**,** 1065-72.

HAWKINS, R. D. & KALANT, H. 1972. The metabolism of ethanol and its metabolic effects. *Pharmacol Rev,* 24**,** 67-157.

HEIDRICH, J. E., CONTOS, L. M., HUNSAKER, L. A., DECK, L. M. & VANDER JAGT, D. L. 2004. Inhibition of pancreatic cholesterol esterase reduces cholesterol absorption in the hamster. *BMC Pharmacol,* 4**,** 5.

HERST, P. M., TAN, A. S., SCARLETT, D. J. & BERRIDGE, M. V. 2004. Cell surface oxygen consumption by mitochondrial gene knockout cells. *Biochim Biophys Acta,* 1656**,** 79-87.

HILLMAN, L. C., PETERS, S. G., FISHER, C. A. & POMARE, E. W. 1986. Effects of the fibre components pectin, cellulose, and lignin on bile salt metabolism and biliary lipid composition in man. *Gut,* 27**,** 29-36.

HOEK, J. B., CAHILL, A. & PASTORINO, J. G. 2002. Alcohol and mitochondria: a dysfunctional relationship. *Gastroenterology,* 122**,** 2049-63.

HUSAIN, S. Z., PRASAD, P., GRANT, W. M., KOLODECIK, T. R., NATHANSON, M. H. & GORELICK, F. S. 2005. The ryanodine receptor mediates early zymogen activation in pancreatitis. *Proc Natl Acad Sci U S A,* 102**,** 14386-91.

IIMURO, Y., BRADFORD, B. U., GAO, W., KADIISKA, M., MASON, R. P., STEFANOVIC, B., BRENNER, D. A. & THURMAN, R. G. 1996. Detection of alpha-hydroxyethyl free radical adducts in the pancreas after chronic exposure to alcohol in the rat. *Mol Pharmacol,* 50**,** 656-61.

IRANI, K., XIA, Y., ZWEIER, J. L., SOLLOTT, S. J., DER, C. J., FEARON, E. R., SUNDARESAN, M., FINKEL, T. & GOLDSCHMIDT-CLERMONT, P. J. 1997. Mitogenic signaling mediated by oxidants in Ras-transformed fibroblasts. *Science,* 275**,** 1649-52.

ITO, K., MIYASHITA, Y. & KASAI, H. 1997. Micromolar and submicromolar Ca2+ spikes regulating distinct cellular functions in pancreatic acinar cells. *Embo J,* 16**,** 242-51.

IWATSUKI, N. & PETERSEN, O. H. 1979. Direct visualization of cell to cell coupling: transfer of fluorescent probes in living mammalian pancreatic acini. *Pflugers Arch,* 380**,** 277-81.

JAISWAL, A. K., MCBRIDE, O. W., ADESNIK, M. & NEBERT, D. W. 1988. Human dioxin-inducible cytosolic NAD(P)H:menadione oxidoreductase. cDNA sequence and localization of gene to chromosome 16. *J Biol Chem,* 263**,** 13572-8.

JAMIESON, J. D. & PALADE, G. E. 1971a. Condensing vacuole conversion and zymogen granule discharge in pancreatic exocrine cells: metabolic studies. *J Cell Biol,* 48**,** 503-22.

JAMIESON, J. D. & PALADE, G. E. 1971b. Synthesis, intracellular transport, and discharge of secretory proteins in stimulated pancreatic exocrine cells. *J Cell Biol,* 50**,** 135-58.

JOHNSON, L. R. (ed.) 1994. *Physiology of the gastrointestinal tract,* New York: Raven Press.

JOSEPH, S. K., NAKAO, S. K. & SUKUMVANICH, S. 2006. Reactivity of free thiol groups in type-I inositol trisphosphate receptors. *Biochem J,* 393**,** 575-82.

JOSEPH, S. K., RYAN, S. V., PIERSON, S., RENARD-ROONEY, D. & THOMAS, A. P. 1995. The effect of mersalyl on inositol trisphosphate receptor binding and ion channel function. *J Biol Chem,* 270**,** 3588-93.

KADLUBAR, F. F., ANDERSON, K. E., HAUSSERMANN, S., LANG, N. P., BARONE, G. W., THOMPSON, P. A., MACLEOD, S. L., CHOU, M. W., MIKHAILOVA, M., PLASTARAS, J., MARNETT, L. J., NAIR, J., VELIC, I. & BARTSCH, H. 1998. Comparison of DNA adduct levels associated with oxidative stress in human pancreas. *Mutat Res,* 405**,** 125-33.

KAISER, A. M., SALUJA, A. K., SENGUPTA, A., SALUJA, M. & STEER, M. L. 1995. Relationship between severity, necrosis, and apoptosis in five models of experimental acute pancreatitis. *Am J Physiol,* 269**,** C1295-304.

KAKKAR, P. & SINGH, B. K. 2007. Mitochondria: a hub of redox activities and cellular distress control. *Mol Cell Biochem,* 305**,** 235-53.

KAPHALIA, B. S. & ANSARI, G. A. 2001. Purification and characterization of rat hepatic microsomal low molecular weight fatty acid ethyl ester synthase and its relationship to carboxylesterases. *J Biochem Mol Toxicol,* 15**,** 165-71.

KAPHALIA, B. S. & ANSARI, G. A. 2003. Purification and characterization of rat pancreatic fatty acid ethyl ester synthase and its structural and functional relationship to pancreatic cholesterol esterase. *J Biochem Mol Toxicol,* 17**,** 338-45.

KAPHALIA, B. S., FRITZ, R. R. & ANSARI, G. A. 1997. Purification and characterization of rat liver microsomal fatty acid ethyl and 2-chloroethyl ester synthase and their relationship with carboxylesterase (pI 6.1). *Chem Res Toxicol,* 10**,** 211-8.

KAPHALIA, B. S., GREEN, S. M. & ANSARI, G. A. 1999. Fatty acid ethyl and methyl ester synthases, and fatty acid anilide synthase in HepG2 and AR42J cells: interrelationships and inhibition by tri-o-tolyl phosphate. *Toxicol Appl Pharmacol,* 159**,** 134-41.

KASAI, H., LI, Y. X. & MIYASHITA, Y. 1993. Subcellular distribution of Ca2+ release channels underlying Ca2+ waves and oscillations in exocrine pancreas. *Cell,* 74**,** 669-77.

KERN, H. F. 1993. *The Pancreas. Biology, pathobiology and disease*, Raven Press.

KIM, J. Y., KIM, K. H., LEE, J. A., NAMKUNG, W., SUN, A. Q., ANANTHANARAYANAN, M., SUCHY, F. J., SHIN, D. M., MUALLEM, S. & LEE, M. G. 2002. Transporter-mediated bile acid uptake causes Ca2+-dependent cell death in rat pancreatic acinar cells. *Gastroenterology,* 122**,** 1941-53.

KLOPPEL, G. & MAILLET, B. 1993. Pathology of acute and chronic pancreatitis. *Pancreas,* 8**,** 659-70.

KNAUF, P. A., PROVERBIO, F. & HOFFMAN, J. F. 1974. Electrophoretic separation of different phophosproteins associated with Ca-ATPase and Na, K-ATPase in human red cell ghosts. *J Gen Physiol,* 63**,** 324-36.

KOHUT, M., NOWAK, A., NOWAKOWSKA-DUIAWA, E. & MAREK, T. 2002. Presence and density of common bile duct microlithiasis in acute biliary pancreatitis. *World J Gastroenterol,* 8**,** 558-61.

KUNITOH, S., IMAOKA, S., HIROI, T., YABUSAKI, Y., MONNA, T. & FUNAE, Y. 1997. Acetaldehyde as well as ethanol is metabolized by human CYP2E1. *J Pharmacol Exp Ther,* 280**,** 527-32.

LANGE, L. G. & SOBEL, B. E. 1983. Mitochondrial dysfunction induced by fatty acid ethyl esters, myocardial metabolites of ethanol. *J Clin Invest,* 72**,** 724-31.

LAPOSATA, E. A. & LANGE, L. G. 1986. Presence of nonoxidative ethanol metabolism in human organs commonly damaged by ethanol abuse. *Science,* 231**,** 497-9.

LAPOSATA, M. 1999. Fatty acid ethyl esters: nonoxidative ethanol metabolites with emerging biological and clinical significance. *Lipids,* 34 Suppl**,** S281-5.

LEITE, M. F., DRANOFF, J. A., GAO, L. & NATHANSON, M. H. 1999. Expression and subcellular localization of the ryanodine receptor in rat pancreatic acinar cells. *Biochem J,* 337 (Pt 2)**,** 305-9.

LERCH, M. M. & AGHDASSI, A. A. 2010. The role of bile acids in gallstone-induced pancreatitis. *Gastroenterology,* 138**,** 429-33.

LERCH, M. M., SALUJA, A. K., DAWRA, R., RAMARAO, P., SALUJA, M. & STEER, M. L. 1992. Acute necrotizing pancreatitis in the opossum: earliest morphological changes involve acinar cells. *Gastroenterology,* 103**,** 205-13.

LETKO, G., WINKLER, U., MATTHIAS, R. & HEINRICH, P. 1991. Studies on lipid peroxidation in pancreatic tissue. In vitro formation of thiobarbituric-acid-reactive substances (TBRS). *Exp Pathol,* 42**,** 151-7.

LEUNG, P. S. & CHAN, Y. C. 2009. Role of oxidative stress in pancreatic inflammation. *Antioxid Redox Signal,* 11**,** 135-65.

LIEBER, C. S. 1992. [Clinical biochemistry of alcohol and its metabolic and hepatic effects]. *Journ Annu Diabetol Hotel Dieu***,** 183-210.

LIND, C., CADENAS, E., HOCHSTEIN, P. & ERNSTER, L. 1990. DT-diaphorase: purification, properties, and function. *Methods Enzymol,* 186**,** 287-301.

LINDBLAD, L., LUNDHOLM, K. & SCHERSTEN, T. 1977. Bile acid concentrations in systemic and portal serum in presumably normal man and in cholestatic and cirrhotic conditions. *Scand J Gastroenterol,* 12**,** 395-400.

LIOU, J., KIM, M. L., HEO, W. D., JONES, J. T., MYERS, J. W., FERRELL, J. E., JR. & MEYER, T. 2005. STIM is a Ca2+ sensor essential for Ca2+-store-depletion-triggered Ca2+ influx. *Curr Biol,* 15**,** 1235-41.

LIU, X., KIM, C. N., YANG, J., JEMMERSON, R. & WANG, X. 1996. Induction of apoptotic program in cell-free extracts: requirement for dATP and cytochrome c. *Cell,* 86**,** 147-57.

LUMENG, L. & CRABB, D. W. 2000. Alcoholic liver disease. *Curr Opin Gastroenterol,* 16**,** 208-18.

LUR, G., HAYNES, L. P., PRIOR, I. A., GERASIMENKO, O. V., FESKE, S., PETERSEN, O. H., BURGOYNE, R. D. & TEPIKIN, A. V. 2009. Ribosome-free terminals of rough ER allow formation of STIM1 puncta and segregation of STIM1 from IP(3) receptors. *Curr Biol,* 19**,** 1648-53.

LYN-COOK, B. D., YAN-SANDERS, Y., MOORE, S., TAYLOR, S., WORD, B. & HAMMONS, G. J. 2006. Increased levels of NAD(P)H: quinone oxidoreductase 1 (NQO1) in pancreatic tissues from smokers and pancreatic adenocarcinomas: A potential biomarker of early damage in the pancreas. *Cell Biol Toxicol,* 22**,** 73-80.

MAKAR, A. B. & TEPHLY, T. R. 1975. Inhibition of monkey liver alcohol dehydrogenase by 4-methylpyrazole. *Biochem Med,* 13**,** 334-42.

MALETH, J., VENGLOVECZ, V., RAZGA, Z., TISZLAVICZ, L., RAKONCZAY, Z., JR. & HEGYI, P. 2010. Non-conjugated chenodeoxycholate induces severe mitochondrial damage and inhibits bicarbonate transport in pancreatic duct cells. *Gut*.

MANGOS, J. A., MARAGOS, N. & MCSHERRY, N. R. 1973. Micropuncture and microperfusion study of glucose excretion in rat parotid saliva. *Am J Physiol,* 224**,** 1260-4.

MARENINOVA, O. A., HERMANN, K., FRENCH, S. W., O'KONSKI, M. S., PANDOL, S. J., WEBSTER, P., ERICKSON, A. H., KATUNUMA, N., GORELICK, F. S., GUKOVSKY, I. & GUKOVSKAYA, A. S. 2009. Impaired autophagic flux mediates acinar cell vacuole formation and trypsinogen activation in rodent models of acute pancreatitis. *J Clin Invest,* 119**,** 3340-55.

MARENINOVA, O. A., SUNG, K. F., HONG, P., LUGEA, A., PANDOL, S. J., GUKOVSKY, I. & GUKOVSKAYA, A. S. 2006. Cell death in pancreatitis: caspases protect from necrotizing pancreatitis. *J Biol Chem,* 281**,** 3370-81.

MASAMUNE, A., WATANABE, T., KIKUTA, K., SATOH, K. & SHIMOSEGAWA, T. 2008. NADPH oxidase plays a crucial role in the activation of pancreatic stellate cells. *Am J Physiol Gastrointest Liver Physiol,* 294**,** G99-G108.

MEISSNER, G. 2002. Regulation of mammalian ryanodine receptors. *Front Biosci,* 7**,** d2072-80.

MELINO, G., KNIGHT, R. A. & NICOTERA, P. 2005. How many ways to die? How many different models of cell death? *Cell Death Differ,* 12 Suppl 2**,** 1457-62.

MERCER, J. C., DEHAVEN, W. I., SMYTH, J. T., WEDEL, B., BOYLES, R. R., BIRD, G. S. & PUTNEY, J. W., JR. 2006. Large store-operated calcium selective currents due to co-expression of Orai1 or Orai2 with the intracellular calcium sensor, Stim1. *J Biol Chem,* 281**,** 24979-90.

MISSIAEN, L., TAYLOR, C. W. & BERRIDGE, M. J. 1991. Spontaneous calcium release from inositol trisphosphate-sensitive calcium stores. *Nature,* 352**,** 241-4.

MIYASAKA, K., OHTA, M., TAKANO, S., HAYASHI, H., HIGUCHI, S., MARUYAMA, K., TANDO, Y., NAKAMURA, T., TAKATA, Y. & FUNAKOSHI, A. 2005. Carboxylester lipase gene polymorphism as a risk of alcohol-induced pancreatitis. *Pancreas,* 30**,** e87-91.

MIZUSHIMA, N., LEVINE, B., CUERVO, A. M. & KLIONSKY, D. J. 2008. Autophagy fights disease through cellular self-digestion. *Nature,* 451**,** 1069-75.

MORTON, C., KLATSKY, A. L. & UDALTSOVA, N. 2004. Smoking, coffee, and pancreatitis. *Am J Gastroenterol,* 99**,** 731-8.

MUALLEM, S., BEEKER, T. & PANDOL, S. J. 1988. Role of Na+/Ca2+ exchange and the plasma membrane Ca2+ pump in hormone-mediated Ca2+ efflux from pancreatic acini. *J Membr Biol,* 102**,** 153-62.

MUKHERJEE, R., CRIDDLE, D. N., GUKOVSKAYA, A., PANDOL, S., PETERSEN, O. H. & SUTTON, R. 2008. Mitochondrial injury in pancreatitis. *Cell Calcium,* 44**,** 14-23.

MURPHY, J. A., CRIDDLE, D. N., SHERWOOD, M., CHVANOV, M., MUKHERJEE, R., MCLAUGHLIN, E., BOOTH, D., GERASIMENKO, J. V., RARATY, M. G., GHANEH, P., NEOPTOLEMOS, J. P., GERASIMENKO, O. V., TEPIKIN, A. V., GREEN, G. M., REEVE, J. R., JR., PETERSEN, O. H. & SUTTON, R. 2008. Direct activation of cytosolic Ca2+ signaling and enzyme secretion by cholecystokinin in human pancreatic acinar cells. *Gastroenterology,* 135**,** 632-41.

NATHAN, C. 2003. Specificity of a third kind: reactive oxygen and nitrogen intermediates in cell signaling. *J Clin Invest,* 111**,** 769-78.

NAUSEEF, W. M. 2007. How human neutrophils kill and degrade microbes: an integrated view. *Immunol Rev,* 219**,** 88-102.

NEDERGAARD, M. 1994. Direct signaling from astrocytes to neurons in cultures of mammalian brain cells. *Science,* 263**,** 1768-71.

NEMOTO, T., KOJIMA, T., OSHIMA, A., BITO, H. & KASAI, H. 2004. Stabilization of exocytosis by dynamic F-actin coating of zymogen granules in pancreatic acini. *J Biol Chem,* 279**,** 37544-50.

NEUSCHWANDER-TETRI, B. A., FERRELL, L. D., SUKHABOTE, R. J. & GRENDELL, J. H. 1992. Glutathione monoethyl ester ameliorates caerulein-induced pancreatitis in the mouse. *J Clin Invest,* 89**,** 109-16.

NEUSCHWANDER-TETRI, B. A., PRESTI, M. E. & WELLS, L. D. 1997. Glutathione synthesis in the exocrine pancreas. *Pancreas,* 14**,** 342-9.

NEWSOME, W. H. & RATTRAY, J. B. M. 1965. The enzymatic esterification of ethanol with fatty acids. *Can J Biochem,* 43**,** 1223-1235.

NICHOLLS, D. G. & BUDD, S. L. 2000. Mitochondria and neuronal survival. *Physiol Rev,* 80**,** 315-60.

NICOTERA, P., LEIST, M. & FERRANDO-MAY, E. 1998. Intracellular ATP, a switch in the decision between apoptosis and necrosis. *Toxicol Lett,* 102-103**,** 139-42.

NIEMELA, O. 2001. Distribution of ethanol-induced protein adducts in vivo: relationship to tissue injury. *Free Radic Biol Med,* 31**,** 1533-8.

NONAKA, A., MANABE, T., ASANO, N., KYOGOKU, T., IMANISHI, K., TAMURA, K., TOBE, T., SUGIURA, Y. & MAKINO, K. 1989a. Direct ESR measurement of free radicals in mouse pancreatic lesions. *Int J Pancreatol,* 5**,** 203-11.

NONAKA, A., MANABE, T., TAMURA, K., ASANO, N., IMANISHI, K. & TOBE, T. 1989b. Changes of xanthine oxidase, lipid peroxide and superoxide dismutase in mouse acute pancreatitis. *Digestion,* 43**,** 41-6.

NONAKA, A., MANABE, T., TAMURA, K., KYOGOKU, T., IMANISHI, K., YAMAKI, K. & TOBE, T. 1989c. [Changes of lipid peroxide (LPO) levels in the development of CDE-diet induced acute pancreatitis in mice: preliminary report]. *Nippon Geka Gakkai Zasshi,* 90**,** 1127.

NORTON, I. D., APTE, M. V., HABER, P. S., MCCAUGHAN, G. W., PIROLA, R. C. & WILSON, J. S. 1998. Cytochrome P4502E1 is present in rat pancreas and is induced by chronic ethanol administration. *Gut,* 42**,** 426-30.

NOUSIA-ARVANITAKIS, S. 1999. Cystic fibrosis and the pancreas: recent scientific advances. *J Clin Gastroenterol,* 29**,** 138-42.

NOVITSKIY, G., TRAORE, K., WANG, L., TRUSH, M. A. & MEZEY, E. 2006. Effects of ethanol and acetaldehyde on reactive oxygen species production in rat hepatic stellate cells. *Alcohol Clin Exp Res,* 30**,** 1429-35.

ODINOKOVA, I. V., SUNG, K. F., MARENINOVA, O. A., HERMANN, K., EVTODIENKO, Y., ANDREYEV, A., GUKOVSKY, I. & GUKOVSKAYA, A. S. 2009. Mechanisms regulating cytochrome c release in pancreatic mitochondria. *Gut,* 58**,** 431-42.

OPIE, E. L. 1901. The etiology of acute hemorrhagic pancreatitis. *Johns Hopkins Hospital Bulletin,* 121**,** 182-188.

ORRENIUS, S., GOGVADZE, V. & ZHIVOTOVSKY, B. 2007. Mitochondrial oxidative stress: implications for cell death. *Annu Rev Pharmacol Toxicol,* 47**,** 143-83.

PALADE, G. 1975a. Intracellular aspects of the process of protein synthesis. *Science,* 189**,** 347-58.

PALADE, G. 1975b. Intracellular aspects of the process of protein synthesis. *Science,* 189**,** 867.

PALMIERI, V. O., GRATTAGLIANO, I. & PALASCIANO, G. 2007. Ethanol induces secretion of oxidized proteins by pancreatic acinar cells. *Cell Biol Toxicol,* 23**,** 459-64.

PANDOL, S. J., SALUJA, A. K., IMRIE, C. W. & BANKS, P. A. 2007. Acute pancreatitis: bench to the bedside. *Gastroenterology,* 133**,** 1056 e1-1056 e25.

PARK, B. K., CHUNG, J. B., LEE, J. H., SUH, J. H., PARK, S. W., SONG, S. Y., KIM, H., KIM, K. H. & KANG, J. K. 2003. Role of oxygen free radicals in patients with acute pancreatitis. *World J Gastroenterol,* 9**,** 2266-9.

PARK, C. Y., HOOVER, P. J., MULLINS, F. M., BACHHAWAT, P., COVINGTON, E. D., RAUNSER, S., WALZ, T., GARCIA, K. C., DOLMETSCH, R. E. & LEWIS, R. S. 2009. STIM1 clusters and activates CRAC channels via direct binding of a cytosolic domain to Orai1. *Cell,* 136**,** 876-90.

PAWAN, G. L. 1972. Metabolism of alcohol (ethanol) in man. *Proc Nutr Soc,* 31**,** 83-9.

PERIDES, G., LAUKKARINEN, J. M., VASSILEVA, G. & STEER, M. L. 2010. Biliary acute pancreatitis in mice is mediated by the G-protein-coupled cell surface bile acid receptor Gpbar1. *Gastroenterology,* 138**,** 715-25.

PEROCCHI, F., GOHIL, V. M., GIRGIS, H. S., BAO, X. R., MCCOMBS, J. E., PALMER, A. E. & MOOTHA, V. K. 2010. MICU1 encodes a mitochondrial EF hand protein required for Ca(2+) uptake. *Nature,* 467**,** 291-6.

PETERSEN, O. H. 1975. Proceedings: Electrical coupling between pancreatic acinar cells. *J Physiol,* 250**,** 2P-4P.

PETERSEN, O. H. 1992. Stimulus-secretion coupling: cytoplasmic calcium signals and the control of ion channels in exocrine acinar cells. *J Physiol,* 448**,** 1-51.

PETERSEN, O. H. 1994. Electrophysiology of salivary and pancreatic acinar cells. *In:* JOHNSON, L. R. (ed.) *Physiology of the Gastrointestinal Tract.* Third Edition ed. New York: Raven Press.

PETERSEN, O. H., BURDAKOV, D. & TEPIKIN, A. V. 1999. Polarity in intracellular calcium signaling. *Bioessays,* 21**,** 851-60.

PETERSEN, O. H. & MARUYAMA, Y. 1984. Calcium-activated potassium channels and their role in secretion. *Nature,* 307**,** 693-6.

PETERSEN, O. H. & SUTTON, R. 2006. Ca2+ signalling and pancreatitis: effects of alcohol, bile and coffee. *Trends Pharmacol Sci,* 27**,** 113-20.

PETERSEN, O. H., SUTTON, R. & CRIDDLE, D. N. 2006. Failure of calcium microdomain generation and pathological consequences. *Cell Calcium,* 40**,** 593-600.

PETERSEN, O. H. & TEPIKIN, A. V. 2008. Polarized calcium signaling in exocrine gland cells. *Annu Rev Physiol,* 70**,** 273-99.

PHAM, C. T. 2006. Neutrophil serine proteases: specific regulators of inflammation. *Nat Rev Immunol,* 6**,** 541-50.

PRAKRIYA, M., FESKE, S., GWACK, Y., SRIKANTH, S., RAO, A. & HOGAN, P. G. 2006. Orai1 is an essential pore subunit of the CRAC channel. *Nature,* 443**,** 230-3.

PULLAR, J. M., VISSERS, M. C. & WINTERBOURN, C. C. 2000. Living with a killer: the effects of hypochlorous acid on mammalian cells. *IUBMB Life,* 50**,** 259-66.

PUSHPAKIRAN, G., MAHALAKSHMI, K. & ANURADHA, C. V. 2004. Taurine restores ethanol-induced depletion of antioxidants and attenuates oxidative stress in rat tissues. *Amino Acids,* 27**,** 91-6.

PUTNEY, J. W., JR. 1976a. Biphasic modulation of potassium release in rat parotid gland by carbachol and phenylephrine. *J Pharmacol Exp Ther,* 198**,** 375-84.

PUTNEY, J. W., JR. 1976b. Stimulation of 45Ca influx in rat parotid gland by carbachol. *J Pharmacol Exp Ther,* 199**,** 526-37.

PUTNEY, J. W., JR. 1977. Muscarinic, alpha-adrenergic and peptide receptors regulate the same calcium influx sites in the parotid gland. *J Physiol,* 268**,** 139-49.

PUTNEY, J. W., JR. 1986. A model for receptor-regulated calcium entry. *Cell Calcium,* 7**,** 1-12.

QUINLAN, G. J., EVANS, T. W. & GUTTERIDGE, J. M. 1994a. Linoleic acid and protein thiol changes suggestive of oxidative damage in the plasma of patients with adult respiratory distress syndrome. *Free Radic Res,* 20**,** 299-306.

QUINLAN, G. J., EVANS, T. W. & GUTTERIDGE, J. M. 1994b. Oxidative damage to plasma proteins in adult respiratory distress syndrome. *Free Radic Res,* 20**,** 289-98.

QUINLAN, G. J., LAMB, N. J., EVANS, T. W. & GUTTERIDGE, J. M. 1996. Plasma fatty acid changes and increased lipid peroxidation in patients with adult respiratory distress syndrome. *Crit Care Med,* 24**,** 241-6.

QUINLAN, G. J., LAMB, N. J., TILLEY, R., EVANS, T. W. & GUTTERIDGE, J. M. 1997. Plasma hypoxanthine levels in ARDS: implications for oxidative stress, morbidity, and mortality. *Am J Respir Crit Care Med,* 155**,** 479-84.

RARATY, M., WARD, J., ERDEMLI, G., VAILLANT, C., NEOPTOLEMOS, J. P., SUTTON, R. & PETERSEN, O. H. 2000. Calcium-dependent enzyme activation and vacuole formation in the apical granular region of pancreatic acinar cells. *Proc Natl Acad Sci U S A,* 97**,** 13126-31.

REEVES, E. P., LU, H., JACOBS, H. L., MESSINA, C. G., BOLSOVER, S., GABELLA, G., POTMA, E. O., WARLEY, A., ROES, J. & SEGAL, A. W. 2002. Killing activity of neutrophils is mediated through activation of proteases by K+ flux. *Nature,* 416**,** 291-7.

RILEY, D. J., KYGER, E. M., SPILBURG, C. A. & LANGE, L. G. 1990. Pancreatic cholesterol esterases. 2. Purification and characterization of human pancreatic fatty acid ethyl ester synthase. *Biochemistry,* 29**,** 3848-52.

ROBERTSON, N., STRATFORD, I. J., HOULBROOK, S., CARMICHAEL, J. & ADAMS, G. E. 1992. The sensitivity of human tumour cells to quinone bioreductive drugs: what role for DT-diaphorase? *Biochem Pharmacol,* 44**,** 409-12.

ROOS, J., DIGREGORIO, P. J., YEROMIN, A. V., OHLSEN, K., LIOUDYNO, M., ZHANG, S., SAFRINA, O., KOZAK, J. A., WAGNER, S. L., CAHALAN, M. D., VELICELEBI, G. & STAUDERMAN, K. A. 2005. STIM1, an essential and conserved component of store-operated Ca2+ channel function. *J Cell Biol,* 169**,** 435-45.

RUAS, M., RIETDORF, K., ARREDOUANI, A., DAVIS, L. C., LLOYD-EVANS, E., KOEGEL, H., FUNNELL, T. M., MORGAN, A. J., WARD, J. A., WATANABE, K., CHENG, X., CHURCHILL, G. C., ZHU, M. X., PLATT, F. M., WESSEL, G. M., PARRINGTON, J. & GALIONE, A. 2010. Purified TPC Isoforms Form NAADP Receptors with Distinct Roles for Ca(2+) Signaling and Endolysosomal Trafficking. *Curr Biol*.

RUTLEDGE, P. L., SALUJA, A. K., POWERS, R. E. & STEER, M. L. 1987. Role of oxygen-derived free radicals in diet-induced hemorrhagic pancreatitis in mice. *Gastroenterology,* 93**,** 41-7.

SAEZ, J. C., CONNOR, J. A., SPRAY, D. C. & BENNETT, M. V. 1989. Hepatocyte gap junctions are permeable to the second messenger, inositol 1,4,5-trisphosphate, and to calcium ions. *Proc Natl Acad Sci U S A,* 86**,** 2708-12.

SAGHIR, M., WERNER, J. & LAPOSATA, M. 1997. Rapid in vivo hydrolysis of fatty acid ethyl esters, toxic nonoxidative ethanol metabolites. *Am J Physiol,* 273**,** G184-90.

SALUJA, A. K., LERCH, M. M., PHILLIPS, P. A. & DUDEJA, V. 2007. Why does pancreatic overstimulation cause pancreatitis? *Annu Rev Physiol,* 69**,** 249-69.

SANDBERG, K., JI, H., IIDA, T. & CATT, K. J. 1992. Intercellular communication between follicular angiotensin receptors and Xenopus laevis oocytes: medication by an inositol 1,4,5-trisphosphate-dependent mechanism. *J Cell Biol,* 117**,** 157-67.

SANFEY, H., BULKLEY, G. B. & CAMERON, J. L. 1984. The role of oxygen-derived free radicals in the pathogenesis of acute pancreatitis. *Ann Surg,* 200**,** 405-13.

SANFEY, H., BULKLEY, G. B. & CAMERON, J. L. 1985. The pathogenesis of acute pancreatitis. The source and role of oxygen-derived free radicals in three different experimental models. *Ann Surg,* 201**,** 633-9.

SCHOENBERG, M. H., BUCHLER, M. & BEGER, H. G. 1994. Oxygen radicals in experimental acute pancreatitis. *Hepatogastroenterology,* 41**,** 313-9.

SCHOENBERG, M. H., BUCHLER, M., GASPAR, M., STINNER, A., YOUNES, M., MELZNER, I., BULTMANN, B. & BEGER, H. G. 1990. Oxygen free radicals in acute pancreatitis of the rat. *Gut,* 31**,** 1138-43.

SENNINGER, N., MOODY, F. G., COELHO, J. C. & VAN BUREN, D. H. 1986. The role of biliary obstruction in the pathogenesis of acute pancreatitis in the opossum. *Surgery,* 99**,** 688-93.

SHAROV, V. S., DREMINA, E. S., GALEVA, N. A., WILLIAMS, T. D. & SCHONEICH, C. 2006. Quantitative mapping of oxidation-sensitive cysteine residues in SERCA in vivo and in vitro by HPLC-electrospray-tandem MS: selective protein oxidation during biological aging. *Biochem J,* 394**,** 605-15.

SIEGEL, D., BOLTON, E. M., BURR, J. A., LIEBLER, D. C. & ROSS, D. 1997. The reduction of alpha-tocopherolquinone by human NAD(P)H: quinone oxidoreductase: the role of alpha-tocopherolhydroquinone as a cellular antioxidant. *Mol Pharmacol,* 52**,** 300-5.

SIEGEL, D., GUSTAFSON, D. L., DEHN, D. L., HAN, J. Y., BOONCHOONG, P., BERLINER, L. J. & ROSS, D. 2004. NAD(P)H:quinone oxidoreductase 1: role as a superoxide scavenger. *Mol Pharmacol,* 65**,** 1238-47.

SINGH, V. P., SALUJA, A. K., BHAGAT, L., HIETARANTA, A. J., SONG, A., MYKONIATIS, A., VAN ACKER, G. J. & STEER, M. L. 2001. Serine protease inhibitor causes F-actin redistribution and inhibition of calcium-mediated secretion in pancreatic acini. *Gastroenterology,* 120**,** 1818-27.

SIRIWARDENA, A. K., MASON, J. M., BALACHANDRA, S., BAGUL, A., GALLOWAY, S., FORMELA, L., HARDMAN, J. G. & JAMDAR, S. 2007. Randomised, double blind, placebo controlled trial of intravenous antioxidant (n-acetylcysteine, selenium, vitamin C) therapy in severe acute pancreatitis. *Gut,* 56**,** 1439-44.

SMITH, M. E. 1961. Interrelations in ethanol and methanol metabolism. *J Pharmacol Exp Ther,* 134**,** 233-7.

STAUFFER, P. L., ZHAO, H., LUBY-PHELPS, K., MOSS, R. L., STAR, R. A. & MUALLEM, S. 1993. Gap junction communication modulates [Ca2+]i oscillations and enzyme secretion in pancreatic acini. *J Biol Chem,* 268**,** 19769-75.

STERLING, J. A. 1954. The common channel for bile and pancreatic ducts. *Surg Gynecol Obstet,* 98**,** 420-4.

STRANGE, R. C. 1984. Hepatic bile flow. *Physiol Rev,* 64**,** 1055-102.

STREHLER, E. E. & TREIMAN, M. 2004. Calcium pumps of plasma membrane and cell interior. *Curr Mol Med,* 4**,** 323-35.

SUH, Y. A., ARNOLD, R. S., LASSEGUE, B., SHI, J., XU, X., SORESCU, D., CHUNG, A. B., GRIENDLING, K. K. & LAMBETH, J. D. 1999. Cell transformation by the superoxide-generating oxidase Mox1. *Nature,* 401**,** 79-82.

SUN, J., XU, L., EU, J. P., STAMLER, J. S. & MEISSNER, G. 2001. Classes of thiols that influence the activity of the skeletal muscle calcium release channel. *J Biol Chem,* 276**,** 15625-30.

SUNDARESAN, M., YU, Z. X., FERRANS, V. J., IRANI, K. & FINKEL, T. 1995. Requirement for generation of H2O2 for platelet-derived growth factor signal transduction. *Science,* 270**,** 296-9.

SUZUKI, Y. J., EDMONDSON, J. D. & FORD, G. D. 1992. Inactivation of rabbit muscle creatine kinase by hydrogen peroxide. *Free Radic Res Commun,* 16**,** 131-6.

SUZUKI, Y. J. & FORD, G. D. 1992. Superoxide stimulates IP3-induced Ca2+ release from vascular smooth muscle sarcoplasmic reticulum. *Am J Physiol,* 262**,** H114-6.

SWAROOP, V. S., CHARI, S. T. & CLAIN, J. E. 2004. Severe acute pancreatitis. *JAMA,* 291**,** 2865-8.

SZABADKAI, G. & DUCHEN, M. R. 2008. Mitochondria: the hub of cellular Ca2+ signaling. *Physiology (Bethesda),* 23**,** 84-94.

SZCZEPIORKOWSKI, Z. M., DICKERSIN, G. R. & LAPOSATA, M. 1995. Fatty acid ethyl esters decrease human hepatoblastoma cell proliferation and protein synthesis. *Gastroenterology,* 108**,** 515-22.

TEPIKIN, A. V., VORONINA, S. G., GALLACHER, D. V. & PETERSEN, O. H. 1992. Pulsatile Ca2+ extrusion from single pancreatic acinar cells during receptor-activated cytosolic Ca2+ spiking. *J Biol Chem,* 267**,** 14073-6.

THORN, P., GERASIMENKO, O. & PETERSEN, O. H. 1994. Cyclic ADP-ribose regulation of ryanodine receptors involved in agonist evoked cytosolic Ca2+ oscillations in pancreatic acinar cells. *Embo J,* 13**,** 2038-43.

THORN, P., LAWRIE, A. M., SMITH, P. M., GALLACHER, D. V. & PETERSEN, O. H. 1993. Local and global cytosolic Ca2+ oscillations in exocrine cells evoked by agonists and inositol trisphosphate. *Cell,* 74**,** 661-8.

TINEL, H., CANCELA, J. M., MOGAMI, H., GERASIMENKO, J. V., GERASIMENKO, O. V., TEPIKIN, A. V. & PETERSEN, O. H. 1999. Active mitochondria surrounding the pancreatic acinar granule region prevent spreading of inositol trisphosphate-evoked local cytosolic Ca(2+) signals. *Embo J,* 18**,** 4999-5008.

TSAI, K., WANG, S. S., CHEN, T. S., KONG, C. W., CHANG, F. Y., LEE, S. D. & LU, F. J. 1998. Oxidative stress: an important phenomenon with pathogenetic significance in the progression of acute pancreatitis. *Gut,* 42**,** 850-5.

TSUJI, N., WATANABE, N., OKAMOTO, T. & NIITSU, Y. 1994. Specific interaction of pancreatic elastase and leucocytes to produce oxygen radicals and its implication in pancreatitis. *Gut,* 35**,** 1659-64.

TUGBA DURLU-KANDILCI, N., RUAS, M., CHUANG, K. T., BRADING, A., PARRINGTON, J. & GALIONE, A. 2010. TPC2 proteins mediate nicotinic acid adenine dinucleotide phosphate (NAADP)- and agonist-evoked contractions of smooth muscle. *J Biol Chem,* 285**,** 24925-32.

TUMA, D. J. & KLASSEN, L. W. 1992. Immune responses to acetaldehyde-protein adducts: role in alcoholic liver disease. *Gastroenterology,* 103**,** 1969-73.

TURRENS, J. F. 2003. Mitochondrial formation of reactive oxygen species. *J Physiol,* 552**,** 335-44.

VAN BUUREN, K. J. & VAN GELDER, B. F. 1974. Biochemical and biophysical studies on cytochrome c oxidase. XIII. Effect of cholate on the enzymic activity. *Biochim Biophys Acta,* 333**,** 209-17.

VENGLOVECZ, V., RAKONCZAY, Z., JR., OZSVARI, B., TAKACS, T., LONOVICS, J., VARRO, A., GRAY, M. A., ARGENT, B. E. & HEGYI, P. 2008. Effects of bile acids on pancreatic ductal bicarbonate secretion in guinea pig. *Gut,* 57**,** 1102-12.

VIGNAIS, P. V. 2002. The superoxide-generating NADPH oxidase: structural aspects and activation mechanism. *Cell Mol Life Sci,* 59**,** 1428-59.

VIRLOS, I. T., MASON, J., SCHOFIELD, D., MCCLOY, R. F., EDDLESTON, J. M. & SIRIWARDENA, A. K. 2003. Intravenous n-acetylcysteine, ascorbic acid and selenium-based anti-oxidant therapy in severe acute pancreatitis. *Scand J Gastroenterol,* 38**,** 1262-7.

VORONINA, S., LONGBOTTOM, R., SUTTON, R., PETERSEN, O. H. & TEPIKIN, A. 2002a. Bile acids induce calcium signals in mouse pancreatic acinar cells: implications for bile-induced pancreatic pathology. *J Physiol,* 540**,** 49-55.

VORONINA, S., SUKHOMLIN, T., JOHNSON, P. R., ERDEMLI, G., PETERSEN, O. H. & TEPIKIN, A. 2002b. Correlation of NADH and Ca2+ signals in mouse pancreatic acinar cells. *J Physiol,* 539**,** 41-52.

VORONINA, S. G., BARROW, S. L., GERASIMENKO, O. V., PETERSEN, O. H. & TEPIKIN, A. V. 2004. Effects of secretagogues and bile acids on mitochondrial membrane potential of pancreatic acinar cells: comparison of different modes of evaluating DeltaPsim. *J Biol Chem,* 279**,** 27327-38.

VORONINA, S. G., BARROW, S. L., SIMPSON, A. W., GERASIMENKO, O. V., DA SILVA XAVIER, G., RUTTER, G. A., PETERSEN, O. H. & TEPIKIN, A. V. 2010. Dynamic changes in cytosolic and mitochondrial ATP levels in pancreatic acinar cells. *Gastroenterology*.

WAKUI, M., OSIPCHUK, Y. V. & PETERSEN, O. H. 1990. Receptor-activated cytoplasmic Ca2+ spiking mediated by inositol trisphosphate is due to Ca2(+)-induced Ca2+ release. *Cell,* 63**,** 1025-32.

WARD, J. B., PETERSEN, O. H., JENKINS, S. A. & SUTTON, R. 1995. Is an elevated concentration of acinar cytosolic free ionised calcium the trigger for acute pancreatitis? *Lancet,* 346**,** 1016-9.

WATANABE, M., HOUTEN, S. M., MATAKI, C., CHRISTOFFOLETE, M. A., KIM, B. W., SATO, H., MESSADDEQ, N., HARNEY, J. W., EZAKI, O., KODAMA, T., SCHOONJANS, K., BIANCO, A. C. & AUWERX, J. 2006. Bile acids induce energy expenditure by promoting intracellular thyroid hormone activation. *Nature,* 439**,** 484-9.

WERNER, J., LAPOSATA, M., FERNANDEZ-DEL CASTILLO, C., SAGHIR, M., IOZZO, R. V., LEWANDROWSKI, K. B. & WARSHAW, A. L. 1997. Pancreatic injury in rats induced by fatty acid ethyl ester, a nonoxidative metabolite of alcohol. *Gastroenterology,* 113**,** 286-94.

WERNER, J., SAGHIR, M., FERNANDEZ-DEL CASTILLO, C., WARSHAW, A. L. & LAPOSATA, M. 2001. Linkage of oxidative and nonoxidative ethanol metabolism in the pancreas and toxicity of nonoxidative ethanol metabolites for pancreatic acinar cells. *Surgery,* 129**,** 736-44.

WILLIAMS, J. A. 1980. Regulation of pancreatic acinar cell function by intracellular calcium. *Am J Physiol,* 238**,** G269-79.

WILLIAMS, J. A. 2001. Intracellular signaling mechanisms activated by cholecystokinin-regulating synthesis and secretion of digestive enzymes in pancreatic acinar cells. *Annu Rev Physiol,* 63**,** 77-97.

WINTERBOURN, C. C. 2008. Reconciling the chemistry and biology of reactive oxygen species. *Nat Chem Biol,* 4**,** 278-86.

WINTERBOURN, C. C., HAMPTON, M. B., LIVESEY, J. H. & KETTLE, A. J. 2006. Modeling the reactions of superoxide and myeloperoxidase in the neutrophil phagosome: implications for microbial killing. *J Biol Chem,* 281**,** 39860-9.

WINTERBOURN, C. C. & METODIEWA, D. 1999. Reactivity of biologically important thiol compounds with superoxide and hydrogen peroxide. *Free Radic Biol Med,* 27**,** 322-8.

WOJCIKIEWICZ, R. J., ERNST, S. A. & YULE, D. I. 1999. Secretagogues cause ubiquitination and down-regulation of inositol 1, 4,5-trisphosphate receptors in rat pancreatic acinar cells. *Gastroenterology,* 116**,** 1194-201.

WU, H., BHOPALE, K. K., ANSARI, G. A. & KAPHALIA, B. S. 2008. Ethanol-induced cytotoxicity in rat pancreatic acinar AR42J cells: role of fatty acid ethyl esters. *Alcohol Alcohol,* 43**,** 1-8.

WU, H., CAI, P., CLEMENS, D. L., JERRELLS, T. R., ANSARI, G. A. & KAPHALIA, B. S. 2006. Metabolic basis of ethanol-induced cytotoxicity in recombinant HepG2 cells: role of nonoxidative metabolism. *Toxicol Appl Pharmacol,* 216**,** 238-47.

YERUSHALMI, B., DAHL, R., DEVEREAUX, M. W., GUMPRICHT, E. & SOKOL, R. J. 2001. Bile acid-induced rat hepatocyte apoptosis is inhibited by antioxidants and blockers of the mitochondrial permeability transition. *Hepatology,* 33**,** 616-26.

YU, J. H., KIM, K. H., KIM, D. G. & KIM, H. 2007. Diphenyleneiodonium suppresses apoptosis in cerulein-stimulated pancreatic acinar cells. *Int J Biochem Cell Biol,* 39**,** 2063-75.

YU, J. H., LIM, J. W., KIM, K. H., MORIO, T. & KIM, H. 2005. NADPH oxidase and apoptosis in cerulein-stimulated pancreatic acinar AR42J cells. *Free Radic Biol Med,* 39**,** 590-602.

YU, L., ALVA, A., SU, H., DUTT, P., FREUNDT, E., WELSH, S., BAEHRECKE, E. H. & LENARDO, M. J. 2004. Regulation of an ATG7-beclin 1 program of autophagic cell death by caspase-8. *Science,* 304**,** 1500-2.

YULE, D. I., STUENKEL, E. & WILLIAMS, J. A. 1996. Intercellular calcium waves in rat pancreatic acini: mechanism of transmission. *Am J Physiol,* 271**,** C1285-94.

ZISSIMOPOULOS, S. & LAI, F. A. 2006. Redox regulation of the ryanodine receptor/calcium release channel. *Biochem Soc Trans,* 34**,** 919-21.

ZUCKERBRAUN, B. S., CHIN, B. Y., BILBAN, M., D'AVILA, J. C., RAO, J., BILLIAR, T. R. & OTTERBEIN, L. E. 2007. Carbon monoxide signals via inhibition of cytochrome c oxidase and generation of mitochondrial reactive oxygen species. *FASEB J,* 21**,** 1099-106.